



UNIVERSITÄT ZU LÜBECK

**From the Institute of Neurobiology
of the University of Lübeck
Director: Prof. Dr. rer. nat. Henrik Oster**

**“Remodelling of the circadian network
by bariatric surgery in mice”**

Dissertation
for Fulfillment of Requirements
for the Doctoral Degree
of the University of Lübeck

from the Department of Natural Sciences

Submitted by

Anne-Marie Neumann
from Rostock, Germany

Lübeck, 2021

First referee: Prof. Dr. rer. nat. Henrik Oster

Second referee: Prof. Dr. rer. nat. Jens Mittag

Date of oral examination: Lübeck, 05.08.2021

Approved for printing. Lübeck, 16.08.2021

Declaration

Herewith, I confirm that I have written the present PhD thesis independently and with no other sources and aids than quoted.

Lübeck, February 2021
Anne-Marie Neumann

"Flower gleam and glow
 Let your powers shine
 Make the clock reverse
 Bring back what once was mine
 Heal what has been hurt
 Change the fates design
 Save what has been lost
 Bring back what once was mine
 What once was mine"
 Rapunzel, *Tangled*

Table of Contents

Abbreviations	1
Summary	6
Zusammenfassung.....	7
1 Introduction.....	9
1.1 Obesity.....	10
1.1.1 Potential causes and risk factors	11
1.1.2 Comorbidities	11
1.1.3 Key aspects of pathophysiology	12
1.2 Weight loss therapies	14
1.2.1 Lifestyle intervention.....	15
1.2.2 Pharmacological intervention	16
1.2.3 Surgical intervention	16
1.3 Circadian clocks	22
1.3.1 The mammalian molecular clock.....	22
1.3.2 The circadian network	24
1.3.3 Tissue-specific entrainment to <i>zeitgebers</i>	26
1.3.4 Circadian regulation of metabolism	28
1.4 Metabolic interventions and the circadian clock	30
1.4.1 Effects of a hypercaloric diet.....	30
1.4.2 Effects of meal scheduling.....	31
1.4.3 Effects of bariatric surgery	33
1.5 Aims and main hypothesis.....	34
2 Material and Methods.....	35
2.1 Animal experiments	35
2.1.1 Housing and diets	35
2.1.2 Activity and food intake measurement.....	35
2.1.3 Bariatric surgery protocol.....	37
2.1.4 Social interaction test with three-chamber paradigm	38
2.1.5 PER2::LUC breeding and genotyping	39
2.1.6 Bioluminescence recordings.....	40
2.1.7 Tissue collection	41
2.2 Molecular experiments	41
2.2.1 Plasma concentrations	41
2.2.2 RNA isolation and quantification.....	42

2.2.3 RNA quality control and sequencing	42
2.2.4 RNA sequencing data processing and presentation.....	42
2.2.5 Transcriptome analysis.....	43
2.2.6 Statistical analysis.....	43
3 Results	45
3.1 Mouse behaviour after surgery.....	45
3.1.1 Diet-induced obesity correlates with dampening of behavioural circadian rhythms.....	45
3.1.2 Weight development after VSG is characterised by two distinct phases	46
3.1.3 Locomotor activity is largely resistant to VSG.....	47
3.1.4 VSG increases food intake rhythmicity.....	49
3.1.5 VSG increases sociability during weight loss	52
3.2 Metabolic state at the CP-AP transition.....	55
3.2.1 Tissue-specific recalibration of PER2 rhythms after VSG	55
3.2.2 VSG reduces plasma concentrations of metabolic markers.....	60
3.2.3 Remodelling of WAT transcriptome rhythms after VSG	62
3.2.4 VSG changes metabolism-associated gene expression.....	67
4 Discussion	75
4.1 VSG is effective in DIO mice	76
4.2 Induction of two distinct behavioural phases <i>post-surgery</i>	78
4.2.1 Circadian behaviour.....	78
4.2.2 Anxiety and the HPA axis.....	80
4.3 Regulation of rhythmic metabolism around the CP-AP transition.....	83
4.3.1 Tissue-specific recalibration of the metabolic circadian network.....	83
4.3.2 Selective uncoupling of WAT rhythmic transcriptome from feeding cycles and local clock	85
4.3.3 WAT adipokine diurnal pattern after VSG.....	90
4.4 Outlook: Translation to the human situation.....	91
References.....	95
Supplements.....	124
List of rhythmic and differently expressed genes	124
Other supplements.....	145
Acknowledgements	151
Curriculum vitae	153

Abbreviations

A	Adenine
<i>Acat1</i>	Gene encoding for Acetyl-Coenzyme A (-CoA) acetyltransferase 1
<i>Adipoq</i>	Gene encoding for Adiponectin
AMP	Adenosine monophosphate
AMPK	AMP-activated protein kinase
ANOVA	Analysis of variance
AP	Anabolic phase
<i>ApIn</i>	Gene encoding for Apelin
ARC	Arcuate nucleus or <i>nucleus arcuatus hypothalami</i>
ATP	Adenosine triphosphate
BMAL1	Brain and muscle aryl hydrocarbon receptor nuclear translocator-like protein 1, also known as ARNTL, encoded by <i>Bmal1/Arntl</i> gene
BMI	Body mass index
C	Cytosine
cAMP	Cyclic adenosine monophosphate
CCG(s)	Clock-controlled gene(s)
CCL2	Chemokine (C-C motif) ligand 2, also referred to as monocyte chemoattractant protein 1 (MCP1), encoded by <i>Ccl2</i> gene
cDNA	Complementary deoxyribonucleic acid
CK1δ/ε	Casein kinase 1 isoform delta/epsilon
CLOCK	Circadian locomotor output cycles kaput, encoded by <i>Clock</i> gene
CP	Catabolic phase
CREB	cAMP response element-binding protein
CRY1/2	Cryptochrome, encoded by <i>Cry1/2</i> genes
CVD	Cardiovascular diseases

DBP	<i>D-box</i> albumin promoter binding protein, encoded by <i>Dbp</i> gene
DD	Constant darkness
ddH ₂ O	Double-distilled water
dFC	Diurnal fold change
DIO	Diet-induced obesity
DMEM	Dulbecco's Modified Eagle's Medium
DNA	Deoxyribonucleic acid
dNTP	2'-Desoxyribonucleosid-5'triphosphate
dsDNA	Double-stranded DNA
<i>e.g.</i>	<i>exempli gratia</i> (Latin), for example
E4BP4	E4 promoter-binding protein 4, also known as NFIL3, encoded by <i>Nfil3</i> gene
<i>E-Box</i>	Enhancer box
EDTA	Ethylenediaminetetraacetic acid
ELISA	Enzyme-linked immunosorbent assay
<i>Elov6</i>	Gene encoding for Elongation of long-chain fatty acids family member 6
<i>et al.</i>	<i>et alia</i> (Latin), and others
EU	European Union
FC	Fold change
FDR	False discovery rate
FELASA	Federation of European Laboratory Animal Science Associations
FFA(s)	Free fatty acid(s)
FGF21	Fibroblast growth factor 21, encoded by <i>Fgf21</i> gene
G	Guanine
GC(s)	Glucocorticoid(s)
GLP-1	Glucagon-like peptide 1

GLUT2	Glucose transporter 2, encoded by <i>Slc2a2</i> gene
GO	Gene ontology
GR	Glucocorticoid receptor
<i>GRE</i>	GC-responsive elements
HBSS	Hanks' Balanced Salt Solution
HEPES	4-(2-Hydroxyethyl)-1-piperazineethanesulfonic acid
HFD	High-fat diet
<i>Hmgcl</i>	Gene encoding for HMG-CoA lyase
HMG-CoA	β -Hydroxy β -methylglutaryl-CoA
<i>Hmgcr</i>	Gene encoding for HMG-CoA reductase
<i>Hmgcs1/2</i>	Gene encoding for HMG-CoA synthase 1 (soluble) / 2 (mitochondrial)
HPA	Hypothalamic-pituitary-adrenal
<i>i.e.</i>	<i>id est</i> (Latin), that is
ID	Identifier
ipRGCs	Intrinsically photosensitive retinal ganglion cells
KEGG	Kyoto Encyclopedia of Genes and Genomes
LD	Light-dark
LD12:12	12-hour light: 12-hour dark
<i>Lep</i>	Gene encoding for Leptin
LiD	Liquid diet
<i>Lipe</i>	Gene encoding for Lipase E or Hormone-sensitive lipase
<i>Lipf</i>	Gene encoding for Lipase F or Gastric triacylglycerol lipase
LL	Constant light
LPL	Lipoprotein lipase, encoded by <i>Lpl</i> gene
LUC	Firefly luciferase, encoded by <i>Luc</i> gene

MAPK	Mitogen-activated protein kinase
MELUR	Ministry of Energy Change, Rural Areas & Consumer Protection
<i>mPer2</i>	Gene encoding for the mouse Period 2
mRNA	Messenger ribonucleic acid
N	Symbol to account for a random nucleobase in a genomic sequence
NaCl	Sodium chloride
NAD	Nicotinamide adenine dinucleotide, oxidised NAD ⁺ , reduced NADH
NCBI	National Center for Biotechnology Information
NPAS2	Neuronal PAS domain protein 2, encoded by <i>Npas2</i> gene
OECD	Organisation for Economic Co-operation and Development
OSA	Obstructive sleep apnoea
<i>Oxct1</i>	Gene encoding for 3-oxoacid CoA-transferase 1
PAI-1	Plasminogen activator inhibitor-1, encoded by <i>Serpine1</i> gene
PCR	Polymerase chain reaction
<i>Pepck1</i>	Gene encoding for Phosphoenolpyruvate carboxykinase
PER1/2/3	Period 1/2/3, encoded by <i>Per1/2/3</i> genes
<i>Pnpl3</i>	Gene encoding for Patatin like phospholipase domain containing 3
PPAR(s)	Peroxisome proliferator-activated receptor(s), PPAR- γ isoform gamma
PRKCA	Protein kinase C alpha
<i>Rarres2</i>	Gene encoding for Chemerin, also known as retinoic acid receptor responder protein 2
REV-ERB(s)	Reverse-erythroblastosis virus nuclear receptor subfamily 1 members, REV-ERB α/β isoforms alpha/beta, also called NR1D1/NR1D2, encoded by <i>Nr1d1/2</i> genes
RHT	Retinohypothalamic tract or <i>tractus retinohypothalamicus</i>
RM	Repeated measures

RNA	Ribonucleic acid
ROR	Retinoic acid related orphan receptor(s)
<i>RORE</i>	ROR-response elements
ROUT	Robust regression and outlier removal
RYGB	Roux-en-Y Gastric Bypass
<i>Scd1</i>	Gene encoding for Stearoyl-CoA desaturase-1
SCN	Suprachiasmatic nucleus or <i>nucleus suprachiasmaticus</i>
scWAT	Subcutaneous white adipose tissue
SDS	Sodium dodecyl sulphate
SEM	Standard error of the mean
SIRT1	Sirtuin 1, also known as NAD-dependent deacetylase sirtuin-1
<i>Sqle</i>	Gene encoding for Squalene monooxygenase, also called squalene epoxidase
T	Thymine
T2DM	Type 2 Diabetes mellitus
TAE	Tris-acetate-EDTA
TAG(s)	Triacylglyceride(s)
TCA	Tricarboxylic acid
Tris	Tris(hydroxymethyl)aminomethane
TTFL	Transcription-translation feedback loop
UK	United Kingdom
US	United States (of America)
VSG	Vertical sleeve gastrectomy
WAT	White adipose tissue
WHO	World Health Organization

Summary

Obesity is a global health issue associated with deadly comorbidities and a reduced quality of life. Its development is caused by a prolonged positive energy balance, but its expression is determined by a variety of underlying factors. For example, disruption of natural rhythms was recognised as an obesity risk factor. Organisms across the globe have developed circadian clocks to anticipate external conditions such as the 24-h light-dark cycle or the availability of food. In mammals, these rhythms are orchestrated by a tight network of communicating tissue clocks based on autonomous but synchronised transcriptional-translational feedback loops in virtually every cell. To effectively adapt to the environment, some clocks can be adjusted by metabolic and endocrine crosstalk.

Bariatric surgery is a popular way to achieve long-term body weight loss. These interventions are more successful in resetting metabolism than conventional strategies, but the mechanisms of action and reasons for varying outcomes are still not clear. Given a tight interplay of the circadian network with the metabolic system, I hypothesised that the clock system can influence bariatric surgical success and *vice versa*. For that reason, vertical sleeve gastrectomy (VSG) was performed in obese mice and behaviour, tissue rhythms, and white adipose tissue (WAT) transcriptome regulation were evaluated. Post-surgical weight development was characterised by two distinct metabolic periods: a catabolic and a subsequent anabolic phase. The gastrointestinal reconstruction induced a unique food intake pattern. An initial caloric restriction gradually normalised in parallel to an increased food intake frequency specifically during the daily active phase. This resulted in a significantly strengthened feeding rhythm in the anabolic phase. The metabolic state during the transition from the catabolic to the anabolic state was further investigated. Bariatric surgery tissue-specifically modulated rhythmicity of the central master pacemaker, the adrenal gland, and the liver. No significant effects were detected in clock function of either epididymal or subcutaneous WAT. Temporal transcriptome analysis of the latter revealed a reduction of cyclic genes transcription after VSG (sham: 2,493 vs. VSG: 1,013 cycling transcripts) independent of sustained rhythms in core clock gene expression. Moreover, VSG altered rhythmic transcriptional regulation of WAT lipid metabolism pathways. This suggests a remodelling of diurnal metabolic rhythms after VSG downstream of the molecular clock machinery in WAT.

In summary, I could show that bariatric surgery can affect daily rhythms of behaviour, tissue clocks, and gene expression. Of note, VSG seems to selectively uncouple the WAT rhythmic transcriptome from, both, the local core clock activity and the feeding rhythms. These metabolic adaptations can likely be applied to the human situation early after surgery in some regard, but the VSG mouse model does not yield long-term weight loss similar to humans. It may, however, be of particular interest in understanding poor first-phase responders.

Zusammenfassung

Übergewicht ist ein globales Gesundheitsproblem assoziiert mit potenziell tödlichen Komorbiditäten und stark eingeschränkter Lebensqualität. Es entsteht aufgrund einer andauernden positiven Energiebalance, allerdings beeinflussen verschiedenste Mechanismen Geschwindigkeit und Schweregrad der Erkrankung. Beispielsweise wurde das Stören natürlicher Tagesrhythmen als Risikofaktor erkannt. Organismen weltweit haben diese sog. *zirkadianen* Rhythmen entwickelt, um externe Verhältnisse wie den Wechsel von Licht und Dunkel oder die Verfügbarkeit von Futter im Laufe des Tages zu antizipieren. In Säugetieren werden diese Rhythmen über ein engmaschiges Netzwerk an inneren Gewebeuhren organisiert, welche auf autonomen, aber synchronisierten Rückkopplungsschleifen von Transkription und Translation in nahezu jeder Zelle basieren. Um effektiv auf Umgebungsänderungen zu reagieren, können manche dieser Uhren von metabolischen oder endokrinen Signalen reguliert werden.

Die bariatrische Chirurgie ist eine populäre Methode zur anhaltenden Gewichtsreduktion. Diese Art Interventionen sind erfolgreicher darin, den Metabolismus zurückzusetzen, als konventionelle Therapien, jedoch bleiben Wirkmechanismus sowie Ursachen für unterschiedliche Ergebnisse weiterhin unklar. In Anbetracht des Zusammenspiels des zirkadianen Netzwerks mit dem metabolischen System nahm ich an, dass circadiane Uhren und bariatrischer Chirurgieerfolg sich gegenseitig beeinflussen. Daher wurde die Schlauchmagenbildung in adipösen Mäusen ausgeführt und Verhalten, Gewebeuhren sowie das Transkriptom des weißen Fettgewebes untersucht. Die postoperative Gewichtsentwicklung zeigte zwei metabolische Intervalle: eine katabole sowie eine darauffolgende anabole Phase. Die Rekonstruktion des Gastrointestinaltrakts induzierte eine veränderte Art der Futteraufnahme. Eine anfängliche Kalorienrestriktion normalisierte sich schrittweise während gleichzeitig die Futteraufnahmehäufigkeit anstieg, besonders in der natürlichen Aktivitätsphase des Tages. Daraus resultierend war der Rhythmus der Futteraufnahme während der anabolen Phase gestärkt. Weiter sollte der metabolische Zustand zum Zeitpunkt des Übergangs von der katabolen in die anabole Phase untersucht werden. Die bariatrische Chirurgie modulierte gewebespezifisch die Uhrenrhythmik des zentralen Schrittmachers, der Nebenniere und der Leber. Weder das epididymale noch das subkutane weiße Fettgewebe zeigten signifikante Veränderungen in ihrer Uhrenfunktion. Transkriptomanalysen des letztgenannten offenbarten eine Reduktion tagesrhythmischer Gene nach bariatrischer Operation (von 2.493 auf 1.013), obwohl die Expression der wichtigsten Uhrengene unverändert blieb. Die rhythmische Regulation von Genen des Lipidstoffwechsels zeigte jedoch Abwandlungen. Dies deutet darauf hin, dass die Schlauchmagenbildung in weißem Fettgewebe die Tagesaktivität metabolischer Rhythmen auf einer der molekularen Uhr nachgeschalteten Ebene reguliert.

Zusammengefasst zeigt meine Arbeit, dass die bariatrische Operation tägliche Rhythmen des Verhaltens, von Gewebeuhren und der Genexpression beeinflussen kann. Bemerkenswerterweise scheint die Operation am Ende der katabolen Phase zu einem gewissen Grad das rhythmische Transkriptom des weißen Fettgewebes sowohl von der konstant laufenden Gewebeuhr als auch der progressiv verstärkten Rhythmik der Futteraufnahme zu entkoppeln. Die metabolischen Anpassungen in der Maus lassen sich wahrscheinlich auch auf den Menschen übertragen – zumindest zu einer frühen Phase nach der Operation. Das Mausmodell ist allerdings nicht geeignet, den beim Menschen üblichen Langzeitgewichtsverlust abzubilden. Stattdessen könnte es Hinweise auf Einflussfaktoren bei jenen Patienten zu liefern, die kaum positiv auf die bariatrische Operation reagieren.

1 Introduction

Modern society pressures more and more people to live a life considered largely unhealthy. The increase of atypical working hours (*e.g.* at night) leads to workers spending more time awake during the biological rest phase. Moreover, people spend less leisure time preparing balanced meals or be physically active. These trends are supported by artificial lighting, 24-h services, and calorie-rich highly processed food options.

Though according to the Organisation for Economic Co-operation and Development (OECD) the annual working hours decrease on average around the world (OECD, 2019), demand for shift work is increasing in many fields (McMenamin, 2007). In the European Union (EU), 19 % of employees work during the night and 21% work in shifts, particularly the physically demanding rotating shifts. In the United States (US) these numbers are even higher with 30 % night-time work and 38 % shift work (European Foundation for the Improvement of Living and Working Conditions. and International Labour Organization (ILO)., 2019). It is estimated that around 5 – 10 % of shift workers suffer from shift work sleep disorder (Drake *et al.*, 2004). Moreover, shift workers necessarily also eat at atypical times. Disruption of daily rhythms by mistimed meals, sleep deprivation, and light at night are associated with adverse health effects. Shift-work is associated with diseases such as diabetes mellitus type 2 (T2DM), obesity, hypertension, impaired cognitive function, depressive symptoms, and cancer (Reid and Abbott, 2015; Torquati *et al.*, 2019; Pickel and Sung, 2020). In parallel, people report a perceived lack of time to prepare healthy meals. More than 40 % of young workers (20 to 31 years old) with > 40 work hours per week somewhat or strongly agreed with the statement of being “too busy to eat healthy foods” and more than 35 % with finding it “hard to find time to sit down and eat a meal”. Furthermore, 71.4 % across the whole study reported eating “fast food” more than once a week (Escoto *et al.*, 2012). A consequence of deregulated biological rhythms in combination with poor eating habits is a substantial and increasing part of the population being overweight or obese (OECD, 2018); a pandemic that burdens health systems globally (Withrow and Alter, 2011).

It is undeniable that environmental factors such as diet or sleep impact physical and mental health. Given the association of disrupted biological rhythms in the pathogenesis of these diseases, a look into the role of (inner) biological clocks in the success of treatment options becomes interesting. Taking the natural daily rhythms into account led to the advancing field of chronomedicine. For example, time-of-day effects were reported for treatments of cancer, asthma, and cardiovascular diseases (CVD; Münch and Kramer, 2019). Moreover, circadian rhythms were shown to influence the success of cardiac surgery (Montaigne *et al.*, 2018) and wound healing (Hoyle *et al.*, 2017). An understanding of the interplay between circadian clocks and specific therapeutical approaches will subsequently lead to more efficient treatments for the diseases of modern civilisation.

1.1 Obesity

Overweight and obesity are complex, multifactorial medical conditions with abnormal or excess body fat accumulation leading to increased health risks. Body weight status is usually categorised by body mass index (BMI). BMI is calculated by dividing a person's weight (in kg) by the square of their height (in m). A person exceeding a BMI of 25 is considered overweight, of 30 obese.

According to the World Health Organization (WHO), the worldwide prevalence of obesity nearly tripled between the years 1975 and 2016. In 2016, 1.9 billion adults (> 18 years of age) were overweight and 650 million of these were obese. This accounts for 39 % and 13 % of the population, respectively. A trend that also impacts health in children, with 18 % of the children aged 5 – 18 years being overweight and around 7 % obese (WHO, 2020). Obesity was long considered a problem of the Western world. However, obesity is also on the rise in large parts of Asia and Africa (WHO, 2020). For example, the overweight rate in Chinese children and adolescents increased from 5 % during 1991 – 1995 to 13.2 % in 2006 – 2010. A particularly high number (11.7 %) of infants (age 0 – 1 years) were reported to be overweight in 2006 – 2010. The prevalence dropped only mildly from 2010 to 2015 (Guo *et al.*, 2019). Today, obesity is seen as a leading cause of death worldwide. This is not a result of obesity by itself, but a reflection of its numerous comorbidities (Fig. 1.1).

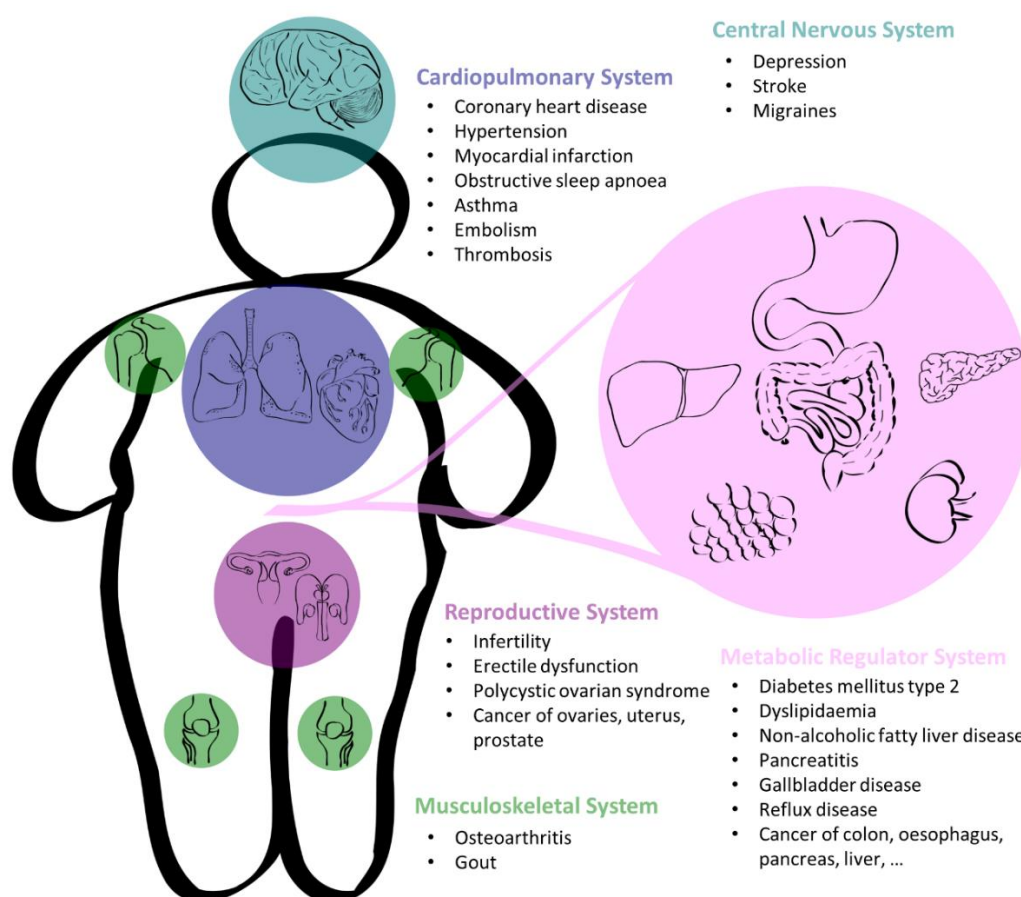


Figure 1.1: Comorbidities of obesity. Obesity is a multifactorial and systemic disease. List of comorbidities taken from Upadhyay *et al.*, 2018 and adapted according to Reimann *et al.*, 2017; Buie *et al.*, 2019.

1.1.1 Potential causes and risk factors

Obesity is a multi-causal disease. In the most basic sense, obesity can be explained by an excessive intake of high-calorie food in combination with a lack of physical activity. However, genetics, underlying humoral diseases, or psychiatric disorders are among the known contributors. The Endocrine Society wrote in 2017 about the complex environment of contributing factors in the pathogenesis of obesity (Schwartz *et al.*, 2017). Data from “overfeeding studies” in normal-weight and obese patients led to the conclusion that some people are biologically predisposed to an elevated level of body fat that is physiologically defended during weight loss and gain (Schwartz *et al.*, 2017).

Genetics potentially work in tandem with environmental factors to favour a positive energy balance. The list of suggested effectors includes diet composition, lifestyle (*e.g.* shift-work), environmental toxins, infections, microbiome alterations, and maternal obesity or diabetes (Schwartz *et al.*, 2017). Though genetic variants were only found to account for a small portion of the obesity risk, epigenetics seem to play an important role (Rohde *et al.*, 2019). Notably, maternal obesity is associated with increased repressive epigenetic markers in neurons of the hypothalamic feeding circuit (Plagemann *et al.*, 2009) as well as epigenetic changes to enhance adipogenic potential of white adipose tissue (WAT; Yang *et al.*, 2013). Parental diet can crucially impact children during development and increase their obesity risk later in life (Ravelli *et al.*, 1976; Sharp *et al.*, 2015). With successful treatment preceding pregnancy such a familial chaining could be broken.

1.1.2 Comorbidities

All-cause mortality increases with abnormal BMI. Moreover, adults of both sexes show a significant reduction in life expectancy by obesity. These effects are greater among the young than old and among men than women. Furthermore, ethnicity plays a role (Smith and Smith, 2016). The main causes of death in relation to obesity include heart attack, stroke, and diabetes-related complications (Upadhyay *et al.*, 2018). T2DM and CVD are not only very common in obese individuals but also the leading reasons for the associated increase in mortality.

Metabolic syndrome is a cluster of at least three of five medical conditions: obesity, high blood pressure (hypertension), hyperglycaemia (insulin resistance), high serum triacylglycerides (TAGs), and low serum high-density lipoprotein (Alberti *et al.*, 2009). In a study of the US population, only 2 % of normal weight subjects developed the metabolic syndrome compared to 22 % of overweight and 60 % of obese individuals (Park *et al.*, 2003). Obesity is generally seen as cause and sign of the metabolic syndrome. A consequence of the obesity-associated metabolic disbalance is the development of T2DM, non-alcoholic fatty liver disease, and CVD (Katsiki *et al.*, 2018; Zafar *et al.*, 2018). However, the risk for CVD increases with BMI independent of the metabolic status. So-called metabolically healthy

obese subjects are still at significantly higher risk of CVD compared to metabolically healthy normal weight (Yeh *et al.*, 2019).

It is established that obesity has diverse effects especially on the cardiovascular and endocrine system. However, as a systemic disease it impacts the body at all levels. Notably, obesity is a major risk factor for severe asthma or certain types of cancer (Upadhyay *et al.*, 2018). While asthma onset was linked with obesity-associated metabolic disturbances (Sideleva *et al.*, 2012), excess fat accumulation also compresses lung capacity by restricting space for sufficient lung expansion, thus, favouring airway collapsibility (Watson *et al.*, 2010). Furthermore, the restrictive effect of visceral body fat is the major preventable risk factor for the pathogenesis of obstructive sleep apnoea (OSA; Young *et al.*, 2004). OSA is defined as interruptions in breathing during sleep by upper airway obstructions and collapse. The subsequent arousal from hypoxia leads to fragmented sleep (Young *et al.*, 2004); a circadian disruption frequently associated with obesity.

Obesity greatly affects physical health. A sometimes less regarded fact, overweight takes a heavy toll on mental health. Not only do obesity and unhealthy diets accelerate the onset of traditionally age-related cognitive impairment (Buie *et al.*, 2019), but they increase the risk of depression and depressive symptoms (Luppino *et al.*, 2010). Moreover, the relationship between major depression and obesity is bidirectional: 55 % of obese individuals develop depression over time and, *vice versa*, 58 % of depressive individuals are obese (Luppino *et al.*, 2010). Depression is characterised by persistent sadness and disinterest. It can disrupt sleep and diet rhythms as well as social structure, thus, heavily impacting on quality of life.

1.1.3 Key aspects of pathophysiology

Although the causality of obesity is still insufficiently understood, physiological dysregulations caused by the disease are extensively described. A prolonged positive energy balance leads to an altered distribution of WAT across the body combined with adaptations in adipocyte size and number, cellular composition, vascularisation, oxidative stress, secretory profile, and inflammatory state (Longo *et al.*, 2019). These adaptations in WAT physiology affect metabolic homeostasis peripherally and centrally.

When healthy, WAT stores energy received from circulating TAGs (*e.g.* from lipoproteins) or glucose as lipid TAG droplets after meals for later release as free fatty acids (FFAs) as starvation energy source. When the lipid storage capacities of adipose tissue are exceeded, plasma concentrations of FFAs and TAGs rise. Elevated circulating lipids are increasingly stored in other metabolic organs such as liver, pancreas, and muscle. Here, they act as lipotoxins and reduce insulin sensitivity (Unger and Orci, 2000).

Research into the field of obesity maintenance and progression gained new momentum with the discovery of leptin (Zhang *et al.*, 1994). Leptin is a satiety inducing hormone secreted from adipose tissue: an adipokine (Campfield *et al.*, 1995). Though leptin deficiency leads to an obese phenotype, the genetically normal obese patient has high levels of the hormone but shows functional resistance similar to diabetic insulin resistance (Maffei *et al.*, 1996). Notably, circulating leptin concentrations strongly correlate with subcutaneous fat mass (Hube *et al.*, 1996; Van Harmelen *et al.*, 1998; Minocci *et al.*, 2000). The resulting leptin resistance in obesity seems to be selective. While exogenous leptin supplementation was able to induce some peripheral effects like increase of blood pressure, it failed to act centrally reduce appetite (Rahmouni *et al.*, 2005; Könner and Brüning, 2012). Consequently, leptin appears to be a driving force in obesity-associated hypertension.

It is unclear, how this selective leptin resistance develops. Proposed mechanisms included tissue-specific disruption of receptor function, altered transportation across the blood-brain-barrier, and semi-protective neuroinflammation in sensitive brain regions (de Git and Adan, 2015; Liu *et al.*, 2018b). TAGs can induce peripheral leptin resistance but were recently shown to also cross the blood-brain barrier and induce leptin and insulin resistance centrally on the receptor level (Banks *et al.*, 2018). Given the importance of leptin in appetite regulation and obesity, more peptide hormones with feeding regulating actions in the brain were investigated. The complementary “hunger” hormone, ghrelin, showed decreased and dysregulated serum levels in obesity but a pivotal role in promoting obesity seems unlikely (Müller *et al.*, 2015). Rising leptin levels develop early in obesity and leptin’s role in insulin sensitivity suggests a contributing part for the development of insulin resistance and T2DM (Levi *et al.*, 2011; D’Elia *et al.*, 2019).

Since adipose tissue is a major place of action in obesity, a large body of studies was conducted into adipose tissue physiology of lean and obese people. Other adipokines besides leptin were associated with disease progression at different levels (Tab. 1.1; Fasshauer and Blüher, 2015). Moreover, adipokines connect metabolism and immunological status. For example, leptin not only regulates appetite and insulin action but is also a proinflammatory cytokine (Lord *et al.*, 1998; Kiguchi *et al.*, 2009). The secretory profile of many adipokines correlates with adipocyte size, fat mass, and cellular composition (Fasshauer and Blüher, 2015). The proinflammatory characteristics of many adipokines and the increase of circulating levels of these contribute to the so-called metainflammation (for metabolic inflammation) in obesity (Unamuno *et al.*, 2018). Metainflammation primary originating in WAT was linked to the progression of insulin resistance in obesity (Winer *et al.*, 2009; Kang *et al.*, 2016).

Table 1.1: Physiological role of selected adipokines and concentrations in obesity. FGF21: Fibroblast growth factor 21; CCL2: chemokine (C-C motif) ligand 2; PAI-1: plasminogen activator inhibitor-1

Adipokine	Main actions	Change in obesity
Adiponectin	Improves insulin sensitivity, antiinflammatory	↓ (1)
Apelin	Inhibits insulin secretion, decrease lipolysis	↑ (1)
Chemerin	Regulates adipogenesis & stimulates lipolysis, chemoattractant	↑ (1)
FGF21	Glucose uptake into adipocytes, improves energy metabolism	↑ (1)
Leptin	Satiety signal, improves insulin sensitivity	↑ (1)
CCL2	Chemoattractant	↑ (1)
Nesfatin-1	Glucose-dependent insulintropic, promotes satiety	↑ (3)
PAI-1	Serine protease inhibitor, suppresses fibrinolysis	↑ (4)
Resistin	Promotes insulin resistance, proinflammatory	↑ (2)
Visfatin	Stimulates NAD biosynthesis for beta-cell function	↑ (2)

Modified after (1) Fasshauer and Blüher, 2015; (2) Rabe et al., 2008; (3) Zhang et al., 2012; (4) Tschoner et al., 2012

Though, both, dysregulated WAT adipokine secretion and immune responses are observed in different WAT depots of obese individuals (Jialal and Devaraj, 2018), some functional differences may play a significant role in the development of the metabolic syndrome. While visceral WAT is more associated with inflammation (Lemieux *et al.*, 2001) and adiponectin secretion (Motoshima *et al.*, 2002), subcutaneous WAT (scWAT) is the major source of leptin (Minocci *et al.*, 2000). Moreover, visceral WAT is prone to lipolysis and generation of FFAs (Zierath *et al.*, 1998; Freedland, 2004), whereas scWAT appears to have a higher capacity to absorb FFAs and TAGs (Freedland, 2004). However, these buffering actions are limited by its adipogenic potential and exhaustion leads to ectopic fat storage in and around other organs. The resulting lipotoxicity further increases inflammation and insulin resistance (Unger and Orci, 2000; Longo *et al.*, 2019). In line with this, expansions of scWAT depots were associated with lower muscle and WAT insulin sensitivity (Camastra *et al.*, 2017). Even though visceral WAT (*e.g. via* waist circumference) is a reliable predictor of mortality, scWAT characteristics appear more crucially involved in the progression of metabolic disturbances in obesity.

1.2 Weight loss therapies

Weight loss is a reliable method to treat obesity and its associated comorbidities. The risk of developing T2DM was reduced by $\geq 50\%$ after a loss of just 5 kg body weight in women (Colditz, 1995). However, sustained reduction of a pathological weight is difficult and demanding. As of now, a small range of approved medications is available in addition to dietary or exercise interventions (see chapter 1.2.2). Bariatric surgery is a well-established surgical intervention to substantially reduce weight and avoid

regaining. Nevertheless, a combination of treatment options is recommended with lifestyle interventions preceding surgical or pharmacological therapies (Tab. 1.2; Yumuk *et al.*, 2015).

Table 1.2: Treatment recommendations based on BMI and comorbidities.

Treatment intervention	BMI (kg/m ²)			
	25.0 – 29.9	30.0 – 34.9	35.0 – 39.9	> 40
Lifestyle	Yes	Yes	Yes	Yes
Pharmaceutical	With comorbidities	With comorbidities	Yes	Yes
Surgical	No	With comorbidities	With comorbidities	Yes

Modified after Yumuk *et al.*, 2015

1.2.1 Lifestyle intervention

Lifestyle interventions are potentially effective for all types of overweight. The most important factor is to reduce the ratio of caloric intake to energy expenditure. Though content-specific diets such as low-fat or low-carbohydrate give good weight loss results initially, compliance is often lacking due to meal monotony. More successful for a long-term change of dietary habits are balanced weight loss diets (*e.g.* Mediterranean diet; Yumuk *et al.*, 2015; Joshi and Mohan, 2018; Chester *et al.*, 2019). Lifestyle interventions can successfully reduce weight by $\geq 5\%$ in 35 – 80 % of participants in the first 6 months and by $\geq 10\%$ in 3 – 42 %. After one year, numbers can go up to 97% ($\geq 5\%$ weight loss) and 70 % ($\geq 10\%$; Lv *et al.*, 2017). However, to achieve comparatively high and reliable weight loss results, a combination of dieting, physical activity, and behavioural therapy is needed (Lv *et al.*, 2017).

A more recently emerging idea is time-restricted eating or intermittent fasting. In intermittent fasting individuals on a recurring basis avoid energy intake for an extend period of time (*e.g.* 16 h) with a short intervening period of normal food intake (Mattson *et al.*, 2017). Interestingly, time-restricted eating is often accompanied by unattempted caloric restriction (Gabel *et al.*, 2018). In a study with matched nutrient content between intervention and control group, participants show no body weight reduction after five weeks but metabolic and cardiovascular improvements (Sutton *et al.*, 2018). In another study comparing time-restricted eating within 4 h or 6 h per day against a control group, participants were able to reduce body weight by approx. 3 % in eight weeks independent of the time frame with a reduction of around 550 kcal/d. No calories were counted or restricted (Cienfuegos *et al.*, 2020). Moreover, lunch timing did also affect success of a diet program in a South Spanish cohort (Garaulet *et al.*, 2013). Night-time working and subsequent night-time eating are associated with an increased risk of obesity (Reid and Abbott, 2015) and shifting active cycles potentiates the effects of excess caloric intake (Kim *et al.*, 2018). Thus, the importance of meal timing in weight loss dieting is not surprising.

1.2.2 Pharmacological intervention

For more severe cases of overweight, especially with comorbidities, pharmaceuticals can be added to the intervention regime. Several drugs are approved to treat specific obesity-associated comorbidities, *e.g.* T2DM. Two mechanisms of action are historically used for the treatment of obesity itself: inhibition of pancreatic lipases to reduce digestion of dietary fats (*e.g.* Orlistat) or appetite suppressants and anorectics (Herdegen and Böhm, 2010).

Most anorectic drugs act by strengthening the biogenic amines response (*e.g.* Amfepramon, Sibutramine) or by inhibiting the cannabinoid receptor 1 (*e.g.* Rimonabant; Herdegen and Böhm, 2010). However, these anorectic drugs come with diverse side effects. Biogenic amines like dopamine, serotonin, or epinephrine and the cannabinoid system act substantially on all levels of the body's physiology including peripheral stress responses and neurotransmission. Subsequently, side effects include damage of the cardiovascular system, sleep disturbances, and, in case of Rimonabant, depression, anxiety, and suicidal thoughts (Herdegen and Böhm, 2010). Combined with a moderate effectiveness, this led to many drugs being taken off the market again after cost-benefit analyses (Herdegen and Böhm, 2010; Srivastava and Apovian, 2018). Still on the market in the EU is Naltrexone SR/Bupropion SR (opioid receptor antagonist/dopamine noradrenaline reuptake inhibitor). Additionally, Orlistat and new drugs like Liraglutide, a glucagon-like peptide 1 (GLP-1) receptor mono-agonist, were approved (Dragano *et al.*, 2020). Effectiveness varies strongly between trials with ranges from 1 to 11 % (Saunders *et al.*, 2018; Srivastava and Apovian, 2018; Dragano *et al.*, 2020). Markets around the world are also flooded with natural supplements to reduce weight; however, these seem to be mostly ineffective and unrecommended, even potentially harmful (Wharton *et al.*, 2020).

Pharmacological treatment of obesity needs careful consideration given the possible metabolic, cardiovascular and psychiatric side effects compared to only moderate success rates. Lifestyle interventions combined with behaviour therapy seem similarly effective with a much lower risk and long-term potential.

1.2.3 Surgical intervention

Bariatric surgery is recommended to be used in tandem with conventional weight loss therapies. With a BMI ≥ 40 kg/m² or a BMI ≥ 35 kg/m² with comorbidities, patients can undergo bariatric or metabolic surgery after conventional therapies have failed. Conventional therapy is considered failed if a patient is incapable of losing 15 % (when BMI 35 – 39.9 kg/m²) or 20 % (when BMI > 40 kg/m²) of weight, alternatively, if the patient cannot sustain weight loss within a year. In patients with a BMI > 50 kg/m² or uncontrollable comorbidities, surgery is recommended without prior lifestyle interventions (Arbeitsgemeinschaft der Wissenschaftlichen Medizinischen Fachgesellschaften e.V., 2018).

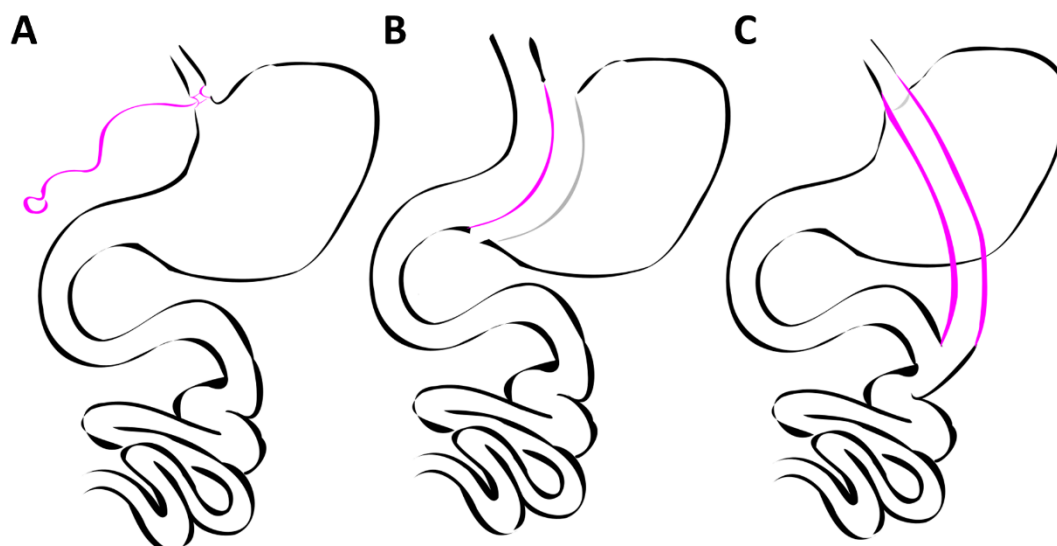


Figure 1.2: Types of bariatric surgery. [A] Adjustable gastric band, [B] vertical sleeve gastrectomy, and [C] Roux-en-Y gastric bypass.

The three most common types of surgeries are gastric band, vertical sleeve gastrectomy (VSG), and Roux-en-Y gastric bypass (RYGB; Fig. 1.2). Less prevalent, more complex and riskier is the biliopancreatic diversion with a duodenal switch (Seelbach and D’Almeida, 2020). While the gastric band is seen as an exclusively restrictive method, the other types reconstruct anatomical structures leading to endocrine adaptations of gastrointestinal physiology. These adaptations can subsequently affect the whole body including the brain, liver, and adipose tissue (Azim and Kashyap, 2016; Landecho *et al.*, 2017).

1.2.3.1 Outcomes

Bariatric surgery is more effective in obtaining long-term weight loss than behavioural interventions. A comprehensive study from Sjöström *et al.* (2007) evaluated surgical outcomes against a control group of, both, conventionally treated and untreated patients from 1987 to 2001. The mean changes in body weight were approximately 23 % at 2 years, 17 % at 10 years, 16 % at 15 years, and 18 % at 20 years *post-surgery* compared to 0 % to 1 % in the control group during those years (Sjöström *et al.*, 2007). Within 18 months, patients undergoing bariatric surgery lost 22.6 % of body weight compared to 6.7 % in a group of conventionally treated patients (Heo *et al.*, 2012). A recent meta-analysis of weight loss at 10 or more years after bariatric surgery showed that RYGB led to an excess body weight loss (relative to ideal body weight) of 55.4 %, gastric banding to 45.9 %, and VSG to 57.0 % (O’Brien *et al.*, 2019).

Additionally, bariatric surgery greatly improves glucose homeostasis: in a small cohort of 60 patients RYGB led to a T2DM remission rate of 81.2 %, VSG of 80.9 %, and gastric banding of 60.8 % over three

years (Abbatini *et al.*, 2010). Interestingly, though metabolic benefits are predicted by the weight loss, T2DM improves prior to any weight loss occurrence and can be maintained in some patients after weight regain (Landecheo *et al.*, 2017). In about 70 % of patients, dyslipidaemia ameliorates after bariatric surgery: low-density lipoprotein and TAGs are reduced, while high-density lipoprotein tends to increase (Buchwald *et al.*, 2004). Moreover, metabolic surgery reduces all-cause mortality, especially in relation to cardiovascular and cerebrovascular diseases (Aminian *et al.*, 2019). Hypertension is resolved or improved in approx. 78.5 % of patients, OSA in 83.6 % (Buchwald *et al.*, 2004).

Of the three most common types of surgeries, gastric banding is overall the least successful type of surgery, but the procedure is comparably mild and easily reversible (Abbatini *et al.*, 2010; O'Brien *et al.*, 2019). In direct comparison, RYGB leads to slightly better metabolic outcomes but also to more *peri-* and *post-*operative complications compared to VSG (Peterli *et al.*, 2018; Nasser *et al.*, 2019). For example, in a group of patients with a BMI of 35 – 49.9 kg/m² primary complications after VSG were observed in 2.55 % and 5.92 % after RYGB, readmission within 30 days in 2.90 % and 5.63 %, respectively (Nasser *et al.*, 2019). However, the chance to develop or worsen a gastroesophageal reflux syndrome, though small, is higher after VSG (Peterli *et al.*, 2018). Overall, VSG is the type of bariatric surgery with the best benefit-risk ratio.

1.2.3.2 Mechanisms of action

Evaluation of bariatric surgery in humans relies mostly on blood and faecal samples. This greatly limits understanding of mechanisms of actions. Given the restricted access to human tissue data, animal models, specifically rodent models, were established to study bariatric surgery in controlled and reproducible conditions (Yin *et al.*, 2012; Shah and Shin, 2020). Combined with the human data, knowledge of physiological adaptations after bariatric surgery has greatly increased recently.

It is well established that surgery leads to an increase of adiponectin, while leptin, proinflammatory signals, fetuin A, and FGF21 are decreased (Faramia *et al.*, 2020). The regulation on some gastrointestinal hormones seems to depend on the type of surgery: *e.g.* ghrelin is reduced after VSG, but the direction of change is unclear after other types of surgery (Tuero *et al.*, 2020). Similar discrepancies are found for incretins and pancreatic hormones (Meek *et al.*, 2016). A randomised clinical trial comparing endocrine blood concentrations found fasting ghrelin reduced after VSG, while it increased after RYGB. Leptin, glucose, and insulin were reduced in both. Glucagon, though at no point significantly different between both types of surgery, was reduced six and twelve months after VSG compared to baseline (Kalinowski *et al.*, 2017). Such variations in hormonal responses may explain in some part the differential outcomes of bariatric surgery procedures. However, experiments with

knockout mouse models have shown that neither ghrelin nor the incretin GLP-1 are necessary for successful outcomes after VSG (Chambers *et al.*, 2013; Wilson-Pérez *et al.*, 2013a). Functioning leptin signalling appears more crucial for sustainability of, both, weight loss and improved glucose homeostasis after bariatric surgery (Hao *et al.*, 2015; Mokadem *et al.*, 2015; Abu-Gazala *et al.*, 2018). Given leptin's proposed central role in obesity pathogenesis (see chapter 1.1.3), the mechanism underlying the impact bariatric surgery has on leptin signalling needs further investigation.

Initially, the effects on body weight are largely contributed to caloric restriction. A smaller stomach capacity enforces smaller meal sizes. However, a study comparing weight loss on an 800-kcal/d diet without or after RYGB found RYGB patients to reach the 10-kg weight loss goal significantly faster than the diet-only group (30 vs. 46.4 days; Halliday *et al.*, 2019). In studies with pair-fed rodents after bariatric or sham surgery, no difference in weight development was detected, but significant differences were found regarding metabolic or cardiovascular outcomes (Douros *et al.*, 2019; Barron *et al.*, 2020).

The beneficial effects of surgery compared to food restriction on glucose homeostasis were thoroughly studied in rodents. Pair-fed sham controls had a higher fasting glucose and lower insulin and incretin response after a mixed-meal tolerance test than VSG animals (Douros *et al.*, 2019). In the California Davis type-2 diabetes mellitus rat, a month after VSG surgery animals had decreased fasting plasma insulin, ghrelin, and lipid concentrations, as well as increased fasting plasma adiponectin independent of weight and after five months a higher amount of circulating bile concentrations (Cummings *et al.*, 2012). Moreover, β -cell islet transcription was significantly modified by the surgery independent of weight loss (Douros *et al.*, 2019). The surgery can improve the diabetic phenotype more than comparable dietary restrictions. However, the mechanisms behind this advantage are still largely unclear.

The faster stomach passage alters the composition of nutrients arriving in the small intestine impacting absorption, bile acid secretion, and the microbiome (Liu *et al.*, 2018a). This probably changes endocrine and paracrine signalling in the digestive system which, in turn, impacts the maintenance of the metabolic syndrome. In rats, both, VSG and RYGB led to similar accelerated gastric emptying rates compared to sham animals (Chambers *et al.*, 2014). Nutrient absorption in the intestine is altered by bariatric surgery. However, the mechanisms in RYGB and VSG appear to initially differ: while after RYGB a large part of the arriving glucose is consumed by a hyperplastic intestine, after VSG absorption seems delayed (in rats; Cavin *et al.*, 2016). More than a year after surgery in humans, a Danish study found accelerated absorption of glucose and proteins in both procedures (Svane *et al.*, 2019). Nevertheless, the delivery of a less digested, nutrient-rich diet to the intestine was proposed to be a crucial mediator of endocrine and metabolic rebalancing after bariatric surgery (Karra *et al.*, 2010).

The liver is a central organ of metabolism, involved in glucose, fat, and protein homeostasis. It was proposed as the major driver of improved peripheral glucose homeostasis after bariatric surgery. Bariatric surgery increases hepatic insulin sensitivity within a week in T2DM patients (Lim *et al.*, 2011). This is accompanied by a decrease of hepatic fat content and endogenous glucose production (Lim *et al.*, 2011; Immonen *et al.*, 2014). A study in mice showed a weight-independent decrease in the abundance of lipid droplets in the liver after VSG (Abu-Gazala *et al.*, 2018). The rate of production of TAG-rich lipoproteins from the liver is reduced after bariatric surgery and their catabolic clearance increased (Padilla *et al.*, 2014). An increase in bile acids induced by bariatric surgery leads to an upregulation of FGF21, a hepato- and adipokine that regulates metabolic processes in several tissues: it increases hepatic fatty acid breakdown while decreasing lipid synthesis and is a key regulator of glucose homeostasis and glycaemic control (Patton *et al.*, 2017). In adipose tissue, FGF21 specifically upregulates glucose uptake (Lewis *et al.*, 2020). The rapid effects of bariatric surgery on hepatic and whole-body glucose metabolism are profound and seemingly relate to changes in bile acid circulation.

Adipose tissue distribution, morphology, and physiology are greatly affected by bariatric surgery. Not only are ectopic WAT depots decreased, but overall adipose tissue inflammation is ameliorated (Labrecque *et al.*, 2017; Adami *et al.*, 2019). Bariatric surgery reduces adipocyte size in scWAT and leptin levels in parallel with systemic metabolic improvements (Eriksson-Hogling *et al.*, 2015; Camastra *et al.*, 2017; Billeter *et al.*, 2017). Bariatric surgery not only normalises expression levels of leptin and adiponectin, but also reduces those of PAI-1 and chemerin (Askarpour *et al.*, 2020). Nine weeks after RYGB in mice, adipose tissue shows a higher degree of browning and increased catabolic metabolism compared to weight-matched controls (Ben-Zvi *et al.*, 2018). Nine days after surgery, these effects are not yet detectable. However, fatty acid metabolism over is marginally decreased. A small study in 13 patients 4 weeks after RYGB raises the question whether the systemic metabolic improvements of T2DM occur independent of the normalisation of adipose tissue function (Katsogiannos *et al.*, 2019). Despite increasing interest in adipose tissue as a metabolic regulator, data on the immediate effects on the tissue after bariatric surgery are still scarce and understanding of the metabolic adaptations leading to sustained weight loss are lacking.

1.2.3.3 Side effects and long-term complications

Despite the many beneficial effects of bariatric surgery, these types of interventions come with some undesirable side effects. A common side effect of the gastrointestinal remodelling is the dumping syndrome, particularly after RYGB (Ramadan *et al.*, 2016). Malabsorption and gastrointestinal adaptations lead to deficits of vitamin D and minerals such as calcium potentially decreasing bone density and increasing fracture risk (Corbeels *et al.*, 2018). A very recent animal study demonstrated a

slightly higher degree of altered bone structure 8 weeks after RYGB compared to VSG (Corbeels *et al.*, 2020). Other common micronutrient deficiencies included B vitamins, especially B12, iron, and folate, all of which are involved in production and functionality of red blood cells. Consequently, patients may suffer from anaemia without sufficient supplementation (Kwon *et al.*, 2014; Weng *et al.*, 2015). Given that bariatric surgery is recommended in combination with lifestyle interventions, screening and surveillance of micronutritional status need to be included to avoid such deficits.

The rapid and massive weight loss as induced by bariatric surgery potentially leads to excess skin. This overhanging skin is often obstructive, hard to hygienically maintain, and decreases body satisfaction. Subsequently, body contouring procedures are performed (Chandawarkar, 2006). The desire for body contouring seems to disproportionally occur in females and is accompanied by a lower score in body satisfaction and higher score of depressive symptoms (Monpellier *et al.*, 2018). However, despite a dependence of amount of excess skin with amount of weight loss, higher total weight loss was associated with fewer depressive symptoms.

The psychological situation of patients after bariatric surgery is complicated. Though surgery-induced weight reduction is generally associated with improvements of anxiety and depression for several years (Rieber *et al.*, 2013; White *et al.*, 2015; Spirou *et al.*, 2020), the ongoing cognitive restraint to adhere to a controlled diet and body image issues can affect patients negatively (Geller *et al.*, 2020). For example, bariatric surgery patients showed higher deterioration of mental health compared to *pre*-surgical baseline and dietary control groups despite stable weight loss 10 years later (Canetti *et al.*, 2016). Psychosocial improvement apparently cannot be reliably sustained (Jumbe *et al.*, 2016; Spirou *et al.*, 2020). Additionally, the decrease of food as a hedonic stimulus or changes in the gut-brain axis and the central reward system after surgery increases the risk to develop substance abuse or alcohol abuse disorder in a subset of patients (King *et al.*, 2017; Orellana *et al.*, 2019). Moreover, relatively few data were reported for the time early *post*-surgery. In one study, a significant decrease in anxiety scores was found already 3 months after surgery and continued to be decreased for up to 12 months (Bužgová *et al.*, 2016). In a small cohort of severely obese adolescents undergoing bariatric surgery, psychopathological symptoms were improved on a group level 4 months *post*-surgery. However, a subgroup of patients presented a decline of psychosocial adjustment despite no prior abnormalities (Järvholm *et al.*, 2012). Consequently, more research is needed to potentially predict the subset of patients mentally suffering after bariatric surgery and a routine physiological follow-up early- and long-term may be needed.

1.3 Circadian clocks

Due to the rotation of the earth around its axis, all organisms had to adapt to a roughly 24-h cycle of environmental changes like light, temperature, humidity, or food availability. To anticipate these changes and orchestrate physiological functions accordingly, so-called circadian clocks (from Latin *circa* “around” and *dies* “day”) have developed in central and peripheral tissues. These clocks are sensitive to potent external time cues or *zeitgeber* (from German “time giver”) such as natural light which entrain the system to a 24-h rhythm. Without these *zeitgebers* circadian clocks can keep running with an endogenous rhythm of approx. 24 hours. This self-sustainment is one of three key characteristics marking a true circadian pacemaker. The two others are being entrainable by a *zeitgeber* and having temperature compensated kinetics. Clocks throughout the body are known to fulfil these criteria only to some extent and are therefore often referred to as “slave” or “secondary” clocks. They rely on synchronising input from a master pacemaker to keep time, which in mammals is located in the hypothalamic *suprachiasmatic nucleus* (SCN; Begemann *et al.*, 2020).

1.3.1 The mammalian molecular clock

Almost all types of cells contain an autonomous circadian clock. This is realised *via* interlocked transcriptional-translational feedback loops (TTFL; Fig. 1.3). In mammals, core clock components are the transcription factors Brain and muscle aryl hydrocarbon receptor nuclear translocator-like protein 1 (BMAL1, also called ARNTL), Circadian locomotor output cycles kaput (CLOCK) or its paralogue Neuronal PAS domain protein 2 (NPAS2), three Period variants (PER1, PER2, PER3), and two Cryptochrome proteins (CRY1, CRY2). The expression, activity, and degradation of these interacting factors is tightly regulated by interposed mechanisms (Takahashi, 2017; Vitaterna *et al.*, 2019).

The positive arm of the main TTFL involves a CLOCK:BMAL1 heterodimer binding to enhancer elements (*i.e.* E-box elements, a *CANNTG* DNA sequence) in the promotor region of the *Per* and *Cry* genes, as well as several clock-controlled genes (CCGs). Forming the negative arm, PER and CRY proteins accumulate during the light phase, heterodimerise, and translocate into the nucleus to inhibit CLOCK:BMAL1-mediated transcriptional activity, therefore, suppressing their own gene expression (Gekakis *et al.*, 1998; Kume *et al.*, 1999; Shearman *et al.*, 2000). With delay, casein kinases (*e.g.* CK1 δ/ϵ) interact with PER:CRY, a complex *post*-translational modification process that is a major determining factor of temporal stability and rhythm period length. In the nucleus, successively phosphorylated PER:CRY heterodimers are ubiquitinated and degraded, thus, allowing CLOCK:BMAL1 activity to increase again (Eide *et al.*, 2005; Meng *et al.*, 2008; Maier *et al.*, 2009; Zhou *et al.*, 2015).

To increase robustness of circadian rhythms, auxiliary loops exist. They involve D-site of albumin promoter binding protein (DBP), E4 binding protein 4 (E4BP4, also called NFIL3), Reverse-erythroblastosis virus alpha/beta nuclear receptor subfamily 1 members (REV-ERB α/β , also called NR1D1/NR1D2), and Retinoic acid related orphan receptors (RORs). While DBP and E4BP4 compete for enhancing and inhibiting, respectively, *e.g.* *Per* expression *via* targeting *D-box* promoter sequences, negative regulators REV-ERBs and positive regulators RORs compete for binding to ROR response elements (RORE) of, *e.g.*, *Bmal1* (Mitsui *et al.*, 2001; Preitner *et al.*, 2002). Consequently, these transcription factors can regulate and fine-tune the expression rates of clock genes or CCGs with the corresponding promoter sequences and stabilise overall clock rhythmicity.

Stabilising circadian clock processes are of notable importance given that environmental factors can induce expression of specific clock genes. Following signalling pathways from the retina, light impulses increase *Per* expression *via* cAMP response element-binding protein (CREB) and Mitogen-activated protein kinase (MAPK) interaction with a cAMP response element (Ding *et al.*, 1997; Travnickova-Bendova *et al.*, 2002). However, *Per1* and *Per2* show different degrees of light responsiveness; *Per3* appears to not play a substantial role in the mechanism (Albrecht *et al.*, 1997; Zylka *et al.*, 1998; Travnickova-Bendova *et al.*, 2002). While *Per1* mRNA expression is immediately induced, *Per2* mRNA expression follows with a delay. Additionally, light-sensitive activation of Protein kinase C alpha (PRKCA) increases *post*-translational stability of PER2 (Jakubcakova *et al.*, 2007). The additional stability of PER2 delays the offset of PER activity specifically at dusk and, consequently, the phase of the rhythms, whereas the acute induction of PER1 advances the phase specifically at dawn (Schwartz *et al.*, 2011). This mechanism plays a crucial role in resetting of light-sensitive circadian clocks and adapting to changes of this *zeitgeber*.

The integration of hormonal signals into the circadian clock is largely responsible for resetting clocks throughout the body to the metabolic status (Landgraf *et al.*, 2017; see chapter 1.3.3). The glucocorticoid (GC) receptor (GR), activated in response to *e.g.* stress and food stimuli, binds to the GC-responsive elements (GRE) in target gene promoters. Binding to GREs, for example, acutely induces *Per1* expression, thus, affecting circadian clock regulation (Yamamoto *et al.*, 2005; Reddy *et al.*, 2012). However, nutrients can also more directly impact on clock gene expression. Fatty acids activate Peroxisome proliferator-activated receptors (PPARs). These were shown to regulate *Bmal1* transcription positively and directly interact with *Per2* (Canaple *et al.*, 2006; Schmutz *et al.*, 2010). Moreover, the energy status affects activity of AMP-activated protein kinase (AMPK), which is involved in PER:CRY degradation, and Sirtuin 1 (SIRT1), which stimulates AMPK and inhibits CLOCK:BMAL1, *via* the AMP/ATP and NAD⁺/NADH balance, respectively (Um *et al.*, 2007; Asher *et al.*, 2008; Nakahata *et al.*, 2008; Lamia *et al.*, 2009).

The circadian transcription *via E-boxes, D-boxes, and RORE* by circadian clock genes and the *zeitgeber*-dependent resetting of molecular rhythms lead to tissue-specific circadian transcriptomes. Recent studies report around 40 – 80 % of mammalian protein-coding gene expression to undergo day to night (= diurnal) variation in selected tissues, thus, potentially being under circadian control (Zhang *et al.*, 2014; Mure *et al.*, 2018). How exactly the circadian output is regulated tissue-specifically remains largely elusive, but specific downstream regulators were proposed (Littleton *et al.*, 2020).

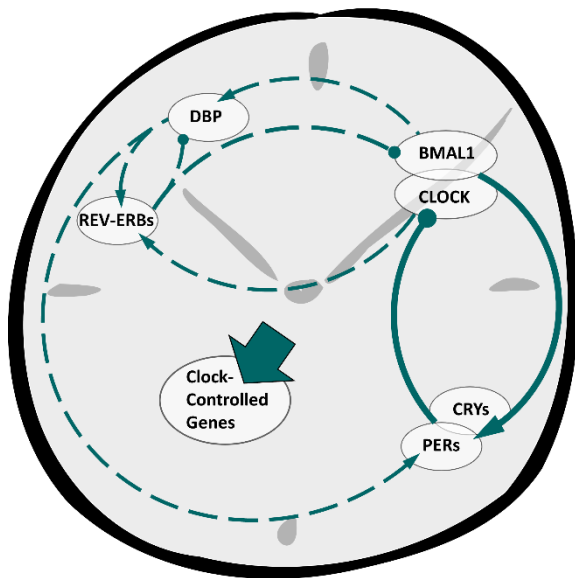


Figure 1.3: Simplified schematic presentation of the core molecular clock TTFL. In the main loop (solid lines) heterodimer CLOCK:BMAL1 induces expression of PER and CRY proteins, which as heterodimer PER:CRY in return repress the transcriptional activity of CLOCK:BMAL1, inhibiting their own expression. Transcription, translation, interaction, and degradation of the involved factors takes approx. 24 h. An auxiliary loop (dashed lines) stabilises the oscillation of the process. CLOCK:BMAL1 induce the expression of DBP and REV-ERBs. While DBP additionally induces production of PERs, REV-ERBs inhibit BMAL1 synthesis. DBP and REV-ERBs also regulate each other. Clock proteins regulate the expression of clock-controlled genes via specific E-box (CLOCK:BMAL1), D-box (DBP) and RORE (REV-ERBs) DNA-sequences. Lines with arrow heads represent induction, lines with circles inhibition of activity.

1.3.2 The circadian network

The molecular circadian clock based on the TTFL is conserved in nucleated cells across species. However, basically all cells, including *e.g.* red blood cells, exhibit circadian oscillations (O'Neill and Reddy, 2011). Synchronising these cellular clocks creates tissue pacemakers to anticipate and organise physiological functions such as digestion, immunity, or behaviour. To balance these functions in time, a master pacemaker synchronises tissue clocks across the whole body to an external *zeitgeber* establishing a hierarchical network (Fig. 1.4).

In mammals, the master pacemaker resides in the hypothalamic SCN and is mostly sensitive to the *zeitgeber* light. It receives this information from photoreceptors in the retina *via* the retinohypothalamic tract (RHT) and is under natural conditions robustly entrained to the current light situation (see chapter 1.3.3). Other input comes from the geniculohypothalamic tract, which also conveys visual information, and the Raphé nuclei, which relay signals from hypothalamic nuclei, the limbic system, and the brainstem (Rosenwasser and Turek, 2015). The afferent serotonergic connections *via* the Raphé nuclei are responsible for incorporating non-photic cues such as arousal into the SCN rhythm (Sumova *et al.*, 1996; Glass *et al.*, 2000). Furthermore, the arcuate nucleus (ARC)

integrates metabolic and homeostatic signals into SCN output; a way for endocrine feedback to modulate SCN activity (Yi *et al.*, 2006; Padilla *et al.*, 2019).

SCN efferents directly innervate predominately hypothalamic regions. These targets distribute the circadian timing signals to regulate activity/sleep-wake behaviour, hormonal axes and melatonin release, feeding behaviour, and body temperature. The prominent role of the SCN in regulating these body functions in a circadian manner became clear from surgical lesion studies or genetically disruption of the clock system within the SCN (Astiz *et al.*, 2019; Begemann *et al.*, 2020). Major targets of the SCN are the *pre*-autonomic neurons of the paraventricular nucleus. Subsequently, the SCN can regulate the sympathetic and parasympathetic output to peripheral organs (Buijs *et al.*, 2003). Moreover, the SCN innervates several hypothalamic regions of endocrine activity and brain regions impacting the endocrine system behaviourally (*e.g.* through feeding behaviour). Notably, the SCN regulates the hypothalamic-pituitary-adrenal (HPA) axis. Basal adrenal GC secretion displays pronounced circadian rhythmicity, peaking with the onset of activity. The SCN exerts its control over the HPA axis *via* the autonomic nervous system as well as by induction of corticotropin-releasing hormone secretion and subsequent release of adrenocorticotrophic hormone from the pituitary (ACTH; Neumann *et al.*, 2019). Circulating GCs are a major synchronisation signal: resetting, buffering, or inducing circadian rhythmicity in non-SCN tissues throughout the body (Balsalobre *et al.*, 2000; Sujino *et al.*, 2012; Pezük *et al.*, 2012). Thus, the SCN can control and fine-tune circadian physiological actions. However, peripheral rhythms can be sustained without a functional clock in the SCN by maintaining rhythmic behaviour driven by the light-dark cycle (so-called “light masking effect”) or by time-restricted feeding (Husse *et al.*, 2014; Kolbe *et al.*, 2019).

In the periphery, circadian clocks adjust tissue activities such as metabolic homeostasis, immunity, and reproduction (Richards and Gumz, 2012). *In vitro*, without SCN input and in constant conditions, most non-SCN central oscillators lose rhythmicity after few cycles indicating a strong lack of self-sustainability (Begemann *et al.*, 2020), while peripheral tissue clock rhythms often persist for several cycles (Yamazaki *et al.*, 2000; Yoo *et al.*, 2004; Molyneux *et al.*, 2008). Tissue-specific ablation of the circadian clock machinery helps to clarify the role of such local circadian input. For example, the adrenal clock was deemed dispensable for the generation of normal corticosterone rhythms (Dumbell *et al.*, 2016). However, under a short unnatural light-dark (LD) cycle (*i.e.* 3.5-h-light/3.5-h-dark) the adrenal clock is needed for stabilisation of GC rhythms (Engeland *et al.*, 2018). The liver clock is required for hepatic and systemic glucose homeostasis (Lamia *et al.*, 2008). Recently, it was shown that only about 10 % of the liver rhythmic transcriptome depends on the liver clock, questioning the degree of its independence (Koronowski *et al.*, 2019). Interestingly, disruption of the adipocyte clock affects plasma concentrations of polyunsaturated fatty acids, subsequently changing the feedback to hypothalamic feeding centres and time-dependent appetite regulation (Paschos *et al.*, 2012).

1.3.3 Tissue-specific entrainment to *zeitgebers*

The phases of clock gene expression rhythms in different peripheral tissues do not match with each other nor with the central pacemaker. This means that tissue-specific communication routes with the SCN and with entrainment factors apply. Peripheral clocks integrate environmental and systemic signals into rhythmic baseline activities to better adapt tissue-specific functions to environmental demands. Consequently, they need to be sensitive to another set of *zeitgebers* than the SCN.

The SCN is entrained primarily by light. Melanopsin-expressing intrinsically photosensitive retinal ganglion cells (ipRGCs) monosynaptically project to the SCN *via* the RHT. The blue-light activated melanopsin conveys gross changes of environmental light. Nevertheless, rods and cones transmitting information about the current light pattern also contribute to SCN entrainment and downstream regulation (Perez-Leon *et al.*, 2006; Bonmati-Carrion *et al.*, 2017; Masís-Vargas *et al.*, 2020). The SCN and SCN-driven locomotor activity robustly entrain to LD cycles between 21 – 28 h when undisturbed (Aton *et al.*, 2004; West *et al.*, 2017; Heyde and Oster, 2019). Though other *zeitgebers* like food intake or arousal were shown to modulate the entrained SCN output, when in conflict the light input outweighs other timing signals (Damiola *et al.*, 2000; Heyde and Oster, 2019). Moreover, SCN rhythmicity is not affected by adrenalectomy and a lack of GC rhythms in contrast to many other clocks (Segall *et al.*, 2006; Sujino *et al.*, 2012; Soták *et al.*, 2016). Of note, ipRGCs do not exclusively project to the SCN (Beier *et al.*, 2020). The perihabenular region was shown to receive ipRGC input that impacts intrinsic clock gene expression and mood regulation (Fernandez *et al.*, 2018). This suggests the existence of SCN-independent, light-sensitive circadian clocks in the brain.

Another very potent *zeitgeber* is food. An SCN-independent, food-entrainable oscillator was suggested due to the phenomenon of food anticipatory activity in SCN-lesioned animals after time-restricted feeding (Mistlberger, 2009). A single central pacemaker for this behaviour was not found yet. However, several mechanisms of entrainment of different clocks to metabolic signals are described. While the SCN itself seems largely resistant to metabolic signals, other central clocks are not (Damiola *et al.*, 2000; Olivo *et al.*, 2014; Begemann *et al.*, 2020). Specifically, clocks in feeding centres are affected by metabolic signalling (Ubaldo-Reyes *et al.*, 2017; Wang *et al.*, 2017). However, ghrelin was able to phase advance SCN-driven locomotor activity after fasting (Yannielli *et al.*, 2007). Additionally, leptin was shown to indirectly normalise SCN function of leptin-deficient mice (Grosbellet *et al.*, 2015). These studies highlight the routes for subtle adjustments in master pacemaker function by the metabolic status, probably mediated by SCN-interplay with metabolic regulatory nuclei such as the ARC (Fig. 1.4).

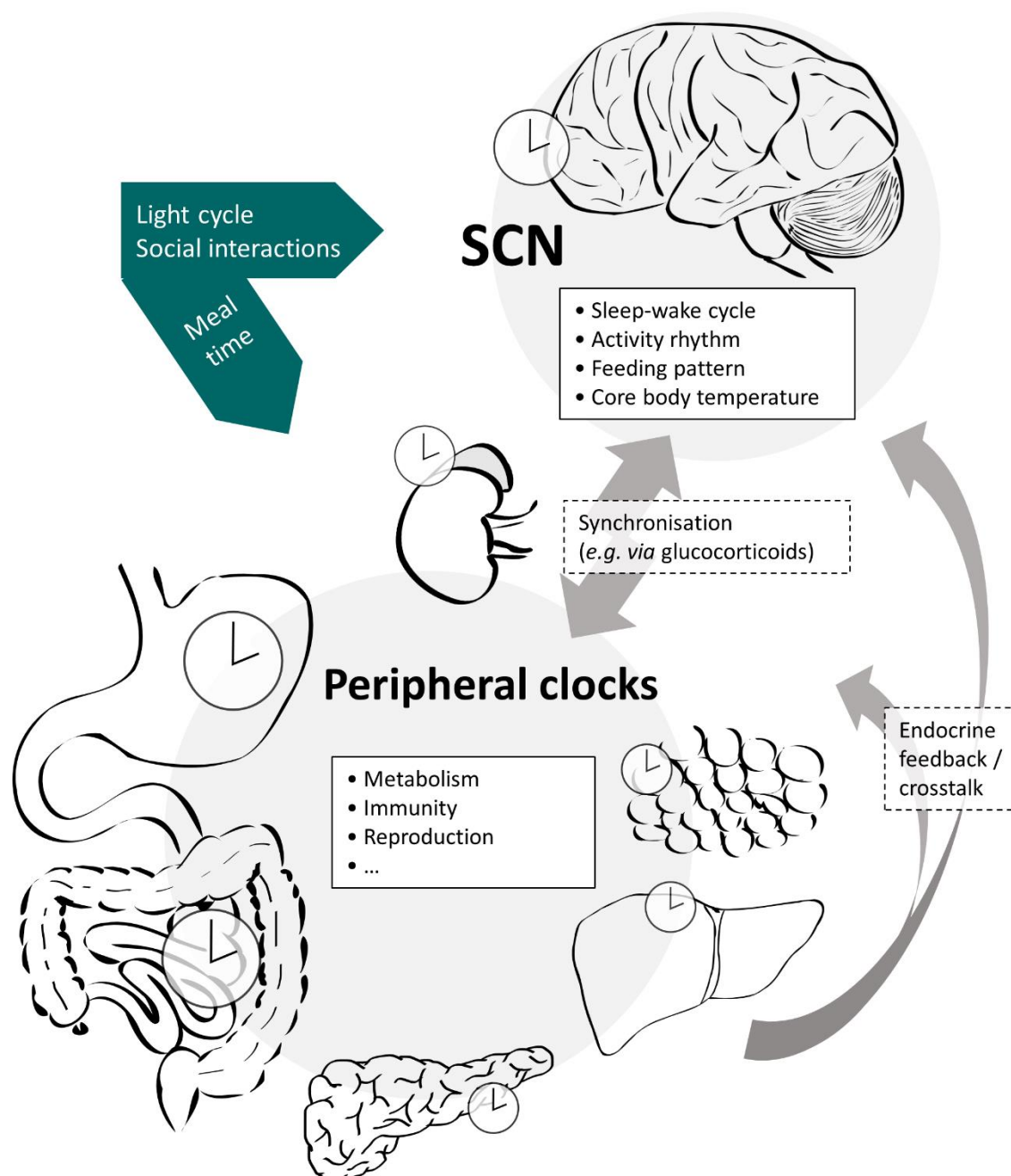


Figure 1.4: Organisation of the circadian network and inter-clock communication. The SCN entrains to the 24-h cycle of light and dark. As a master pacemaker it synchronises other central and peripheral clocks via neuronal projections and regulation of rhythmic glucocorticoid secretion. Zeitgeber like arousal also affect central clocks and the associated signalling can be incorporated into the SCN output. Central clocks regulate systemic functions such as sleep-wake cycle, activity, feeding patterns or core body temperature. Local clocks in the periphery modulate peripheral and tissue metabolism, immune responses, reproduction, and other tissue-specific functions. Secreted factors such as metabolic hormones and nutrients are involved in feedback communication with central clocks and the SCN as well as in crosstalk between peripheral clocks.

Peripheral clocks are particularly responsive to metabolic signals. Notably, although about 60 % of the liver transcriptome synchronises to GCs (Reddy *et al.*, 2007), feeding time seems to be a more dominant *zeitgeber* for the liver clock and its rhythmic transcriptome than GCs (Vollmers *et al.*, 2009; Sujino *et al.*, 2012). Day-time restricted feeding uncouples the liver clock gene expression from the SCN in mice (Damiola *et al.*, 2000). This is mediated by endocrine factors that directly vary in response to the feeding-fasting cycle. The liver clock is sensitive to resetting by insulin and glucagon (Tahara *et al.*, 2011; Chaves *et al.*, 2014; Sun *et al.*, 2015), the incretins GLP-1 and oxyntomodulin (Ando *et al.*, 2013; Landgraf *et al.*, 2015), and ghrelin (Wang *et al.*, 2018).

Contrary to the data from liver, GCs appear to be a stronger *zeitgeber* for WAT clock gene expression than food intake (Su *et al.*, 2016; Soták *et al.*, 2016). Nevertheless, daytime-restricted feeding can phase-shift adipose tissue clock gene expression in parallel to corticosterone rhythms (Zvonic *et al.*, 2006). Rhythmic expression of metabolic genes, however, is lost without a diurnal feeding cycle independent of GC rhythms (Su *et al.*, 2016). Moreover, in parallel to the different metabolic and pathophysiological functions (see chapter 1.1.3), different WAT depots show high variation in rhythmicity of metabolic genes, whereas core clock expression is consistent between depots (van der Spek *et al.*, 2018). This hints at tissue-specific regulation of transcription downstream of the core clock in WAT by metabolic stimuli.

1.3.4 Circadian regulation of metabolism

Circadian clocks cannot only be entrained by metabolic signals, but one of the main functions of the circadian system is to organise energy metabolism according to time-dependent changes of environmental conditions. Global genetic disruption of the molecular clock can lead to dampened feeding rhythms and an increased risk for obesity (Turek *et al.*, 2005; Barclay *et al.*, 2013; Kettner *et al.*, 2015). Similarly, single nucleotide polymorphisms in human clock genes are associated with altered metabolism (Valladares *et al.*, 2015; Lopez-Minguez *et al.*, 2016). For example, the *CLOCK* gene variant *rs1801260* has repeatedly been associated with increased risk of obesity (Scott *et al.*, 2008; Garaulet *et al.*, 2011; Ruiz-Lozano *et al.*, 2016a).

Lesioning of the SCN and close retinal projections abolishes diurnal variation in food intake, hormonal rhythms, and increased hepatic insulin resistance (Stoynev *et al.*, 1982; Kalsbeek *et al.*, 2001; Coomans *et al.*, 2013). Genetic disruption of circadian clock activity exclusively in the SCN leads to arrhythmic feeding behaviour in constant darkness (DD; Kolbe *et al.*, 2019). Despite retained behavioural rhythmicity in LD, certain metabolic genes are dampened in the periphery like *Acat1* (Acetyl-CoA acetyltransferase) in pancreas and *Pepck1* (Phosphoenolpyruvate carboxykinase) in the liver (Kolbe *et al.*, 2019), thus, these depend specifically on SCN pacemaker input. Under constant conditions

(enforced posture, constant dim light, hourly meals, and sleep deprivation) approx. 15 % of human metabolites in plasma and saliva still exhibited a diurnal pattern, confirming a rhythmic regulation of metabolic pathways independent of sleep or feeding (Dallmann *et al.*, 2012).

As mentioned before, the SCN projects to several hypothalamic brain regions, hereby regulating behavioural rhythms including food intake timing. Among these regions are homeostatic centres like the ARC, the dorso- and the ventromedial hypothalamus (Kalsbeek *et al.*, 1993; Méndez-Hernández *et al.*, 2020). Leptin receptor-expressing neurons in the ARC seem to be essential for feeding rhythm generation. A pharmacological disruption does not only result in hyperphagia but also rhythm dampening in LD and arrhythmicity in DD (Li *et al.*, 2012). Ablation of a specific neurotransmitter-expressing subset of these neurons reproduces the disrupted circadian feeding patterns (Wiater *et al.*, 2011). This neuronal subpopulation was proposed to be activated directly by SCN efferents and SCN-driven GCs (Shimizu *et al.*, 2008; Herrera-Moro Chao *et al.*, 2016).

The SCN can synchronise metabolic organs directly *via* the autonomic nervous system. Indirectly, GC rhythms and feeding cycle-associated metabolic factors modulate metabolic functions. As a result, the concentration of many metabolically active hormones and metabolites cycle along the day in parallel to rhythmic food intake (Landgraf *et al.*, 2017; Skene *et al.*, 2018). Still, clock-controlled baseline mRNA expression or protein secretion are reported for cholestekinin, gastrin (Pasley *et al.*, 1987), proglucagon/GLP-1 (Gil-Lozano *et al.*, 2014), ghrelin (Laermans *et al.*, 2015), insulin (La Fleur *et al.*, 2001), and leptin (Kalsbeek *et al.*, 2001; Kettner *et al.*, 2015; Taira *et al.*, 2019). Moreover, mechanisms to enact a hormone's actions may be under circadian control: for example, leptin's blood-brain barrier transport is rhythmically regulated (Pan and Kastin, 2001) and the gastrin receptor is rhythmically expressed, even in fasted rats (Rubin *et al.*, 1988). Also, GLP-1 and insulin actions underly a circadian component (Marcheva *et al.*, 2010; Shi *et al.*, 2013; Gil-Lozano *et al.*, 2014; Biancolin *et al.*, 2020). Summarising, both, the concentration of circulating (metabolic) hormones as well as the magnitude of their effects can be modulated by the circadian clock.

Local clock gene activity induces the expression of CCGs. Interestingly, the overall rhythmic transcriptome is highly tissue-specific and mirrors an organ's role in physiology (Storch *et al.*, 2002; Zhang *et al.*, 2014). To what extent these diurnal oscillations of genes are a result of rhythmic behaviour, of rhythmic systemic signals such as hormones, or direct regulation by (local) clock genes needs further exploration. For example, though the circadian clock in WAT is not strongly affected by feeding cues, the oscillations of many metabolic genes in this tissue are lost without a diurnal feeding rhythm (Su *et al.*, 2016). Nevertheless, specific clock proteins were shown to regulate transcription of metabolic pathways. CLOCK:BMAL1 mediates leptin expression in adipose tissue (Kettner *et al.*, 2015). The pancreatic β -cell clock (*i.e.* *Bmal1/Clock* expression) is necessary for maintenance of glucose

sensitivity and insulin secretion (Marcheva *et al.*, 2010). A liver-specific knock-out of *Bmal1* in mice disrupts hepatic glucose export into the circulation through a constant low expression of GLUT2 (Glucose transporter 2; Lamia *et al.*, 2008). CRYs were shown to block glucagon-mediated gluconeogenic gene expression in the liver, thereby reducing fasting glucose production (Zhang *et al.*, 2010). The transcriptional activity of the lipid metabolism regulator PPAR γ is modulated by PER2 (Schmutz *et al.*, 2010; Grimaldi *et al.*, 2010). REV-ERB α participates in the hepatic control of sterol regulatory element-binding protein activity, cholesterol/bile acid metabolism (Le Martelot *et al.*, 2009) as well as carbohydrate and overall lipid metabolism (Delezie *et al.*, 2012). Moreover, CLOCK was shown to transactivate expression of *Lpl* (Lipoprotein lipase; Delezie *et al.*, 2012). Multiple transcription factors can regulate the expression of the hepato- and adipokine *Fgf21* including REV-ERB, ROR, E4BP4, and PPARs (Erickson and Moreau, 2017). Various key genes of metabolic processes contain *E-boxes*, *D-boxes* or *RORE* in their respective promotor regions (Kang *et al.*, 2007; Rey *et al.*, 2011; Cho *et al.*, 2012; Yoshitane *et al.*, 2019). BMAL1 induces expression of *e.g.* *Elovl6* (Elongation of long-chain fatty acids family member 6) and *Scd1* (Stearoyl-CoA desaturase 1), both key enzymes of fatty acid metabolism (Paschos *et al.*, 2012).

All in all, metabolism is rhythmically organised centrally and peripherally. Though circadian clocks may directly regulate only a subset of these functions, the SCN-induced feeding rhythm is a major pacemaker for rhythmic energy metabolism. Besides, the local clock machinery modulates metabolic pathways and peripheral clock disruption increases the risk of metabolic diseases.

1.4 Metabolic interventions and the circadian clock

The circadian clock regulates metabolism on different levels while at the same time it can be reset by metabolic cues. Subsequently, metabolic diseases can be cause and consequence of circadian disruption. Given such a tight interplay between these two systems, metabolic interventions are bound to affect and be affected by the circadian system.

1.4.1 Effects of a hypercaloric diet

A hypercaloric high-fat diet (HFD) reliably induces obesity and symptoms of the metabolic syndrome in animals and humans (Wang and Liao, 2012). Development of metabolic disturbances under these conditions is preceded and accompanied by circadian disruptions. A dietary switch to HFD induces dampening of behavioural rhythms and a locomotor period lengthening in DD within a week of exposure (Kohsaka *et al.*, 2007; Mendoza *et al.*, 2008b; Pendergast *et al.*, 2013). The rapid changes are assumed to happen predominately *via* dysregulation of feeding and reward centres rather than the

SCN (Blancas-Velazquez *et al.*, 2017; Pickel and Sung, 2020). The master clock remains unresponsive acutely (Pendergast *et al.*, 2013). In a recent study, it was suggested that the SCN-dopamine system is substantially involved in the metabolic modulation after HFD (Luo *et al.*, 2018).

Peripherally, HFD disrupts tissue rhythmicity and synchrony. Particularly the liver and WAT clocks are dampened by hypercaloric diet (Kohsaka *et al.*, 2007; Pendergast *et al.*, 2013; Prasai *et al.*, 2013), and liver and spleen clocks are phase-shifted (Pendergast *et al.*, 2013). Similarly, a sugar enriched HFD shifts clocks in skeletal muscle and brown adipose tissue to different degrees (de Goede *et al.*, 2018a). Additionally, the temporal patterns of plasma levels of glucose, insulin, corticosterone, FFAs, and several adipokines are altered (Kohsaka *et al.*, 2007; Cano *et al.*, 2009). Notably, the diurnal pattern of leptin becomes arrhythmic and FFAs are shifted to an increased expression during the active phase (Kohsaka *et al.*, 2007). Overall, the circadian metabolome is reorganised in a tissue-specific manner with a loss of coherence among tissues (Abbondante *et al.*, 2016; Dyar *et al.*, 2018). Such disruptive effect of HFD on peripheral rhythms was also described in humans (Pivovarovova *et al.*, 2015; Budai *et al.*, 2019). In conclusion, a diet associated with Western lifestyle high in fat and sugar leads to an internal desynchronisation compared to healthy controls. Interestingly, diet reversal back to chow quickly normalises behavioural rhythms, phase regulation of the liver clock, and liver transcriptome rhythms in mice (Eckel-Mahan *et al.*, 2013; Branecky *et al.*, 2015).

The liver is adapting rapidly to the metabolic environment and liver clock function was deemed necessary for glycaemic homeostasis. Thus, the disruptive nature of HFD on liver rhythms plays a crucial role in the development of diet-induced obesity and T2DM. Dampening of liver clock genes parallels dampening of lipogenic gene expression and circulating insulin levels especially during the late active phase (Honma *et al.*, 2016). Degradation of the clock protein CRY1 by autophagy is accelerated by HFD, limiting its time-dependent gluconeogenic control and, thus, contributing to hyperglycaemia (Toledo *et al.*, 2018). Inhibited recruitment of CLOCK:BMAL1 to target genes and increased rhythmic PPAR activity by HFD induces a widespread remodelling of hepatic gene oscillations (Eckel-Mahan *et al.*, 2013; Guan *et al.*, 2018). Interestingly, a ketogenic diet (high in fat, very low in carbohydrates) has rather opposite effects (Tognini *et al.*, 2017). Consequently, a hypercaloric diet disrupts the liver clock and other peripheral rhythms, not the disproportionally increased lipid consumption *per se*.

1.4.2 Effects of meal scheduling

A hypercaloric diet dampens diurnal feeding rhythms by increasing rest phase food intake specifically. Hence, it was found that simply restricting the food availability to the rest phase was already sufficient to disturb metabolic homeostasis. Daytime or rest phase restriction of food intake uncouples

peripheral oscillators from the central pacemaker SCN and disrupts internal synchrony (Damiola *et al.*, 2000; Stokkan *et al.*, 2001; Hara *et al.*, 2001). Of note, the SCN and SCN-dependent GC signalling seems to counteract such phase-shifting effects of mistimed feeding to a certain degree (Le Minh *et al.*, 2001; Saini *et al.*, 2013). Nevertheless, desynchrony is a consequence of mistimed feeding and was proposed to ameliorate the development of the metabolic syndrome. Already after one week, mice restricted to HFD during the rest phase gain more weight and show increased leptin resistance compared to *ad-libitum* controls (Yasumoto *et al.*, 2016; Oishi and Hashimoto, 2018). Moreover, even prolonged standard diet during the rest phase leads to phenotypes of the metabolic syndrome and T2DM in mice (Mukherji *et al.*, 2015b; Mukherji *et al.*, 2015a). Forced activity during the natural rest phase can also shift feeding patterns towards the rest phase and subsequently disrupt glucose tolerance and expression of insulin sensitivity genes (Salgado-Delgado *et al.*, 2008; Marti *et al.*, 2016).

The negative effects of rest phase food intake observed in animals are mirrored in human shift and night work (Reid and Abbott, 2015; Torquati *et al.*, 2019; Pickel and Sung, 2020). The human peripheral circadian system is differently regulated by early or late eating, whereas central rhythms and markers are sustained, confirming a selectively peripheral food timing sensitivity like in animals (Wehrens *et al.*, 2017). In line with this, late lunch, big lunch, and nighttime consumption are associated with the development of obesity and metabolic syndrome (Berg *et al.*, 2009; Bo *et al.*, 2014; Kutsuma *et al.*, 2014; Yoshida *et al.*, 2018). Interestingly, though restricting food intake to few hours a day is beneficial for metabolic health in humans (see chapter 1.2.1), skipping of breakfast or lunch is not (Berg *et al.*, 2009; Kutsuma *et al.*, 2014; Ogata *et al.*, 2019). High caloric intake in humans during the late evening or night is disruptive like rest phase feeding in mice, while intake during the light/early active hours is metabolically preferred. Circadian clocks and peripheral synchrony likely modulate this effect.

Given the adverse effects of rest phase food intake, restricting the diet to the natural active phase was investigated as a strategy to counter circadian and metabolic disruption. As previously mentioned, early lunch increases weight loss efficiency (Garaulet *et al.*, 2013). Moreover, a high-calorie breakfast combined with a small dinner reduces weight and the diabetic phenotype (Jakubowicz *et al.*, 2013; Jakubowicz *et al.*, 2015). In mice, standard chow diet restricted to the active phase barely affects liver clock gene expression compared to the natural *ad-libitum* rhythm (Patel *et al.*, 2016; Greenwell *et al.*, 2019), but restricting the food to the active phase of HFD-fed (obese) mice rescues the dampened liver clock gene expression and improves metabolic regulation (Hatori *et al.*, 2012; Chaix *et al.*, 2014). In mice under constant light (LL), a condition of circadian disruption, the introduction of restricted feeding resynchronises rhythmic genes in liver and WAT (Yamamuro *et al.*, 2020).

Caloric restriction in rodents leads to self-imposed time-restricted feeding (Acosta-Rodríguez *et al.*, 2017). Consequently, timing of the reduced meal affects the circadian system in a similar direction, but

active phase caloric restriction shows stronger benefits for metabolic homeostasis (Velingkaar *et al.*, 2020) and increases the amplitude of liver clock mRNA expression rhythms even in standard diet; an effect absent in clock-deficient mice (Patel *et al.*, 2016). Moreover, caloric restriction reprograms the rhythmic transcriptome of the liver compared to *ad-libitum* feeding with, *e.g.*, lipid pathways gaining rhythmicity (Makwana *et al.*, 2019). Interestingly, though the SCN is resistant to general rest phase food restriction, a mistimed and hypocaloric diet can affect the master clock and its acute light response (Mendoza *et al.*, 2005; Mendoza *et al.*, 2007). The potential of caloric restriction to reset the SCN clock was also shown when meals were given in an ultradian pattern (more than one cycle per day; Mendoza *et al.*, 2008a). Isocaloric ultradian feeding does not shift the master pacemaker (Sen *et al.*, 2017), peripheral rhythms are generally dampened by irregular ultradian feeding patterns (Su *et al.*, 2016; Sen *et al.*, 2017; de Goede *et al.*, 2018b).

1.4.3 Effects of bariatric surgery

Drastic changes in feeding patterns and metabolic homeostasis (*e.g.* meal scheduling, caloric restriction) can influence the circadian network on different levels. In line with this, the circadian system is modulated by a radical metabolic intervention like bariatric surgery. It was shown that bariatric surgery modifies patients' behaviour to avoid circadian disruptions. Sleep disturbances due to obesity-related sleep apnoea are reduced, improving sleep quality profoundly (Dixon *et al.*, 2001). Patients report less night-time hunger (Colles *et al.*, 2008) and food preferences are shifted towards less calorie-dense food in mice and humans, avoiding the dampening effect of HFD (Miras and le Roux, 2010; Wilson-Pérez *et al.*, 2013b; Kapoor *et al.*, 2017).

Data on circadian gene expression after bariatric surgery or massive weight loss is rare. On a molecular level in mice, neither RYGB nor weight-matched dieting affects enrichment of genes diurnally expressed under HFD in the liver. However, circadian clock gene expression is modulated nine weeks *post-surgery*, and these changes seem to correspond to human data (Ben-Zvi *et al.*, 2018). Another type of bypass surgery in rats increases hepatic core clock proteins PER2 and CRY1 (Kim *et al.*, 2015). Moreover, the REV-ERB α diurnal expression pattern in adipose tissue is affected by RYGB in Goto-Kakizaki rats (Zhang *et al.*, 2013).

It is very likely that bariatric surgery and the circadian system interact in achieving metabolic balance and weight loss. However, Arble *et al.* suggest in their study that the circadian system is not necessary for VSG to improve metabolism (2015). Importantly, this does not exclude a possible role of the circadian network in influencing surgical outcomes. Late-eating, for example, is associated with less successful weight loss therapies including bariatric surgery (Garaulet *et al.*, 2013; Ruiz-Lozano *et al.*, 2016b).

1.5 Aims and main hypothesis

Which individual differences affect the outcomes of metabolic interventions such as bariatric surgery is still poorly understood. A diverse set of contributing factors besides simple energy intake are associated with the development of obesity and will subsequently affect weight loss therapies. Given the mutual interaction between circadian clocks and the metabolic system, the main aim of this PhD project was to investigate to what extent VSG in mice can reset or modulate circadian rhythms on different levels of the hierarchical clock network:

1. Effect on intrinsic circadian behaviour and the central pacemaker
2. Effect on peripheral tissue clock rhythmicity
3. Effect on rhythmic regulation of WAT metabolism

I hypothesised that bariatric surgery would lead to a tissue-specific reprogramming of peripheral circadian function in parallel to adaptations of feeding behaviour. Furthermore, a second aim was to expand on the dimensions of behavioural adaptations by studying potentially stress-related anxiety during and after the metabolic and circadian restructuring induced by bariatric surgery. To address these questions, mice were subjected to VSG after obtaining a diet-induced obese phenotype. Intrinsic behaviour was recorded under constant darkness conditions *pre-* and *post-surgery*. Following an understanding of *post-surgical* weight loss development, physiology and behaviour were studied in detail during an early (*i.e.* nine days) and a late (*i.e.* four weeks) time period after surgery.

2 Material and Methods

2.1 Animal experiments

2.1.1 Housing and diets

All animal experiments were carried out in accordance with the German Law for Animal Protection and FELASA's guidelines for animal research and approved by the ethical committee of the Ministry of Energy Change, Rural Areas & Consumer Protection (MELUR) of the State of Schleswig-Holstein (licences 4(76-6/17), 4(99-11/18)).

Male mice (C57BL/6JRj, PER2::LUC/C57BL/6J) were used for the experiments. C57BL/6JRj were bred at and ordered from the mouse breeding facility Janvier Labs (Le Genest-Saint-Isle, France). PER2::LUC/C57BL/6J were bred at the animal facility of the University of Lübeck. These mice were exclusively used for bioluminescence recordings of specific tissues. For more details on the strain see chapter “2.1.5 PER2::LUC breeding and genotyping”. Mice were housed in type-2 microisolation cages (long, open, 530 cm³) in separate cabinet racks for up to 12 cages. Racks and rooms were artificially ventilated (21 – 23 °C, 55 – 65 % humidity). Mice were kept under a 12-hour light: 12-hour dark cycle (LD12:12; light at ca. 300 lux). For food intake and activity rhythm evaluation, mice were maintained under DD at least two weeks before surgery (Fig. 2.1 A). Mice were group-housed (3 – 5 per cage) until one week before the start of *pre*-surgical experiments or two weeks before surgery.

Water and food were accessible *ad libitum*. Mice were received with 3 – 4 weeks after birth and diet was immediately changed to high-fat diet (HFD, D12492i, Research Diets, New Brunswick, US; 60 % energy from fat). Three days before surgery, mice received liquid diet (LiD, Nutricia Fortimel Compact vanilla flavour, Danone, Paris, France; 2.4 kcal/ml) as a choice. HFD was removed two days *prior* to surgery. Mice were fasted overnight before surgery. After surgery mice received LiD exclusively for two days, a choice of LiD and HFD on the third day and only HFD for the remaining experimental period. Weight was recorded weekly until day of surgery. After surgery, mice were weighted daily until day 7, on day 10, on day 12, weekly again from 14 days *post*-surgery onwards, and before sacrifice. Weight measurement and handling of mice in DD was conducted under dim red light. Sham control animals that did not regain weight were excluded from analysis (n = 2).

2.1.2 Activity and food intake measurement

Activity was recorded with custom-made infrared detectors positioned above the cage grid. Activity was plotted in 5-min bin actograms. For analysis, activity in 5-min bins and 15-min bins was used for calculation of periodicity (by χ^2 periodogram analysis with period lengths between 20 and 26 h, Fig. 2.1 B) with ClockLab data acquisition software (ActiMetrics, Wilmette, US). A running period of 5 days

was calculated with high-resolution 5-min bin periods from one week *prior* surgery to 17 days *post*-surgery. Moreover, onsets and total activity were assessed from activity in 15-min bins. Amplitude of the determined periods from the 15-min bin periodogram (corrected by χ^2 value of that period with $p < 0.0001$) and amplitude of the rhythm with the determined period were used as output factors to evaluate the strength of rhythmicity.

Feeding events were recorded using automated food monitors with a separate food hopper (BioDAQ, Research Diets). Feeding bouts ≥ 0.01 g and meals (≥ 0.02 g separated by ≥ 300 s) were exported in 15-min intervals with BioDAQ Data Viewer (Research Diets) and plotted with ActogramJ (Schmid *et al.*, 2011). Applying the activity onsets determined with ClockLab, meal frequency and meal intake of active and rest phase were determined manually. For rhythm analysis, feeding bout and meal frequency data were smoothened using a 3-hour running average. Daily profiles of the smoothened data were then calculated with ActogramJ. Feeding offset ($= 0^\circ$) was defined as a decline in feeding events to below 50 % of the daily average for more than 3 h. This representation of feeding bout and meal activity was plotted in 1-hour bins and analysed with GraphPad Prism8 (GraphPad, San Diego, US). Amplitudes were determined from curve fits of a sine wave with non-zero baseline fixed to a wavelength of 360° . Mice that did not use the food hopper were excluded from further analysis ($n = 5$).

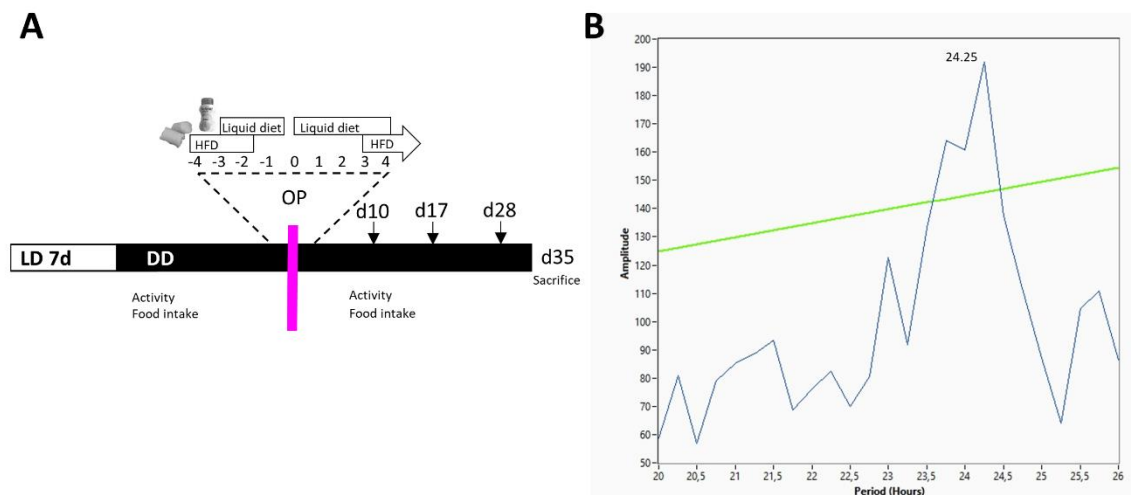


Figure 2.1: Timeline of DD experiments and locomotor period determination with ClockLab. [A] Mice were housed under LD upon arrival and released into DD one week prior pre-surgical recordings. Activity and food intake were measured. Interval borders were day 3, 10, and 17 (food intake and activity rhythms) or 28 (weight) post-surgery. Mice were sacrificed 35 days after surgery. [B] Example periodogram from ClockLab giving a significant period (here 24.25) and corresponding amplitude. Green line indicates a χ^2 significance threshold with $p < 0.0001$.

2.1.3 Bariatric surgery protocol

Bariatric surgery was performed on mice with diet-induced obesity (DIO) weighing at least 35 g before fasting as previously reported (Chambers *et al.*, 2013). Mice were anaesthetised with isoflurane in oxygen (5 % for induction, 1.5 – 2.5 % throughout the surgery), subcutaneously treated for analgesia with 1 mg/kg meloxicam (Metacam 2mg/ml solution for injections, Boehringer Ingelheim) and for antibiosis with 8 mg/kg gentamicin (Gentamicin-ratiopharm 40 mg/ml SF, Ratiopharm) in 1 ml NaCl (against dehydration). Surgeries were performed on a 37 °C-warmed surgery table (DSx Vented Warming Table, VetEquip, Pleasanton, US).



Figure 2.2: Crucial steps of VSG surgery. [A] Opening of abdominal cavity. [B-C] Isolation of the stomach from surrounding tissue and ligaments. [D] Flattening of the stomach. [E-F] Positioning of the stomach between the jaws of stapler. [G] A sleeve of 2-3 mm was kept. [H] Remaining fundus (grey part) was ligated. [I] Wound was closed.

All materials for the surgery were sterilised before usage either by autoclaving or during a surgical session with a hot bead steriliser (18000-45, FST Fine Science Tools, Heidelberg, Germany). The abdominal cavity was opened with a scalpel (#11 blade) and fine scissors for skin and peritoneum, respectively (Fig. 2.2 A). The stomach was isolated from surrounding tissue and major ligaments were cut (Fig. 2.2 B-C). After flattening with a cotton bud, the stomach was positioned between the jaws of

a 45-mm vascular/thin-tissue stapler (Fig. 2.2 D-F; Endopath ETS-Flex 45, Ethicon, Sommersville, US) with 2.5-mm loads (Endopath ETS45 2.5mm Reloads TR45W, Ethicon). A sleeve of 2 – 3 mm was left open as connection between esophagus and duodenum after resection or blockage of ca. 80 % of the stomach (Fig. 2.2 G). The remaining fundus was ligated with 4-0 silk suture material (Fig. 2.2 H; Perma-Hand EH6722, Ethicon) and the wound was closed with a rapidly absorbable 5-0 suture (Fig. 2.2 I; Coated Vicryl Rapide MPVR4930, Ethicon). During sham surgery the stomach was positioned between large forceps (without using the teeth) and exposed to 15 – 20 seconds of mechanical pressure. Mice were kept in a 37°C-warmed and ventilated wake-up chamber (MediHEAT TM, Peco Service, Cumbria, UK). Analgesic treatment was repeated daily until four days *post-surgery*.

2.1.4 Social interaction test with three-chamber paradigm

The social interaction test was performed according to Kuti and Page (2011). Briefly, all mice were continuously housed in closed racks in the room of testing. The arena was 60 x 30 x 30 cm in dimensions. Each chamber was 30 x 20 cm and separated by a wall with a gate of 7.5 x 7.5 cm. Stimulus tubes were ca. 10 cm in diameter, 20 cm high and perforated with several holes of ca. 1 cm in diameter. A source of light and a camera were positioned directly above the arena. Light intensity in the middle chamber was ca. 450 lux. Three age-matched stimulus mice were trained to stay calm in the tubes for 10 min every day for a week before testing. A coloured cap was put on top of the tubes to keep mice for climbing up the walls. Moreover, stimulus mice were housed in a separate cabinet rack *prior* to the testing sessions. For final acclimatisation, test mice were put up on tables in the room 30 min to 1 h before beginning of a session. Mice were tested on day 9 and 30 *post-surgery*.

A test session consisted of the habituation and the social test (Fig. 2.3). First, mice could run freely for 5 min to explore the arena (= habituation). Full entry of every mouse *per* chamber was counted manually and used to determine every individual's preferred chamber. After that, mice were shortly limited to the middle chamber while both stimulus tubes were put in the outer chambers. In the tube of the disliked chamber, one random social stimulus mouse was presented. Exploration and social behaviour (= social test) were video recorded for 10 min. After every test, the stimulus mouse was exchanged. Chambers and tubes were cleaned with 75 % ethanol between sessions.

In ANY-maze (Stoelting Co., Dublin, Ireland), the arena was mapped into chamber zones and tube zones and social behaviour was analysed (Fig. 2.3). Distance travelled, entry per zone with mouse's head, time per zone, time immobile per zone as well as distance to subject or object were calculated automatically by the program. The zone of approx. 4 cm around the tubes was used to determine the proportion of time specifically spent interacting since head entry into the zone was associated with sniffing and mounting.

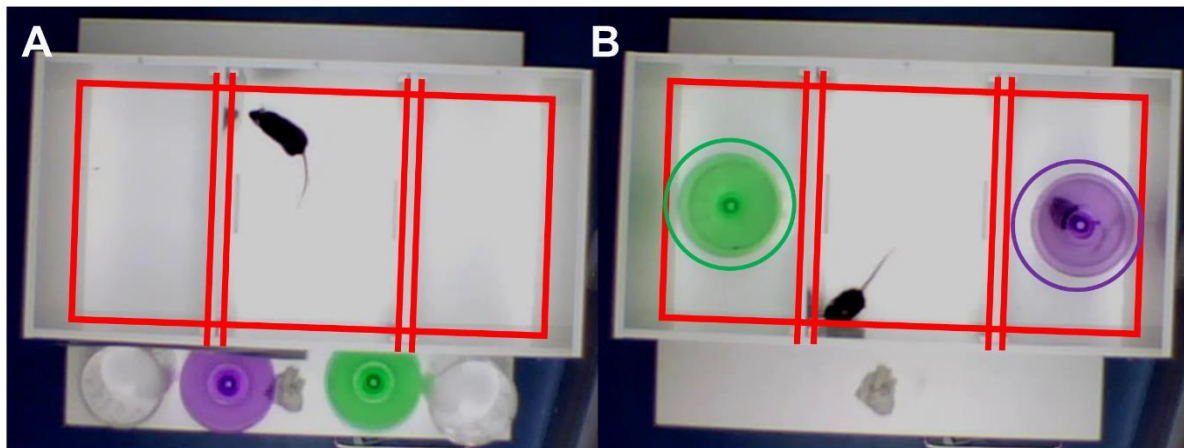


Figure 2.3: Social interaction test with three-chamber paradigm. [A] Habituation: mice could run freely for 5 min to explore. [B] Social test: a stimulus mouse in a perforated tube (purple cap) and a similar tube without mouse (green cap) were placed in the disliked and liked corner chambers, respectively. Exploration and social behaviour were recorded for 10 min. Interaction zones are indicated by circles around the tubes.

2.1.5 PER2::LUC breeding and genotyping

PER2::LUC mice are a circadian reporter mouse line. The *Luc* (Luciferase) gene is fused in-frame to the 3' end of the endogenous *mPer2* gene (Yoo *et al.*, 2004). This way all regulatory elements are preserved, and transcriptional and *post*-transcriptional dynamics function normally. The parallel expression of luciferase with the core clock component PER2 allows for real-time recordings of circadian clock activity when keeping tissues cultured in a luciferin-containing medium.

PER2::LUC heterozygous mice were used for all bioluminescence experiments. After weaning at around 3 weeks of age, ear biopsies were taken for genotyping. For DNA isolation, 20 μ l of DNA extraction buffer (50 mM Tris, 2 mM NaCl, 10 mM EDTA, 1 % SDS; pH 8.0) was added with 1 μ l 10 mg/ml proteinase K (Roche, Basel, Switzerland) to every ear snip. After incubation for 1 h at 55 °C shaking (450 rpm), reaction tubes were vortexed briefly. If needed reaction time was prolonged by 20 min to assure complete digestion of tissue. Distilled water (ddH₂O; 500 μ l) was added and the solution incubated for 10 min at 95 °C shaking (450 rpm) to inactive proteinase K. Samples were stored at 4 °C.

To verify the genotype of mice, polymerase chain reaction (PCR) was used:

1. Per reaction: 0.5 μ l DNA sample, 1 μ l 10x ammonium buffer (Ampliqon, Odense, Denmark), 0.1 μ l 10 mM dNTPs (Thermo Scientific, Waltham, US), 0.2 μ l Taq polymerase (5 units/ μ l; Ampliqon), 7.8 μ l ddH₂O + primer (10 pmol/ μ l; Eurofins, Luxemburg)
 - a. 0.2 μ l forward primer: 5'-CGCTGTGTTTACTGCGAGAGTGAGG-3'
 - b. 0.1 μ l reverse primer 1: 5'-CCACAAGATCTTCCCCCTTCCG-3'

c. 0.1 µl reverse primer 2: 5'-GTCCCTATCGAAGGACTCTGGCAC-3'

2. PCR conditions: 3 min at 95 °C (initial denaturation), 36 cycles of 30 s at 94 °C (denaturation) + 30 s at 65 °C (annealing) + 1 min at 72 °C (elongation), 7 min at 72 °C (final elongation), 4 °C ∞ (cooling)

PCR products were analysed using 1.5-% agarose gel electrophoresis (Fig. 2.4 A). Samples were mixed with 2 µl 6x loading buffer (0.25 % bromophenol blue, 30 % glycerol, in ddH₂O). Agarose gel was prepared in 1x TAE buffer (400 mM Tris, 200 mM acetic acid, 10 mM EDTA (pH 8.0), H₂O) with 1:10,000 SYBR Safe DNA Gel stain (Invitrogen, Carlsbad, US). Samples and 4 µl SimplyLoad 100 bp DNA Ladder (Lonza, Basel, Switzerland) run at a constant voltage of 80 V for 15 – 30 min in 1x TAE buffer. Wildtype *mPer2* product was 200 bp, transgenic *mPer2^{Luc}* product 780 bp. Gel pictures were taken with the FastGene Blue/Green GelPic LED Box Imaging System (Nippon Genetics, Tokyo, Japan).

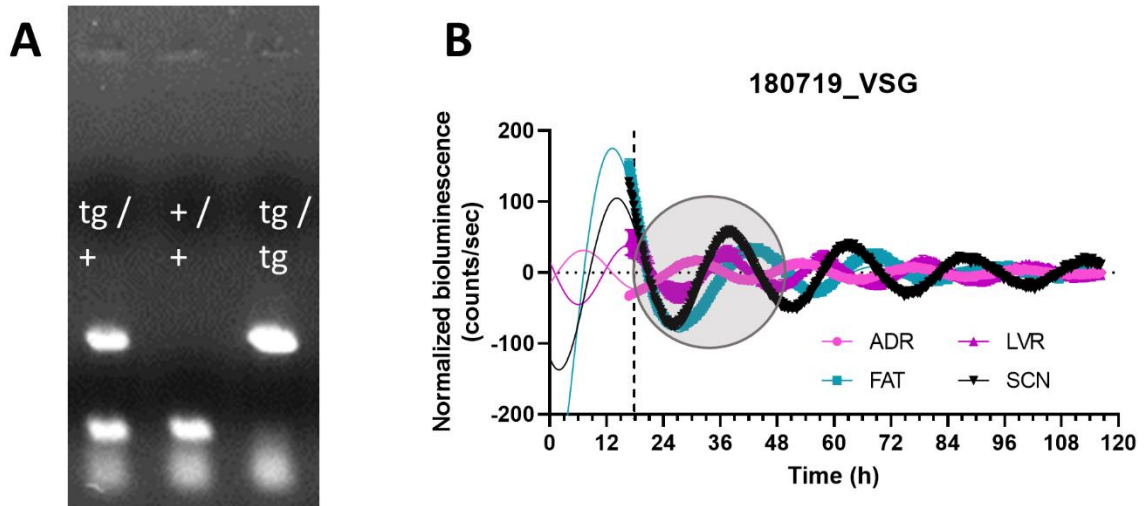


Figure 2.4: *PER2::LUC* genotyping and bioluminescence analysis. [A] Exemplary genotyping result from a heterozygous transgenic (tg/+), a wildtype (+/+), and a homozygous transgenic (tg/tg) mouse. [B] Example bioluminescence analysis. Dampened sine waves were fitted onto averages of individual tissue recordings (starting ca. ZT6) after exclusion of the first 12 h of recording (~ ZT18, marked by the dashed line) and 24-hour running average baseline subtraction. The first cycle after 12 h of recording was evaluated for troughs, peaks, and zero transitions.

2.1.6 Bioluminescence recordings

Tissues of *PER2::LUC* mice were harvested between ZT3 – 5 (ZT0 = "lights on") and kept in ice-cold Hanks' Balanced Salt Solution (HBSS). 300 µm thick slices of SCN, adrenal gland, or liver tissue were prepared with a vibratome (HM650V, Thermo Fisher Scientific) and immediately placed onto tissue culture inserts (PICMORG50; Merck Millipore, Burlington, US). White adipose tissue (epididymal) was manually cut into 1.5-mm pieces with a scalpel and arranged free-floating. Preparations were cultivated in Dulbecco's Modified Eagle Medium (DMEM) supplemented with 0.7 mM luciferin, 4 g/l

glucose, 2 mM stable glutamine, 10 mM HEPES, 100 units/ml penicillin, 0.1 mg/ml streptomycin, 2 % B27, and 0.075 % sodium bicarbonate at 32 °C and 5 % CO₂ (Yoo *et al.*, 2004). Tissue bioluminescence was recorded every 10 min for 1 min up to 7 days starting from approx. ZT6 using a LumiCycle luminometer (ActiMetrics). Raw data were baseline-subtracted using a 24-hour running average and dampened sine waves fitted using LumiCycle Analysis software (ActiMetrics). Only recordings with a goodness of fit $\geq 50\%$ were used. The first 12 h of recording were excluded from all analyses (Fig. 2.4 B). For period determination, best-fit dampened sine wave models were calculated with GraphPad Prism on the average of all recordings of an individual tissue ($n = 1 - 4$ slices). Phase was determined *via* the first ascending zero transition of the model fit; amplitudes and dampening were defined as the difference and ratio between the first maximum and the following minimum, respectively. These parameters were calculated from the model fit with Matlab (The MathWorks, Natick, US). For phase distribution Rayleigh tests of uniformity were performed with Oriana v2.0 (Kovach Computing, Pentraeth, UK). The SCN tissue explants were prepared by **Violetta Pilorz** from the Institute of Neurobiology (University of Lübeck).

2.1.7 Tissue collection

Mice were sacrificed by cervical dislocation every 6 h starting at ZT1 on day 9 *post-surgery*. Trunk blood was collected in EDTA-coated tubes, kept on ice, and later centrifuged (30 min, 1,500 x g) to obtain plasma. Tissues were snap-frozen on dry ice. Samples were stored at -80 °C until further use.

2.2 Molecular experiments

2.2.1 Plasma concentrations

Plasma levels of leptin (Mouse Leptin ELISA Kit, Cat# 90030, Crystal Chem, Zaandam, The Netherlands), adiponectin (Adiponectin (Mouse) ELISA Kit, Cat# AG-45A-0004YEK-KI01, AdipoGen Life Sciences, Liestal, Switzerland), triglycerides (Triglyceride Colorimetric Assay Kit, Cat# 10010303, Cayman Chemical, Ann Arbor, US), free fatty acids (96-well Serum/Plasma Fatty Acid Kit, Cat# SFA-1, Zen-bio, Durham, US), and corticosterone (Corticosterone ELISA kit, Cat# ADI-900-097, Enzo Life Sciences, Farmingdale, US) were measured according to the manufacturers' instructions. Corticosterone ELISA measurement was performed by **Iwona Olejniczak** from the Institute of Neurobiology (University of Lübeck).

2.2.2 RNA isolation and quantification

Subcutaneous white adipose tissue biopsies were homogenised with ~ 10 ceramic beads in 900 µl TRIzol reagent (Qiagen, Hilden, Germany). The bench homogenizer Omni Bead Ruptor (Omni International, Kennesaw, US) was used with the program: 4.5 m/s speed, 3 cycles, 20 s, 3 s decay. Lipids were removed by centrifugation for 3 min at 14,000 x g. After adding 900 µl pure ethanol, the mix was transferred stepwise onto columns of the RNeasy Mini Kit (Cat# 74104, Qiagen) and total RNA was isolated with on-column DNase digestion according to the manufacturer's protocol. RNA concentration was measured with microplate spectrophotometer (Epoch Microplate Spectrophotometer, BioTek Instruments, Winooski, US) and the Gen5 software, version 2.0 (BioTek Instruments). The 260 nm to 280 nm absorbance ratio was used for quantification and purity control. RNA purity in the 260/280 ratio of more than 1.9 was accepted. Samples were stored at -80 °C.

2.2.3 RNA quality control and sequencing

RNA-seq library generation and sequencing were performed at the Transcriptome and Genome Analysis Core Unit, University Medical Center Göttingen (Wilms *et al.*, 2019). Briefly, using a standard sensitivity RNA Analysis Kit (DNF-471), 200 ng of total RNA were checked for quality and integrity with the Fragment Analyzer (Advanced Analytical, Ames, US). All samples selected for sequencing exhibited an RNA integrity number > 8. Libraries were prepared with the TruSeq RNA Library Preparation Kit (version 2, set A, 48 samples, 12 indexes) and the Illumina RS-1222001 protocol (Illumina, San Diego, US). Optimisation steps were performed to increase ligation efficiency (> 94 %) and to avoid PCR duplication artefacts and primer dimers. A fluorometry-based system (QuantiFluor dsDNA System, Promega, Madison, US) was used for quantitation of cDNA libraries. Average size (~ 300 bp) of final cDNA libraries was determined with the dsDNA 905 Reagent Kit (Fragment Analyzer, Advanced Analytical). Pooled libraries were sequenced on a HiSeq 2000 (Illumina) generating 50-bp single-end reads (at 25 Mio. reads/sample).

2.2.4 RNA sequencing data processing and presentation

Sequence images were transformed with Illumina software (BaseCaller, Illumina, San Diego, US) to BCL files (binary base call), which were demultiplexed to fastq files with bcl2fastq (version 2.17.1.14; Dodt *et al.*, 2012). FastQC (version 0.11.5; Babraham Bioinformatics, Cambridge, UK) was used for quality control. Data procession and analysis were done in the R/Bioconductor environment (Gentleman *et al.*, 2004). Sequence alignments with the genome of *Mus musculus* (mm10) were performed using Bowtie (version 2.1.0), conversion and sorting using Samtools (version 0.1.19), and read counting using

Htseq (version 0.5.4p3). Normalisation of raw counts and analysis of differential gene expression analysis was done with the DESeq2 R package (v 1.12.3; Love *et al.*, 2014). Data processing was performed by **Orr Shomroni** from the Transcriptome and Genome Analysis Core Unit (University Medical Center Göttingen).

Principle component analysis was calculated and plotted with Matlab. Genes with the Log2(fold change; FC) of at least ± 1 between conditions and a Benjamini-Hochberg adjusted p-value < 0.05 were considered differently expressed. KEGG enrichment analysis (FDR < 0.05 , Top10 categories, minimum number of IDs 5 and maximum 500 per category) of these was performed in Webgestalt (Liao *et al.*, 2019) and visualised with the R package GoPlot (version 1.0.2; Walter *et al.*, 2015).

2.2.5 Transcriptome analysis

For rhythm analysis (JTK_CYCLEv3 for R, FDR-corrected p-values < 0.05 , assumed period of 24 h; Hughes *et al.*, 2010) only transcripts expressed in all replicates of at least one time point in sham or VSG conditions were included. A list consisting of the differentially expressed and differentially rhythmic genes (“differently regulated”) was used for gene ontology (GO) enrichment analysis using the BiNGO plugin for Cytoscape (version 3.7.2; Shannon *et al.*, 2003; Maere *et al.*, 2005). Overrepresented biological processes were detected using hypergeometric tests and an FDR correction of $p < 0.05$ against the whole *Mus musculus* annotation library. The network was filtered to only show nodes with a size > 16 . Top10 categories of the enrichment analysis and the central GO terms were labelled. Heatmaps were created based on baseline-normalised z-scores corrected by each ZT standard deviation. Phase and amplitude were calculated using JTK_Cycle. Oriana was used to visualise phase-shifts. For baseline comparisons, individual gene expression counts were normalised against sham control gene average (= sham-normalised), and, for rhythmicity comparisons, against the corresponding group gene average (= baseline-normalised). Diurnal fold change (dFC) was defined as difference between maximum and minimum normalised by baseline, sum of Lorentzian curve-fits was calculated on dFC distribution with GraphPad Prism. Gene lists for analysis of pathway regulation were taken from [wikipathways.org](http://www.wikipathways.org) (WP33, WP157, WP336, WP386, WP3588; Slenter *et al.*, 2018). Data sets are accessible through NCBI’s Gene Expression Omnibus (accession number GSE162671).

2.2.6 Statistical analysis

All data are presented as means of the sample \pm SEM. Data were statistically analysed and plotted using GraphPad Prism. P-values < 0.05 were considered significant. For comparison of one variable across the two groups, *t*-tests were performed (*e.g.* bioluminescence recordings). To evaluate changes

from baseline, *t*-tests against a hypothetical mean were calculated. For comparisons between groups across different time points, repeated measures (RM) 2-way analyses of variance (ANOVA) were performed (*e.g.* body weight development, meal intake). When the number of animals differed across time (*e.g.* comparing *pre*-surgical status vs. VSG *post*-surgery) mixed-effects analyses were chosen. Sidak's multiple comparison test was performed for *post hoc* statistics. Pearson correlation was used to evaluate relationships between variables; for visual presentation simple linear regression was performed. ROUT method of identifying outlier was used per time point, for plasma concentrations specifically with a maximum desired FDR < 0.05, in all other experiments < 0.01.

3 Results

In this doctoral thesis, the effect of bariatric surgery on biological rhythms of HFD-induced obese mice was investigated. *Post*-surgical constant darkness behaviour was monitored, tissue rhythms evaluated, and white adipose tissue transcriptome analysed.

3.1 Mouse behaviour after surgery

3.1.1 Diet-induced obesity correlates with dampening of behavioural circadian rhythms

Short-term HFD (1 month) is known to disrupt circadian rhythms (Kohsaka *et al.*, 2007; Pendergast *et al.*, 2013). Withstanding of VSG-induced weight loss needs mice to weigh at least 35 g. To archive this, mice received HFD exclusively from week 3 – 4 of age for ca. 10 weeks. The minimum surgical weight was reached after 9 weeks on HFD (Fig. 3.1 A; $n = 27$). Mice gained an average of 8.3 ± 0.22 % per week before *pre*-surgical experiments started (Fig. 3.1 A, B) and a total of 90.4 ± 3.83 % until the day of surgery (Fig. 3.1 C). To examine the effects of HFD and subsequent bariatric surgery on endogenous circadian rhythms, mice were observed in DD and free-running behaviour was studied. The overall weight gain correlated negatively with the amplitude of the detected period from the periodogram of locomotor activity (Fig. 3.1 D; $n = 16$) and the amplitude of the mean meal activity rhythm (Fig. 3.1 E; $n = 13$). These results are confirmatory regarding a disruptive effect of HFD on rodent circadian behaviour.

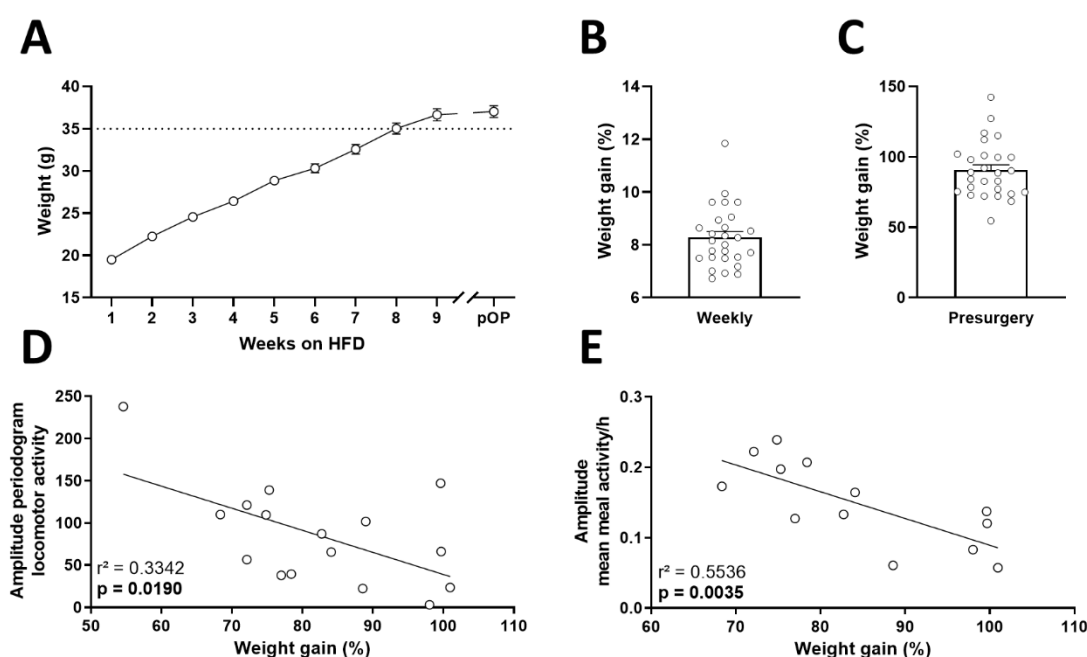


Figure 3.1: Weight development by HFD exposure and associated dampening of rhythms. [A] Weight development of mice on HFD ($n = 27$). [B] Weekly weight gain and [C] overall gain before surgery. [D] Overall weight gain correlates negatively with periodogram amplitude of locomotor activity ($n = 16$) and [E] amplitude of mean meal activity ($n = 13$), simple linear regression, squared correlation coefficient and corresponding p-value stated. pOP: pre-surgery.

3.1.2 Weight development after VSG is characterised by two distinct phases

First, the success of VSG needed verification by evaluating body weight development *post-surgery* under DD conditions. Body weight loss is the major output parameter of a successful bariatric surgery. Weight data until day 28 *post-surgery* were analysed. VSG mice displayed an immediate weight loss after surgery compared to a period of weight stagnation in sham mice up to day 10 (Fig. 3.2 A-C; VSG: $n = 13$ vs. sham: $n = 8$). This catabolic phase (CP) was followed by a phase of weight regain, an anabolic phase (AP). Notably, most VSG mice (10 out of 13) did not reach their *pre-surgical* weight throughout the experimental period (Fig. 3.2 A, C), while all sham mice exceeded their initial weight after ca. 10 days.

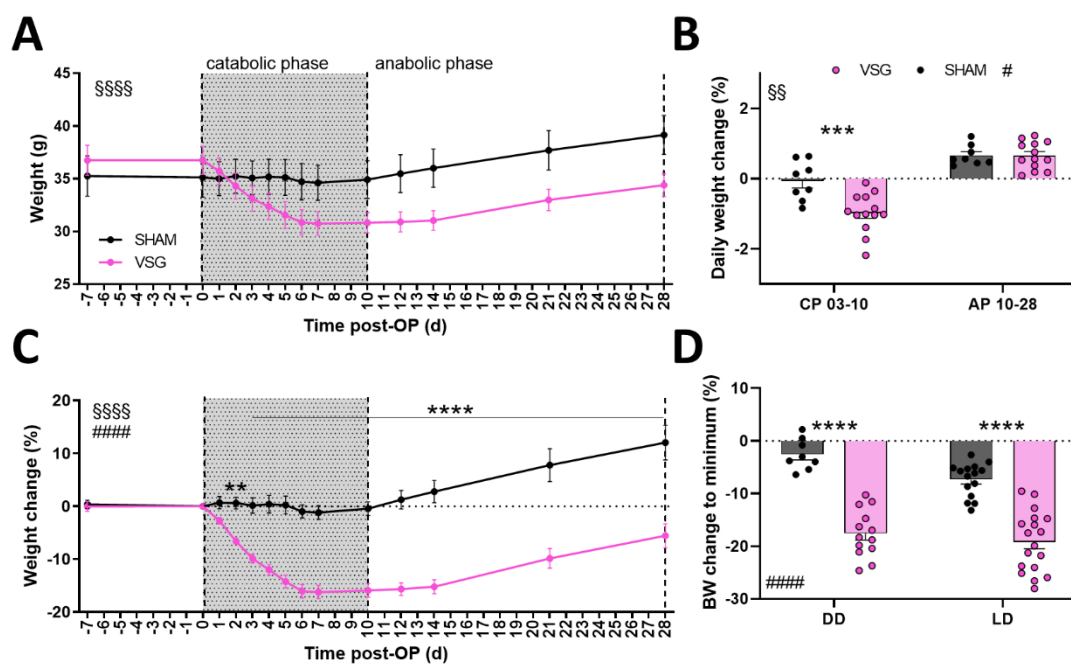


Figure 3.2: Weight development after bariatric surgery. [A] Absolute weight development after surgery, 2-way RM-ANOVA. [B] Average daily weight change during catabolic phase (CP, day 3 – 10) and anabolic phase (AP, day 10 – 28), 2-way RM-ANOVA. [C] Relative weight development after surgery, 2-way RM-ANOVA. [D] Overall body weight (BW) change to the initial minimum post-surgery under constant darkness (DD) or a 12h-light:12h-dark cycle (LD), 2-way ANOVA. In [A] and [C] beginning and ending of post-surgical intervals are indicated by dashed lines; CP is highlighted. VSG/sham $n = 13/8$. Legend: interaction \$\$\$\$ $p < 0.0001$, §§ $p < 0.01$; group effect ##### $p < 0.0001$, # $p < 0.05$; Sidak's post hoc comparison **** $p < 0.0001$, *** $p < 0.001$, ** $p < 0.01$.

When comparing absolute weight development between groups, only an interaction effect was detected (Fig. 3.2 A; 2-way RM-ANOVA, interaction $p < 0.0001$). However, relative body weight data was significantly different after VSG and sham. VSG induced a daily weight change in CP of -1.0 ± 0.16 % compared to -0.1 ± 0.20 % for sham (Fig. 3.2 B, C; 2-way RM-ANOVA, $p < 0.001$). Daily weight development did not differ during AP (VSG: 0.7 ± 0.11 % vs. sham: 0.7 ± 0.10 %). The weight change effect was significant from day 2 *post-surgery* (Fig. 3.2 C; VSG: -6.6 ± 0.60 vs. sham: 0.6 ± 1.12 , 2-way RM-ANOVA, $p < 0.01$). Around the CP-AP transition animals had reached the lowest *post-surgical* body

weight. This corresponded to a change of $-17.6 \pm 1.26\%$ (-10.3 to -24.7%) from their initial body weight for VSG animals and $-2.6 \pm 1.05\%$ for sham animals (Fig. 3.2 D; 2.1 to -6.4% , 2-way ANOVA, $p < 0.0001$). VSG and sham mice kept under LD12:12 conditions showed a comparable weight change (VSG: $-19.2 \pm 1.35\%$, -9.55 to -28.06% , $n = 18$, vs. sham mice: $-7.4 \pm 0.82\%$, -2.65 to -13.19% , $n = 15$, 2-way ANOVA, $p < 0.0001$).

In summary, bariatric surgery was followed by two distinct phases of initial weight loss and subsequent weight gain. VSG decreased body weight by almost 20 % compared to ca. 5 % by sham surgery. Maximum weight loss was reached after one week in both groups.

3.1.3 Locomotor activity is largely resistant to VSG

Locomotor activity rhythms are a reliable output parameter for SCN activity (see chapter 1.3). Locomotion was observed by infrared detector beam breaks until day 17 *post-surgery*. No major differences between VSG and sham animals were seen in 5-min bin actograms (Fig. 3.3 A, B; VSG: $n = 9$ vs. sham: $n = 7$). Occasionally, increased total activity counts could be observed during the first few days after surgery in both groups. This corresponded with the time mice received LiD (exclusively until day 3, marked by coloured lines in actograms) and analgesic treatment (until day 5).

When analysing the 5-day running period of mice, a minor alteration was detected *post-surgery* between VSG and sham mice (Fig. 3.3 C; 2-way RM-ANOVA, interaction $p < 0.05$). While period lengths for sham-operated mice fluctuated closely around *pre-surgical* baselines, periods of VSG mice were lengthened around day 9 (VSG: 0.45 ± 0.169 h vs. sham: -0.12 ± 0.208 h, $p < 0.05$). This corresponded with the end of CP and transition into AP. Average period over either interval, CP or AP, did not differ significantly between sham and VSG mice (Fig. 3.3 D; CP VSG: 23.9 ± 0.08 h vs. sham: 23.8 ± 0.08 h, AP VSG: 23.9 ± 0.04 h vs. sham: 23.7 ± 0.04 h, 2- way RM-ANOVA), but a trend for an overall *post-surgical* lengthening of periods was found (group effect $p = 0.0504$). Activity distribution along the subjective day between rest and active phase did not change after any type of surgery compared to *pre-surgical* baselines (Fig. 3.3 E; active phases: pre: 0.70 ± 0.015 , CP VSG: 0.66 ± 0.022 or sham: 0.68 ± 0.033 , AP VSG: 0.70 ± 0.022 or sham: 0.69 ± 0.028 , mixed effects model; rest phases: pre: 0.31 ± 0.015 , CP VSG: 0.34 ± 0.022 or sham: 0.35 ± 0.027 , AP VSG: 0.30 ± 0.022 or sham: 0.33 ± 0.025 , mixed effects model). After normalising total activity counts by the LD12:12 baseline, an overall decrease was found *post-surgery* in both groups with a tendency of a stronger decrease after VSG compared to sham (Fig. 3.3 F; CP VSG: 0.56 ± 0.048 vs. sham: 0.71 ± 0.087 , AP VSG: 0.55 ± 0.043 vs. sham: 0.73 ± 0.100 , 2-way RM-ANOVA, group effect $p = 0.0845$).

Collectively, these results suggest a certain resistance of locomotor activity – and, presumably, the activity rhythm generating SCN – to the metabolic alterations induced by VSG. Though minor changes were detected, these were not sustained across the surgical interval (running period) or only seen as a tendency (interval periods, total activity).

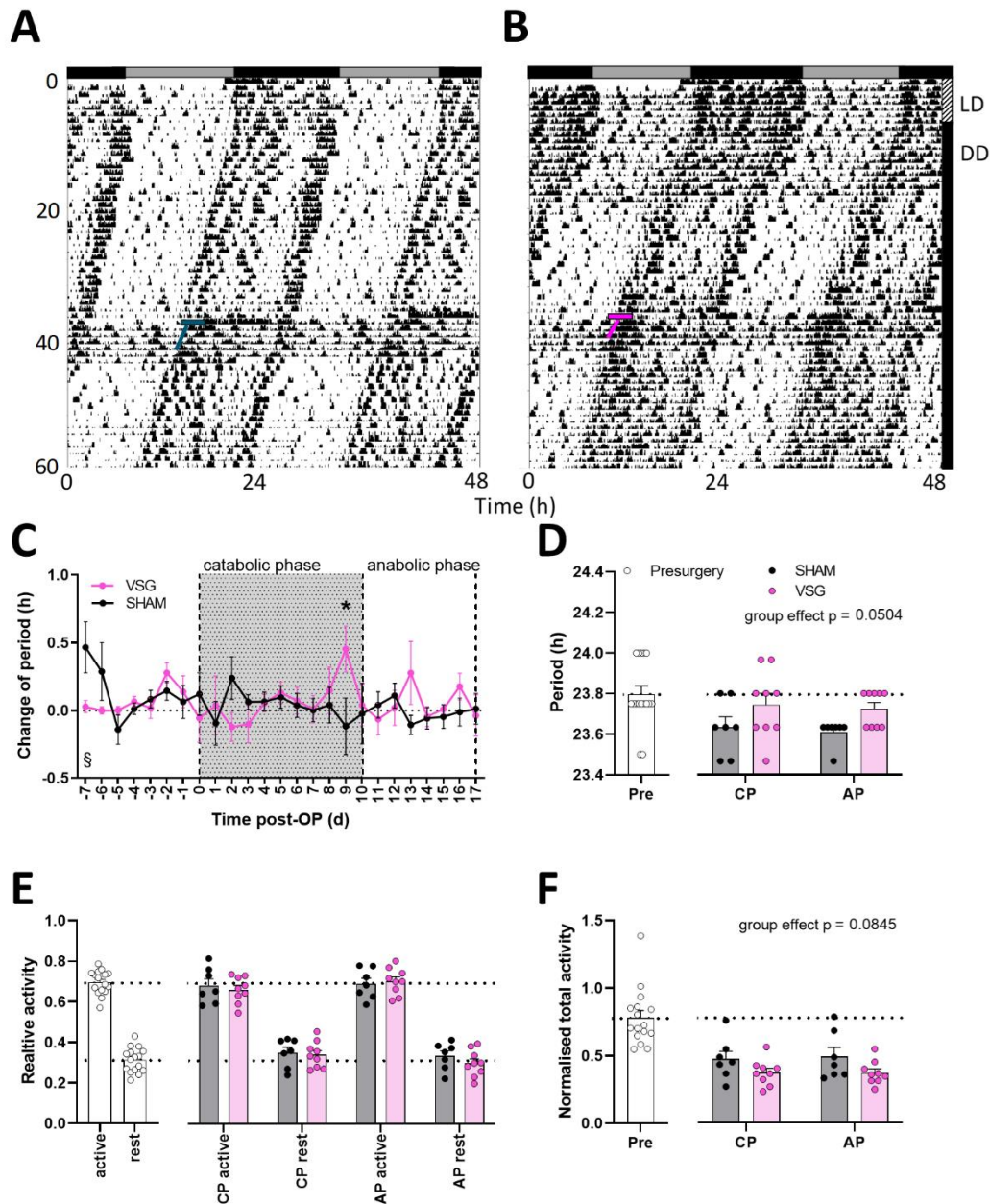


Figure 3.3: Resistance of locomotor activity to VSG. [A] Representative 5-min bin locomotor activity actograms of a sham-operated and [B] a VSG-operated mouse; coloured bars indicate time of surgery, coloured lines period of post-operative care with liquid diet. Observation started with a LD12:12 cycle (here LD) followed by constant darkness (DD), original light-dark schedule is indicated on top of the actograms. [C] Running period of 5 days along the experimental time, beginning and ending of post-surgical intervals are indicated by dotted lines, CP is highlighted, 2-way RM-ANOVA. [D] Average period during pre-surgical, CP and AP intervals, 2-way RM ANOVA on post-surgical conditions, group effect p-value is stated. [E] Relative activity before and after surgery during the respective active and rest phases against pre-surgical baseline, mixed effects model on active and rest phases separately. [F] Total activity counts normalised to LD12:12 baseline activity, 2-way RM-ANOVA on post-surgical conditions, group effect p-value is stated. VSG/sham $n = 9/7$. Legend: interaction § $p < 0.05$; Sidak's post hoc comparison * $p < 0.05$.

3.1.4 VSG increases food intake rhythmicity

VSG limits the food storage capacity of the stomach. The intervention leads to well-documented metabolic adaptations (*e.g.* Azim and Kashyap, 2016). To investigate how these adaptations impact feeding rhythms, food intake behaviour was measured by automatic food hopper and analysed until day 17 *post-surgery*.

Meal pattern microstructure was analysed first. No obvious differences were seen in actograms of meal activity (Fig. 3.4 A, B; VSG: $n = 8$, sham: $n = 5$). Average meal size was reduced by VSG immediately in CP and remained reduced in AP compared to sham (Fig. 3.4 C; CP VSG: 0.07 ± 0.004 g vs. sham: 0.11 ± 0.003 g, AP VSG: 0.09 ± 0.010 g vs. sham: 0.13 ± 0.012 g, 2-way RM-ANOVA, group effect $p < 0.01$). Similarly, after VSG total daily intake was reduced over both *post-surgical* periods compared to sham (Fig. 3.4 D; CP VSG: 1.5 ± 0.07 g vs. sham: 2.0 ± 0.24 g, AP VSG: 2.4 ± 0.10 g vs. sham: 2.9 ± 0.17 g, mixed effects model, group effect $p < 0.5$). Notably, VSG mice increased meal frequency during AP (Fig. 3.4 E, CP VSG: 20.3 ± 1.10 vs. sham: 18.4 ± 1.80 , AP VSG: 30.7 ± 1.23 vs. sham: 22.0 ± 1.70 , 2-way RM-ANOVA, AP VSG vs. AP sham $p < 0.001$).

Looking into when these changes happen across the subjective day, VSG and sham mice behaved differently compared to the *pre-surgical* state (Fig. 3.4 F, G). Meal size did not show daytime-dependent variation within any group (data not shown). While both, sham and VSG animals, significantly reduced CP active phase food intake compared to *pre-surgical* baseline, the effect was stronger after VSG (Fig. 3.4 F; pre: 2.0 ± 0.09 g, CP VSG: 1.1 ± 0.05 g or sham: 1.4 ± 0.15 g, AP VSG: 1.8 ± 0.08 g or sham: 2.1 ± 0.11 g, mixed effects model, pre vs. CP sham $p < 0.05$, pre vs. CP VSG $p < 0.0001$). Moreover, VSG animals showed reduced rest phase food intake in CP but not in AP, whereas sham surgery increased rest phase food intake in AP but not in CP (pre: 0.7 ± 0.07 g, CP VSG: 0.4 ± 0.04 g or sham: 0.6 ± 0.12 g, AP VSG: 0.6 ± 0.06 g or sham: 0.8 ± 0.08 g, mixed effects model, pre vs. CP VSG $p < 0.05$, pre vs. AP sham $p < 0.05$). Neither active nor rest phase meal frequency in sham animals showed significant differences compared to *pre-surgery* (Fig. 3.4 G; active phases: pre: 17.6 ± 1.34 , CP sham: 13.1 ± 1.06 , AP sham: 15.9 ± 1.59 , mixed effects model; rest phases: pre: 5.9 ± 0.49 , CP sham: 5.2 ± 0.86 , AP sham: 6.1 ± 0.52 , mixed effects model). Meal frequencies during the rest phase were also not affected by VSG surgery during any *post-surgical* period. However, AP active phase meal frequency was increased (active phases: pre: 17.6 ± 1.34 , CP VSG: 14.1 ± 0.84 , AP VSG: 22.8 ± 1.29 , mixed effects model, pre vs. AP VSG $p < 0.05$; rest phases: pre: 5.9 ± 0.49 , CP VSG: 6.2 ± 0.45 , AP VSG: 7.9 ± 0.67 , mixed effects model). Interestingly, body weight change to the *post-surgical* minimum showed a tendency to correlate negatively with AP active phase frequency (Fig. 3.4 H; simple linear regression, $p = 0.0595$) and correlated significantly with AP rest phase frequency (Fig. 3.4 I; simple linear regression, $p < 0.05$).

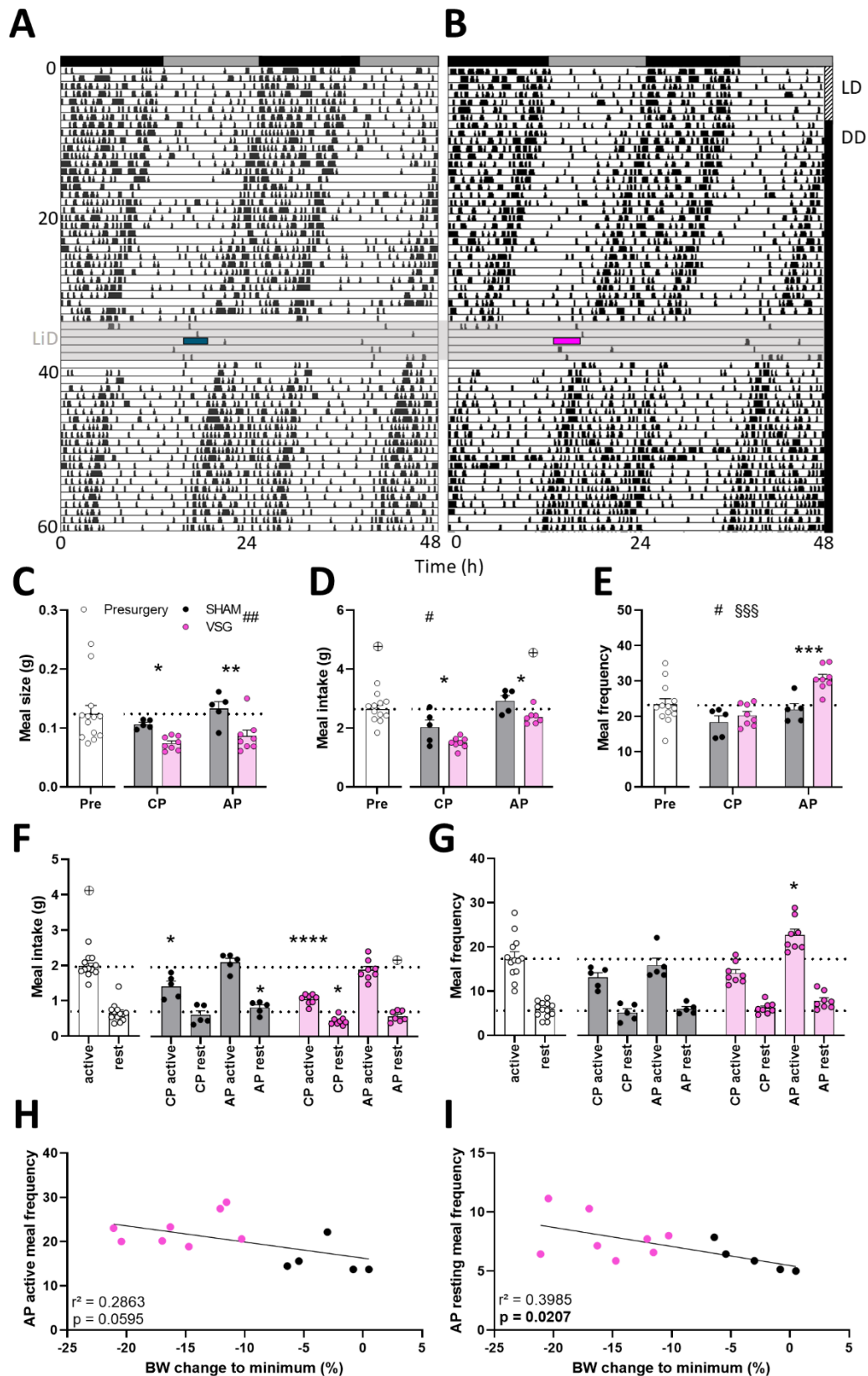


Figure 3.4: VSG reduces meal size and increases meal frequency. (Caption continues next page)

[A] Representative 15-min bin meal intake actograms of a sham- and [B] of a VSG-operated mouse. Coloured bars indicate time of surgery, shaded area indicates time of liquid diet (LiD) exposure. The daily cage check could result in false bouts being detected. Observation started with an LD12:12 cycle (here LD) followed by constant darkness (DD). The original light-dark schedule is indicated on top of the actograms. [C] Average meal size, 2-way RM-ANOVA, [D] daily meal intake, mixed effects model, exclusion of 1 % outlier, and [E] daily meal intake frequency, 2-way RM-ANOVA, [C-E] statistics were done on post-surgical conditions. [F] Distribution of meal intakes and [G] meal frequency across the day, mixed effects model against pre-surgical baseline on active and rest phases separately, exclusion of 1 % outlier. [H] AP active and [I] rest phase meal frequency plotted against BW change to initial minimum, simple linear regression, squared correlation coefficient and p-value stated. VSG/sham $n = 8/5$. Legend: crossed circle indicates 1 % outlier data point; interaction §§§ $p < 0.001$; group effect ## $p < 0.01$, # $p < 0.05$; Sidak's post hoc comparisons **** $p < 0.0001$, *** $p < 0.001$, ** $p < 0.01$, * $p < 0.05$.

To further clarify a daytime-dependent increase of feeding activity, daily profiles were studied. For this, both, feeding bout (≥ 0.01 g) and meal intake (≥ 0.02 g separated by ≥ 300 s) frequencies were smoothed, plotted, and analysed (= mean activity). Mean bout activity *per hour* did not significantly differ during CP between VSG and sham (Fig. 3.5 A; 2-way RM-ANOVA, VSG/sham $n = 8/5$), but an interaction effect was detected ($p < 0.05$). The difference between sham and VSG was heavily affected by one sham mouse displaying a triphasic daily profile. Though not statistically verified, a reduction of feeding events at the end of the active phase in both groups compared to *pre-surgical* baseline was seen. No significant alteration was detected in AP regarding feeding bout activity (Fig. 3.5 B; 2-way RM-ANOVA). However, the shape of the VSG curve was notably less biphasic compared to sham. Mean meal activity *per hour* in CP showed a similar trend than bout activity, but the interaction effect is even clearer (Fig. 3.5 C; 2-way RM-ANOVA, $p < 0.0001$). Meal consumption at the end of the active phase after sham appeared particularly affected compared to *pre-surgery*. Interestingly, meal activity during AP in VSG did not necessarily appear less biphasic but was clearly increased over the whole active phase (Fig. 3.5 D; 2-way RM-ANOVA, group effect $p < 0.01$), while sham activity seemed almost identical to *pre-surgical* baseline. In line with this, VSG animals during AP showed significantly increased meal activity amplitudes (Fig. 3.5 E; pre: 0.15 ± 0.016 counts/h, CP VSG: 0.12 ± 0.012 counts/h vs. sham: 0.10 ± 0.008 counts/h, AP VSG: 0.21 ± 0.021 counts/h vs. sham: 0.14 ± 0.014 counts/h, 2-way RM-ANOVA, AP VSG vs. AP sham $p < 0.05$).

To summarize the feeding data, both manipulations induced an initial reduction of food intake but did not considerably impact feeding rhythmicity early *post-surgery*. Sham animals normalised back to *pre-surgical* behaviour during the CP-AP transition. VSG animals increased meal frequency particularly in the AP active phase which strengthened the overall feeding rhythms.

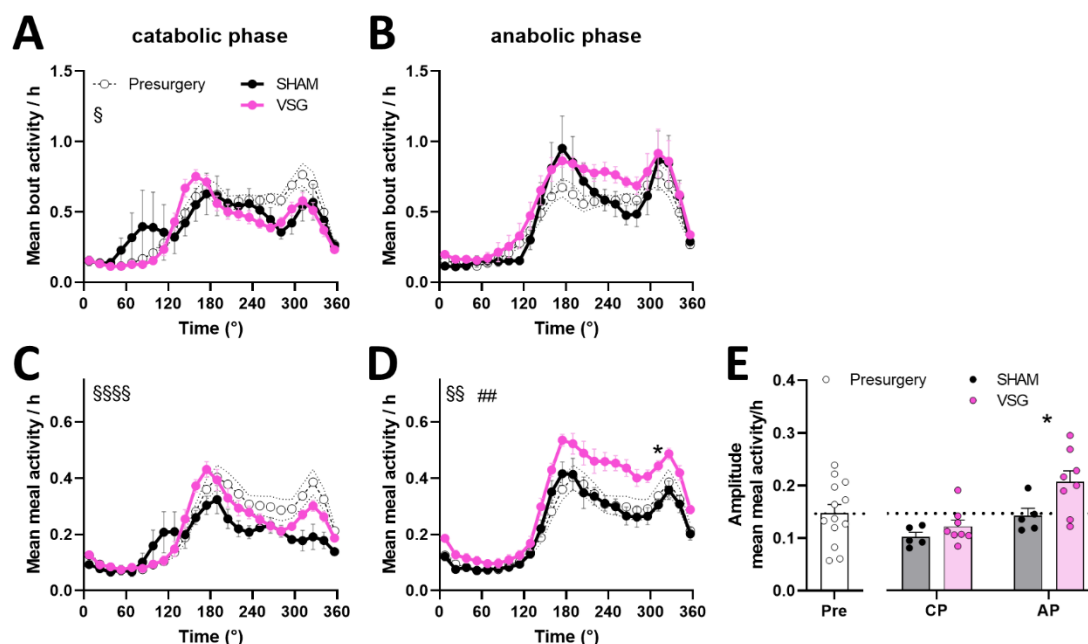


Figure 3.5: VSG increases feeding rhythmicity during AP. Mean bout activity per hour during [A] the catabolic and [B] the anabolic phase. Mean meal activity per hour during [C] the catabolic and [D] the anabolic phase. [E] Daily profile amplitudes of the mean meal activity. [A-E] 2-way RM-ANOVA on post-surgical conditions, VSG/sham $n = 8/5$. Legend: interaction §§§§ $p < 0.0001$, §§ $p < 0.01$, § $p < 0.05$; group effect ## $p < 0.01$; Sidak's post hoc comparison * $p < 0.05$.

3.1.5 VSG increases sociability during weight loss

Psychosocial factors could potentially affect bariatric surgery outcomes and influence circadian behaviour (Kalarchian and Marcus, 2019). To broaden the understanding of *post-surgical* behaviour, a social interaction test using the three-chamber paradigm was performed in VSG mice. Mice were kept in LD12:12 to reduce potential mood effects from housing under DD conditions (Monje *et al.*, 2011; Rosenwasser *et al.*, 2020).

Overall, 14 VSG and 13 sham mice were recorded for the experiment. One VSG mouse was excluded from day 9 analysis because of not displaying any explorative behaviour during that test. Another was excluded from day 30 analysis because it re-entered a catabolic state shortly before testing. First, it was verified that type of surgery does not impact basic locomotor activity in the arena. Distance travelled during the habituation was recorded and no differences between groups were found either 9 or 30 days *post-surgery* (Fig. 3.6 A; d9 VSG: 17.5 ± 1.03 m vs. sham: 19.1 ± 1.3 m, d30 VSG: 20.3 ± 1.32 m vs. sham: 19.8 ± 1.67 m, mixed effects model). Next, curiosity was evaluated by counting the times a mouse entered a chamber with its head ("peeking"). Type of surgery affected peeking behaviour into the test chambers: while sham animals showed no shifted preference for the social chamber after habituation, VSG animals significantly increased peeking into the chamber with an interaction partner at 30 days *post-surgery* (Fig. 3.6 B; VSG d9 habituation: 0.96 ± 0.054 vs. test: 1.17 ± 0.076 , d30 habituation: 0.86 ± 0.023 vs. test: 1.07 ± 0.049 , sham d9 habituation: 0.81 ± 0.040

vs. test: 1.01 ± 0.086 , d30 habituation: 0.84 ± 0.043 vs. test: 0.87 ± 0.051 , mixed effect model, group effect $p < 0.001$, VSG d30 habituation vs. test $p < 0.01$).

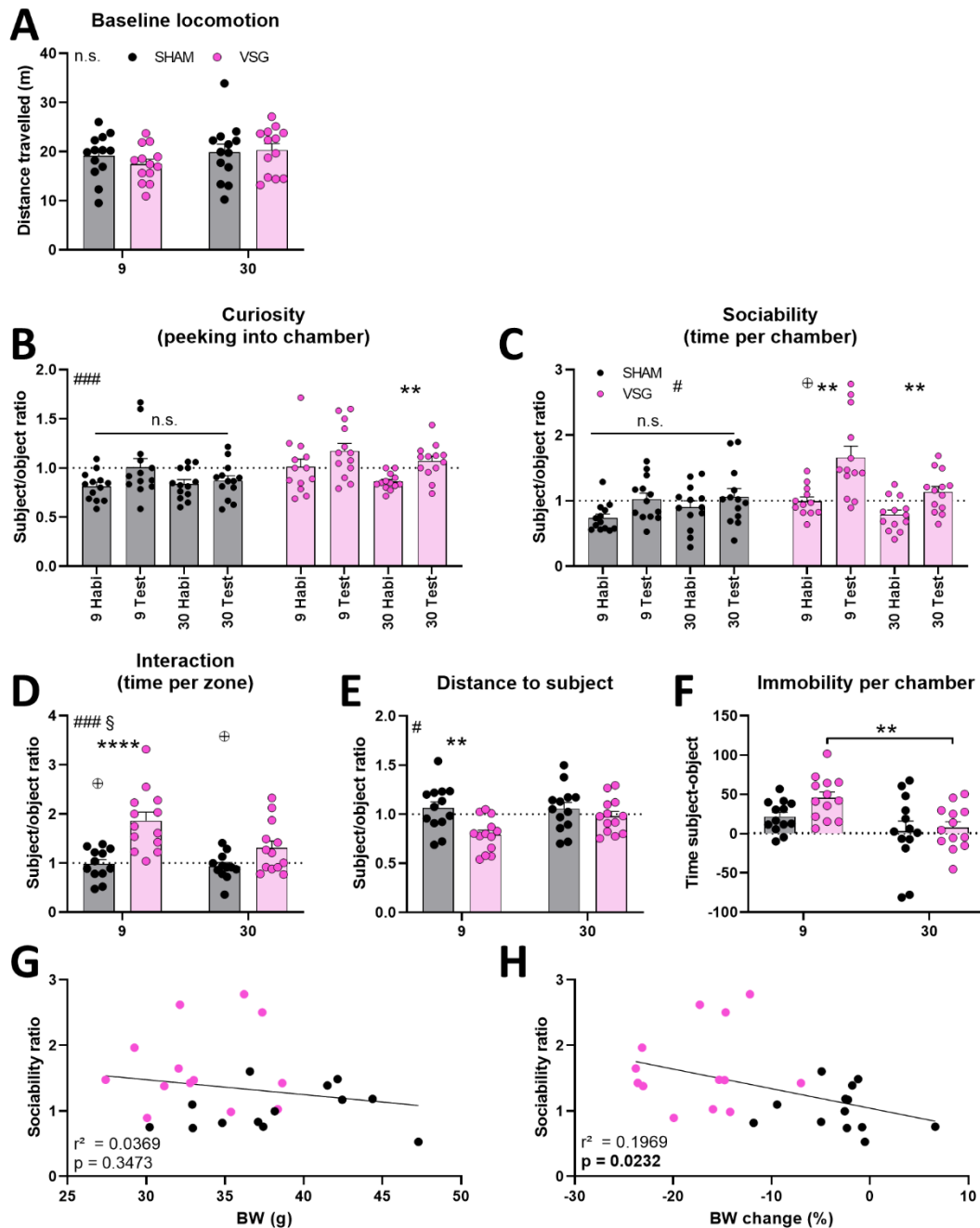


Figure 3.6: VSG-induced catabolism increases sociability 9 days post-surgery. [A] Distance travelled by mice during habituation (indicator of basic locomotion). [B] Ratio between the times mice moved with their heads across borders of subject vs. object chambers (= peeking, indicator of curiosity). [C] Ratio between times spent in subject vs. object chambers (indicator of sociability; = sociability ratio). [D] Ratio between times spent in proximity of subject vs. object (indicator of interacting behaviour). [E] Ratio between average distances to subject vs. object. [F] Difference between times spent immobile in subject and object chambers. [A-F] Mixed effects model, Sidak's post hoc comparisons [B, C, F] within surgical groups or [A, D, E] between surgical conditions. [G] Day 9 body weight (BW) or [H] BW change plotted against sociability ratio, simple linear regression, squared correlation coefficient and p-value stated. VSG/sham $n = 13/13$ per time point. Legend: crossed circle indicates 1 % outlier data point; interaction § $p < 0.05$; group effect ### $p < 0.001$, # $p < 0.05$; Sidak's post hoc comparison **** $p < 0.0001$, ** $p < 0.01$.

A more pronounced effect was detectable when analysing the ratio of total times spend between each test chambers, an indicator of sociability. Here, at both time points, 9 and 30 days *post-surgery*, VSG mice showed a shifted preference towards the subject chamber compared to habituation (Fig. 3.6 C; VSG d9 habituation: 0.99 ± 0.066 vs. test: 1.66 ± 0.173 , d30 habituation: 0.79 ± 0.069 vs. test: 1.13 ± 0.087 , sham d9 habituation: 0.74 ± 0.059 vs. test: 1.03 ± 0.091 , d30 habituation: 0.90 ± 0.094 vs. test: 1.06 ± 0.123 , mixed effects model, group effect $p < 0.05$, VSG d9 and d30 habituation vs. test $p < 0.01$). To make the results clearer, times spent in the zone close around the test object or subject, times spent immobile in each chamber, and distance kept to the object or subject were additionally recorded (Fig. 3.6 D-F). VSG mice spent significantly more time in the subject zone, presumably interacting with the partner (Fig. 3.6 D; d9 VSG: 1.86 ± 0.175 vs. sham: 0.98 ± 0.090 , d30 VSG: 1.30 ± 0.144 vs. 0.93 ± 0.078 , mixed effects model, d9 VSG vs. sham $p < 0.0001$), and overall closer to the subject (Fig. 3.6 E; d9 VSG: 0.79 ± 0.048 vs. sham: 1.06 ± 0.065 , d30 VSG: 0.98 ± 0.049 vs. sham: 1.05 ± 0.065 , mixed effects model, d9 VSG vs. sham $p < 0.01$) compared to their sham counterparts at day 9 *post-surgery*. Though no group differences were detected between times spent immobile, VSG mice were less immobile in the subject chamber 30 days compared to 9 days *post-surgery* (Fig. 3.6 F; VSG d9: 45.5 ± 7.58 s vs. d30: 7.4 ± 7.67 s, sham d9: 21.7 ± 5.47 s vs. d30: 3.3 ± 12.59 s, mixed effects model, VSG d9 vs. d30 $p < 0.01$).

VSG clearly increased social behaviours 9 days *post-surgery*. Moreover, though the sociability ratio did not correlate with body weight at day 9, it significantly correlated with body weight change at day 9 (Fig. 3.6 G, H; simple linear regression, $p = 0.3473$, $p < 0.05$, respectively). Collectively, it seems that bariatric surgery-induced weight loss increases willingness to socialise in mice.

3.2 Metabolic state at the CP-AP transition

Given the diverse effects found in behaviour at the CP-AP transition, at around 10 days *post-surgery*, more experiments were performed to elicit the metabolic state and metabolic rhythms at that time. Nine days after surgery was chosen as day of tissue collection for analysis. For these experiments, animals were kept in a LD12:12 cycle to reduce diurnal variation and have a stronger translational relevance with regard to human patients.

3.2.1 Tissue-specific recalibration of PER2 rhythms after VSG

Peripheral and central rhythms are differently affected by metabolic challenges. Using the *PER2::LUC* reporter mouse it is possible to investigate rhythmicity of several tissues simultaneously from one individual, thus allowing for better analysis of effects on the circadian network. SCN (Fig. 3.7), adrenal gland (Fig. 3.8), liver (Fig. 3.9), and WAT samples (Fig. 3.10) were collected and luminescence recorded.

3.2.1.1 Suprachiasmatic nucleus

The SCN showed robust rhythms up to 6 days in culture (Fig. 3.7 A, B). One to two slices per animal were analysed (Fig. 3.7 A; VSG: $n = 6$, sham: $n = 5$). Modelled rhythms appeared largely in sync between individuals. When plotting the mean of all models, SCN of VSG animals displayed a phase-delay (Fig. 3.7 B). This phase-delay of 1.31 h was significant in a direct comparison of the second ascending zero-point (Fig. 3.7 D; VSG: 32.4 ± 0.17 h vs. sham: 31.1 ± 0.28 h, unpaired *t*-test, $p < 0.01$). Period (Fig. 3.7 C; VSG: 24.5 ± 0.23 h vs. sham: 24.3 ± 0.11 h, unpaired *t*-test), amplitude (Fig. 3.7 E; VSG: 51.7 ± 12.92 counts/s vs. sham: 42.0 ± 10.53 counts/s, unpaired *t*-test), and dampening (Fig. 3.7 F; VSG: 0.74 ± 0.041 vs. sham: 0.74 ± 0.035 , unpaired *t*-test) did not show significant variation between surgical groups. Interestingly, similar to what was seen in the social interaction experiment, phase did not correlate with body weight but with body weight change at day 9 *post-surgery* (Fig. 3.7 G, H; simple linear regression, $p = 0.1654$, $p < 0.01$, respectively).

To summarize, SCN from LD-entrained animals showed a phase-shift between VSG and sham animals. This result potentially contradicts the results from the DD locomotor activity data; however, minor alterations were observed there, too. Overall, locomotor activity as the major SCN output was largely resistant to type of surgery (see chapter 3.1.3). Conclusively, the SCN itself should be largely resistant to the type of surgery, though subtle and time point-specific effects cannot be excluded.

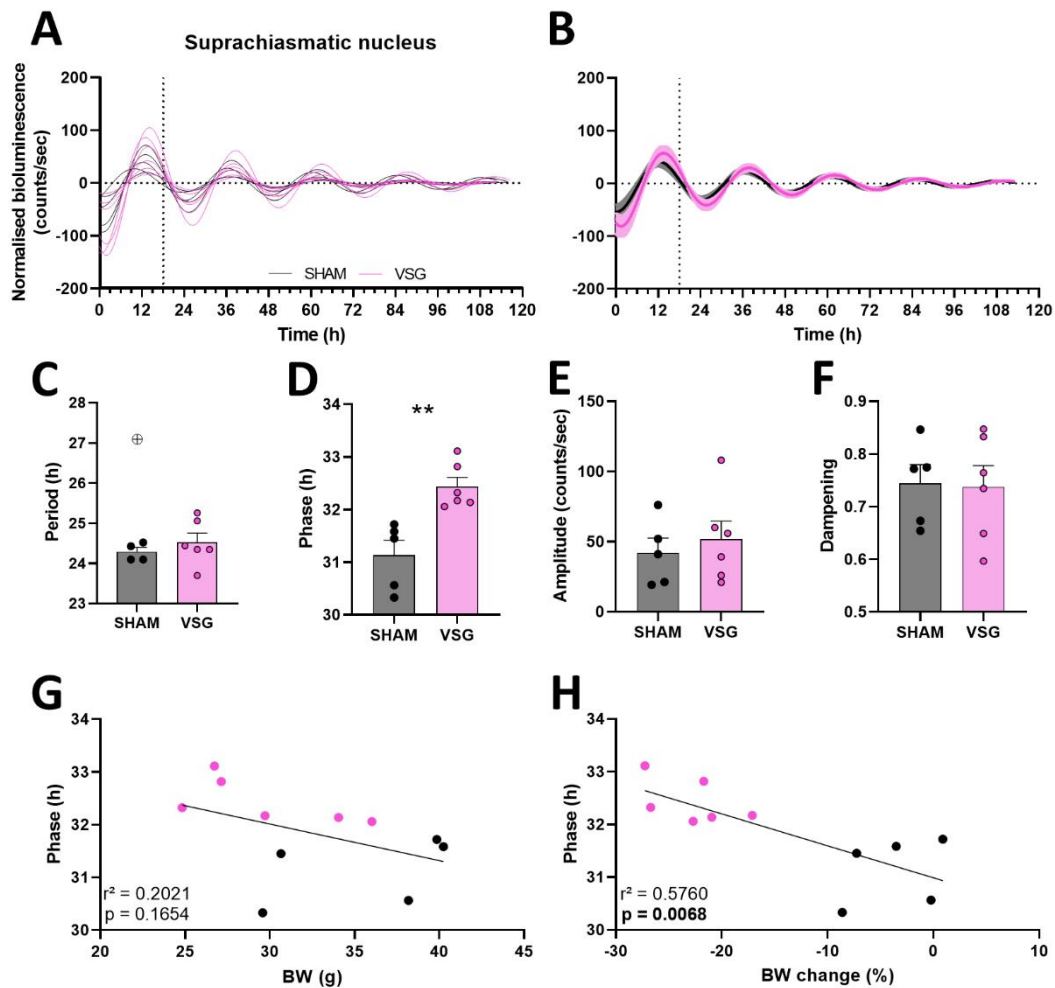


Figure 3.7: Tissue rhythms of SCN explants after surgery. [A] Dampened sine wave models of averaged tissue recordings per individual. [B] Average curve of grouped models. [C] Period, [D] phase, [E] amplitude, and [F] dampening of SCN tissue recording models, unpaired *t*-test. [G] Body weight and [H] body weight change at sacrifice plotted against phase values, simple linear regression, squared correlation coefficient and *p*-value stated. VSG/sham *n* = 6/5. Legend: crossed circle indicates 1 % outlier data point, unpaired *t*-test ** *p* < 0.01. Tissue preparation by Violetta Pilorz.

3.2.1.2 Adrenal gland

Adrenal glucocorticoids are major regulators of the circadian network (Balsalobre *et al.*, 2000). The adrenal clock receives input from the SCN but also integrates peripheral metabolic feedback (Heyde and Oster, 2019). As an important link between central and peripheral clock organisation, PER2 rhythms after metabolic surgery were evaluated (Fig. 3.8).

One to four adrenal slices per individual were cultured (Fig. 3.8 A, VSG: *n* = 6, sham: *n* = 7). Notably, sham curve-fits seemed greatly out of sync compared to VSG. There was no difference by type of surgery when comparing the average group rhythms (Fig. 3.8 B). Circadian parameters period (Fig. 3.8 C; VSG: 22.8 ± 0.19 h vs. sham: 23.1 ± 0.15 h, unpaired *t*-test), phase (Fig. 3.8 D; VSG: 23.2 ± 0.51 vs. sham: 26.8 ± 1.93 , unpaired *t*-test), amplitude (Fig. 3.8 E; VSG: 35.5 ± 7.05 counts/s vs. sham: 44.5 ± 8.49 counts/s, unpaired *t*-test) and dampening (Fig. 3.8 F; VSG: 0.71 ± 0.033 vs. sham:

0.80 ± 0.030 , unpaired t -test) were very similar between VSG and sham animals. However, as indicated by the out of sync individual sham curves, variances of phases between VSG and sham were significantly different (Fig. 3.8 A, D; F-test to compare variances, $p < 0.01$). Moreover, sham phase values proved to not have a significant direction of the mean (Fig. 3.8 G; Rayleigh z -test $p = 0.318$) in contrast to VSG (data not shown, $p < 0.001$). VSG induced a higher degree of synchronicity within the group possibly hinting at adrenal de-synchronicity in sham controls. Phase values, however, did not correlate with BW change (Fig. 3.8 H; simple linear regression).

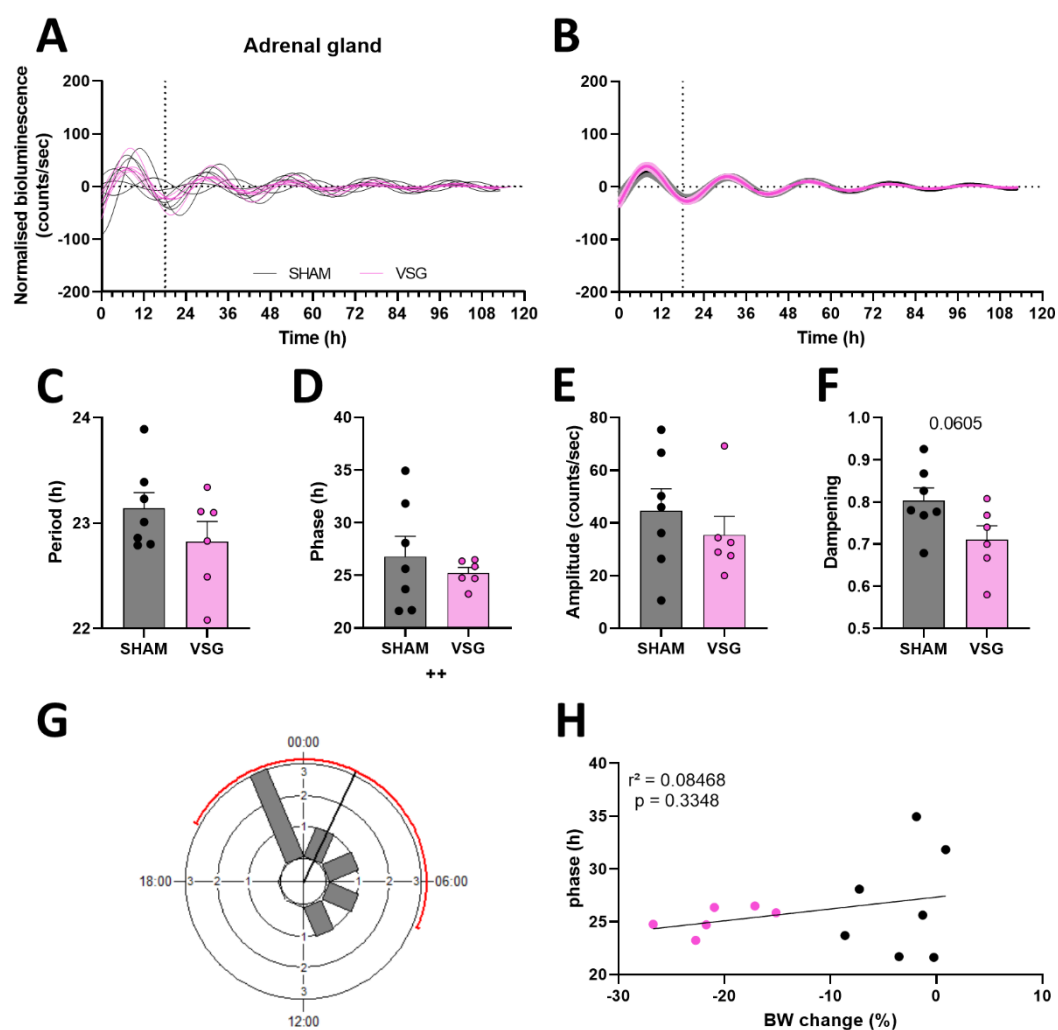


Figure 3.8: Tissue rhythms of the adrenal gland explants after surgery. [A] Dampened sine wave models of averaged tissue recordings per individual. [B] Average curve of grouped models. [C] Period, [D] phase, [E] amplitude, and [F] dampening of adrenal tissue recording models, unpaired t -test, trend p -value stated. [G] Circular plot of phase timing, Rayleigh z -test, red arch indicates standard deviation of mean vector direction. [H] Body weight change plotted against phase values, simple linear regression, squared correlation coefficient and p -value stated. VSG/sham $n = 6/7$. Legend: F-test to compare variances ++ $p < 0.01$.

3.2.1.3 Liver

The liver is particularly receptive to metabolic changes and liver rhythms were previously shown to react to metabolic feedback (Vollmers *et al.*, 2009; Sujino *et al.*, 2012). Thus, the effect of bariatric surgery on liver clock function was studied (Fig. 3.9).

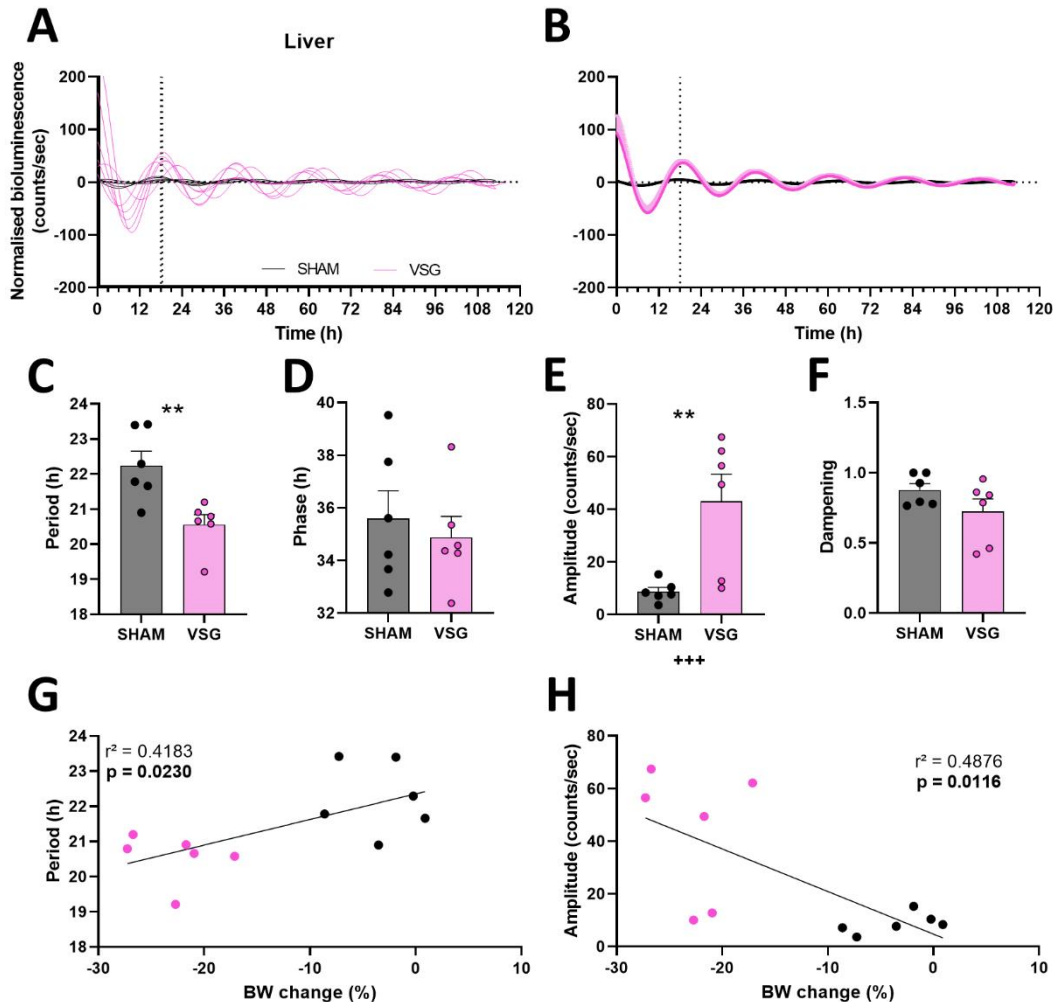


Figure 3.9: Tissue rhythms of liver explants after surgery. [A] Dampened sine wave models of averaged tissue recordings per individual. [B] Average curve of grouped models. [C] Period, [D] phase, [E] amplitude, and [F] damping of liver tissue recording models, unpaired *t*-test. [G] Body weight change plotted against period and [H] amplitude, simple linear regression, squared correlation coefficient and *p*-value stated. VSG/sham *n* = 6/6. Legend: ** *p* < 0.01, *F*-test to compare variances *** *p* < 0.001.

Slices of six VSG and six sham animals were recorded. Looking into individual and averaged curve fits, VSG livers clearly showed more pronounced rhythmicity compared to sham (Fig. 3.9 A, B). Without SCN input, VSG animals had an accelerated PER2 expression rhythm with a period of 20.6 ± 0.28 h vs. sham with 22.2 ± 0.41 h (Fig. 3.9 C, unpaired *t*-test, *p* < 0.01), while the phase remained unaffected (Fig. 3.9 D; VSG: 34.9 ± 0.80 h vs. sham: 35.6 ± 1.06 h, unpaired *t*-test). Moreover, amplitude after VSG was increased (Fig. 3.9 E; VSG: 57.4 ± 10.31 counts/s vs. sham: 11.7 ± 1.59 counts/s, unpaired *t*-test,

$p < 0.01$ with Welch's correction $p < 0.05$), whereas dampening showed no significant difference (Fig. 3.9 F; VSG: 0.72 ± 0.092 vs. sham: 0.88 ± 0.046 , unpaired t -test). Both altered circadian parameters, period and amplitude, correlated with BW change at the time (Fig. 3.9 G and Fig. 3.9 H, respectively; simple linear regression).

3.2.1.4 White adipose tissue

WAT is substantially restructured following bariatric surgery (see chapter 1.2.3.2). Therefore, as the final cultured tissue, WAT explants were recorded and analysed (Fig. 3.10, VSG/sham $n = 6/6$). Rhythms dampened slightly faster after VSG surgery (Fig. 3.10 A, B) and dampening rate had significantly different variances between groups (Fig. 3.10 F; VSG: 0.60 ± 0.071 vs. sham: 0.72 ± 0.025 , F-test to compare variances $p < 0.05$). However, no circadian parameter showed a significant difference of the means in direct comparison (Fig. 3.10 C-F; period VSG: 26.3 ± 1.13 h vs. sham: 26.8 ± 0.56 h; phase VSG: 35.6 ± 0.88 h vs. sham: 37.7 ± 1.05 h; amplitude VSG: 45.2 ± 18.93 counts/s vs. sham: 23.3 ± 8.03 counts/s; unpaired t -tests). Dampening did also not correlate with BW or BW change (data not shown; simple linear regression). In sum, circadian clock machinery in WAT seemed to be largely resistant to the metabolic changes 9 days after surgery.

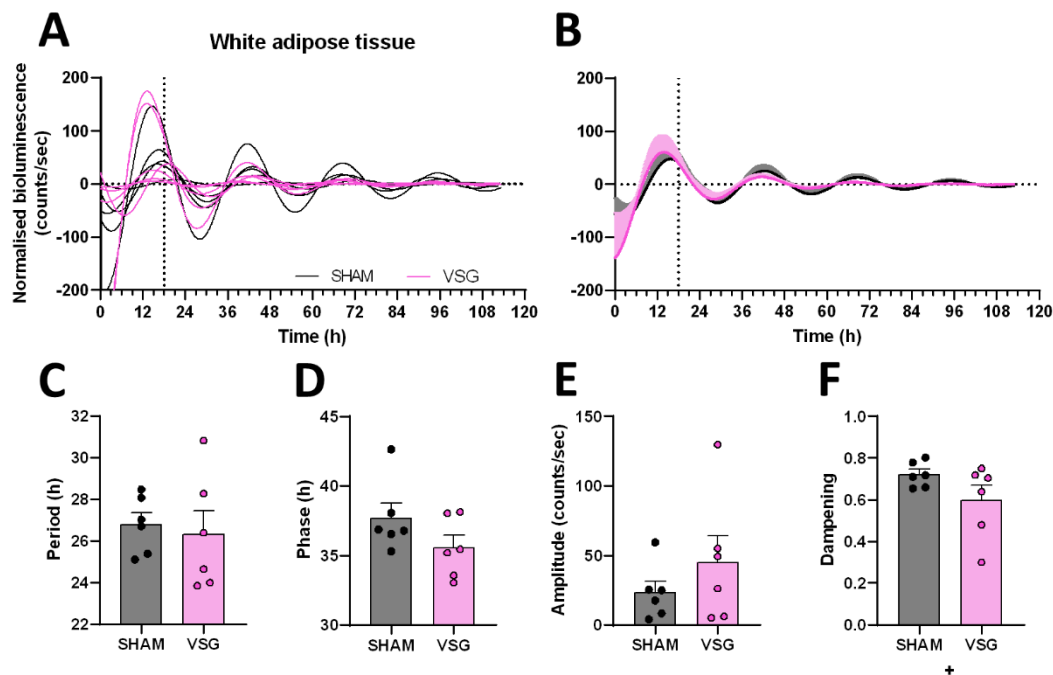


Figure 3.10: Tissue rhythms of WAT explants after surgery. [A] Dampened sine wave models of averaged tissue recordings per individual. [B] Average curve of grouped models. [C] Period, [D] phase, [E] amplitude, and [F] dampening of WAT tissue recording models, unpaired t -test. VSG/sham $n = 6/6$. Legend: F-test to compare variances + $p < 0.05$.

3.2.2 VSG reduces plasma concentrations of metabolic markers

3.2.2.1 Corticosterone

Adrenal clocks were less synchronised to the *zeitgeber* light in sham animals (see chapter 3.2.1.2). Therefore, corticosterone plasma concentrations were measured as an adrenal output factor. No rhythmicity was detected after either VSG or sham (Fig. 3.11; JTK_Cycle, $n = 4 - 6$ per time point per group). However, while corticosterone after VSG as expected was highest at the beginning of the active phase, such an increase was lacking in sham animals (ZT1 VSG: 5.88 ± 3.153 ng/ml vs. sham: 3.77 ± 0.994 ng/ml, ZT7 VSG: 13.85 ± 3.420 ng/ml vs. sham: 10.66 ± 2.570 ng/ml, ZT13 VSG: 18.40 ± 6.140 ng/ml vs. sham: 2.93 ± 0.752 ng/ml, ZT19 VSG: 16.88 ± 4.923 ng/ml vs. sham: 13.23 ± 3.945 ng/ml, 2-way ANOVA, ZT13 VSG vs. sham $p < 0.05$). Instead, sham corticosterone levels exhibited a second trough. Overall, baseline showed a trend towards increased secretion after VSG (VSG: 13.97 ± 2.396 ng/ml vs. sham: 8.17 ± 1.636 ng/ml, unpaired t -test, $p = 0.057$).

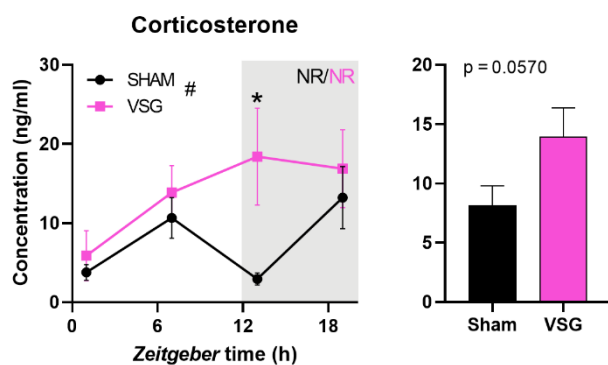


Figure 3.11: Diurnal variation and corresponding baseline of plasma corticosterone concentrations on day 9 after VSG. Statistics of daily profiles with 2-way ANOVA, Sidak's post hoc comparison, and JTK_Cycle, baseline comparison with unpaired t -test, trend p -value stated. $n = 4 - 6$ per group/time point. Legend: NR = no rhythm detected with JTK_Cycle $p < 0.05$, group effect # $p < 0.05$, direct comparison * $p < 0.05$. Measurement by Iwona Olejniczak.

3.2.2.2 Circulating lipids and adipokines

WAT mass loss is arguably the most dramatic effect of VSG-induced weight loss. Due to the unresponsiveness of PER2 rhythms of cultured WAT tissue explants from day 9 *post-surgery* to VSG, a deeper look into WAT functionality was conducted. Plasma levels of FFAs, TAGs, and the adipokines leptin and adiponectin were measured. All plasma levels were significantly reduced by VSG (Fig. 3.12 A-D, $n = 2-4$ per time point per group).

Independent of type of surgery, FFAs cycled significantly (Fig. 3.12 A; JTK_Cycle $p < 0.05$) and were highest during the middle of the dark and early light phase (ZT1 VSG: 858.5 ± 53.98 μ M vs. sham: 1505.5 ± 224.81 μ M, ZT7 VSG: 670.6 ± 251.83 μ M vs. sham: 778.3 ± 231.71 μ M, ZT13 VSG: 709.4 ± 89.48 μ M vs. sham: 1057.9 ± 133.66 μ M, ZT19 VSG: 896.0 ± 82.52 μ M vs. sham: 1737.1 ± 227.28 μ M). Moreover, concentrations were significantly different between groups at these time points (2-way ANOVA, ZT1 VSG vs. sham $p < 0.05$, ZT19 VSG vs. sham $p < 0.01$). Overall, VSG FFAs baseline was reduced (VSG: 742.1 ± 57.96 μ M vs. sham: 1269.7 ± 134.27 μ M, unpaired t -test, $p < 0.01$).

TAGs cycled significantly only in sham controls (Fig. 3.12 B; JTK_Cycle $p < 0.05$). Moreover, the time of peak concentrations was shifted from early morning in sham to late night in VSG (ZT1 VSG: 93.6 ± 1.95 mg/dl vs. sham: 155.5 ± 10.64 mg/dl, ZT7 VSG: 71.5 ± 4.39 mg/dl vs. sham: 117.2 ± 7.32 mg/dl, ZT13 VSG: 70.0 ± 13.43 mg/dl vs. sham: 97.8 ± 9.19 mg/dl, ZT19 VSG: 104.3 ± 14.75 mg/dl vs. sham: 121.1 ± 18.69 mg/dl). Concentrations were significantly different at ZT1 (2-way ANOVA, ZT1 VSG vs. sham $p < 0.01$). VSG surgery clearly decreased baseline levels (VSG: 85.7 ± 6.24 mg/dl vs. sham: 122.9 ± 7.67 mg/dl, unpaired t -test, $p < 0.001$).

Adiponectin concentrations lost rhythmicity after VSG surgery as compared to sham (Fig. 3.12 C; JTK_Cycle $p < 0.05$). Baseline secretion was downregulated (VSG: 75.4 ± 7.65 μ g/ml vs. sham: 115.3 ± 10.28 μ g/ml, unpaired t -test, $p < 0.01$). Along the day, significant difference occurred during the active phase peak (ZT1 VSG: 77.4 ± 23.40 μ g/ml vs. sham: 105.2 ± 11.44 μ g/ml, ZT7 VSG: 61.9 ± 3.17 μ g/ml vs. sham: 90.9 ± 8.31 μ g/ml, ZT13 VSG: 67.6 ± 11.13 μ g/ml vs. sham: 123.9 ± 16.86 μ g/ml, ZT19 VSG: 96.8 ± 7.74 μ g/ml vs. sham: 171.6 ± 39.04 μ g/ml, 2-way ANOVA, ZT19 VSG vs. sham $p < 0.05$).

The most pronounced VSG effects were seen for leptin concentrations (Fig. 3.12 D). Though neither sham nor VSG levels cycled significantly (JTK_Cycle), both displayed strong daily variations. Plasma leptin in sham controls was highest during the dark phase and peaked around ZT13, while in VSG levels were lowest during the active phase and highest in the inactive (light) phase (ZT1 VSG: 14.0 ± 6.96 ng/ml vs. sham: 23.6 ± 9.46 ng/ml, ZT7 VSG: 10.2 ± 3.66 ng/ml vs. sham: 24.8 ± 8.86 ng/ml, ZT13 VSG: 1.3 ± 0.05 ng/ml vs. sham: 55.0 ± 2.29 ng/ml, ZT19 VSG: 1.9 ± 0.57 ng/ml vs. sham: 38.3 ± 10.53 ng/ml, 2-way ANOVA, interaction $p < 0.05$, group effect $p < 0.0001$). Consequently, differences in the active phase were significant (ZT13 VSG vs. sham $p < 0.001$, ZT19 VSG vs. sham $p < 0.01$) and baseline was strongly reduced (VSG: 6.9 ± 2.46 ng/ml vs. sham: 33.9 ± 5.59 ng/ml, unpaired t -test, $p < 0.001$).

To summarize, all obesity-associated plasma concentrations were reduced on day 9 after VSG. FFAs were downregulated particularly during the active phase. TAGs peak plasma concentrations were shifted into the active phase. Somewhat surprisingly, also adiponectin levels were reduced during the night. Interestingly, leptin concentrations showed an antiphasic secretion after VSG. Hence, WAT functionality and circadian regulation of WAT activity appeared strongly affected by bariatric surgery.

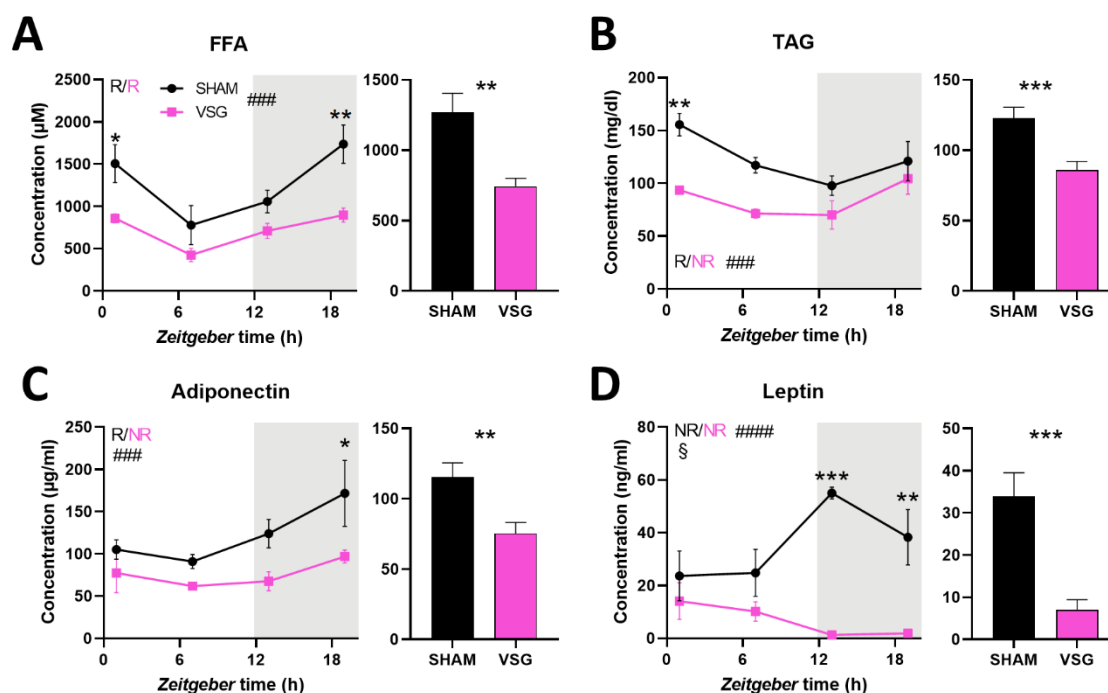


Figure 3.12: Daily variation of metabolic marker plasma concentrations and corresponding baseline levels on day 9 after VSG. [A] Concentrations of free fatty acids (FFAs), [B] triglycerides (TAGs), [C] adiponectin, and [D] leptin 9 days post-surgery. Daily profiles with 2-way ANOVA with Sidak's post hoc comparison and JTK_Cycle, baseline comparison with unpaired t-test. $n = 2-4$ per group/time point. Legend: R = rhythmicity detected with JTK_Cycle $p < 0.05$, NR = no rhythm, interaction $\$ p < 0.05$, group effect ##### $p < 0.0001$, ### $p < 0.001$, direct comparison *** $p < 0.001$, ** $p < 0.01$, * $p < 0.05$.

3.2.3 Remodelling of WAT transcriptome rhythms after VSG

Next, mRNA from subcutaneous WAT biopsies ($n = 4$ per group/time point) were sequenced and expression counts analysed. 18,124 transcripts were detected. The 1st principle component accounted for 46.59% of variances, the 2nd for 22.79% and the 3rd for 11.33% (Fig. 3.13 A). The two groups could be clearly separated in the principle component analysis, except for one sham animal. Nevertheless, this animal was not excluded from further analysis as it was not an outlier in any consecutive analyses. 426 differently expressed genes were detected with a $\log_2(\text{FC})$ of -3.01 (overexpressed in sham, $n = 163$) to -1.00 and 1.00 to 3.01 (overexpressed in VSG, $n = 263$). Using KEGG, these genes were associated with pathways of mostly the immune system (Fig. 3.13 B; 5/10). Additionally, genes of lipid metabolism (3/10) and "Neuroactive ligand-receptor interaction" were differently expressed. According to the KEGG database, the last is associated with, among other diseases, leptin deficiency.

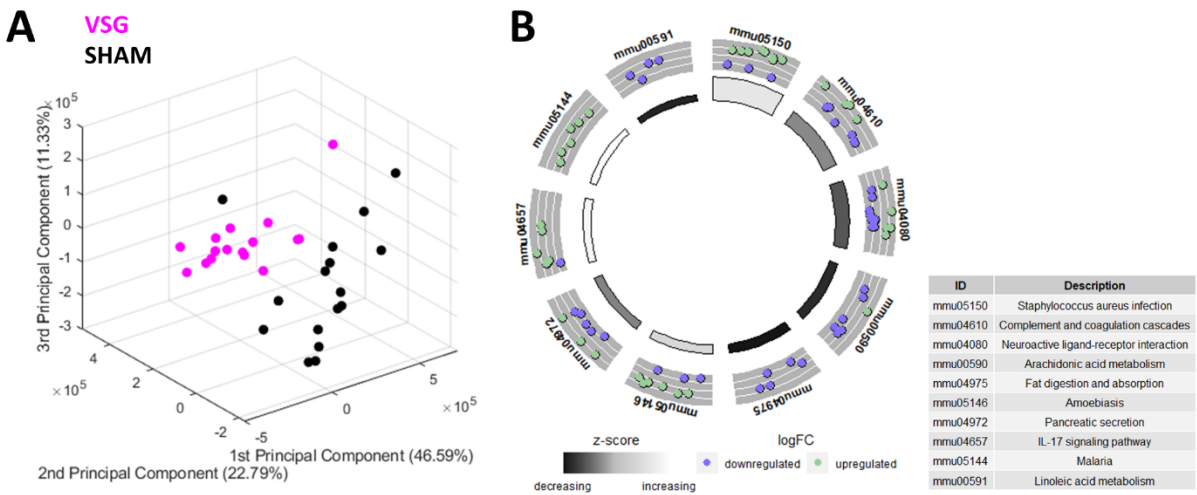


Figure 3.13: Principle component analysis and KEGG pathway enrichment of differently expressed genes. [A] Principle component analysis of 18,124 detected genes. [B] KEGG pathway enrichment of differently expressed genes detected by $\log_2(\text{FC})$ (here, $\log\text{FC}$) and legend of associated pathways.

To study the diurnal transcriptome, JTK_Cycle analysis was performed over all sequenced genes. In sham-operated mice, 2,493 transcripts were significantly rhythmic compared to 1,013 in VSG mice (JTK_CYCLE, $p < 0.05$). Combined with the 263 up- and 163 downregulated genes after VSG, a group of 3,039 differently regulated genes and 405 shared rhythmic genes were found (Fig. 3.14 A; Tab. S1). Using the Cytoscape plug-in BiNGO, a GO enrichment analysis against the whole mouse annotation library was conducted. Top10 GO categories included mostly metabolic processes (5/10) with a cluster frequency between 36.6 % and 23.3 % (Fig. 3.14 B). The most enriched category was “cellular process” with 52.7 %. Moreover, the resulting Cytoscape network showed five main clusters and one big subcluster (Fig. 3.14 C). The subcluster as well as one major cluster were associated with metabolic processes. The other clusters were of processes involved in development and cellular structure, organisation and transportation, biological regulation, and response mechanisms.

In summary, the broad transcriptome analyses indicated acute inflammatory processes in analysed WAT biopsies after VSG. Moreover, VSG induced a higher loss of rhythmic genes compared to a minor gain of rhythmicity. Pathways impacted by dysregulation included to a high degree metabolic pathways. To further clarify the effects on the rhythmic transcriptome, phase and amplitude of cycling genes as well as clock gene expression were evaluated.

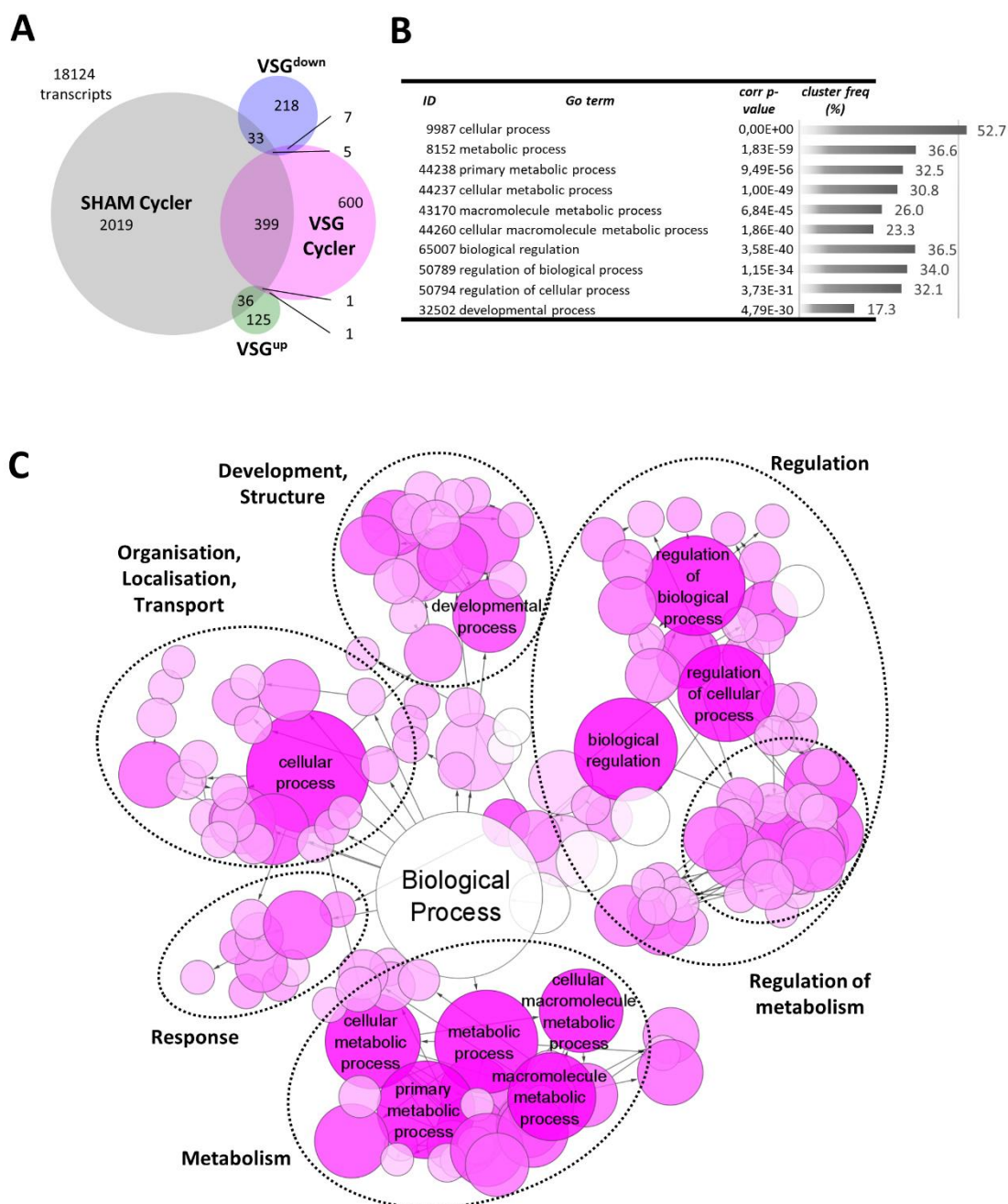


Figure 3.14: Differently regulated genes are metabolism-associated. [A] Venn diagram of rhythmic and up- or downregulated gene groups. [B] Top10 enriched gene ontology categories via Cytoscape plug-in BiNGO. [C] Cytoscape network as a result of the complete BiNGO analysis. Node size was limited to > 16 and corresponds to test genes annotated to gene set, colour to enrichment p-values. Clusters were identified using Cytoscape's search engine with key words.

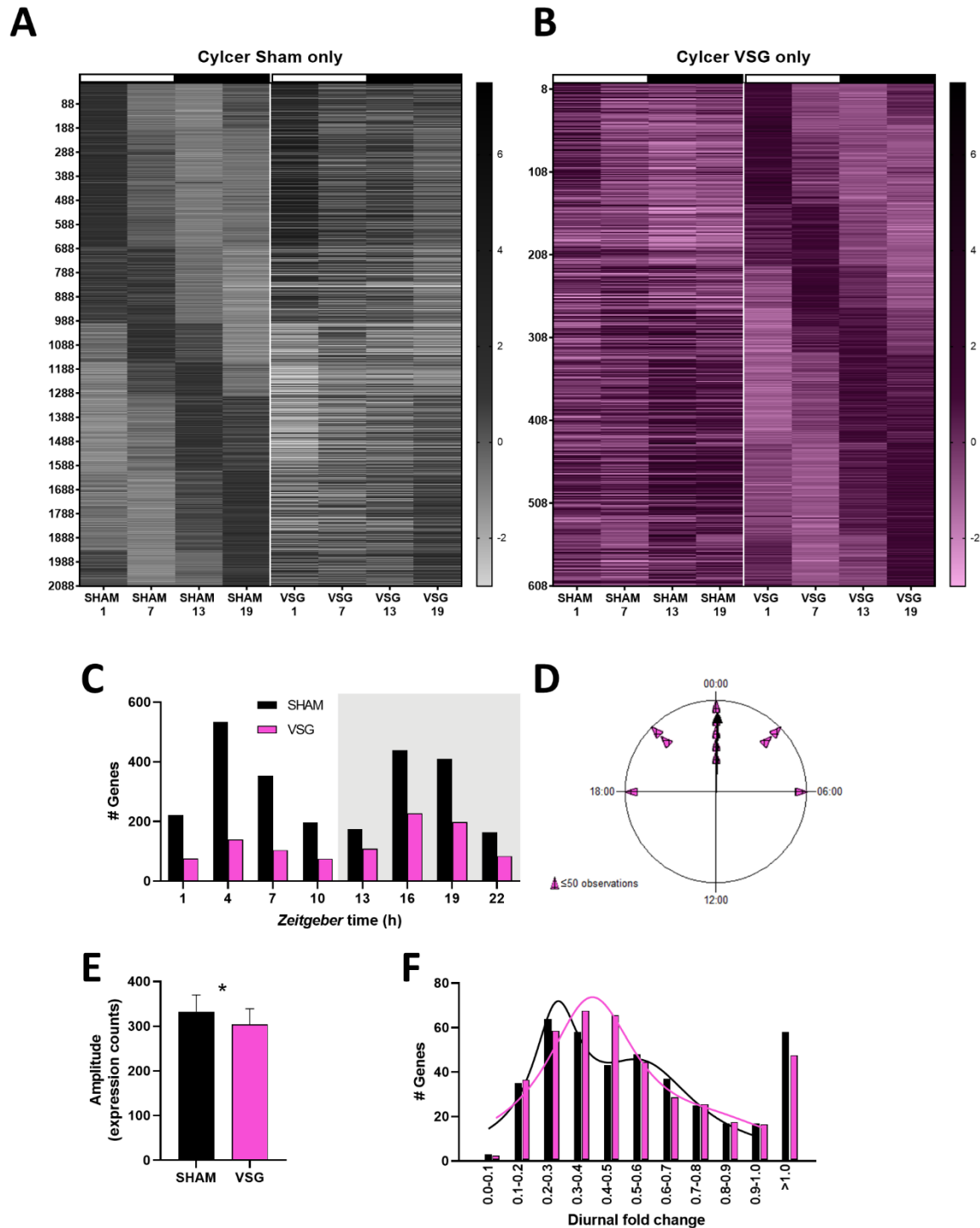


Figure 3.15: Modulation of transcriptome rhythms by VSG. [A] Normalised expression (ZT-SD-controlled z-score) of genes significantly rhythmic in sham only and sorted by sham-phase compared to VSG expression, and [B] of genes significantly rhythmic in VSG only sorted by VSG-phase compared to sham expression. Rhythmicity analysis via JTK_Cycle, $p < 0.05$. [C] Distribution of peak times of rhythmic genes in sham and VSG. [D] ± 12 -hour phase shifts of common cyclus genes grouped by max. 50 observations per symbol. [E] JTK amplitude comparison of common cyclus, paired t-test. [F] Distribution of diurnal FC of common cyclus, curve fits with sum of Lorentzians to show peak(s) of distribution. Legend: * $p < 0.05$.

Rhythmic genes of each group were phase-sorted. After the exclusion of common cyclers, *i.e.* genes with rhythmic expression after VSG and sham, the part of the transcriptome cycling significantly only in WAT of sham controls showed diffuse diurnal expression in VSG and *vice versa* (Fig. 3.15 A, B; JTK_Cycle $p < 0.05$). Next, peak distribution of all genes detected as rhythmic in either one of the groups were compared. Cycling genes showed a biphasic expression pattern with increased numbers peaking during the middle of the day and night (Fig. 3.15 C; VSG vs. sham: ZT1 76 vs. 222, ZT4 140 vs. 534, ZT7 104 vs. 354, ZT10 75 vs. 196, ZT13 109 vs. 175, ZT16 227 vs. 438, ZT19 198 vs. 410, ZT22 84 vs. 164, peak calculation JTK_Cycle). Overall, 52.39 % of cycling genes in sham controls peaked during the day compared to only 38.99 % in VSG. In sham-operated mice, most genes peaked at ZT4 (VSG: 13.82 % vs. sham: 21.42 %) compared to ZT16 in VSG mice (sham: 17.57 % vs. VSG: 22.41 %). Genes rhythmic in both surgical groups displayed similar phasing (Fig. 3.15 D; $n = 405$, mean \pm 12-hour phase shift 0.08 h) and only slight alterations in amplitudes (Fig. 3.15 E; VSG: 303.5 ± 35.33 counts vs. sham: 332.6 ± 33.55 counts, paired t-test, $p < 0.05$). Interestingly, amplitude distribution across the genes rhythmic under both conditions was slightly shifted towards higher middle range values after VSG in parallel to a loss of genes with a FC > 1.0 (Fig. 3.15 F; sum of two Lorentzians curve-fit, data Tab. S2).

These specific changes of general transcriptome regulation were contrasted by a largely unaffected core clock machinery (Fig. 3.16 A-I; data Tab. S3). *Bmal1*, *Dbp*, *Per1*, *Per2*, *Nr1d1*, *Nr1d2*, and *Cry1* showed no significant differences in daily expression of mRNA between surgical groups. However, *Dbp* showed a trend towards higher expression levels during the light phase in VSG mice (Fig. 3.16 B; ZT7 VSG vs. sham $p = 0.075$). Noted exceptions were *Clock* (Fig. 3.16 C; amplitude VSG: 206.08 counts vs. sham: 161.96 counts, mean expression VSG: 1337.2 ± 64.51 counts vs. sham: 1556.4 ± 46.05 counts, 2-way ANOVA, group effect $p < 0.01$, ZT1 VSG vs. sham $p < 0.05$) and the *Clock* paralogue *Npas2* (Fig. 3.16 F; amplitude VSG: 97.09 counts vs. sham: 72.57 counts, mean expression VSG: 101.0 ± 20.77 counts vs. sham: 80.6 ± 21.30 counts, 2-way ANOVA, group effect $p < 0.05$, ZT19 VSG vs. sham $p < 0.05$). Moreover, all selected clock genes, but *Clock*, showed pronounced daily FC variation (clock genes mean: VSG: 1.31 ± 0.162 , 0.41 to 1.92, vs. sham: 1.34 ± 0.215 , 0.23 to 2.48, *Clock* FC VSG: 0.41 vs. sham: 0.23). Furthermore, *Clock* diurnal FC was increased after VSG. *Clock* expression was reduced during the light phase and the beginning of the dark phase. Maximum measured expression was shifted from early day to late night, though JTK_Cycle did not detect different peak times (VSG: ZT1 vs. sham: ZT1).

Overall, the rhythmic transcriptome of WAT in VSG appeared blunted with a shift towards nighttime peak phases and very partially increased amplitudes. Despite the effects on potentially clock controlled genes or pathways, core clock component mRNA regulation was largely normal. This affirms the results from the bioluminescence recordings of PER2 expression in WAT and the conclusion of a stable tissue core clock.

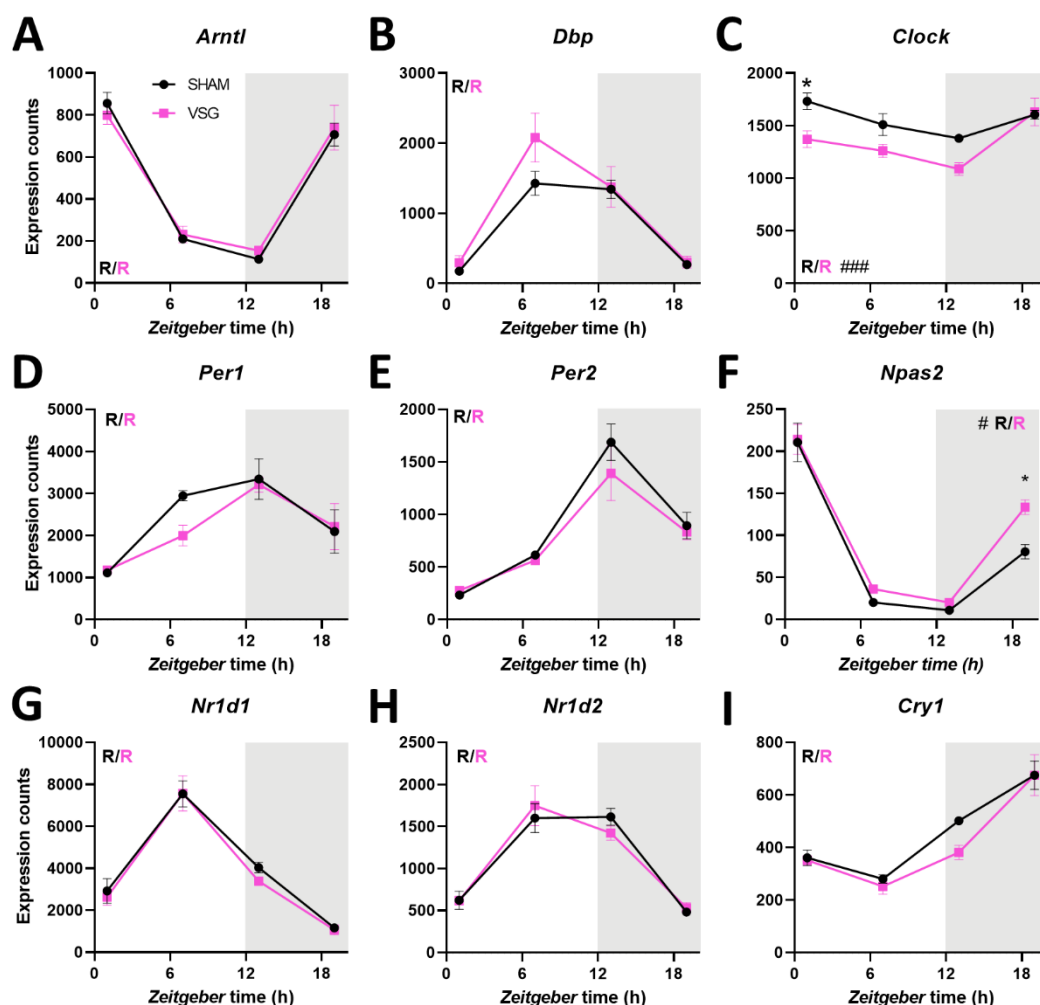


Figure 3.16: Clock gene machinery mRNA expression after bariatric surgery. Expression counts of clock genes [A] *Bmal1* (*Arntl*), [B] *Dbp*, [C] *Clock*, [D] *Per1*, [E] *Per2*, [F] *Npas2*, [G] *Nr1d1*, [H] *Nr1d2* and [I] *Cry1*. $n = 4$ per group/time point. Legend: R = Rhythmicity detected with *JTK_Cycle* $p < 0.05$, group effect ### $p < 0.001$, # $p < 0.05$, *Sidak's* post hoc comparison * $p < 0.05$.

3.2.4 VSG changes metabolism-associated gene expression

Given the clustering of metabolic processes enriched among the differently regulated genes, lipid and glucose metabolism were analysed further. Sham control-normalised expression of pathway-associated genes were compared to screen for potentially affected pathways (Fig. S1-3). Moreover, adipokine gene expression was investigated to confirm effects seen in diurnal plasma concentrations.

3.2.4.1 Lipid metabolism

Pathways of lipid homeostasis were evaluated. Catabolic processes (e.g. fatty acid breakdown) seemed slightly upregulated during the day and rather downregulated during the night by bariatric surgery, though none of these effects were significant (Fig. 3.17 A; 31 genes compared, ZT1 VSG: 1.05 ± 0.215 vs. sham: 0.99 ± 0.080 , ZT7 VSG: 1.09 ± 0.095 vs. sham: 0.93 ± 0.046 , ZT13 VSG: 0.99 ± 0.084 vs. sham:

0.92 ± 0.032 , ZT19 VSG: 0.95 ± 0.053 vs. sham: 1.16 ± 0.083 , 2-way ANOVA). No baseline change was detected (Fig. 3.17 B; 2.13 ± 7.050 , one sample *t*-test). Comparing the change of phase per time point between VSG and sham after baseline correction, the increase during day in parallel to the decrease during the night led to a diurnal pattern (Fig. 3.17 C; JTK_Cycle $p < 0.05$, ZT1 -2.11 ± 4.694 , ZT7 49.13 ± 34.920 , ZT13 11.10 ± 9.463 , ZT19 -6.40 ± 5.173). This indicates a phase-specific upregulation of transcriptional activity during the rest phase.

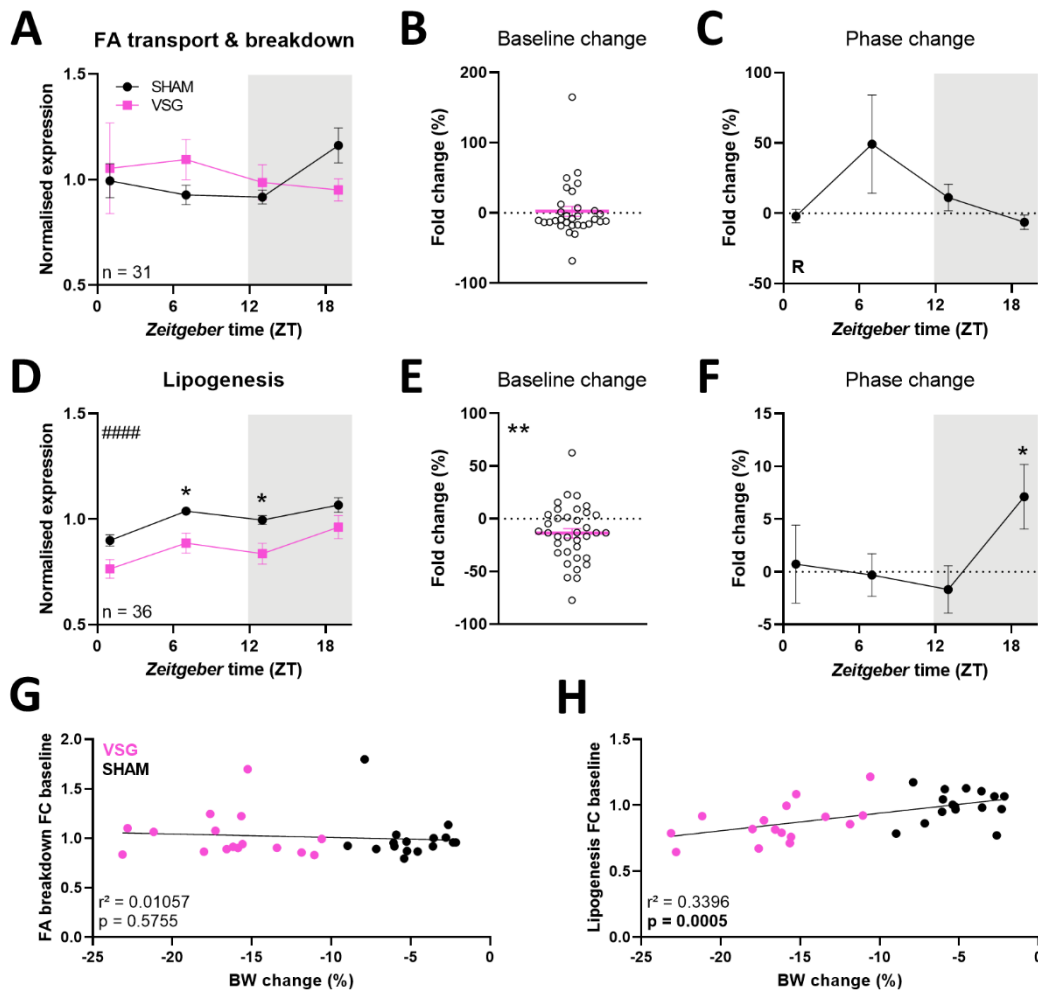


Figure 3.17: Diurnal regulation of lipid homeostasis pathways. [A] Expression of fatty acid (FA) transport and breakdown-associated genes normalised to sham controls, 2-way ANOVA + Sidak's post hoc test. [B] Change in baseline expression of these genes by VSG, one sample *t*-test against the hypothetical mean 0. [C] Change in phase-dependent baseline-normalised expression of these genes. [D] To sham control normalised expression of lipogenesis genes, 2-way ANOVA + Sidak's post hoc. [E] Change in baseline expression of these genes by VSG, one sample *t*-test against the hypothetical mean 0. [F] Change in phase-dependent of baseline-normalised expression of these genes, one sample *t*-tests against the hypothetical mean 0. [G] FA breakdown and [H] lipogenesis baseline expression plotted against weight change at sacrifice, simple linear regression, squared correlation coefficient and corresponding *p*-value stated. Legend: R = rhythmicity detected with JTK_Cycle $p < 0.05$, group effect #### $p < 0.0001$, direct comparison ** $p < 0.01$, * $p < 0.05$.

In contrast, anabolic processes (lipogenesis) were globally downregulated by VSG (Fig. 3.17 D; 36 genes compared, ZT1 VSG: 0.76 ± 0.045 vs. sham: 0.90 ± 0.027 , ZT7 VSG: 0.89 ± 0.047 vs. sham: 1.04 ± 0.019 , ZT13 VSG: 0.84 ± 0.049 vs. sham: 1.00 ± 0.035 , ZT19 VSG: 0.96 ± 0.055 vs. sham:

1.07 ± 0.035 , 2-way ANOVA, group effect $p < 0.0001$). In both conditions, expression was increased during the active phase but had an additional smaller peak during the rest phase. Expectably, baseline levels were significantly reduced by ca. 14 % after VSG (Fig. 3.17 E; -13.74 ± 4.488 , one sample t -test, $p < 0.01$). Even though the expression pattern between VSG and sham seemed very alike, comparing the phase change of baseline-normalised expression revealed an upregulation specifically during the late active phase (Fig. 3.17 F; ZT1: 0.73 ± 3.699 , ZT7: -0.31 ± 2.028 , ZT13: -1.68 ± 2.245 , ZT19: 7.12 ± 3.048 , one sample t -tests, ZT19 $p < 0.05$).

While fatty acid catabolism showed an upregulation in associated mRNA expression during the day, lipogenesis regulation was upregulated during the night. Moreover, normalised expression baseline of lipogenesis correlated significantly with weight change at sacrifice, whereas baseline of fatty acid breakdown did not (Fig. 3.17 G, H; simple linear regression). Conclusively, lipid metabolism was affected by VSG in, both, a baseline and phase-dependent manner. To elaborate on these results, exemplary key enzymes of other lipid-associated pathways (*i.e.* lipolysis, cholesterol biosynthesis, ketone body metabolism; Fig. 3.18, data in Tab. S4) were evaluated.

Lip encodes for the Lipoprotein lipase and hydrolyses TAGs from lipoproteins. Expression was significantly reduced (Fig. 3.18 A; 2-way ANOVA, group effect $p < 0.0001$). Similarly, expression of *Pnpla3* (Patatin like phospholipase domain containing 3, the triacylglycerol lipase of the adipocytes) and *Lipf* (Gastric triacylglycerol lipase) was downregulated (Fig. 3.18 B, C; 2-way ANOVA, group effect $p < 0.001$ and $p < 0.0001$, respectively). These genes break down mostly circulating TAGs to diacylglycerides and fatty acids. Expression of *Lipe* (Hormone-sensitive lipase), which degrades intracellular lipid droplets, was unchanged (data not shown, 2-way ANOVA).

Cholesterol biosynthesis is high during the rest phase. This was reflected in sham expression of all three sterol synthesis genes investigated. *Hmgcs1* encodes for HMG-CoA synthase 1, an essential early enzyme of the pathway. The expression was strongly decreased by VSG (Fig. 3.18 D; 2-way ANOVA, group effect $p < 0.0001$). Moreover, expression lost its rhythmicity after bariatric surgery (JTK_Cycle $p < 0.05$). Daily variation was less clear in VSG compared to sham. For *Hmgcr*, however, which encodes for the rate-limiting HMG-CoA reductase of the mevalonate pathway, no such pronounced effects were seen, but a trend towards reduced expression was detected (Fig. 3.18 E; 2-way ANOVA, $p = 0.0780$). *Sqle* encodes for squalene monooxygenase and is considered one of the rate-limiting steps later in sterol biosynthesis. Here, expression was again reduced (Fig. 3.18 F; 2-way ANOVA, group effect $p < 0.001$).

Lastly, ketone body metabolism was evaluated. The transcripts of two anabolic enzymes, *Hmgcs2* (HMG-CoA synthase 2) and *Hmgcl* (HMG-CoA lyase), were both significantly upregulated after VSG (Fig. 3.18 G, H; 2-way ANOVA, group effect $p < 0.0001$ and $p < 0.001$, respectively). Additionally, VSG

expression rhythms of *Hmgcl* appeared antiphasic compared to those in sham, with the highest expression in the middle of the rest phase (VSG) vs. the end of the active phase (sham). Expression of the catabolic enzyme *Oxct1* (3-oxoacid CoA-transferase 1), however, was decreased after VSG (Fig. 3.18 I; 2-way ANOVA, group effect $p < 0.0001$). These results indicated a consistent upregulation of ketone body production in WAT.

In summary, lipid metabolism in WAT is diversely affected by bariatric surgery. A decrease of lipogenesis, lipolysis, and sterol synthesis was detected. A shift towards ketone body metabolism was indicated. Moreover, VSG impacted transcriptional regulation of some lipid pathways in a phase-dependent manner.

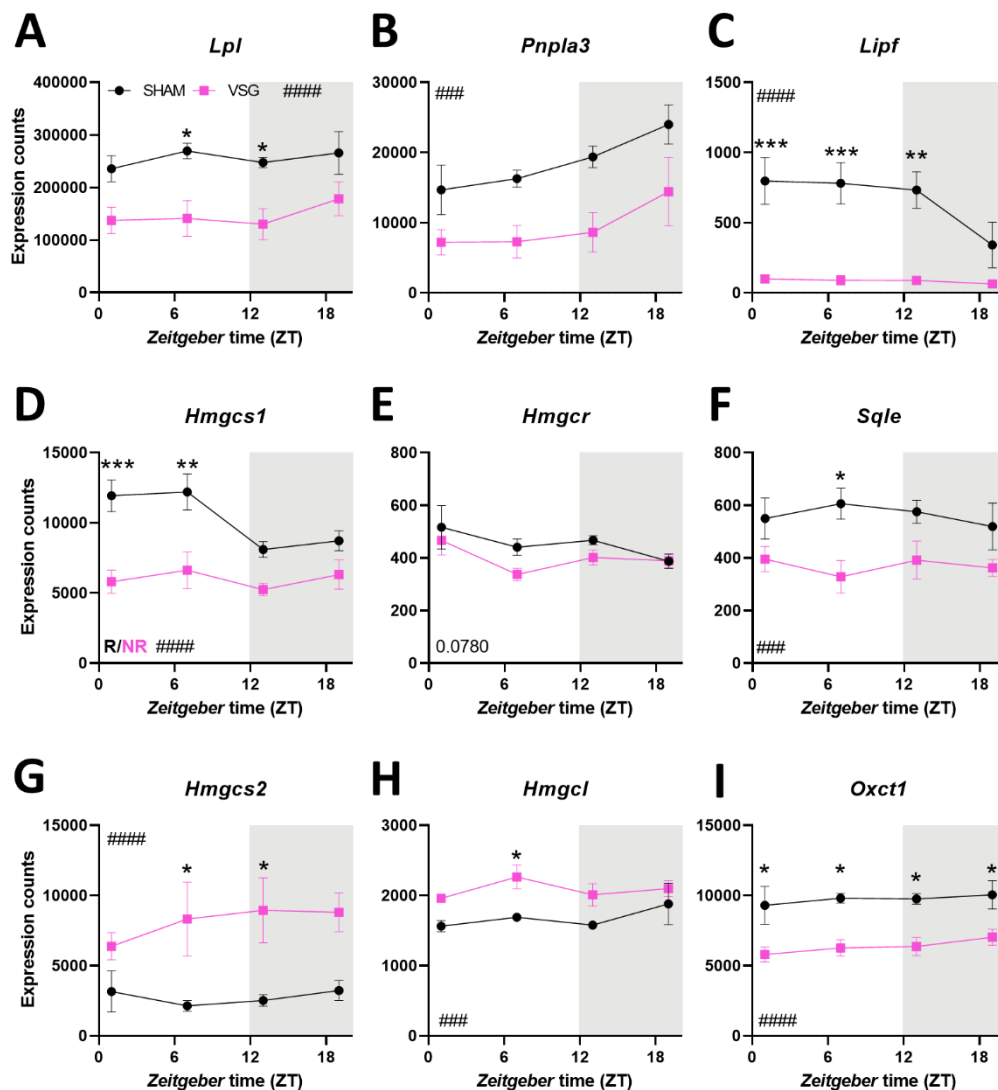


Figure 3.18: Expression of exemplary genes of specific lipid pathways. Lipolysis genes [A] *Lpl*, [B] *Pnpla3*, [C] *Lipf*, sterol synthesis genes [D] *Hmgcs1*, [E] *Hmgcr* (group effect p -value stated), [F] *Sqle*, and ketone body metabolism genes [G] *Hmgcs2*, [H] *Hmgcl*, [I] *Oxct1*, 2-way ANOVA. $n = 4$ per group/time point. Legend: R = rhythmicity detected with JTK_Cycle $p < 0.05$, NR no rhythm, group effect ##### $p < 0.0001$, ### $p < 0.001$, Sidak's post hoc comparison *** $p < 0.001$, ** $p < 0.01$, * $p < 0.05$.

3.2.4.2 Glucose metabolism and citric acid cycle

Since diurnal regulation of lipid metabolism was affected by bariatric surgery, other metabolic pathways were studied. Glucose metabolism, pyruvate breakdown, and the tricarboxylic acid (TCA) cycle were evaluated for their baseline- and phase-dependent changes.

When looking into genes associated with glucose metabolism, no significant differences were observed (Fig. 3.19 A-C, $n = 28$). VSG phase seemed to be slightly delayed compared to sham with the peak occurring at ZT19 vs. ZT13 after sham (Fig. 3.19 A; ZT1 VSG: 1.01 ± 0.083 vs. sham: 1.00 ± 0.046 , ZT7 VSG: 0.95 ± 0.064 vs. sham: 0.95 ± 0.038 , ZT13 VSG: 0.93 ± 0.063 vs. sham: 1.04 ± 0.072 , ZT19 VSG: 1.14 ± 0.119 vs. sham: 1.01 ± 0.045 , 2-way ANOVA). However, a phase-dependent change was not detected (Fig. 3.19 C, ZT1: 1.13 ± 3.581 , ZT7: 0.89 ± 3.186 , ZT13: -0.53 ± 6.606 , ZT19: 27.00 ± 22.939 , one sample t -tests); neither was a baseline change (Fig. 3.19 B; 0.67 ± 5.670 , one sample t -test).

Genes that are specific for either glycolysis or gluconeogenesis were evaluated next (Fig. 3.19 D-F, Fig. S4). Due to the low number of genes ($n = 8$ and $n = 5$, respectively) some effects may have been masked by high variations. When sham-normalised, glycolysis-specific gene expression showed a similar trend towards a phase delay as global glucose metabolism (Fig. 3.19 D; ZT1 VSG: 0.95 ± 0.190 vs. sham: 0.98 ± 0.092 , ZT7 VSG: 0.90 ± 0.156 vs. sham: 1.00 ± 0.033 , ZT13 VSG: 0.98 ± 0.169 vs. sham: 1.08 ± 0.055 , ZT19 VSG: 0.99 ± 0.091 vs. sham: 0.93 ± 0.046 , 2-way ANOVA). Here, phase-dependent changes of expression regulation were detected (Fig. 3.19 F; ZT1: 2.70 ± 10.516 , ZT7: -7.81 ± 6.644 , ZT13: -4.02 ± 5.564 , ZT19: 18.69 ± 5.217 , one sample t -tests, ZT19 $p < 0.01$, JTK_Cycle $p < 0.05$). No change of baseline expression was found (Fig. 3.19 E; -4.77 ± 14.775). Gluconeogenesis-specific genes did not show significant alterations in any of the analyses (Fig. S4).

In summary, glucose metabolism-associated genes were not strongly affected by bariatric surgery. Glycolysis-specific genes showed a change of phase-related regulation with an increase of transcriptional activity during the middle of the night. Though regulation of WAT glucose metabolism seemed largely resistant to the metabolic impact of VSG, the downstream pathway of pyruvate breakdown and the metabolic centre pathway TCA cycle were both significantly altered (Fig. 3.20 A-F).

Genes involved in pyruvate breakdown were significantly decreased by VSG compared to sham (Fig. 3.20 A; $n = 9$, ZT1 VSG: 0.62 ± 0.022 vs. sham: 0.89 ± 0.016 , ZT7 VSG: 0.80 ± 0.027 vs. sham: 1.02 ± 0.018 , ZT13 VGS: 0.73 ± 0.014 vs. sham: 1.00 ± 0.008 , ZT19 VSG: 0.87 ± 0.030 vs. sham: 1.09 ± 0.022 , 2-way ANOVA, group effect $p < 0.0001$). Baseline expression levels were reduced by ca. 25 % (Fig. 3.20 B; -24.61 ± 1.978 , one sample t -test, $p < 0.0001$). Phase-dependent regulation from baseline-normalised expression profiles revealed a more pronounced biphasic pattern with lower minima and higher maxima after VSG (Fig. 3.20 C; ZT1: -6.62 ± 1.528 , ZT7: 3.52 ± 1.857 , ZT13: -3.53 ± 2.204 , ZT19: 5.81 ± 1.931 , one sample t -tests, ZT1 $p < 0.01$, ZT19 $p < 0.05$).

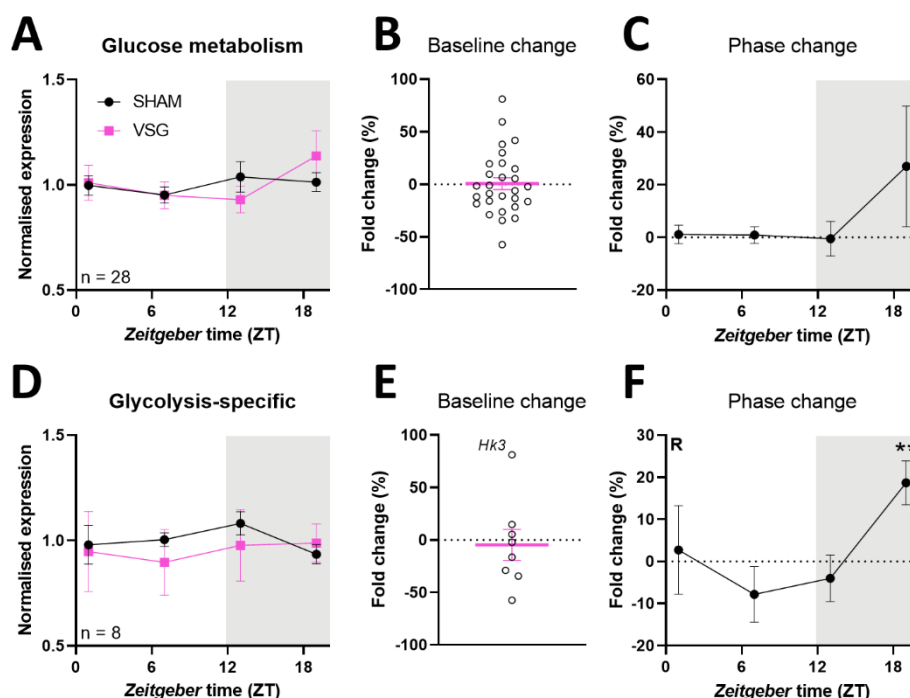


Figure 3.19: Regulation of glucose metabolism after bariatric surgery. [A] Expression of glucose metabolism genes normalised to sham controls, 2-way ANOVA. [B] Change of baseline expression of these genes by VSG, one sample t-test against hypothetical mean 0. [C] Change of phase-dependent baseline-normalised expression, one sample t-tests against hypothetical mean 0. [D] Sham-normalised gene expression of glycolysis-specific genes, 2-way ANOVA. [E] Change of baseline expression by VSG of these genes, Hk3 is stated since its regulation showed a markedly different direction but was statistically no outlier, one sample t-test against hypothetical mean 0. [F] Change of phase-dependent baseline-normalised expression, one sample t-tests against hypothetical mean 0. Legend: R = rhythmicity detected with JTK_Cycle $p < 0.05$, ** $p < 0.01$.

A similar picture was seen when looking into the genes involved in the TCA cycle. Again, VSG led to a decrease of gene expression except at ZT7 (Fig. 3.20 D; $n = 19$, ZT1 VSG: 0.82 ± 0.020 vs. sham: 0.91 ± 0.009 , ZT7 VSG: 1.00 ± 0.025 vs. sham: 1.02 ± 0.011 , ZT13 VSG: 0.84 ± 0.019 vs. sham: 0.95 ± 0.008 , ZT19 VSG: 1.01 ± 0.019 vs. sham: 1.12 ± 0.012 , 2-way ANOVA, group effect $p < 0.0001$, interaction $p < 0.05$). Baseline was reduced by ca. 8 % (Fig. 3.20 E; -8.13 ± 1.949 , one sample t-test, $p < 0.001$). Transcriptional activity of daily expression was upregulated during the middle of light phase and downregulated during night and the beginning of the light phase (Fig. 3.20 F; ZT1: -2.41 ± 0.894 , ZT7: 6.55 ± 0.874 , ZT13: -2.69 ± 0.736 , ZT19: -1.29 ± 1.277 , one sample t-tests, ZT1 $p < 0.05$, ZT7 $p < 0.0001$, ZT13 $p < 0.01$).

Taken together, these results indicated a largely unaffected regulation of glucose metabolism, whereas gene expression of pyruvate breakdown and TCA cycle was strongly reduced with more pronounced daily biphasic expression patterns. Phase-dependent activity of transcription was particularly upregulated for pyruvate breakdown during the late night and downregulated in the early morning, while TCA cycle genes were also downregulated in the early morning, but significantly upregulated during the middle of the day.

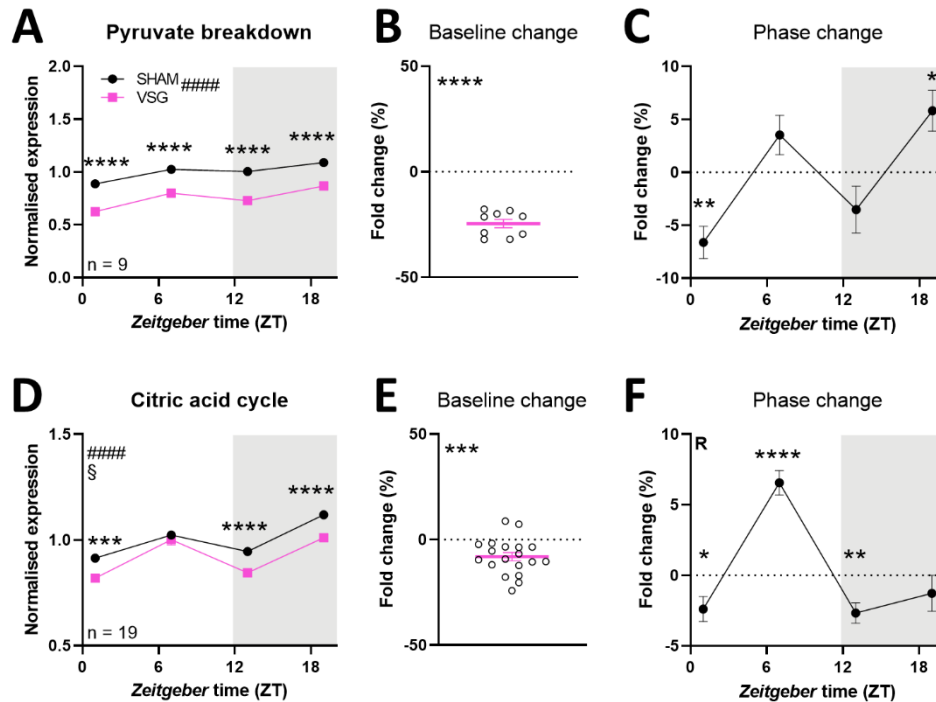


Figure 3.20: Regulation of pyruvate breakdown and citric acid cycle. [A] Expression of pyruvate breakdown genes normalised to sham controls, 2-way ANOVA + Sidak's post hoc test. [B] Change of baseline expression of these genes by VSG, one sample t-test against hypothetical mean 0. [C] Change of phase-dependent baseline-normalised expression of pyruvate breakdown genes, one sample t-tests against hypothetical mean 0. [D] Sham-normalised gene expression of citric acid cycle genes, 2-way ANOVA + Sidak's post hoc. [E] Change of baseline expression of these genes by VSG, one sample t-test against hypothetical mean 0. [F] Change of phase-dependent baseline-normalised expression of citric acid cycle genes, one sample t-tests against hypothetical mean 0. Legend: R=rhythmicity detected with JTK_Cycle $p < 0.05$, interaction § $p < 0.05$, group effect #### $p < 0.0001$, direct comparison **** $p < 0.0001$, *** $p < 0.001$, ** $p < 0.01$, * $p < 0.05$.

3.2.4.3 Adipokines

Lastly, to get a better idea on WAT functionality, adipokine gene expression was compared between surgical conditions. In plasma, leptin and adiponectin were significantly downregulated 9 days *post*-surgery after VSG. Here, *Lep* (Leptin), *Adipoq* (Adiponectin), *Ap1n* (Apelin), *Rarres2* (Chemerin), *Serpine1* (PAI-1) and *Ccl2* (CCL2 or MCP1, Monocyte chemoattractant protein 1) mRNA levels were evaluated (Fig. 3.21; data in Tab. S5).

In line with the changes observed for plasma concentration levels, *Lep* expression was strongly downregulated at all recorded time points (Fig. 3.21 A; 2-way ANOVA, $p < 0.0001$). However, contrary to the plasma values, no strong daily variation was detected in either VSG or sham animals (JTK_Cycle, 2-way ANOVA time effect $p = 0.4608$, interaction $p = 0.6973$). *Adipoq* expression was also reduced, but by a much smaller margin (Fig. 3.21 B; 2-way ANOVA, group effect $p < 0.05$). Again, contrary to the plasma concentrations, no rhythms in mRNA expression were detected in either surgical group (JTK_Cycle). This indicates that daily variation of leptin and adiponectin largely depend on *post*-transcriptional mechanisms and VSG is primarily reducing baseline expression.

Expression of *Apln*, an adipokine factor increased in obesity, was reduced by VSG (Fig. 3.21 C; 2-way ANOVA, group effect $p < 0.0001$). While expression in sham decreased from morning to middle of the night, in VSG expression remained mostly steady across the day. Gene expression *Rarres2*, an adipokine that stimulates intracellular droplet lipolysis, in turn, was increased after VSG (Fig. 3.21 D, 2-way ANOVA, group effect $p < 0.01$). PAI-1 is increased in obesity and *Serpine1* was significantly reduced by VSG (Fig. 3.21 E; 2-way ANOVA, group effect $p < 0.0001$). Moreover, reduced mRNA levels were specifically observed during the light phase (interaction $p < 0.01$, ZT1 VSG vs. sham $p < 0.05$, ZT7 $p < 0.0001$), whereas nighttime expression was not much different between groups. *Serpine1* mRNA cycled in both surgical groups, but with a reduced amplitude in VSG (JTK_Cycle $p < 0.05$, VSG: 722.81 counts vs. sham: 2045.11 counts). Gene expression of metaflammation-associated *Ccl2* was reduced during the early light phase (Fig. 3.21 F; 2-way ANOVA, ZT1 VSG vs. sham $p < 0.05$) and lost rhythmicity after VSG compared to sham (JTK_Cycle $p < 0.05$). To summarize, mRNAs of adipokine factors largely showed trends associated with a beneficial endocrine crosstalk after VSG (reduction of *Lep*, *Apln*, *Serpine*, *Ccl2*). *Adipoq* and *Rarres2* were not reduced as expected.

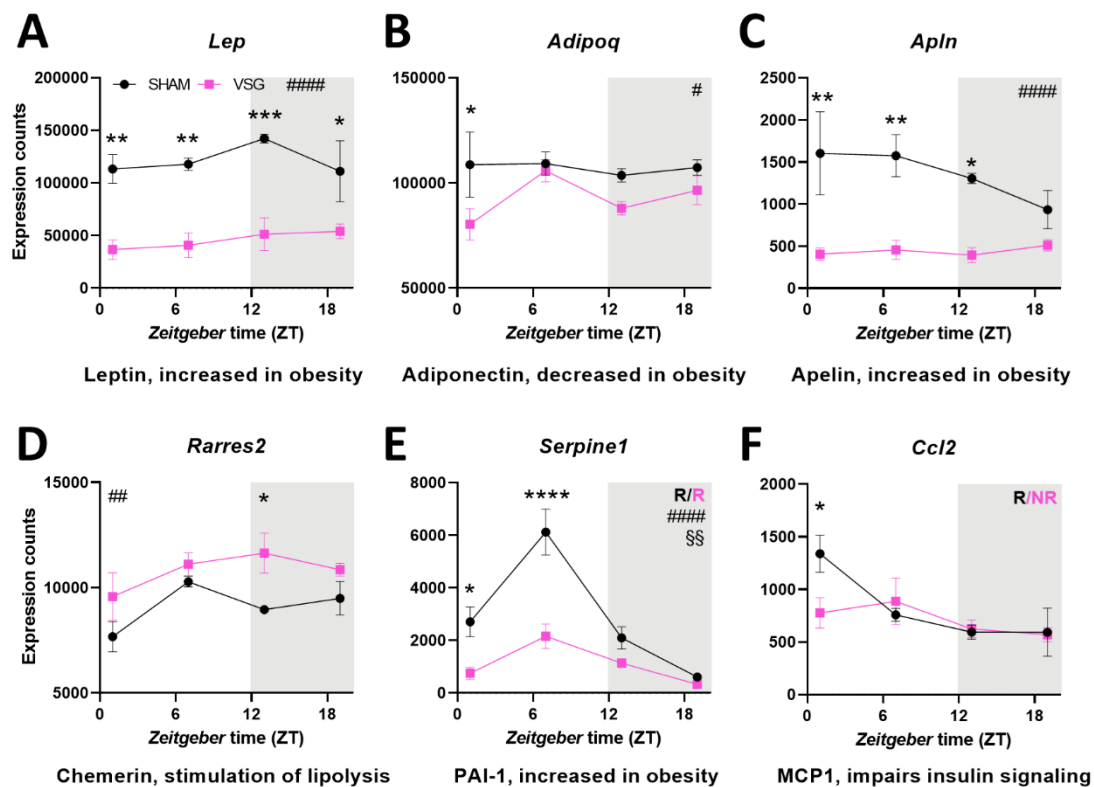


Figure 3.21: Adipokine mRNA expression after bariatric surgery. Expression values for [A] *Lep*, [B] *Adipoq*, [C] *Apln*, [D] *Rarres2* (or chemerin), [E] *Serpine1* (or PAI-1) and [F] *Ccl2* (or MCP1), 2-way ANOVA. $n = 4$ per group/time point. Legend: R = rhythmicity detected by JTK_Cycle $p < 0.05$, NR = no rhythm, interaction §§ $p < 0.01$, group effect ##### $p < 0.0001$, ## $p < 0.01$, # $p < 0.05$, Sidak's post hoc comparison **** $p < 0.0001$, *** $p < 0.001$, ** $p < 0.01$, * $p < 0.05$.

4 Discussion

Metabolic and circadian disruption go hand in hand in our modern world. This is rooted in a tight mutual interaction between the network of circadian clocks, which efficiently organises physiology according to time-dependent environmental circumstances, and whole-body metabolism. The circadian system is structured somewhat like a constitutional monarchy: the master pacemaker, the SCN, transmits light cycle-aligned time signals to central and peripheral clocks to bring tissue functions in synch with the daily 24-h cycle. At the same time, other *zeitgebers* such as food intake can reset metabolically sensitive clocks independent of the SCN to fine-tune tissue rhythms according to their unique responsibilities (Landgraf *et al.*, 2017; Astiz *et al.*, 2019; Begemann *et al.*, 2020). The result is a delicate balance in which the SCN governs the circadian clock network, but its orders can be vetoed under specific circumstances. When *zeitgebers* confer conflicting time information, *e.g.* when eating during the natural rest/sleep phase, this temporal order is perturbed, which may give rise to pathologies like obesity, cancer, or mental disorders (Reid and Abbott, 2015; Torquati *et al.*, 2019).

The hierarchical circadian network orchestrates whole-body physiology. Consequently, it plays an important but often still disregarded role in disease treatments. Chronomedicine is an emerging field and will help construct more effective therapeutical strategies and a better understanding of interindividual variances in success rates. More than half of the most used drugs in the US target a CCG while at the same time having a rather short half-life (*i.e.* < 6 h; Zhang *et al.*, 2014), thus, being sensitive to treatment timing. Furthermore, time-of-day dependencies were reported for therapies of cancer, asthma, and CVDs (Münch and Kramer, 2019) as well as for surgery outcomes and wound healing (Hoyle *et al.*, 2017; Montaigne *et al.*, 2018).

Metabolism and circadian clocks affect each other profoundly (Landgraf *et al.*, 2017; Takahashi, 2017; Wehrens *et al.*, 2017; Astiz *et al.*, 2019). Unsurprisingly, the risk for obesity increases in chronodisruptive environments (Reid and Abbott, 2015). At the same time, circadian disturbance may be one consequence of obesity (Young *et al.*, 2004; Colles *et al.*, 2008). Hence, it is tempting to speculate a modulating role of the circadian system in the treatment of obesity. First evidence shows that meal timing impacts weight loss efforts (Garaulet *et al.*, 2013; Ruiz-Lozano *et al.*, 2016b). Such changes in meal intake can reprogram aspects of the circadian system (Ben-Zvi *et al.*, 2018; Makwana *et al.*, 2019). However, a deeper characterisation of the underlying mechanisms is lacking. In this PhD thesis, I showed that weight loss surgery (VSG) affects the circadian system on behavioural, tissue, and molecular levels in mice and that these adaptations correlate with weight loss. Bariatric surgery enables a tissue-specific restructuring of the WAT circadian system, in which metabolic transcriptome rhythms are uncoupled from, both, centrally controlled feeding rhythms and local (WAT) clock function.

4.1 VSG is effective in DIO mice

HFD feeding induces obesity in many mammals accompanied by insulin resistance and hyperlipidaemia (Wang and Liao, 2012). To efficiently approach the investigation of the potential of bariatric surgery to modulate the circadian system, I first wanted to verify its effectiveness under my experimental conditions. The VSG mouse model is well established in an LD12:12 cycle and associated with weight loss, reduced food intake, improved glucose regulation, reduced arterial blood pressure, and increased circulating bile acid concentrations (Arble *et al.*, 2015; Ding *et al.*, 2016; Hao *et al.*, 2017; McGavigan *et al.*, 2017a; McGavigan *et al.*, 2017b).

Weight loss is the major outcome of bariatric surgery (O'Brien *et al.*, 2019). In this project, mice underwent VSG or sham after reaching or exceeding 35 g of weight. Under DD and LD conditions, mice lost a maximum of 18 % and 19 % (~ 6 g) of their (fasted) presurgical weight by VSG, respectively, compared to 3 % and 7 % (~ 2 g) under sham conditions (Fig. 3.2 D). Maximum weight loss occurred within the first ten days followed by a plateau and subsequent weight regain (Fig. 3.2 C). Weight change under DD conditions has not been previously reported. Under LD conditions, a similar initial weight loss (day 0 – 9) of about 18 % after both, VSG and RYGB, was shown in mice by Hao *et al.* (2017). In another study, mice lost approx. 20 % of their body weight two weeks *post-surgery* (Pressler *et al.*, 2015). Several more mouse studies plot body weight development in absolute values, but these do not explicitly mention the maximum weight loss. Estimated from the figures, mice appear to lose between approx. 8 – 10 g (after ≤ 10 days in LD or LL; Ryan *et al.*, 2014; Arble *et al.*, 2015; Hao *et al.*, 2017; Douros *et al.*, 2019) after VSG when starting from a similar baseline of 35 – 38 g. Sham surgery seems to induce a weight loss of 5 % (Pressler *et al.*, 2015; Hao *et al.*, 2017) or < 4 g (Ryan *et al.*, 2014; Arble *et al.*, 2015; Hao *et al.*, 2017). As opposed to RYGB, the VSG rodent model induces only a transient weight loss (Ryan *et al.*, 2014; Ding *et al.*, 2016; Hao *et al.*, 2017; McGavigan *et al.*, 2017b). After an initial phase of maximum weight loss (day 0 – 10), I found VSG mice to gain weight at an identical daily rate as control animals (0.7 % per day; Fig. 3.2 B). This fact insinuates that the VSG-induced weight gap between sham and VSG is stable. Collectively, despite slight variations depending on the exact protocol, mice lose reliably up to 20 % of their *pre-surgical* body weight within the first two weeks after VSG independent of the light cycle conditions. Of note, neither weight loss nor gain seem to correlate with sleeve size indicating that other physiological systems may impact the outcome (Hao *et al.*, 2017). The maximum body weight reduction by VSG in mice is comparable to other rodents (Chambers *et al.*, 2013) and humans after nine months to two years (Sjöström *et al.*, 2007; Heo *et al.*, 2012).

One proposed mechanism of reducing body weight after VSG is caloric restriction induced by a smaller stomach. Mice in my study significantly reduced meal sizes after VSG (Fig. 3.4 C). Moreover, overall daily meal intake slightly decreased compared to sham controls, but this seemed to normalise at a

later timepoint (Fig. 3.4 D; F). This normalisation was accompanied by an increased meal intake frequency that correlated with the extent of the initial weight change (Fig. 3.4 E). Meal pattern changes after bariatric surgery in rodents were reviewed recently (Shah and Shin, 2020). An initial decrease in food intake followed by a normalisation is well established after VSG. An accompanying increase in meal frequency was also described previously (Stefater *et al.*, 2010; Arble *et al.*, 2015). The phase of caloric restriction parallels that of weight loss, while the normalisation of caloric intake happens during weight regain phase. Concluding, to compensate for the reduced meal size as a consequence of the stomach reduction resulting in a catabolic state, VSG animals after some time learn to increase meal frequency to switch metabolism back to an anabolic state. This adaption process appears to be stronger the more weight an animal had lost in body weight due to the surgery.

Human studies on the effects of bariatric surgery on eating patterns are rather rare. Though the treatment generally increases healthy eating habits, some patients were observed to switch to snacking or sweet treats after VSG (Nikiforova *et al.*, 2019). A study in patients after RYGB showed that the number of daily meals significantly increases one year after surgery. Of note, this is not associated with weight loss up to two years *post-surgery* (Laurenus *et al.*, 2012). Nevertheless, patients experiencing less improvements of eating behaviour (*i.e.* disinhibition/loss of control, hunger) one year after bariatric surgery have poorer weight loss outcomes up to ten years later (Kontinen *et al.*, 2015). Two years *post-surgery*, however, mark only the beginning of weight recovery in humans (Sjöström *et al.*, 2007) and data on meal patterns and long-term weight development are needed to evaluate to what extent an increased meal frequency can predict surgical outcomes.

Besides weight loss, hallmarks of a successful surgical intervention are improvements in glucose homeostasis and the normalisation of obesity and diabetes-associated plasma markers, especially those related to or derived from the adipose tissue (Abbatini *et al.*, 2010; Eriksson-Hogling *et al.*, 2015; Abu-Gazala *et al.*, 2018; Faramia *et al.*, 2020). The amount of weight loss observed after bariatric surgery mostly corresponds to a reduction of fat mass (Ryan *et al.*, 2014; Ding *et al.*, 2016; Hao *et al.*, 2017). Therefore, in my project I focused on adipose tissue-related metabolic adaptations. At the time of maximum weight loss (*i.e.* day 9 – 10), plasma from LD-entrained animals was collected and analysed for a selection of obesity markers. Levels of leptin, adiponectin, FFAs, and TAGs were significantly reduced by VSG (Fig. 3.12). Able *et al.* reported a reduction of TAGs and non-esterified fatty acids in HFD-fed mice *post-surgery* (Arble *et al.*, 2015). Similarly, a study in rats shows a reduction of TAGs one month after VSG as well as an increase of adiponectin and a reduction of leptin after one and three months, respectively (Cummings *et al.*, 2012). The decrease of leptin concentrations in VSG mice exceeds pair-fed controls 2 – 3 months *post-surgery*, but it fails to reach or maintain the improvements of RYGB (Hao *et al.*, 2017; McGavigan *et al.*, 2017b). Gene expression data from the adipose tissue

confirmed the trends seen in plasma concentrations of leptin and adiponectin (Fig. 3.21 A, B). However, VSG only mildly reduced *Adipoq* expression in scWAT.

Bariatric surgery is known to reliably reduce dyslipidaemia and leptin as well as to increase adiponectin in humans (Askarpour *et al.*, 2020; Rafei *et al.*, 2020; Piché *et al.*, 2020). The lack of an increase in adiponectin levels in my model may be due to temporal reasons. One month after bariatric surgery in humans, adiponectin plasma concentrations are still largely unaffected, whereas leptin concentrations are already sharply decreasing (Shimizu *et al.*, 2017; Stephens *et al.*, 2019; Min *et al.*, 2020). Weight loss-induced adaptations of adiponectin signalling presumably happen after the decline in leptin levels. Thus, nine days *post-surgery* may have been too early to detect changes in this direction. Moreover, the rapid loss of adipose tissue may initially account for a decrease of adiponectin secretion.

Three strong indicators of a successful metabolic surgery are body weight loss, caloric restriction due to smaller meals, and the reduction of obesity markers. Data from my study were consistent with those from published literature using VSG animal models in rhythmic environmental conditions (*i.e.* LD). Consequently, VSG in DIO mice had transient weight effects independent of lighting conditions. As expected, physiological changes during the initial phase of weight loss after bariatric surgery in obese mice mirrored the short-term surgical outcomes of human patients.

4.2 Induction of two distinct behavioural phases *post-surgery*

4.2.1 Circadian behaviour

Circadian disruption, specifically of rhythmic behaviour, after exposure to HFD precedes metabolic dysregulation (Kohsaka *et al.*, 2007; Pendergast *et al.*, 2013). Given the metabolic benefits from VSG, whether and how the intervention can modulate or even rescue HFD-induced circadian system disruption needed further investigation. To verify such a circadian disruption in mice after ≥ 10 weeks of HFD, which was the time needed to induce the obesity phenotype (Fig. 3.1 A-C), I correlated *pre-surgical* circadian parameters under DD with weight development. As expected, behavioural rhythms were dampened by HFD-induced weight gain. This was indicated by a negative correlation with the amplitude of the locomotor activity periodogram (Fig. 3.1 D) and the overall amplitude of the meal activity rhythm (Fig. 3.1 E). A similar correlation of weight gain under HFD with locomotor rhythm amplitude was shown before (Bravo *et al.*, 2014). After surgery, weight development could be separated in two phases: a CP until day 10 and an AP from day 10 onwards (Fig. 3.2 A-C). These intervals were applied on the longitudinal recordings of locomotor activity and feeding behaviour to evaluate weight loss-associated changes of circadian behaviour.

Locomotor activity under LD was previously reported unchanged during the first four weeks after VSG in mice (Arble *et al.*, 2015), whereas a slight increase of dark phase activity bouts was measured four to six weeks *post-surgery* in rats (Stefater *et al.*, 2010). Under DD conditions, I found locomotor activity to be largely unaffected by the VSG-induced metabolic reset (Fig. 3.3). Neither average period, total activity, nor diurnal distribution of activity were significantly different between VSG and sham controls during any *post-surgical* interval. A lengthening effect by VSG was detected when analysing the activity rhythm period length continuously across the whole experiment. However, this difference was not sustained and significant exclusively around nine days *post-surgery*. Conclusively, it can be assumed that locomotor activity and the SCN output as the major driver of activity rhythms are mostly unresponsive to metabolic alterations after bariatric surgery. In line with this, the SCN is considered largely resistant to metabolic challenges in contrast to the peripheral circadian system (Damiola *et al.*, 2000; Stokkan *et al.*, 2001; Hara *et al.*, 2001). The subtle period effects observed after VSG may be in relation to food intake changes around the CP-AP transition. As mentioned above, mice switch from CP to AP by increasing their meal frequency and, thus, slowly normalising overall caloric intake. A hypercaloric diet *ad libitum* was previously shown to lengthen free-running rhythms, but not immediately (Kohsaka *et al.*, 2007). Interestingly, I found the phase of the PER2 protein rhythms of explants of LD-entrained SCN at day nine to be shifted (delayed) by 1.3 h after VSG and to correlate with weight change, but no changes of period were detected here (Fig. 3.7 C, H). Detecting a phase delay in SCN tissue culture as opposed to a period effect as indicated in the locomotor activity may reflect the light entrainment of the cultured tissues. Only a combination of time and caloric restriction was previously shown to have minor effects on SCN circadian phase (Mendoza *et al.*, 2005; Mendoza *et al.*, 2008a). Such a unique feeding pattern may also be involved here.

When food is available freely, feeding rhythms naturally follow activity rhythms. I did not observe any marked changes in the diurnal pattern of locomotor activity at any time *post-surgery*. VSG decreased meal size and meal intake during CP and AP compared to sham, while it increased meal frequency during AP compared to control animals (Fig. 3.4 C-E). When comparing the diurnal pattern of feeding activity with the *pre-surgical* state, I found sham mice to initially reduce active phase meal intake slightly initially, probably due to the *post-surgical* recovery, and later increase rest phase intake in AP. Given that circadian rhythms dampen with weight gain, this flat diurnal pattern of caloric intake found in sham controls late after surgery may be indicative of a continuation of the inherent effect of HFD on circadian rhythms. In VSG animals, meal intake was reduced in the active and the rest phase during CP with no significant differences during AP compared to the *pre-surgical* baseline (Fig. 3.4 F). However, meal frequency was increased significantly after VSG during the AP active phase (Fig. 3.4 G). This indicated a strengthening of the feeding activity diurnal pattern that was confirmed when evaluating the mean meal frequency *per hour*: the amplitude of this rhythm was increased after VSG in AP (Fig.

3.5 D-E). Analogous, in an LD12:12 cycle, increased dark phase feeding bouts were seen in mice after VSG but also increased light phase bouts were observed in one control cohort (Arble *et al.*, 2015). Moreover, an overall increased activity along the whole day was reported in rats (Stefater *et al.*, 2010). Rhythm amplitudes have not been evaluated in these studies, however. While AP active phase meal frequency only showed a trend to correlate with the body weight change to the *post*-surgical minimum, AP rest phase meal frequency correlated significantly (Fig. 3.4 H-I). This indicates that VSG increases feeding (specifically meal) frequency in both phases, but the effect is more pronounced during the active phase, thus, resulting in an overall strengthening of the diurnal feeding rhythm.

Taken together, VSG in rodents shows potential to modulate locomotor activity rhythms and does increase feeding rhythmicity significantly after the transient weight loss period. Thus, VSG may induce a unique metabolic pattern that combines caloric restriction with altered timing of food intake specifically around the CP-AP transition (nine to ten days) after VSG which is subsequently able to induce time point-specific effects in locomotor rhythms and SCN circadian activity. The peripheral reorganisation of metabolism following VSG may feedback to central centres of homeostatic control and modulate behavioural output.

4.2.2 Anxiety and the HPA axis

Metabolic state as well as circadian behaviour are differently regulated early and later after bariatric surgery. Notably, both systems have the potential to affect and be affected by mood and anxiety. A common comorbidity of obesity is depression, and circadian disruption was linked to mental health disturbances (Luppino *et al.*, 2010; Walker *et al.*, 2020). In both cases, the relationship is described as bidirectional. Bariatric surgery was generally shown to reduce anxiety and depression scores long-term, but unresponsive subgroups exist (see chapter 1.2.3.3). Therefore, I hypothesised that in parallel to the adaptations of metabolism and the circadian system, VSG may also modulate anxiety-related symptoms. Animals underwent a social interaction test nine and 30 days *post*-surgery to account for both metabolic phases seen after VSG (*i.e.* CP, AP). The absence of circadian entrainment is potentially a mild stressor, hence, I tested mice entrained to an LD12:12 cycle (Monje *et al.*, 2011; Rosenwasser *et al.*, 2020). The three-chambered social approach test used in this project is a way of social behaviour evaluation. Social avoidance is indicated by less time spent in the social compartment as opposed to the neutral and/or non-social compartment (Toth and Neumann, 2013).

Mice showed a decreased social anxiety after VSG as indicated by increased social interaction seeking behaviour (*i.e.* they resided longer in proximity of an interaction partner; Fig. 3.6 B-F) compared to sham controls, whereas baseline locomotor activity was similar (Fig. 3.6 A). I found a difference in “curiosity” (*i.e.* peeking into the social chamber; Fig. 3.6 B) only 30 days *post*-surgery, while close

interaction time and the average distance kept to the subject were significant specifically nine days after (Fig. 3.6 D, E). It was previously shown that full entries into a chamber are an insufficient parameter to evaluate social activity and are more predictive for explorative behaviour (Nadler *et al.*, 2004). Hence, the entry with the head only may also be prone to insensitivity. The sociability ratio (time spent *per* chamber with the subject vs. the object) was significantly increased at both times after VSG and correlated after nine days with body weight change (Fig. 3.6 G, H). In conclusion, it seems that the initial reduction of body weight improves social anxiety-related behaviour and that the subsequent relapse to weight gain weakens this.

Obesity in rodents alters the emotional state at different levels. Long-term HFD induces depressive-like behaviour and increases anxiety (Aslani *et al.*, 2015; Dutheil *et al.*, 2016; Arcego *et al.*, 2018). Aberrant social behaviour is a symptom associated with both (Toth and Neumann, 2013). DIO rats show metabolic disturbances (*e.g.* increased TAGs and total cholesterol) after eight weeks of HFD while also spending significantly less time socially interacting in an open field (Gancheva *et al.*, 2017). An intermittent hypercaloric diet (2 h/day) for 28 days reduces social interaction in group-housed rats (Reichelt *et al.*, 2020), but neither *ad libitum* nor intermittent HFD affects social behaviour after just 10 days of feeding in single-housed mice (Otsuka *et al.*, 2019). Of note, at least two studies found partially contradicting evidence regarding the reduction of social interaction in DIO rodents (Buchenauer *et al.*, 2009; Takase *et al.*, 2016). Changes in social behaviour as another effect of HFD-induced anxiety and depression are still relatively unexplored and the results seem highly sensitive to experimental parameters such as length of exposure, testing set-up, and housing differences (group-housed vs. single-housed). To the best of my knowledge, social behaviour with the three-chamber paradigm was not yet evaluated in DIO mice. Wildtype, healthy mice are expected to show a strong preference for the social chamber (Landauer and Balster, 1982; Nadler *et al.*, 2004). Such a preference was abolished in sham animals, which indicates that the prolonged exposure to HFD and the development of obesity did indeed decrease the interest in social activities. For the first time, I could show that VSG to some degree restored social preference in male mice (Fig. 3.6). This effect depended on weight loss. Bariatric surgery in rodents was previously shown to alter reward behaviour (*i.e.* decrease preference for palatable food, increase ethanol intake; Wilson-Pérez *et al.*, 2013b; Davis *et al.*, 2013) and improve cognition (Grayson *et al.*, 2014). VSG in female rats reduces exploratory behaviour while at the same time decreasing anxiety in the elevated plus maze more than five weeks after surgery (Himel *et al.*, 2018). Caloric restriction, but not repeated fasting and refeeding (both approx. 20 % reduction of food intake), reduces anxiety and depressive-like symptoms assessed by different tests (Yamamoto *et al.*, 2009). Overall, this suggests that the multi-dimensional emotional state is very specifically modulated by the metabolic state, *e.g.*, during the different phases following bariatric surgery. This mirrors the fact that also human patients not always improve behavioural

abnormalities *post-surgery* (Järvholm *et al.*, 2012). Further research is needed to understand the underlying physiological adaptations mediating these effects.

Anxiety and aberrant sociality increase with chronic stress (Sandi and Haller, 2015; Radley *et al.*, 2015). Prolonged, obesity-inducing exposure to HFD is mostly seen as an environmental stressor that increases HPA axis tone (Packard *et al.*, 2016). For example, 12 weeks of HFD in mice increases anxiety-related behaviour and stress-induced corticosterone levels (Sharma and Fulton, 2013). In rats, eight weeks of HFD starting after weaning increases symptoms of depression (assessed *via* forced swim test) and anxiety (assessed *via* elevated plus maze) in parallel to increased light-phase corticosterone serum levels (Aslani *et al.*, 2015). Until a decade ago, the body of data was still very inconclusive on the effects of HFD on HPA axis activity (Tannenbaum *et al.*, 1997; Auvinen *et al.*, 2011), but more recent studies conclusively support the idea that obesity leads to HPA axis hyperactivity (Dutheil *et al.*, 2016; Yokoyama *et al.*, 2020; Werdermann *et al.*, 2021). Discrepancies may result from differences in HFD exposure time, degree of obesity, and dietary compositions (Incollingo Rodriguez *et al.*, 2015; Packard *et al.*, 2016).

Given such dysregulation of the HPA axis under long-term HFD feeding and the rescue effect of VSG on social anxiety in my experiments, it appears likely that bariatric surgery may affect basal HPA axis activity. As one potential output, I evaluated individual adrenal tissue circadian rhythms in explants nine days *post-surgery*. Though no rhythm parameter was significantly altered by VSG in mice compared to sham controls, the phases of adrenals from VSG animals were more in sync with the external *zeitgeber* light (Fig. 3.8 D, G). Alternatively, sham adrenals could be more sensitive to resetting (*in vivo* or *ex vivo*). Adrenal tissue rhythms after bariatric surgery have not been investigated previously. Interestingly, several weeks after VSG HFD-fed female rats increase open arm entry durations (in the elevated plus maze) and plasma corticosterone 2 h before “lights off” (Himel *et al.*, 2018). In line with this, corticosterone plasma levels from sham animals lacked the marked early active phase peak in corticosterone plasma levels compared to VSG animals (Fig. 3.11). Moreover, VSG baseline concentrations showed a trend towards increased levels. Though the adrenal clock may not be crucial for the generation of GC circulating levels (Dumbell *et al.*, 2016), it may modulate basal and stress-induced GC release (Oster *et al.*, 2006; Son *et al.*, 2008; Leliavski *et al.*, 2014; Engeland *et al.*, 2018; Neumann *et al.*, 2019). Chronic stress from or in combination with disrupted rhythms, as seen under prolonged HFD feeding, dampens GC rhythms in mammals (Désir *et al.*, 1981; Kohsaka *et al.*, 2007; Aslani *et al.*, 2015; Koch *et al.*, 2017). Already after one week of HFD, also the pituitary of animals seems to have higher peak time variation compared to chow-fed animals (not statistically evaluated; Pendergast *et al.*, 2013). If HPA rhythms are indeed more prone to be out of sync in sham controls, this could result in false conclusions from pooled data with lower expression at suspected peak times (*i.e.* just before the active phase) and an impression of dampening. This might also explain why there is

remaining ambiguity about the effect of obesity on basal HPA axis activity despite clearly related behavioural disruptions. Future experiments should include individual GC analyses, consider the possibly affected circadian rhythmicity of the axis, and in case of bariatric surgery study the acute adaptational phase.

4.3 Regulation of rhythmic metabolism around the CP-AP transition

4.3.1 Tissue-specific recalibration of the metabolic circadian network

The behavioural changes induced by bariatric surgery particularly during the CP-AP transition will naturally influence physiological processes across the body. Since bariatric surgery is first and foremost a metabolic intervention, I focused on the body's metabolic state at the critical time of nine to ten days *post-surgery*. As mentioned above, feeding rhythmicity is overall strengthened during AP after VSG (in DD; Fig. 3.4, Fig. 3.5), but it cannot be excluded that this adaptation of the diurnal meal frequency pattern already initiates during CP (Fig. 3.5 A, C). Feeding patterns affect peripheral clocks substantially (see chapter 1.3.3), hence, I hypothesised that the CP-AP transition and associated behavioural changes will impact the circadian clock network downstream of the SCN or, in other words, an increased feeding rhythmicity may stabilise metabolic clock activity.

Under natural conditions, the adrenal clock ticks in line with the SCN stabilising HPA axis rhythmicity and GC release rhythms, but when in temporal conflict feeding rhythms and the light-sensitive SCN can independently affect the GC secretion and induce biphasic patterns (Chung *et al.*, 2011; Chung *et al.*, 2017; Engeland *et al.*, 2018). In my model, adrenal PER2 rhythms nine days after VSG were neither strengthened like the feeding rhythm nor shifted (like the SCN; Fig. 3.5, 3.7, 3.8). This supports the notion that the adrenal clock is not entirely dependent on either tissue but integrates multiple signals for its rhythmic endocrine output. Adrenal explants after sham surgery were less synchronised to external time between individuals (Fig. 3.8 D, G). This may be due to higher sensitivity to circadian resetting by an obesity-induced hyperactivity of the HPA axis (see previous chapter 4.2.2). Adrenal GCs are major peripheral synchronisers, and their rhythms are the driving force of peripheral circadian rhythmicity (Balsalobre *et al.*, 2000). Sham animals lacked the marked early active phase peak in corticosterone plasma levels (Fig. 3.11). However, neither liver nor WAT explants from sham animals presented any desynchronicity or increased variance like the adrenal glands (Fig. 3.8, 3.9, 3.10). The lack of other phase effects indicates that peripheral synchronicity is not systemically disrupted at the level of the core clocks in sham animals. Feeding rhythms play a crucial role in entrainment of metabolic tissues such as liver and WAT (see chapter 1.3.3), hence, any variation in adrenal rhythmic activity may be buffered.

Contrary to the adrenal gland, I found type of surgery to significantly affect period and amplitude of the liver tissue and both these parameters correlated with body weight change (Fig. 3.9). VSG induced a shorter period and increased the amplitude compared to sham (Fig. 3.9 C, E). Though I have not evaluated feeding data in the same animals I sacrificed for tissue culture, the increased amplitude likely comes from and parallels an increased feeding rhythm. The liver is known to be sensitive to metabolic challenges, especially when these occur in a time-dependent manner (Hatori *et al.*, 2012; Yamamuro *et al.*, 2020). Timed HFD feeding not only prevents or improves obesity (Hatori *et al.*, 2012; Chaix *et al.*, 2014), restricting food intake to the natural active phase also stabilises circadian rhythms. Nighttime-restricted feeding increases liver clock amplitudes in different models of obesity (Kudo *et al.*, 2004; Hatori *et al.*, 2012) and circadian disruption (Chaix *et al.*, 2014; Yamamuro *et al.*, 2020). Interestingly, these beneficial effects are independent of any caloric restriction and happen in parallel to restoration of diurnal activities of nutrient regulators such as CREB and AMPK as well as of rhythmic hepatic glucose and lipid metabolism (Hatori *et al.*, 2012). The strengthening of the feeding rhythm with an unproportionally increased meal frequency during the active phase starting around the CP-AP transition seems to inflict a restoration of the liver circadian clock after VSG just like HFD-restriction to the active phase and will likely lead to similar metabolic improvements. Admittedly, VSG does not induce a strict time-restricted pattern, however, it additionally reduces caloric intake, especially during CP (see chapter 4.1). Also, caloric restriction of normal chow diet was shown to affect liver clock function and increase the expression amplitude of selected clock genes (Patel *et al.*, 2016; Sato *et al.*, 2017; Velingkaar *et al.*, 2020). Moreover, nighttime-restricted feeding and caloric restriction can affect the phase of clock gene mRNAs (Hatori *et al.*, 2012; Branecky *et al.*, 2015; Velingkaar *et al.*, 2020). I did not find shifts of the liver clock in cultured tissue rhythms but an accelerated rhythm (*i.e.* a shorter period). Most previously mentioned studies measured liver clock gene expression on pooled time point samples within a window of 24 hours. They, thus, may not be suited to detect period changes sufficiently.

Taken together, the liver was expectedly sensitive to the metabolic interventions in my study. VSG itself or the unique VSG-induced feeding pattern were able to increase liver clock amplitude and to shorten the period of the molecular rhythm. This sensitivity may also explain why liver parameters correlated with body weight change. Given the resetting potential of incretins and glucagon for the liver clock (Ando *et al.*, 2013; Sun *et al.*, 2015; Landgraf *et al.*, 2015) and their adjusted secretion after bariatric surgery (Kalinowski *et al.*, 2017), these may be possible modulators of the increased liver rhythmicity. However, at least GLP-1 was deemed unnecessary for the reduction of body weight, energy intake, and glucose intolerance after VSG (Wilson-Pérez *et al.*, 2013a). Further research into the rhythmicity of candidate modulators and their possible interaction sides with the hepatic clock are needed to elicit the underlying mechanisms in restoration of liver rhythms after VSG.

As the metabolic tissue that is most heavily reorganised following gut reconstruction (Labrecque *et al.*, 2017; Adami *et al.*, 2019), I evaluated WAT. Surprisingly, I did not find any impact of type of surgery on the functionality of the core clock in epididymal WAT explants (Fig. 3.10) nor on the level of clock gene mRNA expression in scWAT biopsies (Fig. 3.16). Metabolic challenges or interventions like ultradian or circadian time-restricted feeding tend to affect liver and WAT clock rhythms in a similar way (Su *et al.*, 2016; de Goede *et al.*, 2018b; Yamamuro *et al.*, 2020). However, it was previously suggested that the WAT clock needs longer time to adapt to a new metabolic state (Pickel and Sung, 2020). Nevertheless, plasma lipid and leptin levels indicating WAT metabolic activity were already normalising after nine days (*i.e.* reduced; Fig. 3.12). Interestingly, adiponectin, TAGs, and leptin exhibited an altered diurnal blood rhythm after VSG surgery. The data from tissue culture rhythms in adrenal, liver, and WAT combined with the altered rhythms of plasma concentrations hint towards a tissue-specific recalibration of circadian clocks during the CP-AP transition.

4.3.2 Selective uncoupling of WAT rhythmic transcriptome from feeding cycles and local clock

Local tissue clocks organise a tissue's physiological role. A conflicting *zeitgeber* can lead to an uncoupling of rhythms from the light-driven circadian system. Such effects are the result of distinct adaptations of the tissue transcriptome and can happen in parallel or independent of the local clock (see chapter 1.3.3, Su *et al.*, 2016). I wanted to further investigate how the WAT after CP is affected by VSG given the dramatic substance loss in this tissue (Ryan *et al.*, 2014; Ding *et al.*, 2016; Hao *et al.*, 2017). mRNAs from scWAT biopsies were sequenced at six-hour intervals on day nine *post-surgery* and diverse regulations of especially metabolic gene transcription were detected (Fig. 4.1).

As mentioned above, the core clock in epididymal WAT tissue culture explants appeared resistant to VSG-induced weight loss and metabolic adaptations. In line with this, the mRNA expression rhythms of core clock components in scWAT were similarly resistant except for *Clock* and its paralogue *Npas2*, which showed increased amplitudes after VSG (Fig. 3.16). The molecular clock is known to cycle consistently across different WAT depots, while other (*e.g.* metabolic) genes show a higher variation of rhythmicity between adipose tissues (van der Spek *et al.*, 2018). Though I cannot exclude that the response of *Clock* and *Npas2* mRNA expression is the initial signal of the whole clock machinery adapting to the new feeding rhythm, it more likely reflects a non-circadian function. For example, CLOCK is a positive regulator of NF- κ B-mediated transcription in a BMAL1-independent way (Nuclear factor 'kappa-light-chain-enhancer' of activated B-cells; Spengler *et al.*, 2012). Given the role of NF- κ B in inflammation, an altered expression of *Clock* may affect acute and chronic adipose tissue inflammation. Moreover, CLOCK was shown to promote adipogenesis and play a role in suppressing

apoptosis *in vitro* (Wang *et al.*, 2016; Zhu *et al.*, 2016). Thus, an adjusted expression may relate to the morphological reconstruction of WAT *post-surgery*.

Despite an unresponsive core clock, I found the rhythmic transcriptome after VSG to have a reduced number of cycling genes (sham: 2,493 vs. VSG: 1,013; Fig. 3.14 A) and shared cyclers to have an overall decreased amplitude in parallel to a shift towards genes with medium rhythmicity (FC 0.3 – 0.5; Fig. 3.15). This indicates that the loss of lipid depots following bariatric surgery and the associated anatomical adaptations disrupt and blunt the rhythmic transcriptome independent of the core clock. Of note, more than half of the rhythmic genes of sham animals peaked during the light phase, while most rhythmic genes peaked during the dark phase after VSG surgery (Fig. 3.15 C). This disproportional loss of active phase peaking genes could be a consequence of strengthened feeding rhythms and a modulation of metabolic genes. An initial KEGG pathway analysis of globally up- or downregulated genes revealed significant differential expression of immune responses and acute inflammatory pathways (Fig. 3.13 B). This may reflect residual *post-operative* wound healing after VSG. However, when evaluating all differently regulated genes, *i.e.*, all genes differently expressed and differently rhythmic together, genes of metabolic pathways and regulation of metabolic pathways were indeed specifically enriched (Fig. 3.14 B, C). Transcriptome analyses following bariatric surgery are rare. Moreover, the WAT transcriptome was previously shown to react rather slow to metabolic challenges and weight loss (Pohjanvirta *et al.*, 2008; Antunes *et al.*, 2018). In an elaborate study, several tissues were investigated nine days and nine weeks after RYGB in mice and compared to dieting (Ben-Zvi *et al.*, 2018). Here, an early increase in leukocyte, B-cell, and T-cell markers was detected in scWAT, hence, affirming the idea that during CP and maximum weight loss immune responses (still) play a substantial role. Moreover, the authors found only minor metabolic gene expression changes during the early adaptational phase and more pronounced upregulation of lipid metabolic pathways later *post-surgery* (Ben-Zvi *et al.*, 2018). In another study in rats from the same group, they found WAT to upregulate glucose uptake after surgery (Saeidi *et al.*, 2013). With a sustained weight loss as seen in the RYGB animal model, metabolic pathways are prone to be differently expressed later and long-term. Similar trends were confirmed in a human microarray study: here, two years after RYGB a switch from inflammation and cell proliferation to lipid metabolism was detected in abdominal WAT (Ortega *et al.*, 2015). Nevertheless, metabolism-associated genes were differently regulated already shortly after bariatric surgery in my study.

Since glucose and lipid metabolism were shown to be eventually modulated after RYGB (Ben-Zvi *et al.*, 2018), I analysed respective pathways in more detail. To my knowledge, no study on the diurnal regulation of metabolic pathways following bariatric surgery has so far been published. The main role of adipose tissue – besides its endocrine function – is to store excess energy, *e.g.*, during the active phase, and make it available in times of need, *e.g.*, during resting. The diurnal pattern of plasma TAG

levels reflects dietary intake, while FFAs as an energy source rise during the fasting period, but also transiently after food intake (Kumar Jha *et al.*, 2015; Poggiogalle *et al.*, 2018). Subsequently, the lipid breakdown of circulating dietary fat as well as the generation of lipids for storage is induced after feeding. Genes involved in the transport, metabolism, and storage of lipids follow a diurnal pattern paralleling the feeding-fasting cycle. Circulating TAGs are broken down to glycerol and fatty acids (*i.e.* lipolysis). Mainly in the liver, but also in other tissues, after fatty acid breakdown and glycolysis, acetyl-CoA enters the Krebs or TCA cycle. Excess energy is stored in lipid droplets (*i.e.* after lipogenesis), which in healthy individuals happens primarily in WAT. These are broken down during fasting (*i.e.* lipid droplet lipolysis) and released as FFAs into the blood stream (Kumar Jha *et al.*, 2015; Kiehn *et al.*, 2017; Song *et al.*, 2018). In states of low energy intake ketone bodies can be produced from fatty acids (Fukao *et al.*, 2004). In sham animals, the rhythm of plasma FFAs showed an active phase rise with a peak just before wake time and a sharp decline during the rest phase (Fig. 3.12 A). This rhythm is appeared shifted compared to published data from healthy rodents, in which FFAs rise during fasting and decline during feeding (Kumar Jha *et al.*, 2015). After VSG these rhythms were dampened and the baseline reduced. However, the described lean state diurnal pattern was not fully restored. This is probably a result of the still increased dietary intake of fat vs. carbohydrates compared to a standard chow diet. The rhythms of TAGs peaked just after the active phase in sham animals, while it peaked earlier after VSG; the baseline was also significantly lower (Fig. 3.12 B). The reduction of overall food intake and the increased active phase meal frequency following bariatric surgery decreased the spillover of circulating TAGs into the rest phase, possibly relaxing rest phase lipid metabolism.

Corroborating the decrease of circulating TAGs, I found a reduction of selected genes that break these down (*i.e.* *Lpl*, *Pnpla3*, *Lipf*; Fig. 3.18 A-C). Moreover, lipogenesis was downregulated and modulated in a phase-dependent manner (Fig. 3.17 D-F). The increased late active phase transcriptional regulation of lipogenesis possibly relates to the shifted peak of plasma TAGs concentrations into the late active phase. Both are likely a consequence of the increasing active phase meal frequency around the CP-AP transition. The overall downregulation of lipogenesis genes was correlated with body weight change nine days after VSG (Fig. 3.17 H), something that was previously shown for selected genes of *de novo* lipogenesis seven months after bariatric surgery in humans (Garrido-Sánchez *et al.*, 2012). Despite these changes in plasma concentrations, TAG degradation/lipolysis genes, and lipid generation/lipogenesis genes, genes of fatty acid catabolism only showed an increased light-phase expression after VSG and no overall pathway baseline changes (Fig. 3.17 A-C). Slight diurnal adjustments may be due to a change in energy demand during the rest/fasting phase. Fittingly, I found expression of TCA cycle components to be diurnally upregulated during the late rest phase (Fig. 3.20 F). Compared to weight-matched sham controls, mice nine days after RYGB showed selected genes of lipid lipolysis downregulated, while genes of β -oxidation and TCA cycle are rather unaffected (Ben-Zvi

et al., 2018). Of note, WAT samples in that study were taken at a single time point during the early rest phase from fasted animals. However, this contrast in initial baseline regulation of lipid pathways may indicate that the effects observed in my study are mostly weight loss dependent.

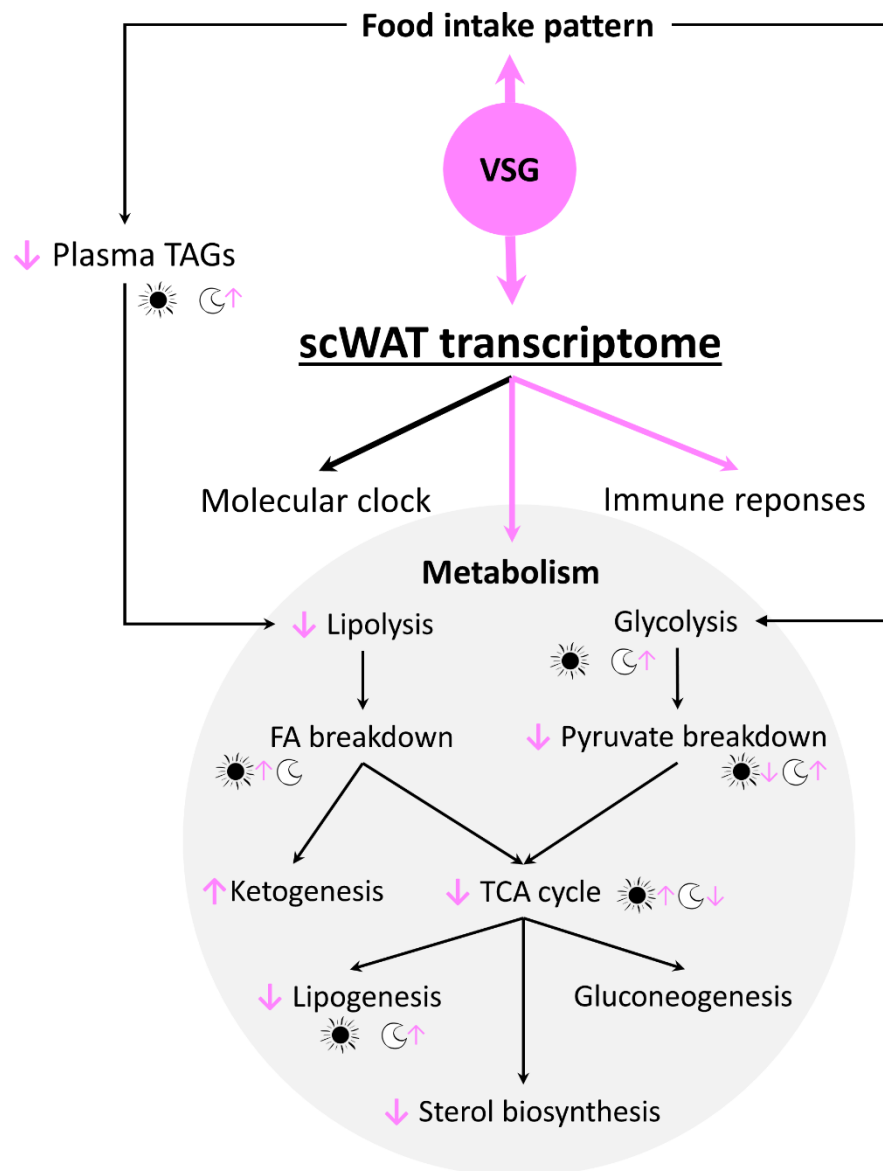


Figure 4.1: VSG-induced remodelling of the scWAT transcriptome. After VSG the scWAT transcriptome shows differential regulation of immune responses and metabolic pathways, whereas the transcription of genes of the molecular clock is largely unaffected. Transcription of many metabolic pathways are overall downregulated (i.e. lipolysis, pyruvate breakdown, TCA cycle, lipogenesis, and sterol biosynthesis). Ketogenesis is upregulated, while baseline of fatty acid (FA) breakdown, glycolysis, and gluconeogenesis remain stable. The diurnal expression patterns of some of these pathways are phase-specifically changed (light-phase regulation indicated by a sun, dark-phase regulation by a moon). Since VSG modulates the food intake pattern, it is likely that some of these diurnal regulations in metabolic gene expression happen in parallel to the adaptations in the feeding-fasting cycle and circulating dietary triacylglycerides (TAGs).

In my model, the key enzymes of ketone body synthesis were upregulated, while ketone body degradation was downregulated (Fig. 3.18 G-I). A metabolic switch to ketogenesis seems plausible given a general early increase of ketone bodies during fasting, dieting, or after surgical interventions (Tulipani *et al.*, 2016). Additionally, while the pacemaker enzyme of the sterol synthesis *Hmgcr* showed only trend of downregulation, I found other key enzymes reduced (Fig. 3.18 D-F). *Hmgcs1* was not only downregulated but also losing its diurnal expression rhythms (Fig. 3.18 D). In a mouse model of the metabolic syndrome, total cholesterol is reduced by RYGB and liver cholesterol metabolism is among the differently regulated pathways (Tarasco *et al.*, 2019). Moreover, it was previously reported that sleeve gastrectomy reduces systemic cholesterol synthesis markers in humans (De Vuono *et al.*, 2017). In that context, a reduction of WAT-dependent cholesterol metabolism may be postulated after VSG in mice.

Lipid metabolism was diversely modified by bariatric surgery in scWAT, revealed by pathway-specific changes of baseline and diurnal regulation pattern. Though overall tissue glucose metabolism was unchanged by VSG, glycolysis-specific genes were transcriptionally upregulated at the end of the dark phase (Fig. 3.19 D-F). Moreover, pyruvate breakdown was at most times downregulated but showed an increased transcription specifically during the late dark phase (Fig. 3.20 A-C). This corresponds to the end of the feeding period and may be related to an altered feeding pattern with an increased meal intake frequency in the active phase. VSG globally shifts adipose tissue metabolism towards a decrease of lipid storage as indicated by a decrease of lipogenesis and sterol biosynthesis genes. The caloric restriction also leads to a reduction in the expression of lipases associated with the degradation of dietary lipids and of pyruvate breakdown and TCA cycle genes. In line with this, ketogenesis was upregulated to buffer shortcomings in energy availability.

From a circadian perspective, the diurnal regulation of WAT transcriptome is multifaceted (Fig. 4.1). The core clock remains largely unaffected by the metabolic adaptations. Despite a sustained clock machinery and in contrast to an increased feeding rhythm around the CP-AP transition, the rhythmic transcriptome appears globally blunted. The possibility to uncouple the rhythmic transcriptome from the local clock has been shown before in liver (Greenwell *et al.*, 2019). Regulation of the DNA-binding capacity of clock proteins and interaction with various transcription factors has been suggested as mechanism for a tissue-specific control of the rhythmic transcriptome depending on environmental signals (Perelis *et al.*, 2015; Beytebiere *et al.*, 2019). Circadian regulation in WAT tissue maintenance may be overwritten by the radical morphological reconstructions (Eriksson-Hogling *et al.*, 2015; Camastra *et al.*, 2017). Nevertheless, pathways of glucose and lipid metabolism showed adjustments in their diurnal expression patterns that could reflect altered feeding rhythms. It was previously shown that GCs are a strong *zeitgeber* for adipose tissue clocks and that a diurnal feeding rhythm is necessary for rhythmicity of metabolic genes (Su *et al.*, 2016). Interestingly, lipid metabolites represent > 75 % of

all evaluated compounds detected as rhythmic under constant conditions in humans (Dallmann *et al.*, 2012). The circadian clock may be more directly involved in the regulation of lipid metabolism, but this not necessarily happens *via* transcription in WAT. Taken together, the adipose rhythmic transcriptome is selectively uncoupled from, both, the local molecular clock and the feeding cycle, while some metabolic genes remain sensitive to changes in diurnal feeding cues.

4.3.3 WAT adipokine diurnal pattern after VSG

Gene expression of adipokines confirmed the improved baseline trends I had detected in plasma concentrations (Fig. 3.12 C, D; see also chapter 4.1). The obesity-associated increase in mRNA expression of *Lep*, *Apel*, and PAI-1 encoding *Serpine1* was reduced (Fig. 3.21 A, C, E). Interestingly, leptin presented an antiphasic diurnal pattern in plasma levels after VSG surgery (Fig. 3.12 D). Leptin concentrations in diurnal and nocturnal rodents show a *post*-prandial increase and a peak occurring during the natural feeding period (Cuesta *et al.*, 2009). While such a pattern was seen in sham mice, after VSG this rhythm was somehow shifted, and diurnal variation was not detected after either type of surgery in scWAT on mRNA level (Fig. 3.21 A). Leptin is secreted in response to energy intake as a signal of satiety; the caloric restriction due to a reduced stomach capacity may prolong the feeling of hunger after VSG in mice and subsequently shift the peak secretion of leptin into the rest phase. In humans, meal timing elevates leptin, but the natural peak occurs during the night (Kumar Jha *et al.*, 2015). Early after bariatric surgery, no significant changes in plasma concentrations rhythms of leptin or adiponectin were observed in a small study on humans, the rest phase rise of lean subjects was not (yet) restored (Costa Justus *et al.*, 2016). Long-term data on adipokine rhythms after surgery are missing so far.

As the only rhythmic gene in both conditions, the active phase peak of *Serpine1* was strongly reduced. The expression of this adipokine was previously shown to be sensitive to the feeding rhythm and to increase after food intake (Kudo *et al.*, 2004). *Ccl2* was decreased at the beginning of the rest phase after VSG and as a result lost the rhythm detected in sham animals (Fig. 3.21 F). Diurnal variation, however, was still seen. CCL2 (or MCP1) is a marker of metabolic inflammation (Unamuno *et al.*, 2018; Longo *et al.*, 2019). Its gene expression is induced after intake of dietary fat in adipose tissue (Meneses *et al.*, 2011). The observed reduction of early rest phase expression after VSG in mice is probably linked to the caloric restriction during the active phase. Chemerin and adiponectin, adipokines up- and downregulated in obesity, respectively, were not yet normalised by VSG as expected from human studies (Askarpour *et al.*, 2020). Nine days *post*-surgery may have been too early for these to show the anticipated effects. Specifically, chemerin stimulates genes of intracellular lipid droplet degradation (Fu *et al.*, 2018), a process that may be upregulated following VSG to account for the reduced dietary

intake of lipids but will subsequently stabilise after the initial phase of catabolism. In summary, VSG in mice induces most expected effects on the adipokine profile already after CP. Changes in the diurnal pattern of leptin plasma levels and *Ccl2* expression may be related to the caloric restriction particularly during the active phase.

4.4 Outlook: Translation to the human situation

It was previously established that the metabolic reset in the VSG rodent model is comparable to the human situation and I was able to confirm selected aspects of this in my study: VSG induced a substantial reduction in body weight accompanied by decreased food intake and improved plasma parameters of lipids and leptin (see chapter 4.1). The transient weight loss following VSG in rodents, however, does not correspond with what is known from patients. Bariatric surgery is generally seen as a good method for long-term weight loss (*e.g.* still 18 % after 20 years; Sjöström *et al.*, 2007) and VSG outcomes do not considerably differ from RYGB (see chapter 1.2.3.1). Moreover, I found VSG to modulate the circadian feeding behaviour. After undergoing a phase of catabolism, mice increased their meal intake frequency and presented a strengthened feeding rhythm. How bariatric surgery modulates feeding patterns in humans has not been investigated thoroughly so far. Few studies report on eating habits after surgery. Even fewer studies evaluated diurnal aspects of such behaviours. In line with my results, patients experience less nighttime hunger *post-surgery* (Colles *et al.*, 2008). Moreover, eating late or in the night as opposed to three structured meals across the day was more common among patients with less weight loss success (Ruiz-Lozano *et al.*, 2016b; Cossec *et al.*, 2021). However, time definitions are inconsistent among these studies and confounding factors were not always sufficiently excluded (*e.g.* daily schedule, caloric intake; Cossec *et al.*, 2021). Though an increased feeding rhythmicity would rescue of HFD-induced dampened rhythms and could be involved in lasting metabolic improvements, I suspect the overall increase in meal intake frequency to rather indicate the magnitude of weight regain since the AP rest phase frequency correlated with weight changes. The subset of patients that tend to snacking and sweet treats already *pre-surgery* present poorer weight loss results after VSG (Ruiz-Tovar *et al.*, 2015). Some patients after VSG modify their eating habits: in that context, binge eating and emotional patterns are associated with worse weight loss outcomes (Sioka *et al.*, 2013).

Taken together, the VSG mouse model may be a suitable paradigm to understand the metabolic adaptations around the phase of maximum weight loss in humans. It is, however, less suitable to study successful long-term results. A combination of surgery with a dietary change (*e.g.* a switch to normal chow diet) leads to sustained total weight loss of 15% after VSG in rats (up to 42 days; Dohmen *et al.*, 2020). Of note, the HFD used in my study contains 60 % fat which exceeds the amount in a standard

Western human diet (Bastías-Pérez *et al.*, 2020; Stott and Marino, 2020). Subsequently, the metabolic response to bariatric surgery will be different and possibly buffered. The VSG rodent model is more a representation of a subset of patients that struggle to maintain the achieved weight loss and would need strict dietary control *post-surgery*. This also fits with the initial rescue of social anxiety and subsequent reversion back to social avoidance that I observed in the three-chamber paradigm. Conclusively, without adaptations (*e.g.* dietary switch, time-restricted feeding) to the experimental protocol, this model of bariatric surgery may be uniquely equipped to study the population of patients with unsuccessful long-term improvements in body weight and behaviour.

Despite the limitations of the mouse model with regard to lasting outcomes, the initial phase of weight loss is still a valid period to elicit the physiological adjustments directly following bariatric surgery in humans. Around the CP-AP transition mice experience caloric restriction while increasing their feeding frequency during the active phase. From my results it can be concluded that VSG-induced weight loss is accompanied by a unique diurnal feeding pattern and a tissue-specific recalibration of the circadian network (Fig. 4.2). Particularly, the adrenal gland appears more synchronised with the *zeitgeber* light (or less sensitive to perturbations) and the liver clock is accelerated as well as its rhythm amplitude increased. Bariatric surgery was also shown to modulate GC metabolism tissue-specifically in humans and possibly reduce the HPA axis drive (Woods *et al.*, 2015). A dampened or disrupted liver clock is associated with metabolic disturbances (Kohsaka *et al.*, 2007; Lamia *et al.*, 2008; Hatori *et al.*, 2012). Thus, the increased liver rhythmicity following bariatric surgery may be involved in improving hepatic metabolism and health (Dash *et al.*, 2016; Borges-Canha *et al.*, 2020). Despite an unresponsive core clock machinery in WAT in parallel to the increasing feeding rhythmicity at the end of the CP, I found the WAT rhythmic transcriptome to be globally blunted, therefore, apparently uncoupled from both *zeitgebers*, light and food. The circadian clock may play a subordinated role in the multiple anatomical and anti-inflammatory adaptations following VSG-induced weight loss and fat-content reduction. Nevertheless, the diurnal regulation patterns of some metabolic pathways such as lipogenesis, TCA cycle, and glycolysis were altered *post-surgery*. Though circadian adipose tissue gene expression following bariatric surgery was never investigated, for example, the baseline reduction of lipogenesis genes was previously described (Garrido-Sánchez *et al.*, 2012). However, obese patients with T2DM show reduced amplitudes of core clock genes and a reduction of rhythmic genes in scWAT (Stenvers *et al.*, 2019). One would suspect bariatric surgery to revoke these observations while improving the T2DM phenotype. Moreover, contrary to my results, an upregulation of many metabolic pathways was described several years after bariatric surgery (González-Plaza *et al.*, 2016; Varela-Rodríguez *et al.*, 2020). It is possible that the metabolic improvements early after bariatric surgery are not substantially driven by WAT circadian metabolism. As recently suggested, the WAT clock may need more time to adapt to a new metabolic state (Pickel and Sung, 2020). Similarly, a small Swedish study in patients

after RYGB recently showed that the increased systemic insulin sensitivity seems to happen independent of WAT insulin sensitivity (Katsogiannos *et al.*, 2019). Instead, the long-term changes in adipose tissue inflammation may be a more interesting factor in understanding successful bariatric surgery (Kerr *et al.*, 2020). Given the very transient weight loss, the VSG rodent model as used in my study may not be the most suitable approach for such an investigation. Moreover, other metabolically active tissues besides liver and WAT, such as pancreas, skeletal muscle, or the intestine, all of which have a functional local clock that can modulate metabolic homeostasis, may be of relevance for the *post-surgical* improvements (Stenvers *et al.*, 2019).

In summary, I could show that VSG in mice combines aspects of caloric restriction and time-restricted feeding in reorganising the circadian system. Many of these circadian adaptations correlate with body weight change and likely also occur in humans initially after bariatric surgery. It is not entirely clear from my study whether the change in diurnal feeding patterns are metabolically beneficial. More studies are needed to clarify the role of the circadian system in the metabolic rescue after bariatric surgery. Since mice are starting to relapse body weight quickly after the early radical loss in parallel to an increased meal frequency, the VSG model may offer opportunities for understanding the interactions of the circadian system with metabolic homeostasis in poorly responding patients. Behavioural interventions targeting these circadian rhythms may further improve the success rates of bariatric surgery.

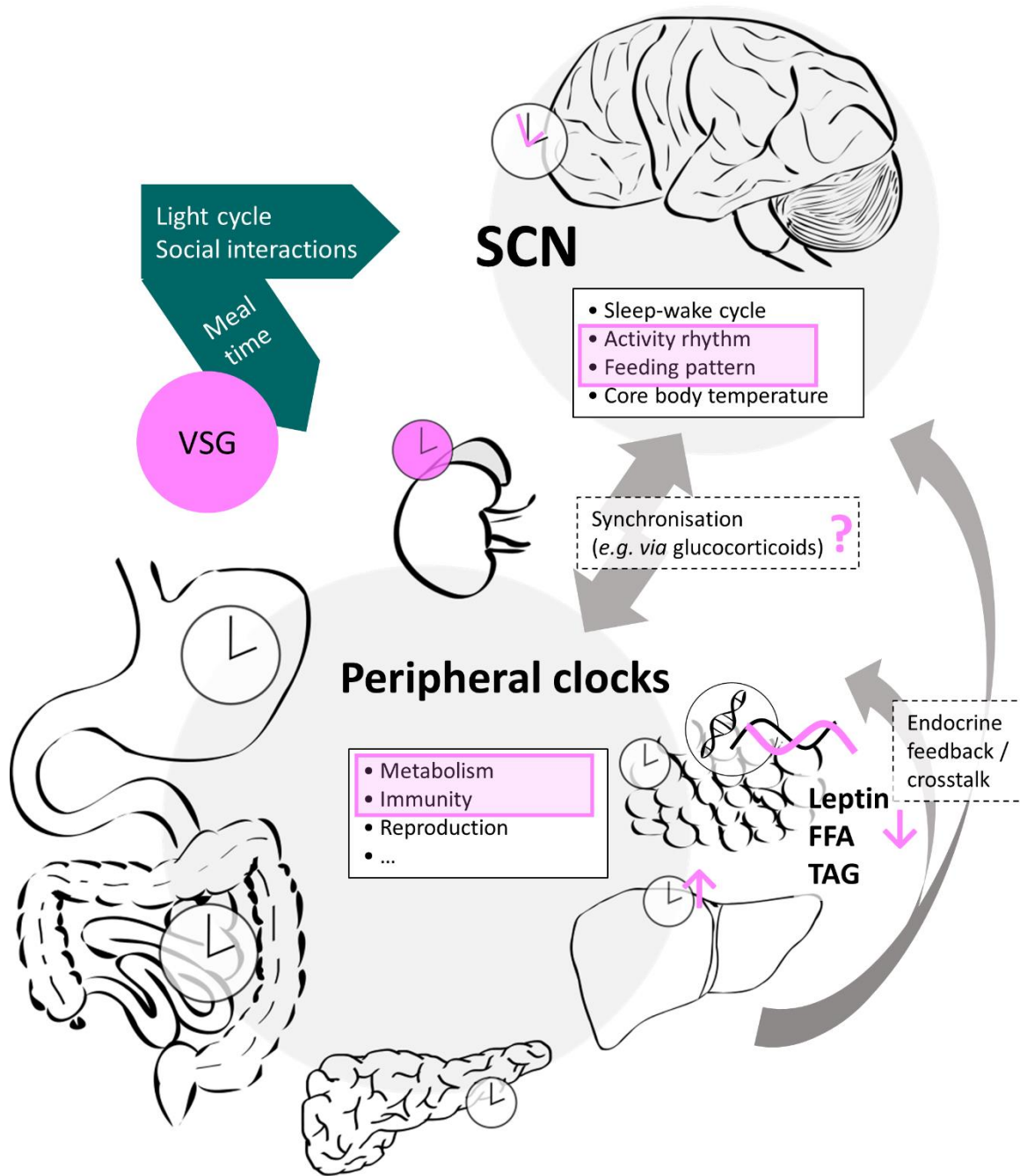


Figure 4.2: Effects of VSG in mice on the circadian network around the CP-AP transition. VSG affects feeding patterns specifically: it reduces caloric intake while switching to an increased intake frequency that globally strengthens the feeding rhythm. Potentially via these feeding pattern changes, VSG can subtly modulate SCN and activity rhythms. In the periphery the metabolic changes lead to a more stably synchronised adrenal clock, an increased liver clock amplitude, a shorter liver clock period and the reduction and diurnal modulation of obesity-associated plasma parameters such as leptin, free fatty acids (FFAs), and triacylglycerides (TAGs). These adaptations are changing the endocrine crosstalk (likely including glucocorticoids), however, overall peripheral synchronisation may not substantially be affected. In white adipose tissue, transcription of metabolism and immunity-associated genes is differently regulated. Specific metabolic pathways and genes present adjusted diurnal regulation while the rhythmic transcriptome as a whole appears blunted.

References

- Abbatini, F., Rizzello, M., Casella, G., Alessandri, G., Capoccia, D., Leonetti, F., and Basso, N. (2010) Long-term effects of laparoscopic sleeve gastrectomy, gastric bypass, and adjustable gastric banding on type 2 diabetes. *Surg Endosc* **24**: 1005–1010.
- Abbondante, S., Eckel-Mahan, K.L., Ceglia, N.J., Baldi, P., and Sassone-Corsi, P. (2016) Comparative Circadian Metabolomics Reveal Differential Effects of Nutritional Challenge in the Serum and Liver. *J Biol Chem* **291**: 2812–2828.
- Abu-Gazala, S., Horwitz, E., Ben-Haroush Schyr, R., Bardugo, A., Israeli, H., Hija, A., *et al.* (2018) Sleeve Gastrectomy Improves Glycemia Independent of Weight Loss by Restoring Hepatic Insulin Sensitivity. *Diabetes* **67**: 1079–1085.
- Acosta-Rodríguez, V.A., Groot, M.H.M. de, Rijo-Ferreira, F., Green, C.B., and Takahashi, J.S. (2017) Mice under Caloric Restriction Self-Impose a Temporal Restriction of Food Intake as Revealed by an Automated Feeder System. *Cell Metab* **26**: 267–277.e2.
- Adami, G.F., Carbone, F., Montecucco, F., Camerini, G., and Cordera, R. (2019) Adipose Tissue Composition in Obesity and After Bariatric Surgery. *OBES SURG* **29**: 3030–3038.
- Alberti, K.G.M.M., Eckel, R.H., Grundy, S.M., Zimmet, P.Z., Cleeman, J.I., Donato, K.A., *et al.* (2009) Harmonizing the Metabolic Syndrome: A Joint Interim Statement of the International Diabetes Federation Task Force on Epidemiology and Prevention; National Heart, Lung, and Blood Institute; American Heart Association; World Heart Federation; International Atherosclerosis Society; and International Association for the Study of Obesity. *Circulation* **120**: 1640–1645.
- Albrecht, U., Sun, Z.S., Eichele, G., and Lee, C.C. (1997) A Differential Response of Two Putative Mammalian Circadian Regulators, *mper1* and *mper2*, to Light. *Cell* **91**: 1055–1064.
- Aminian, A., Zajichek, A., Arterburn, D.E., Wolski, K.E., Brethauer, S.A., Schauer, P.R., *et al.* (2019) Association of Metabolic Surgery With Major Adverse Cardiovascular Outcomes in Patients With Type 2 Diabetes and Obesity. *JAMA* **322**: 1271.
- Ando, H., Ushijima, K., and Fujimura, A. (2013) Indirect effects of glucagon-like peptide-1 receptor agonist exendin-4 on the peripheral circadian clocks in mice. *PLoS One* **8**: e81119.
- Antunes, M.M., Almeida-Souza, C.B. de, Godoy, G., Crisma, A.R., Masi, L.N., Curi, R., and Bazotte, R.B. (2018) Adipose tissue is less responsive to food restriction anti-inflammatory effects than liver, muscle, and brain in mice. *Braz J Med Biol Res* **52**: e8150.
- Arbeitsgemeinschaft der Wissenschaftlichen Medizinischen Fachgesellschaften e.V. (2018) S3-Leitlinie: Chirurgie der Adipositas und metabolischer Erkrankungen. .
- Arble, D.M., Sandoval, D.A., Turek, F.W., Woods, S.C., and Seeley, R.J. (2015) Metabolic effects of bariatric surgery in mouse models of circadian disruption. *Int J Obes (Lond)* **39**: 1310–1318.
- Arcego, D.M., Toniazzo, A.P., Krolow, R., Lampert, C., Berlitz, C., Santos Garcia, E. dos, *et al.* (2018) Impact of High-Fat Diet and Early Stress on Depressive-Like Behavior and Hippocampal Plasticity in Adult Male Rats. *Mol Neurobiol* **55**: 2740–2753.
- Asher, G., Gatfield, D., Stratmann, M., Reinke, H., Dibner, C., Kreppel, F., *et al.* (2008) SIRT1 regulates circadian clock gene expression through PER2 deacetylation. *Cell* **134**: 317–328.

- Askarpour, M., Alizadeh, S., Hadi, A., Symonds, M.E., Miraghajani, M., Sheikhi, A., and Ghaedi, E. (2020) Effect of Bariatric Surgery on the Circulating Level of Adiponectin, Chemerin, Plasminogen Activator Inhibitor-1, Leptin, Resistin, and Visfatin: A Systematic Review and Meta-Analysis. *Horm Metab Res* **52**: 207–215.
- Aslani, S., Vieira, N., Marques, F., Costa, P.S., Sousa, N., and Palha, J.A. (2015) The effect of high-fat diet on rat's mood, feeding behavior and response to stress. *Transl Psychiatry* **5**: e684.
- Astiz, M., Heyde, I., and Oster, H. (2019) Mechanisms of Communication in the Mammalian Circadian Timing System. *Int J Mol Sci* **20**.
- Aton, S.J., Block, G.D., Tei, H., Yamazaki, S., and Herzog, E.D. (2004) Plasticity of circadian behavior and the suprachiasmatic nucleus following exposure to non-24-hour light cycles. *J Biol Rhythms* **19**: 198–207.
- Auvinen, H., Romijn, J., Biermasz, N., Havekes, L., Smit, J.W., Rensen, P.C., and Pereira, A. (2011) Effects of High Fat Diet on the Basal Activity of the Hypothalamus-Pituitary-Adrenal Axis in Mice: A Systematic Review. *Horm Metab Res* **43**: 899–906.
- Azim, S., and Kashyap, S.R. (2016) Bariatric Surgery. *Endocrinology and Metabolism Clinics of North America* **45**: 905–921.
- Balsalobre, A., Brown, S.A., Marcacci, L., Tronche, F., Kellendonk, C., Reichardt, H.M., *et al.* (2000) Resetting of circadian time in peripheral tissues by glucocorticoid signaling. *Science* **289**: 2344–2347.
- Banks, W.A., Farr, S.A., Salameh, T.S., Niehoff, M.L., Rhea, E.M., Morley, J.E., *et al.* (2018) Triglycerides cross the blood-brain barrier and induce central leptin and insulin receptor resistance. *Int J Obes (Lond)* **42**: 391–397.
- Barclay, J.L., Shostak, A., Leliavski, A., Tsang, A.H., Jöhren, O., Müller-Fielitz, H., *et al.* (2013) High-fat diet-induced hyperinsulinemia and tissue-specific insulin resistance in Cry-deficient mice. *Am J Physiol Endocrinol Metab* **304**: E1053-1063.
- Barron, M., Atkinson, S.N., Kirby, J., and Kindel, T. (2020) Sleeve gastrectomy prevents hypertension associated with unique shifts in the gut microbiome. *Surg Endosc* <http://link.springer.com/10.1007/s00464-020-08036-y>. Accessed November 18, 2020.
- Bastías-Pérez, M., Serra, D., and Herrero, L. (2020) Dietary Options for Rodents in the Study of Obesity. *Nutrients* **12**.
- Begemann, K., Neumann, A.-M., and Oster, H. (2020) Regulation and function of extra-SCN circadian oscillators in the brain. *Acta Physiol (Oxf)* **229**: e13446.
- Beier, C., Zhang, Z., Yurgel, M., and Hattar, S. (2020) Projections of iPRGCs and conventional RGCs to retinorecipient brain nuclei. *J Comp Neurol* cne.25061.
- Ben-Zvi, D., Meoli, L., Abidi, W.M., Nestoridi, E., Panciotti, C., Castillo, E., *et al.* (2018) Time-Dependent Molecular Responses Differ between Gastric Bypass and Dieting but Are Conserved Across Species. *Cell Metab* **28**: 310-323.e6.
- Berg, C., Lappas, G., Wolk, A., Strandhagen, E., Torén, K., Rosengren, A., *et al.* (2009) Eating patterns and portion size associated with obesity in a Swedish population. *Appetite* **52**: 21–26.

- Beytebiere, J.R., Greenwell, B.J., Sahasrabudhe, A., and Menet, J.S. (2019) Clock-controlled rhythmic transcription: is the clock enough and how does it work? *Transcription* **10**: 212–221.
- Biancolin, A.D., Martchenko, A., Mitova, E., Gurses, P., Michalchyshyn, E., Chalmers, J.A., *et al.* (2020) The core clock gene, *Bmal1*, and its downstream target, the SNARE regulatory protein secretagogin, are necessary for circadian secretion of glucagon-like peptide-1. *Molecular Metabolism* **31**: 124–137.
- Billeter, A.T., Vittas, S., Israel, B., Scheurlen, K.M., Hidmark, A., Fleming, T.H., *et al.* (2017) Gastric bypass simultaneously improves adipose tissue function and insulin-dependent type 2 diabetes mellitus. *Langenbecks Arch Surg* **402**: 901–910.
- Blancas-Velazquez, A., Fleur, S.E. Ia, and Mendoza, J. (2017) Effects of a free-choice high-fat high-sugar diet on brain PER2 and BMAL1 protein expression in mice. *Appetite* **117**: 263–269.
- Bo, S., Musso, G., Beccuti, G., Fadda, M., Fedele, D., Gambino, R., *et al.* (2014) Consuming more of daily caloric intake at dinner predisposes to obesity. A 6-year population-based prospective cohort study. *PLoS One* **9**: e108467.
- Bonmati-Carrion, M.A., Baño-Otalora, B., Madrid, J.A., and Rol, M.A. (2017) Light color importance for circadian entrainment in a diurnal (*Octodon degus*) and a nocturnal (*Rattus norvegicus*) rodent. *Sci Rep* **7**: 8846.
- Borges-Canha, M., Neves, J.S., Mendonça, F., Silva, M.M., Costa, C., Cabral, P.M., *et al.* (2020) The Impact of Bariatric Surgery on Hepatic Function and Predictors of Liver Steatosis and Fibrosis. *Obes Surg* **30**: 2935–2941.
- Branecky, K.L., Niswender, K.D., and Pendergast, J.S. (2015) Disruption of Daily Rhythms by High-Fat Diet Is Reversible. *PLoS One* **10**: e0137970.
- Bravo, R., Cubero, J., Franco, L., Mesa, M., Galán, C., Rodríguez, A.B., *et al.* (2014) Body weight gain in rats by a high-fat diet produces chronodisruption in activity/inactivity circadian rhythm. *Chronobiology International* **31**: 363–370.
- Buchenauer, T., Behrendt, P., Bode, F.J., Horn, R., Brabant, G., Stephan, M., and Nave, H. (2009) Diet-induced obesity alters behavior as well as serum levels of corticosterone in F344 rats. *Physiology & Behavior* **98**: 563–569.
- Buchwald, H., Avidor, Y., Braunwald, E., Jensen, M.D., Pories, W., Fahrbach, K., and Schoelles, K. (2004) Bariatric Surgery: A Systematic Review and Meta-analysis. *JAMA* **292**: 1724.
- Budai, Z., Balogh, L., and Sarang, Z. (2019) Short-term high-fat meal intake alters the expression of circadian clock-, inflammation-, and oxidative stress-related genes in human skeletal muscle. *Int J Food Sci Nutr* **70**: 749–758.
- Buie, J.J., Watson, L.S., Smith, C.J., and Sims-Robinson, C. (2019) Obesity-related cognitive impairment: The role of endothelial dysfunction. *Neurobiology of Disease* **132**: 104580.
- Buijs, R.M., Fleur, S.E. Ia, Wortel, J., Heyningen, C. van, Zuiddam, L., Mettenleiter, T.C., *et al.* (2003) The suprachiasmatic nucleus balances sympathetic and parasympathetic output to peripheral organs through separate preautonomic neurons. *J Comp Neurol* **464**: 36–48.

- Bužgová, R., Bužga, M., Holéczy, P., and Zonča, P. (2016) Evaluation of Quality of Life, Clinical Parameters, and Psychological Distress after Bariatric Surgery: Comparison of the Laparoscopic Sleeve Gastrectomy and Laparoscopic Greater Curvature Plication. *Bariatric Surgical Practice and Patient Care* **11**: 169–176.
- Camasta, S., Vitali, A., Anselmino, M., Gastaldelli, A., Bellini, R., Berta, R., *et al.* (2017) Muscle and adipose tissue morphology, insulin sensitivity and beta-cell function in diabetic and nondiabetic obese patients: effects of bariatric surgery. *Sci Rep* **7**: 9007.
- Campfield, L., Smith, F., Guisez, Y., Devos, R., and Burn, P. (1995) Recombinant mouse OB protein: evidence for a peripheral signal linking adiposity and central neural networks. *Science* **269**: 546–549.
- Canaple, L., Rambaud, J., Dkhissi-Benyahya, O., Rayet, B., Tan, N.S., Michalik, L., *et al.* (2006) Reciprocal regulation of brain and muscle Arnt-like protein 1 and peroxisome proliferator-activated receptor alpha defines a novel positive feedback loop in the rodent liver circadian clock. *Mol Endocrinol* **20**: 1715–1727.
- Canetti, L., Bachar, E., and Bonne, O. (2016) Deterioration of mental health in bariatric surgery after 10 years despite successful weight loss. *Eur J Clin Nutr* **70**: 17–22.
- Cano, P., Cardinali, D.P., Ríos-Lugo, M.J., Fernández-Mateos, M.P., Reyes Toso, C.F., and Esquifino, A.I. (2009) Effect of a high-fat diet on 24-hour pattern of circulating adipocytokines in rats. *Obesity (Silver Spring)* **17**: 1866–1871.
- Cavin, J.-B., Couvelard, A., Lebtahi, R., Ducroc, R., Arapis, K., Voitellier, E., *et al.* (2016) Differences in Alimentary Glucose Absorption and Intestinal Disposal of Blood Glucose After Roux-en-Y Gastric Bypass vs Sleeve Gastrectomy. *Gastroenterology* **150**: 454-464.e9.
- Chaix, A., Zarrinpar, A., Miu, P., and Panda, S. (2014) Time-restricted feeding is a preventative and therapeutic intervention against diverse nutritional challenges. *Cell Metab* **20**: 991–1005.
- Chambers, A.P., Kirchner, H., Wilson-Perez, H.E., Willency, J.A., Hale, J.E., Gaylinn, B.D., *et al.* (2013) The effects of vertical sleeve gastrectomy in rodents are ghrelin independent. *Gastroenterology* **144**: 50-52.e5.
- Chambers, A.P., Smith, E.P., Begg, D.P., Grayson, B.E., Sisley, S., Greer, T., *et al.* (2014) Regulation of gastric emptying rate and its role in nutrient-induced GLP-1 secretion in rats after vertical sleeve gastrectomy. *American Journal of Physiology-Endocrinology and Metabolism* **306**: E424–E432.
- Chandawarkar, R.Y. (2006) Body contouring following massive weight loss resulting from bariatric surgery. *Adv Psychosom Med* **27**: 61–72.
- Chaves, I., van der Horst, G.T.J., Schellevis, R., Nijman, R.M., Koerkamp, M.G., Holstege, F.C.P., *et al.* (2014) Insulin-FOXO3 Signaling Modulates Circadian Rhythms via Regulation of Clock Transcription. *Current Biology* **24**: 1248–1255.
- Chester, B., Babu, J.R., Greene, M.W., and Geetha, T. (2019) The effects of popular diets on type 2 diabetes management. *Diabetes Metab Res Rev* **35** <https://onlinelibrary.wiley.com/doi/abs/10.1002/dmrr.3188>. Accessed November 3, 2020.
- Cho, H., Zhao, X., Hatori, M., Yu, R.T., Barish, G.D., Lam, M.T., *et al.* (2012) Regulation of circadian behaviour and metabolism by REV-ERB- α and REV-ERB- β . *Nature* **485**: 123–127.

- Chung, S., Lee, E.J., Cha, H.K., Kim, J., Kim, D., Son, G.H., and Kim, K. (2017) Cooperative roles of the suprachiasmatic nucleus central clock and the adrenal clock in controlling circadian glucocorticoid rhythm. *Sci Rep* **7**: 46404.
- Chung, S., Son, G.H., and Kim, K. (2011) Adrenal peripheral oscillator in generating the circadian glucocorticoid rhythm: Adrenal peripheral oscillator in generating the circadian glucocorticoid rhythm. *Annals of the New York Academy of Sciences* **1220**: 71–81.
- Cienfuegos, S., Gabel, K., Kalam, F., Ezpeleta, M., Wiseman, E., Pavlou, V., *et al.* (2020) Effects of 4- and 6-h Time-Restricted Feeding on Weight and Cardiometabolic Health: A Randomized Controlled Trial in Adults with Obesity. *Cell Metabolism* **32**: 366–378.e3.
- Colditz, G.A. (1995) Weight Gain as a Risk Factor for Clinical Diabetes Mellitus in Women. *Ann Intern Med* **122**: 481.
- Colles, S.L., Dixon, J.B., and O'Brien, P.E. (2008) Grazing and Loss of Control Related to Eating: Two High-risk Factors Following Bariatric Surgery. *Obesity* **16**: 615–622.
- Coomans, C.P., Berg, S.A.A. van den, Lucassen, E.A., Houben, T., Pronk, A.C.M., Spek, R.D. van der, *et al.* (2013) The Suprachiasmatic Nucleus Controls Circadian Energy Metabolism and Hepatic Insulin Sensitivity. *Diabetes* **62**: 1102–1108.
- Corbeels, K., Verlinden, L., Lannoo, M., Khalil, R., Deleus, E., Mertens, A., *et al.* (2020) The curious fate of bone following bariatric surgery: bone effects of sleeve gastrectomy (SG) and Roux-en-Y gastric bypass (RYGB) in mice. *Int J Obes* **44**: 2165–2176.
- Corbeels, K., Verlinden, L., Lannoo, M., Simoens, C., Matthys, C., Verstuyf, A., *et al.* (2018) Thin bones: Vitamin D and calcium handling after bariatric surgery. *Bone Rep* **8**: 57–63.
- Cossec, M., Atger, F., Blanchard, C., and Jacobi, D. (2021) Daily Timing of Meals and Weight Loss After Bariatric Surgery: a Systematic Review. *OBES SURG* <http://link.springer.com/10.1007/s11695-021-05278-0>. Accessed February 24, 2021.
- Costa Justus, J.F., Ligocki Campos, A.C., Figueroa, A.L.C., Gomis, R., Santo, M.A., Fávero, G.M., *et al.* (2016) Early Effect of Bariatric Surgery on the Circadian Rhythms of Adipokines in Morbidly Obese Women. *Metabolic Syndrome and Related Disorders* **14**: 16–22.
- Cuesta, M., Clesse, D., Pévet, P., and Challet, E. (2009) From daily behavior to hormonal and neurotransmitters rhythms: comparison between diurnal and nocturnal rat species. *Horm Behav* **55**: 338–347.
- Cummings, B.P., Bettaieb, A., Graham, J.L., Stanhope, K.L., Kowala, M., Haj, F.G., *et al.* (2012) Vertical Sleeve Gastrectomy Improves Glucose and Lipid Metabolism and Delays Diabetes Onset in UCD-T2DM Rats. *Endocrinology* **153**: 3620–3632.
- Dallmann, R., Viola, A.U., Tarokh, L., Cajochen, C., and Brown, S.A. (2012) The human circadian metabolome. *Proc Natl Acad Sci U S A* **109**: 2625–2629.
- Damiola, F., Le Minh, N., Preitner, N., Kornmann, B., Fleury-Olela, F., and Schibler, U. (2000) Restricted feeding uncouples circadian oscillators in peripheral tissues from the central pacemaker in the suprachiasmatic nucleus. *Genes Dev* **14**: 2950–2961.
- Dash, S., Xiao, C., and Lewis, G.F. (2016) Effects of bariatric surgery on hepatic and intestinal lipoprotein particle metabolism. *Curr Opin Lipidol* **27**: 14–18.

- Davis, J.F., Tracy, A.L., Schurdak, J.D., Magrisso, I.J., Grayson, B.E., Seeley, R.J., and Benoit, S.C. (2013) Roux en Y Gastric Bypass Increases Ethanol Intake in the Rat. *OBES SURG* **23**: 920–930.
- De Vuono, S., Ricci, M.A., Siepi, D., Boni, M., Gentili, A., Scavizzi, M., *et al.* (2017) Laparoscopic sleeve gastrectomy modifies cholesterol synthesis but not cholesterol absorption. *Obes Res Clin Pract* **11**: 118–122.
- Delezie, J., Dumont, S., Dardente, H., Oudart, H., Gréchez-Cassiau, A., Klosen, P., *et al.* (2012) The nuclear receptor REV-ERB α is required for the daily balance of carbohydrate and lipid metabolism. *FASEB j* **26**: 3321–3335.
- D’Elia, L., Strazzullo, P., Iacone, R., Russo, O., and Galletti, F. (2019) Leptin levels predict the development of insulin resistance in a sample of adult men—The Olivetti Heart Study. *Nutrition, Metabolism and Cardiovascular Diseases* **29**: 39–44.
- Désir, D., Van Cauter, E., Fang, V.S., Martino, E., Jadot, C., Spire, J.-P., *et al.* (1981) Effects of “Jet Lag” on Hormonal Patterns. I. Procedures, Variations in Total Plasma Proteins, and Disruption of Adrenocorticotropin-Cortisol Periodicity*. *The Journal of Clinical Endocrinology & Metabolism* **52**: 628–641.
- Ding, J.M., Faiman, L.E., Hurst, W.J., Kuriashkina, L.R., and Gillette, M.U. (1997) Resetting the biological clock: mediation of nocturnal CREB phosphorylation via light, glutamate, and nitric oxide. *J Neurosci* **17**: 667–675.
- Ding, L., Sousa, K.M., Jin, L., Dong, B., Kim, B.-W., Ramirez, R., *et al.* (2016) Vertical sleeve gastrectomy activates GPBAR-1/TGR5 to sustain weight loss, improve fatty liver, and remit insulin resistance in mice. *Hepatology* **64**: 760–773.
- Dixon, J.B., Schachter, L.M., and O’Brien, P.E. (2001) Sleep disturbance and obesity: changes following surgically induced weight loss. *Arch Intern Med* **161**: 102–106.
- Dodt, M., Roehr, J.T., Ahmed, R., and Dieterich, C. (2012) FLEXBAR-Flexible Barcode and Adapter Processing for Next-Generation Sequencing Platforms. *Biology (Basel)* **1**: 895–905.
- Dohmen, J., Praktijnjo, M., Rudeloff, A., Uschner, F.E., Klein, S., Plamper, A., *et al.* (2020) Impact of sleeve gastrectomy and dietary change on metabolic and hepatic function in an obesity rat model - Experimental research. *International Journal of Surgery* **75**: 139–147.
- Douros, J.D., Niu, J., Sdao, S., Gregg, T., Fisher-Wellman, K., Bharadwaj, M., *et al.* (2019) Sleeve gastrectomy rapidly enhances islet function independently of body weight. *JCI Insight* **4**.
- Dragano, N.R.V., Fernø, J., Diéguez, C., López, M., and Milbank, E. (2020) Recent Updates on Obesity Treatments: Available Drugs and Future Directions. *Neuroscience* **437**: 215–239.
- Drake, C.L., Roehrs, T., Richardson, G., Walsh, J.K., and Roth, T. (2004) Shift Work Sleep Disorder: Prevalence and Consequences Beyond that of Symptomatic Day Workers. *Sleep* **27**: 1453–1462.
- Dumbell, R., Leliavski, A., Matveeva, O., Blaum, C., Tsang, A.H., and Oster, H. (2016) Dissociation of Molecular and Endocrine Circadian Rhythms in Male Mice Lacking Bmal1 in the Adrenal Cortex. *Endocrinology* **157**: 4222–4233.
- Dutheil, S., Ota, K.T., Wohleb, E.S., Rasmussen, K., and Duman, R.S. (2016) High-Fat Diet Induced Anxiety and Anhedonia: Impact on Brain Homeostasis and Inflammation. *Neuropsychopharmacol* **41**: 1874–1887.

- Dyar, K.A., Lutter, D., Artati, A., Ceglia, N.J., Liu, Y., Armenta, D., *et al.* (2018) Atlas of Circadian Metabolism Reveals System-wide Coordination and Communication between Clocks. *Cell* **174**: 1571-1585.e11.
- Eckel-Mahan, K.L., Patel, V.R., Mateo, S. de, Orozco-Solis, R., Ceglia, N.J., Sahar, S., *et al.* (2013) Reprogramming of the circadian clock by nutritional challenge. *Cell* **155**: 1464–1478.
- Eide, E.J., Woolf, M.F., Kang, H., Woolf, P., Hurst, W., Camacho, F., *et al.* (2005) Control of mammalian circadian rhythm by CKIepsilon-regulated proteasome-mediated PER2 degradation. *Mol Cell Biol* **25**: 2795–2807.
- Engeland, W.C., Massman, L., Mishra, S., Yoder, J.M., Leng, S., Pignatti, E., *et al.* (2018) The Adrenal Clock Prevents Aberrant Light-Induced Alterations in Circadian Glucocorticoid Rhythms. *Endocrinology* **159**: 3950–3964.
- Erickson, A., and Moreau, R. (2017) The regulation of FGF21 gene expression by metabolic factors and nutrients. *Hormone Molecular Biology and Clinical Investigation* **30** <https://www.degruyter.com/doi/10.1515/hmbci-2016-0016>. Accessed December 22, 2020.
- Eriksson-Hogling, D., Andersson, D.P., Bäckdahl, J., Hoffstedt, J., Rössner, S., Thorell, A., *et al.* (2015) Adipose tissue morphology predicts improved insulin sensitivity following moderate or pronounced weight loss. *Int J Obes (Lond)* **39**: 893–898.
- Escoto, K.H., Laska, M.N., Larson, N., Neumark-Sztainer, D., and Hannan, P.J. (2012) Work Hours and Perceived Time Barriers to Healthful Eating Among Young Adults. *Am J Hlth Behav* **36**: 786–796.
- European Foundation for the Improvement of Living and Working Conditions. and International Labour Organization (ILO). (2019) *Working conditions in a global perspective*. Publications Office, LU. <https://data.europa.eu/doi/10.2806/870542>. Accessed February 18, 2021.
- Faramia, J., Ostinelli, G., Drolet-Labelle, V., Picard, F., and Tchernof, A. (2020) Metabolic adaptations after bariatric surgery: adipokines, myokines and hepatokines. *Current Opinion in Pharmacology* **52**: 67–74.
- Fasshauer, M., and Blüher, M. (2015) Adipokines in health and disease. *Trends in Pharmacological Sciences* **36**: 461–470.
- Fernandez, D.C., Fogerson, P.M., Lazzerini Ospri, L., Thomsen, M.B., Layne, R.M., Severin, D., *et al.* (2018) Light Affects Mood and Learning through Distinct Retina-Brain Pathways. *Cell* **175**: 71-84.e18.
- Freedland, E.S. (2004) Role of a critical visceral adipose tissue threshold (CVATT) in metabolic syndrome: implications for controlling dietary carbohydrates: a review. *Nutr Metab (Lond)* **1**: 12.
- Fu, Y.-Y., Hu, B.-H., Chen, K.-L., and Li, H.-X. (2018) Chemerin induces lipolysis through ERK1/2 pathway in intramuscular mature adipocytes of dairy bull calves. *J Cell Biochem* .
- Fukao, T., Lopaschuk, G.D., and Mitchell, G.A. (2004) Pathways and control of ketone body metabolism: on the fringe of lipid biochemistry. *Prostaglandins Leukot Essent Fatty Acids* **70**: 243–251.
- Gabel, K., Hoddy, K.K., Haggerty, N., Song, J., Kroeger, C.M., Trepanowski, J.F., *et al.* (2018) Effects of 8-hour time restricted feeding on body weight and metabolic disease risk factors in obese adults: A pilot study. *NHA* **4**: 345–353.

- Gancheva, S., Galunska, B., and Zhelyazkova-Savova, M. (2017) Diets rich in saturated fat and fructose induce anxiety and depression-like behaviours in the rat: is there a role for lipid peroxidation? *Int J Exp Path* **98**: 296–306.
- Garaulet, M., Gómez-Abellán, P., Albuquerque-Béjar, J.J., Lee, Y.-C., Ordovás, J.M., and Scheer, F.A.J.L. (2013) Timing of food intake predicts weight loss effectiveness. *Int J Obes* **37**: 604–611.
- Garaulet, M., Sánchez-Moreno, C., Smith, C.E., Lee, Y.-C., Nicolás, F., and Ordovás, J.M. (2011) Ghrelin, Sleep Reduction and Evening Preference: Relationships to CLOCK 3111 T/C SNP and Weight Loss. *PLoS ONE* **6**: e17435.
- Garrido-Sánchez, L., Vendrell, J., Fernández-García, D., Ceperuelo-Mallafré, V., Chacón, M.R., Ocaña-Wilhelmi, L., *et al.* (2012) De novo lipogenesis in adipose tissue is associated with course of morbid obesity after bariatric surgery. *PLoS One* **7**: e31280.
- Gekakis, N., Staknis, D., Nguyen, H.B., Davis, F.C., Wilsbacher, L.D., King, D.P., *et al.* (1998) Role of the CLOCK protein in the mammalian circadian mechanism. *Science* **280**: 1564–1569.
- Geller, S., Dahan, S., Levy, S., Goldzweig, G., Hamdan, S., and Abu-Abeid, S. (2020) Body Image and Emotional Eating as Predictors of Psychological Distress Following Bariatric Surgery. *OBES SURG* **30**: 1417–1423.
- Gentleman, R.C., Carey, V.J., Bates, D.M., Bolstad, B., Dettling, M., Dudoit, S., *et al.* (2004) Bioconductor: open software development for computational biology and bioinformatics. *Genome Biol* **5**: R80.
- Gil-Lozano, M., Mingomataj, E.L., Wu, W.K., Ridout, S.A., and Brubaker, P.L. (2014) Circadian Secretion of the Intestinal Hormone GLP-1 by the Rodent L Cell. *Diabetes* **63**: 3674–3685.
- Git, K.C.G. de, and Adan, R.A.H. (2015) Leptin resistance in diet-induced obesity: the role of hypothalamic inflammation: Leptin resistance and inflammation. *Obes Rev* **16**: 207–224.
- Glass, J.D., DiNardo, L.A., and Ehlen, J.C. (2000) Dorsal raphe nuclear stimulation of SCN serotonin release and circadian phase-resetting. *Brain Research* **859**: 224–232.
- Goede, P. de, Sen, S., Oosterman, J.E., Foppen, E., Jansen, R., Fleur, S.E. la, *et al.* (2018a) Differential effects of diet composition and timing of feeding behavior on rat brown adipose tissue and skeletal muscle peripheral clocks. *Neurobiol Sleep Circadian Rhythms* **4**: 24–33.
- Goede, P. de, Sen, S., Su, Y., Foppen, E., Poirel, V.-J., Challet, E., and Kalsbeek, A. (2018b) An Ultradian Feeding Schedule in Rats Affects Metabolic Gene Expression in Liver, Brown Adipose Tissue and Skeletal Muscle with Only Mild Effects on Circadian Clocks. *Int J Mol Sci* **19**.
- González-Plaza, J.J., Gutiérrez-Repiso, C., García-Serrano, S., Rodríguez-Pacheco, F., Garrido-Sánchez, L., Santiago-Fernández, C., *et al.* (2016) Effect of Roux-en-Y gastric bypass-induced weight loss on the transcriptomic profiling of subcutaneous adipose tissue. *Surgery for Obesity and Related Diseases* **12**: 257–263.
- Grayson, B.E., Fitzgerald, M.F., Hakala-Finch, A.P., Ferris, V.M., Begg, D.P., Tong, J., *et al.* (2014) Improvements in hippocampal-dependent memory and microglial infiltration with calorie restriction and gastric bypass surgery, but not with vertical sleeve gastrectomy. *Int J Obes* **38**: 349–356.

- Greenwell, B.J., Trott, A.J., Beytebiere, J.R., Pao, S., Bosley, A., Beach, E., *et al.* (2019) Rhythmic Food Intake Drives Rhythmic Gene Expression More Potently than the Hepatic Circadian Clock in Mice. *Cell Rep* **27**: 649–657.e5.
- Grimaldi, B., Bellet, M.M., Katada, S., Astarita, G., Hirayama, J., Amin, R.H., *et al.* (2010) PER2 controls lipid metabolism by direct regulation of PPAR γ . *Cell Metab* **12**: 509–520.
- Grosbellet, E., Gournelen, S., Pévet, P., Criscuolo, F., and Challet, E. (2015) Leptin Normalizes Photic Synchronization in Male ob/ob Mice, via Indirect Effects on the Suprachiasmatic Nucleus. *Endocrinology* **156**: 1080–1090.
- Guan, D., Xiong, Y., Borck, P.C., Jang, C., Doulias, P.-T., Papazyan, R., *et al.* (2018) Diet-Induced Circadian Enhancer Remodeling Synchronizes Opposing Hepatic Lipid Metabolic Processes. *Cell* **174**: 831–842.e12.
- Guo, Y., Yin, X., Wu, H., Chai, X., and Yang, X. (2019) Trends in Overweight and Obesity Among Children and Adolescents in China from 1991 to 2015: A Meta-Analysis. *International Journal of Environmental Research and Public Health* **16**.
- Halliday, T.M., Polsky, S., Schoen, J.A., Legget, K.T., Tregellas, J.R., Williamson, K.M., and Cornier, M. (2019) Comparison of surgical versus diet-induced weight loss on appetite regulation and metabolic health outcomes. *Physiol Rep* **7**: e14048.
- Hao, Z., Münzberg, H., Rezai-Zadeh, K., Keenan, M., Coulon, D., Lu, H., *et al.* (2015) Leptin deficient ob/ob mice and diet-induced obese mice responded differently to Roux-en-Y bypass surgery. *Int J Obes* **39**: 798–805.
- Hao, Z., Townsend, R.L., Mumphrey, M.B., Morrison, C.D., Münzberg, H., and Berthoud, H.-R. (2017) RYGB Produces more Sustained Body Weight Loss and Improvement of Glycemic Control Compared with VSG in the Diet-Induced Obese Mouse Model. *Obes Surg* **27**: 2424–2433.
- Hara, R., Wan, K., Wakamatsu, H., Aida, R., Moriya, T., Akiyama, M., and Shibata, S. (2001) Restricted feeding entrains liver clock without participation of the suprachiasmatic nucleus: Restricted feeding-induced *Per* genes in the liver. *Genes to Cells* **6**: 269–278.
- Hatori, M., Vollmers, C., Zarrinpar, A., DiTacchio, L., Bushong, E.A., Gill, S., *et al.* (2012) Time-restricted feeding without reducing caloric intake prevents metabolic diseases in mice fed a high-fat diet. *Cell Metab* **15**: 848–860.
- Heo, Y.-S., Park, J.-M., Kim, Y.-J., Kim, S.-M., Park, D.-J., Lee, S.-K., *et al.* (2012) Bariatric surgery versus conventional therapy in obese Korea patients: a multicenter retrospective cohort study. *J Korean Surg Soc* **83**: 335.
- Herdegen, T., and Böhm, R. (2010) *Kurzlehrbuch Pharmakologie und Toxikologie: 328 Tabellen*. 2., aktualisierte Aufl., Thieme, Stuttgart.
- Herrera-Moro Chao, D., León-Mercado, L., Foppen, E., Guzmán-Ruiz, M., Basualdo, M.C., Escobar, C., and Buijs, R.M. (2016) The Suprachiasmatic Nucleus Modulates the Sensitivity of Arcuate Nucleus to Hypoglycemia in the Male Rat. *Endocrinology* **157**: 3439–3451.
- Heyde, I., and Oster, H. (2019) Differentiating external zeitgeber impact on peripheral circadian clock resetting. *Sci Rep* **9**: 20114.

- Himel, A.R., Cabral, S.A., Shaffery, J.P., and Grayson, B.E. (2018) Anxiety behavior and hypothalamic-pituitary-adrenal axis altered in a female rat model of vertical sleeve gastrectomy. *PLoS One* **13**: e0200026.
- Honma, K., Hikosaka, M., Mochizuki, K., and Goda, T. (2016) Loss of circadian rhythm of circulating insulin concentration induced by high-fat diet intake is associated with disrupted rhythmic expression of circadian clock genes in the liver. *Metabolism* **65**: 482–491.
- Hoyle, N.P., Seinkmane, E., Putker, M., Feeney, K.A., Krogager, T.P., Chesham, J.E., *et al.* (2017) Circadian actin dynamics drive rhythmic fibroblast mobilization during wound healing. *Sci Transl Med* **9**: eaal2774.
- Hube, F., Lietz, U., Igel, M., Jensen, P., Tornqvist, H., Joost, H.-G., and Hauner, H. (1996) Difference in Leptin mRNA Levels Between Omental and Subcutaneous Abdominal Adipose Tissue From Obese Humans. *Horm Metab Res* **28**: 690–693.
- Hughes, M.E., Hogenesch, J.B., and Kornacker, K. (2010) JTK_CYCLE: an efficient nonparametric algorithm for detecting rhythmic components in genome-scale data sets. *J Biol Rhythms* **25**: 372–380.
- Husse, J., Leliavski, A., Tsang, A.H., Oster, H., and Eichele, G. (2014) The light-dark cycle controls peripheral rhythmicity in mice with a genetically ablated suprachiasmatic nucleus clock. *FASEB J* **28**: 4950–4960.
- Immonen, H., Hannukainen, J.C., Iozzo, P., Soinio, M., Salminen, P., Saunavaara, V., *et al.* (2014) Effect of bariatric surgery on liver glucose metabolism in morbidly obese diabetic and non-diabetic patients. *Journal of Hepatology* **60**: 377–383.
- Incollingo Rodriguez, A.C., Epel, E.S., White, M.L., Standen, E.C., Seckl, J.R., and Tomiyama, A.J. (2015) Hypothalamic-pituitary-adrenal axis dysregulation and cortisol activity in obesity: A systematic review. *Psychoneuroendocrinology* **62**: 301–318.
- Jakubcakova, V., Oster, H., Tamanini, F., Cadenas, C., Leitges, M., Horst, G.T.J. van der, and Eichele, G. (2007) Light entrainment of the mammalian circadian clock by a PRKCA-dependent posttranslational mechanism. *Neuron* **54**: 831–843.
- Jakubowicz, D., Barnea, M., Wainstein, J., and Froy, O. (2013) High caloric intake at breakfast vs. dinner differentially influences weight loss of overweight and obese women. *Obesity (Silver Spring)* **21**: 2504–2512.
- Jakubowicz, D., Wainstein, J., Ahrén, B., Bar-Dayana, Y., Landau, Z., Rabinovitz, H.R., and Froy, O. (2015) High-energy breakfast with low-energy dinner decreases overall daily hyperglycaemia in type 2 diabetic patients: a randomised clinical trial. *Diabetologia* **58**: 912–919.
- Järvholm, K., Olbers, T., Marcus, C., Mårild, S., Gronowitz, E., Friberg, P., *et al.* (2012) Short-term psychological outcomes in severely obese adolescents after bariatric surgery. *Obesity (Silver Spring)* **20**: 318–323.
- Jialal, I., and Devaraj, S. (2018) Subcutaneous adipose tissue biology in metabolic syndrome. *Hormone Molecular Biology and Clinical Investigation* **33** <https://www.degruyter.com/doi/10.1515/hmbci-2017-0074>. Accessed October 26, 2020.
- Joshi, S., and Mohan, V. (2018) Pros & cons of some popular extreme weight-loss diets. *Indian J Med Res* **148**: 642.

- Jumbe, S., Bartlett, C., Jumbe, S.L., and Meyrick, J. (2016) The effectiveness of bariatric surgery on long term psychosocial quality of life - A systematic review. *Obes Res Clin Pract* **10**: 225–242.
- Kalarchian, M.A., and Marcus, M.D. (2019) Psychosocial Concerns Following Bariatric Surgery: Current Status. *Curr Obes Rep* **8**: 1–9.
- Kalinowski, P., Paluszkiwicz, R., Wróblewski, T., Remiszewski, P., Grodzicki, M., Bartoszewicz, Z., and Krawczyk, M. (2017) Ghrelin, leptin, and glycemic control after sleeve gastrectomy versus Roux-en-Y gastric bypass—results of a randomized clinical trial. *Surgery for Obesity and Related Diseases* **13**: 181–188.
- Kalsbeek, A., Fliers, E., Romijn, J.A., Fleur, S.E. la, Wortel, J., Bakker, O., *et al.* (2001) The Suprachiasmatic Nucleus Generates the Diurnal Changes in Plasma Leptin Levels. *Endocrinology* **142**: 2677–2685.
- Kalsbeek, A., Teclemariam-Mesbah, R., and Péavet, P. (1993) Efferent projections of the suprachiasmatic nucleus in the golden hamster (*Mesocricetus auratus*): SCN EFFERENT PROJECTIONS IN THE GOLDEN HAMSTER. *J Comp Neurol* **332**: 293–314.
- Kang, H.S., Angers, M., Beak, J.Y., Wu, X., Gimble, J.M., Wada, T., *et al.* (2007) Gene expression profiling reveals a regulatory role for ROR α and ROR γ in phase I and phase II metabolism. *Physiological Genomics* **31**: 281–294.
- Kang, Y.-H., Cho, M.-H., Kim, J.-Y., Kwon, M.-S., Peak, J.-J., Kang, S.-W., *et al.* (2016) Impaired macrophage autophagy induces systemic insulin resistance in obesity. *Oncotarget* **7**: 35577–35591.
- Kapoor, N., Al-Najim, W., Roux, C.W. le, and Docherty, N.G. (2017) Shifts in Food Preferences After Bariatric Surgery: Observational Reports and Proposed Mechanisms. *Curr Obes Rep* **6**: 246–252.
- Karra, E., Yousseif, A., and Batterham, R.L. (2010) Mechanisms facilitating weight loss and resolution of type 2 diabetes following bariatric surgery. *Trends in Endocrinology & Metabolism* **21**: 337–344.
- Katsiki, N., Perez-Martinez, P., Anagnostis, P., Mikhailidis, D.P., and Karagiannis, A. (2018) Is Nonalcoholic Fatty Liver Disease Indeed the Hepatic Manifestation of Metabolic Syndrome? *CVP* **16**: 219–227.
- Katsogiannis, P., Kamble, P.G., Boersma, G.J., Karlsson, F.A., Lundkvist, P., Sundbom, M., *et al.* (2019) Early Changes in Adipose Tissue Morphology, Gene Expression, and Metabolism After RYGB in Patients With Obesity and T2D. *The Journal of Clinical Endocrinology & Metabolism* **104**: 2601–2613.
- Kerr, A.G., Andersson, D.P., Rydén, M., Arner, P., and Dahlman, I. (2020) Long-term changes in adipose tissue gene expression following bariatric surgery. *J Intern Med* **288**: 219–233.
- Kettner, N.M., Mayo, S.A., Hua, J., Lee, C., Moore, D.D., and Fu, L. (2015) Circadian Dysfunction Induces Leptin Resistance in Mice. *Cell Metab* **22**: 448–459.
- Kiehn, J.-T., Tsang, A.H., Heyde, I., Leinweber, B., Kolbe, I., Leliavski, A., and Oster, H. (2017) Circadian Rhythms in Adipose Tissue Physiology. In *Comprehensive Physiology*. Terjung, R. (ed.). John Wiley & Sons, Inc., Hoboken, NJ, USA. pp. 383–427 <http://doi.wiley.com/10.1002/cphy.c160017>. Accessed February 10, 2021.
- Kiguchi, N., Maeda, T., Kobayashi, Y., Fukazawa, Y., and Kishioka, S. (2009) Leptin enhances CC-chemokine ligand expression in cultured murine macrophage. *Biochemical and Biophysical Research Communications* **384**: 311–315.

- Kim, M., Son, Y.G., Kang, Y.N., Ha, T.K., and Ha, E. (2015) Changes in Glucose Transporters, Gluconeogenesis, and Circadian Clock after Duodenal–Jejunal Bypass Surgery. *OBES SURG* **25**: 635–641.
- Kim, S.-M., Neuendorff, N., Alaniz, R.C., Sun, Y., Chapkin, R.S., and Earnest, D.J. (2018) Shift work cycle-induced alterations of circadian rhythms potentiate the effects of high-fat diet on inflammation and metabolism. *FASEB J* **32**: 3085–3095.
- King, W.C., Chen, J.-Y., Courcoulas, A.P., Dakin, G.F., Engel, S.G., Flum, D.R., *et al.* (2017) Alcohol and other substance use after bariatric surgery: prospective evidence from a U.S. multicenter cohort study. *Surgery for Obesity and Related Diseases* **13**: 1392–1402.
- Koch, C.E., Leinweber, B., Drengberg, B.C., Blaum, C., and Oster, H. (2017) Interaction between circadian rhythms and stress. *Neurobiol Stress* **6**: 57–67.
- Kohsaka, A., Laposky, A.D., Ramsey, K.M., Estrada, C., Joshu, C., Kobayashi, Y., *et al.* (2007) High-fat diet disrupts behavioral and molecular circadian rhythms in mice. *Cell Metab* **6**: 414–421.
- Kolbe, I., Leinweber, B., Brandenburger, M., and Oster, H. (2019) Circadian clock network desynchrony promotes weight gain and alters glucose homeostasis in mice. *Mol Metab* **30**: 140–151.
- Könner, A.C., and Brüning, J.C. (2012) Selective Insulin and Leptin Resistance in Metabolic Disorders. *Cell Metabolism* **16**: 144–152.
- Konttinen, H., Peltonen, M., Sjöström, L., Carlsson, L., and Karlsson, J. (2015) Psychological aspects of eating behavior as predictors of 10-y weight changes after surgical and conventional treatment of severe obesity: results from the Swedish Obese Subjects intervention study. *The American Journal of Clinical Nutrition* **101**: 16–24.
- Koronowski, K.B., Kinouchi, K., Welz, P.-S., Smith, J.G., Zinna, V.M., Shi, J., *et al.* (2019) Defining the Independence of the Liver Circadian Clock. *Cell* **177**: 1448–1462.e14.
- Kudo, T., Akiyama, M., Kuriyama, K., Sudo, M., Moriya, T., and Shibata, S. (2004) Night-time restricted feeding normalises clock genes and *Pai-1* gene expression in the db/db mouse liver. *Diabetologia* **47**: 1425–1436.
- Kumar Jha, P., Challet, E., and Kalsbeek, A. (2015) Circadian rhythms in glucose and lipid metabolism in nocturnal and diurnal mammals. *Molecular and Cellular Endocrinology* **418**: 74–88.
- Kume, K., Zylka, M.J., Sriram, S., Shearman, L.P., Weaver, D.R., Jin, X., *et al.* (1999) mCRY1 and mCRY2 are essential components of the negative limb of the circadian clock feedback loop. *Cell* **98**: 193–205.
- Kuti, O.J., and Page, D.T. (2011) Assessment of Social Approach Behavior in Mice. In *Mood and Anxiety Related Phenotypes in Mice*. Gould, T.D. (ed.). Humana Press, Totowa, NJ. pp. 83–95 http://link.springer.com/10.1007/978-1-61779-313-4_5. Accessed February 19, 2021.
- Kutsuma, A., Nakajima, K., and Suwa, K. (2014) Potential Association between Breakfast Skipping and Concomitant Late-Night-Dinner Eating with Metabolic Syndrome and Proteinuria in the Japanese Population. *Scientifica (Cairo)* **2014**: 253581.
- Kwon, Y., Kim, H.J., Lo Menzo, E., Park, S., Szomstein, S., and Rosenthal, R.J. (2014) Anemia, iron and vitamin B12 deficiencies after sleeve gastrectomy compared to Roux-en-Y gastric bypass: a meta-analysis. *Surg Obes Relat Dis* **10**: 589–597.

- La Fleur, Kalsbeek, Wortel, and Buijs (2001) A Suprachiasmatic Nucleus Generated Rhythm In Basal Glucose Concentrations: A glucose rhythm generated by the SCN. *Journal of Neuroendocrinology* **11**: 643–652.
- Labrecque, J., Laforest, S., Michaud, A., Biertho, L., and Tchernof, A. (2017) Impact of Bariatric Surgery on White Adipose Tissue Inflammation. *Canadian Journal of Diabetes* **41**: 407–417.
- Laermans, J., Vancleef, L., Tack, J., and Depoortere, I. (2015) Role of the clock gene Bmal1 and the gastric ghrelin-secreting cell in the circadian regulation of the ghrelin-GOAT system. *Sci Rep* **5**: 16748.
- Lamia, K.A., Sachdeva, U.M., DiTacchio, L., Williams, E.C., Alvarez, J.G., Egan, D.F., *et al.* (2009) AMPK regulates the circadian clock by cryptochrome phosphorylation and degradation. *Science* **326**: 437–440.
- Lamia, K.A., Storch, K.-F., and Weitz, C.J. (2008) Physiological significance of a peripheral tissue circadian clock. *Proc Natl Acad Sci U S A* **105**: 15172–15177.
- Landauer, M.R., and Balster, R.L. (1982) A new test for social investigation in mice: Effects of d-amphetamine. *Psychopharmacology* **78**: 322–325.
- Landecheo, M.F., Valentí, V., Moncada, R., and Frühbeck, G. (2017) Eligibility and Success Criteria for Bariatric/Metabolic Surgery. In *Obesity and Lipotoxicity*. Engin, A.B., and Engin, A. (eds). Springer International Publishing, Cham. pp. 529–543 http://link.springer.com/10.1007/978-3-319-48382-5_23. Accessed November 12, 2020.
- Landgraf, D., Neumann, A.-M., and Oster, H. (2017) Circadian clock-gastrointestinal peptide interaction in peripheral tissues and the brain. *Best Pract Res Clin Endocrinol Metab* **31**: 561–571.
- Landgraf, D., Tsang, A.H., Leliavski, A., Koch, C.E., Barclay, J.L., Drucker, D.J., and Oster, H. (2015) Oxyntomodulin regulates resetting of the liver circadian clock by food. *eLife* **4**: e06253.
- Laurenus, A., Larsson, I., Bueter, M., Melanson, K.J., Bosaeus, I., Forslund, H.B., *et al.* (2012) Changes in eating behaviour and meal pattern following Roux-en-Y gastric bypass. *Int J Obes (Lond)* **36**: 348–355.
- Le Martelot, G., Claudel, T., Gatfield, D., Schaad, O., Kornmann, B., Sasso, G.L., *et al.* (2009) REV-ERB α Participates in Circadian SREBP Signaling and Bile Acid Homeostasis. *PLoS Biol* **7**: e1000181.
- Le Minh, N., Damiola, F., Tronche, F., Schütz, G., and Schibler, U. (2001) Glucocorticoid hormones inhibit food-induced phase-shifting of peripheral circadian oscillators. *EMBO J* **20**: 7128–7136.
- Leliavski, A., Shostak, A., Husse, J., and Oster, H. (2014) Impaired Glucocorticoid Production and Response to Stress in Arntl-Deficient Male Mice. *Endocrinology* **155**: 133–142.
- Lemieux, I., Pascot, A., Prud'homme, D., Alméras, N., Bogaty, P., Nadeau, A., *et al.* (2001) Elevated C-Reactive Protein: Another Component of the Atherothrombotic Profile of Abdominal Obesity. *Arterioscler Thromb Vasc Biol* **21**: 961–967.
- Levi, J., Gray, S.L., Speck, M., Huynh, F.K., Babich, S.L., Gibson, W.T., and Kieffer, T.J. (2011) Acute Disruption of Leptin Signaling in Vivo Leads to Increased Insulin Levels and Insulin Resistance. *Endocrinology* **152**: 3385–3395.

- Lewis, J.E., Monnier, C., Marshall, H., Fowler, M., Green, R., Cooper, S., *et al.* (2020) Whole-body and adipose tissue-specific mechanisms underlying the metabolic effects of fibroblast growth factor 21 in the Siberian hamster. *Molecular Metabolism* **31**: 45–54.
- Li, A.-J., Wiater, M.F., Oostrom, M.T., Smith, B.R., Wang, Q., Dinh, T.T., *et al.* (2012) Leptin-sensitive neurons in the arcuate nuclei contribute to endogenous feeding rhythms. *Am J Physiol Regul Integr Comp Physiol* **302**: R1313–1326.
- Liao, Y., Wang, J., Jaehnig, E.J., Shi, Z., and Zhang, B. (2019) WebGestalt 2019: gene set analysis toolkit with revamped UIs and APIs. *Nucleic Acids Res* **47**: W199–W205.
- Lim, E.L., Hollingsworth, K.G., Aribisala, B.S., Chen, M.J., Mathers, J.C., and Taylor, R. (2011) Reversal of type 2 diabetes: normalisation of beta cell function in association with decreased pancreas and liver triacylglycerol. *Diabetologia* **54**: 2506–2514.
- Littleton, E.S., Childress, M.L., Gosting, M.L., Jackson, A.N., and Kojima, S. (2020) Genome-wide correlation analysis to identify amplitude regulators of circadian transcriptome output. *Sci Rep* **10**: 21839.
- Liu, H., Hu, C., Zhang, X., and Jia, W. (2018a) Role of gut microbiota, bile acids and their cross-talk in the effects of bariatric surgery on obesity and type 2 diabetes. *J Diabetes Investig* **9**: 13–20.
- Liu, J., Yang, X., Yu, S., and Zheng, R. (2018b) The Leptin Resistance. In *Neural Regulation of Metabolism*. Wu, Q., and Zheng, R. (eds). Springer Singapore, Singapore. pp. 145–163 http://link.springer.com/10.1007/978-981-13-1286-1_8. Accessed October 16, 2020.
- Longo, M., Zatterale, F., Naderi, J., Parrillo, L., Formisano, P., Raciti, G.A., *et al.* (2019) Adipose Tissue Dysfunction as Determinant of Obesity-Associated Metabolic Complications. *IJMS* **20**: 2358.
- Lopez-Minguez, J., Gómez-Abellán, P., and Garaulet, M. (2016) Circadian rhythms, food timing and obesity. *Proc Nutr Soc* **75**: 501–511.
- Lord, G.M., Matarese, G., Howard, J.K., Baker, R.J., Bloom, S.R., and Lechler, R.I. (1998) Leptin modulates the T-cell immune response and reverses starvation-induced immunosuppression. *Nature* **394**: 897–901.
- Love, M.I., Huber, W., and Anders, S. (2014) Moderated estimation of fold change and dispersion for RNA-seq data with DESeq2. *Genome Biol* **15**: 550.
- Luo, S., Zhang, Y., Ezrokhi, M., Li, Y., Tsai, T.-H., and Cincotta, A.H. (2018) Circadian peak dopaminergic activity response at the biological clock pacemaker (suprachiasmatic nucleus) area mediates the metabolic responsiveness to a high-fat diet. *J Neuroendocrinol* **30**.
- Luppino, F.S., Wit, L.M. de, Bouvy, P.F., Stijnen, T., Cuijpers, P., Penninx, B.W.J.H., and Zitman, F.G. (2010) Overweight, Obesity, and Depression: A Systematic Review and Meta-analysis of Longitudinal Studies. *Arch Gen Psychiatry* **67**: 220.
- Lv, N., Azar, K.M.J., Rosas, L.G., Wulfovich, S., Xiao, L., and Ma, J. (2017) Behavioral lifestyle interventions for moderate and severe obesity: A systematic review. *Preventive Medicine* **100**: 180–193.
- Maere, S., Heymans, K., and Kuiper, M. (2005) BiNGO: a Cytoscape plugin to assess overrepresentation of gene ontology categories in biological networks. *Bioinformatics* **21**: 3448–3449.

- Maffei, M., Stoffel, M., Barone, M., Moon, B., Dammerman, M., Ravussin, E., *et al.* (1996) Absence of Mutations in the Human OB Gene in Obese/Diabetic Subjects. *Diabetes* **45**: 679–682.
- Maier, B., Wendt, S., Vanselow, J.T., Wallach, T., Reischl, S., Oehmke, S., *et al.* (2009) A large-scale functional RNAi screen reveals a role for CK2 in the mammalian circadian clock. *Genes Dev* **23**: 708–718.
- Makwana, K., Gosai, N., Poe, A., and Kondratov, R.V. (2019) Calorie restriction reprograms diurnal rhythms in protein translation to regulate metabolism. *FASEB J* **33**: 4473–4489.
- Marcheva, B., Ramsey, K.M., Buhr, E.D., Kobayashi, Y., Su, H., Ko, C.H., *et al.* (2010) Disruption of the clock components CLOCK and BMAL1 leads to hypoinsulinaemia and diabetes. *Nature* **466**: 627–631.
- Marti, A., Meerlo, P., Grønli, J., Hasselt, S. van, Mrdalj, J., Pallesen, S., *et al.* (2016) Shift in Food Intake and Changes in Metabolic Regulation and Gene Expression during Simulated Night-Shift Work: A Rat Model. *Nutrients* **8**: 712.
- Masís-Vargas, A., Ritsema, W.I.G.R., Mendoza, J., and Kalsbeek, A. (2020) Metabolic Effects of Light at Night are Time- and Wavelength-Dependent in Rats. *Obesity (Silver Spring)* **28 Suppl 1**: S114–S125.
- Mattson, M.P., Longo, V.D., and Harvie, M. (2017) Impact of intermittent fasting on health and disease processes. *Ageing Res Rev* **39**: 46–58.
- McGavigan, A.K., Garibay, D., Henseler, Z.M., Chen, J., Bettaieb, A., Haj, F.G., *et al.* (2017a) TGR5 contributes to glucoregulatory improvements after vertical sleeve gastrectomy in mice. *Gut* **66**: 226–234.
- McGavigan, A.K., Henseler, Z.M., Garibay, D., Butler, S.D., Jayasinghe, S., Ley, R.E., *et al.* (2017b) Vertical sleeve gastrectomy reduces blood pressure and hypothalamic endoplasmic reticulum stress in mice. *Dis Model Mech* **10**: 235–243.
- McMenamin, T.M. (2007) A time to work: recent trends in shift work and flexible schedules. *Monthly Labor Review* .
- Meek, C.L., Lewis, H.B., Reimann, F., Gribble, F.M., and Park, A.J. (2016) The effect of bariatric surgery on gastrointestinal and pancreatic peptide hormones. *Peptides* **77**: 28–37.
- Méndez-Hernández, R., Escobar, C., and Buijs, R.M. (2020) Suprachiasmatic Nucleus-Arcuate Nucleus Axis: Interaction Between Time and Metabolism Essential for Health. *Obesity (Silver Spring)* **28 Suppl 1**: S10–S17.
- Mendoza, J., Drevet, K., Pévet, P., and Challet, E. (2008a) Daily meal timing is not necessary for resetting the main circadian clock by calorie restriction. *J Neuroendocrinol* **20**: 251–260.
- Mendoza, J., Graff, C., Dardente, H., Pévet, P., and Challet, E. (2005) Feeding cues alter clock gene oscillations and photic responses in the suprachiasmatic nuclei of mice exposed to a light/dark cycle. *J Neurosci* **25**: 1514–1522.
- Mendoza, J., Pévet, P., and Challet, E. (2007) Circadian and photic regulation of clock and clock-controlled proteins in the suprachiasmatic nuclei of calorie-restricted mice. *Eur J Neurosci* **25**: 3691–3701.
- Mendoza, J., Pévet, P., and Challet, E. (2008b) High-fat feeding alters the clock synchronization to light. *J Physiol* **586**: 5901–5910.

- Meneses, M.E., Camargo, A., Perez-Martinez, P., Delgado-Lista, J., Cruz-Teno, C., Jimenez-Gomez, Y., *et al.* (2011) Postprandial inflammatory response in adipose tissue of patients with metabolic syndrome after the intake of different dietary models. *Mol Nutr Food Res* **55**: 1759–1770.
- Meng, Q.-J., Logunova, L., Maywood, E.S., Gallego, M., Lebiecki, J., Brown, T.M., *et al.* (2008) Setting clock speed in mammals: the CK1 epsilon tau mutation in mice accelerates circadian pacemakers by selectively destabilizing PERIOD proteins. *Neuron* **58**: 78–88.
- Min, T., Prior, S.L., Dunseath, G., Churm, R., Barry, J.D., and Stephens, J.W. (2020) Temporal Effects of Bariatric Surgery on Adipokines, Inflammation and Oxidative Stress in Subjects with Impaired Glucose Homeostasis at 4 Years of Follow-up. *Obes Surg* **30**: 1712–1718.
- Minocci, A., Savia, G., Lucantoni, R., Berselli, M., Tagliaferri, M., Calò, G., *et al.* (2000) Leptin plasma concentrations are dependent on body fat distribution in obese patients. *Int J Obes* **24**: 1139–1144.
- Miras, A.D., and Roux, C.W. le (2010) Bariatric surgery and taste: novel mechanisms of weight loss: *Current Opinion in Gastroenterology* **26**: 140–145.
- Mistlberger, R.E. (2009) Food-anticipatory circadian rhythms: concepts and methods. *European Journal of Neuroscience* **30**: 1718–1729.
- Mitsui, S., Yamaguchi, S., Matsuo, T., Ishida, Y., and Okamura, H. (2001) Antagonistic role of E4BP4 and PAR proteins in the circadian oscillatory mechanism. *Genes Dev* **15**: 995–1006.
- Mokadem, M., Zechner, J.F., Uchida, A., and Aguirre, V. (2015) Leptin Is Required for Glucose Homeostasis after Roux-en-Y Gastric Bypass in Mice. *PLoS ONE* **10**: e0139960.
- Molyneux, P.C., Dahlgren, M.K., and Harrington, M.E. (2008) Circadian entrainment aftereffects in suprachiasmatic nuclei and peripheral tissues in vitro. *Brain Research* **1228**: 127–134.
- Monje, F.J., Cabatic, M., Divisch, I., Kim, E.-J., Herkner, K.R., Binder, B.R., and Pollak, D.D. (2011) Constant darkness induces IL-6-dependent depression-like behavior through the NF- κ B signaling pathway. *J Neurosci* **31**: 9075–9083.
- Monpellier, V.M., Antoniou, E.E., Mulkens, S., Janssen, I.M.C., Molen, A.B.M. van der, and Jansen, A.T.M. (2018) Body image dissatisfaction and depression in postbariatric patients is associated with less weight loss and a desire for body contouring surgery. *Surgery for Obesity and Related Diseases* **14**: 1507–1515.
- Montaigne, D., Marechal, X., Modine, T., Coisne, A., Mouton, S., Fayad, G., *et al.* (2018) Daytime variation of perioperative myocardial injury in cardiac surgery and its prevention by Rev-Erba antagonism: a single-centre propensity-matched cohort study and a randomised study. *The Lancet* **391**: 59–69.
- Motoshima, H., Wu, X., Sinha, M.K., Hardy, V.E., Rosato, E.L., Barbot, D.J., *et al.* (2002) Differential Regulation of Adiponectin Secretion from Cultured Human Omental and Subcutaneous Adipocytes: Effects of Insulin and Rosiglitazone. *The Journal of Clinical Endocrinology & Metabolism* **87**: 5662–5667.
- Mukherji, A., Kobiita, A., and Chambon, P. (2015a) Shifting the feeding of mice to the rest phase creates metabolic alterations, which, on their own, shift the peripheral circadian clocks by 12 hours. *Proc Natl Acad Sci U S A* **112**: E6683–6690.

- Mukherji, A., Kobiita, A., Damara, M., Misra, N., Meziane, H., Champy, M.-F., and Chambon, P. (2015b) Shifting eating to the circadian rest phase misaligns the peripheral clocks with the master SCN clock and leads to a metabolic syndrome. *Proc Natl Acad Sci U S A* **112**: E6691-6698.
- Müller, T.D., Nogueiras, R., Andermann, M.L., Andrews, Z.B., Anker, S.D., Argente, J., *et al.* (2015) Ghrelin. *Molecular Metabolism* **4**: 437–460.
- Münch, M., and Kramer, A. (2019) Timing matters: New tools for personalized chronomedicine and circadian health. *Acta Physiol* **227** <https://onlinelibrary.wiley.com/doi/abs/10.1111/apha.13300>. Accessed October 7, 2020.
- Mure, L.S., Le, H.D., Benegiamo, G., Chang, M.W., Rios, L., Jillani, N., *et al.* (2018) Diurnal transcriptome atlas of a primate across major neural and peripheral tissues. *Science* **359**: eaao0318.
- Nadler, J.J., Moy, S.S., Dold, G., Simmons, N., Perez, A., Young, N.B., *et al.* (2004) Automated apparatus for quantitation of social approach behaviors in mice. *Genes Brain Behav* **3**: 303–314.
- Nakahata, Y., Kaluzova, M., Grimaldi, B., Sahar, S., Hirayama, J., Chen, D., *et al.* (2008) The NAD⁺-dependent deacetylase SIRT1 modulates CLOCK-mediated chromatin remodeling and circadian control. *Cell* **134**: 329–340.
- Nasser, H., Ivanics, T., Leonard-Murali, S., Shakaroun, D., and Genaw, J. (2019) Perioperative outcomes of laparoscopic Roux-en-Y gastric bypass and sleeve gastrectomy in super-obese and super-super-obese patients: a national database analysis. *Surgery for Obesity and Related Diseases* **15**: 1696–1703.
- Neumann, A.-M., Schmidt, C.X., Brockmann, R.M., and Oster, H. (2019) Circadian regulation of endocrine systems. *Autonomic Neuroscience* **216**: 1–8.
- Nikiforova, I., Barnea, R., Azulai, S., and Susmallian, S. (2019) Analysis of the Association between Eating Behaviors and Weight Loss after Laparoscopic Sleeve Gastrectomy. *Obes Facts* **12**: 618–631.
- O'Brien, P.E., Hindle, A., Brennan, L., Skinner, S., Burton, P., Smith, A., *et al.* (2019) Long-Term Outcomes After Bariatric Surgery: a Systematic Review and Meta-analysis of Weight Loss at 10 or More Years for All Bariatric Procedures and a Single-Centre Review of 20-Year Outcomes After Adjustable Gastric Banding. *Obes Surg* **29**: 3–14.
- OECD (2018) Overweight or obese population. <https://www.oecd-ilibrary.org/content/data/86583552-en>. Accessed February 18, 2021.
- OECD (2019) Hours worked. <https://www.oecd-ilibrary.org/content/data/47be1c78-en>. Accessed February 18, 2021.
- Ogata, H., Kayaba, M., Tanaka, Y., Yajima, K., Iwayama, K., Ando, A., *et al.* (2019) Effect of skipping breakfast for 6 days on energy metabolism and diurnal rhythm of blood glucose in young healthy Japanese males. *Am J Clin Nutr* **110**: 41–52.
- Oishi, K., and Hashimoto, C. (2018) Short-term time-restricted feeding during the resting phase is sufficient to induce leptin resistance that contributes to development of obesity and metabolic disorders in mice. *Chronobiol Int* **35**: 1576–1594.
- Olivo, D., Caba, M., Gonzalez-Lima, F., Vázquez, A., and Corona-Morales, A. (2014) Circadian feeding entrains anticipatory metabolic activity in piriform cortex and olfactory tubercle, but not in suprachiasmatic nucleus. *Brain Research* **1592**: 11–21.

- O'Neill, J.S., and Reddy, A.B. (2011) Circadian clocks in human red blood cells. *Nature* **469**: 498–503.
- Orellana, E.R., Covasa, M., and Hajnal, A. (2019) Neuro-hormonal mechanisms underlying changes in reward related behaviors following weight loss surgery: Potential pharmacological targets. *Biochem Pharmacol* **164**: 106–114.
- Ortega, F.J., Mercader, J.M., Moreno-Navarrete, J.M., Nonell, L., Puigdecanet, E., Rodriguez-Hermosa, J.I., *et al.* (2015) Surgery-Induced Weight Loss Is Associated With the Downregulation of Genes Targeted by MicroRNAs in Adipose Tissue. *The Journal of Clinical Endocrinology & Metabolism* **100**: E1467–E1476.
- Oster, H., Damerow, S., Kiessling, S., Jakubcakova, V., Abraham, D., Tian, J., *et al.* (2006) The circadian rhythm of glucocorticoids is regulated by a gating mechanism residing in the adrenal cortical clock. *Cell Metabolism* **4**: 163–173.
- Otsuka, A., Shiuchi, T., Chikahisa, S., Shimizu, N., and Séi, H. (2019) Sufficient intake of high-fat food attenuates stress-induced social avoidance behavior. *Life Sciences* **219**: 219–230.
- Packard, A.E.B., Egan, A.E., and Ulrich-Lai, Y.M. (2016) HPA Axis Interactions with Behavioral Systems. *Compr Physiol* **6**: 1897–1934.
- Padilla, N., Maraninchi, M., Béliard, S., Berthet, B., Nogueira, J.-P., Wolff, E., *et al.* (2014) Effects of Bariatric Surgery on Hepatic and Intestinal Lipoprotein Particle Metabolism in Obese, Nondiabetic Humans. *Arterioscler Thromb Vasc Biol* **34**: 2330–2337.
- Padilla, S.L., Perez, J.G., Ben-Hamo, M., Johnson, C.W., Sanchez, R.E.A., Bussi, I.L., *et al.* (2019) Kisspeptin Neurons in the Arcuate Nucleus of the Hypothalamus Orchestrate Circadian Rhythms and Metabolism. *Curr Biol* **29**: 592-604.e4.
- Pan, W., and Kastin, A.J. (2001) Diurnal variation of leptin entry from blood to brain involving partial saturation of the transport system. *Life Sci* **68**: 2705–2714.
- Park, Y.-W., Zhu, S., Palaniappan, L., Heshka, S., Carnethon, M.R., and Heymsfield, S.B. (2003) The Metabolic Syndrome: Prevalence and Associated Risk Factor Findings in the US Population From the Third National Health and Nutrition Examination Survey, 1988-1994. *Arch Intern Med* **163**: 427.
- Paschos, G.K., Ibrahim, S., Song, W.-L., Kunieda, T., Grant, G., Reyes, T.M., *et al.* (2012) Obesity in mice with adipocyte-specific deletion of clock component Arntl. *Nat Med* **18**: 1768–1777.
- Pasley, J.N., Barnes, C.L., and Rayford, P.L. (1987) Circadian rhythms of serum gastrin and plasma cholecystokinin in rodents. *Prog Clin Biol Res* **227A**: 371–378.
- Patel, S.A., Velingkaar, N., Makwana, K., Chaudhari, A., and Kondratov, R. (2016) Calorie restriction regulates circadian clock gene expression through BMAL1 dependent and independent mechanisms. *Sci Rep* **6**: 25970.
- Patton, A., Khan, F.H., and Kohli, R. (2017) Impact of Fibroblast Growth Factors 19 and 21 in Bariatric Metabolism. *Dig Dis* **35**: 191–196.
- Pendergast, J.S., Branecky, K.L., Yang, W., Ellacott, K.L.J., Niswender, K.D., and Yamazaki, S. (2013) High-fat diet acutely affects circadian organisation and eating behavior. *Eur J Neurosci* **37**: 1350–1356.

- Perelis, M., Marcheva, B., Ramsey, K.M., Schipma, M.J., Hutchison, A.L., Taguchi, A., *et al.* (2015) Pancreatic β cell enhancers regulate rhythmic transcription of genes controlling insulin secretion. *Science* **350**: aac4250.
- Perez-Leon, J.A., Warren, E.J., Allen, C.N., Robinson, D.W., and Brown, R.L. (2006) Synaptic inputs to retinal ganglion cells that set the circadian clock. *Eur J Neurosci* **24**: 1117–1123.
- Peterli, R., Wölnerhanssen, B.K., Peters, T., Vetter, D., Kröll, D., Borbély, Y., *et al.* (2018) Effect of Laparoscopic Sleeve Gastrectomy vs Laparoscopic Roux-en-Y Gastric Bypass on Weight Loss in Patients With Morbid Obesity: The SM-BOSS Randomized Clinical Trial. *JAMA* **319**: 255.
- Pezük, P., Mohawk, J.A., Wang, L.A., and Menaker, M. (2012) Glucocorticoids as Entraining Signals for Peripheral Circadian Oscillators. *Endocrinology* **153**: 4775–4783.
- Piché, M.-E., Tardif, I., Auclair, A., and Poirier, P. (2020) Effects of bariatric surgery on lipid-lipoprotein profile. *Metabolism* **115**: 154441.
- Pickel, L., and Sung, H.-K. (2020) Feeding Rhythms and the Circadian Regulation of Metabolism. *Front Nutr* **7**: 39.
- Pivovarova, O., Jürchott, K., Rudovich, N., Hornemann, S., Ye, L., Möckel, S., *et al.* (2015) Changes of Dietary Fat and Carbohydrate Content Alter Central and Peripheral Clock in Humans. *The Journal of Clinical Endocrinology & Metabolism* **100**: 2291–2302.
- Plagemann, A., Harder, T., Brunn, M., Harder, A., Roepke, K., Wittrock-Staar, M., *et al.* (2009) Hypothalamic proopiomelanocortin promoter methylation becomes altered by early overfeeding: an epigenetic model of obesity and the metabolic syndrome: Nutritionally induced alterations of POMC promoter methylation. *The Journal of Physiology* **587**: 4963–4976.
- Poggiogalle, E., Jamshed, H., and Peterson, C.M. (2018) Circadian regulation of glucose, lipid, and energy metabolism in humans. *Metabolism* **84**: 11–27.
- Pohjanvirta, R., Boutros, P.C., Moffat, I.D., Lindén, J., Wendelin, D., and Okey, A.B. (2008) Genome-wide effects of acute progressive feed restriction in liver and white adipose tissue. *Toxicol Appl Pharmacol* **230**: 41–56.
- Prasai, M.J., Mughal, R.S., Wheatcroft, S.B., Kearney, M.T., Grant, P.J., and Scott, E.M. (2013) Diurnal variation in vascular and metabolic function in diet-induced obesity: divergence of insulin resistance and loss of clock rhythm. *Diabetes* **62**: 1981–1989.
- Preitner, N., Damiola, F., Lopez-Molina, L., Zakany, J., Duboule, D., Albrecht, U., and Schibler, U. (2002) The orphan nuclear receptor REV-ERB α controls circadian transcription within the positive limb of the mammalian circadian oscillator. *Cell* **110**: 251–260.
- Pressler, J.W., Haller, A., Sorrell, J., Wang, F., Seeley, R.J., Tso, P., and Sandoval, D.A. (2015) Vertical Sleeve Gastrectomy Restores Glucose Homeostasis in Apolipoprotein A-IV KO Mice. *Diabetes* **64**: 498–507.
- Rabe, K., Lehrke, M., Parhofer, K.G., and Broedl, U.C. (2008) Adipokines and insulin resistance. *Mol Med* **14**: 741–751.
- Radley, J., Morilak, D., Viau, V., and Campeau, S. (2015) Chronic stress and brain plasticity: Mechanisms underlying adaptive and maladaptive changes and implications for stress-related CNS disorders. *Neurosci Biobehav Rev* **58**: 79–91.

- Rafey, M.F., Fang, C.E.H., Ioana, I., Griffin, H., Hynes, M., O'Brien, T., *et al.* (2020) The leptin to adiponectin ratio (LAR) is reduced by sleeve gastrectomy in adults with severe obesity: a prospective cohort study. *Sci Rep* **10**: 16270.
- Rahmouni, K., Morgan, D.A., Morgan, G.M., Mark, A.L., and Haynes, W.G. (2005) Role of Selective Leptin Resistance in Diet-Induced Obesity Hypertension. *Diabetes* **54**: 2012–2018.
- Ramadan, M., Loureiro, M., Laughlan, K., Caiazzo, R., Iannelli, A., Brunaud, L., *et al.* (2016) Risk of Dumping Syndrome after Sleeve Gastrectomy and Roux-en-Y Gastric Bypass: Early Results of a Multicentre Prospective Study. *Gastroenterology Research and Practice* **2016**: 1–5.
- Ravelli, G.P., Stein, Z.A., and Susser, M.W. (1976) Obesity in young men after famine exposure in utero and early infancy. *N Engl J Med* **295**: 349–353.
- Reddy, A.B., Maywood, E.S., Karp, N.A., King, V.M., Inoue, Y., Gonzalez, F.J., *et al.* (2007) Glucocorticoid signaling synchronizes the liver circadian transcriptome. *Hepatology* **45**: 1478–1488.
- Reddy, T.E., Gertz, J., Crawford, G.E., Garabedian, M.J., and Myers, R.M. (2012) The hypersensitive glucocorticoid response specifically regulates period 1 and expression of circadian genes. *Mol Cell Biol* **32**: 3756–3767.
- Reichelt, A.C., Loughman, A., Bernard, A., Raipuria, M., Abbott, K.N., Dachtler, J., *et al.* (2020) An intermittent hypercaloric diet alters gut microbiota, prefrontal cortical gene expression and social behaviours in rats. *Nutritional Neuroscience* **23**: 613–627.
- Reid, K.J., and Abbott, S.M. (2015) Jet Lag and Shift Work Disorder. *Sleep Medicine Clinics* **10**: 523–535.
- Reimann, M., Qin, N., Gruber, M., Bornstein, S.R., Kirschbaum, C., Ziemssen, T., and Eisenhofer, G. (2017) Adrenal medullary dysfunction as a feature of obesity. *Int J Obes* **41**: 714–721.
- Rey, G., Cesbron, F., Rougemont, J., Reinke, H., Brunner, M., and Naef, F. (2011) Genome-Wide and Phase-Specific DNA-Binding Rhythms of BMAL1 Control Circadian Output Functions in Mouse Liver. *PLoS Biol* **9**: e1000595.
- Richards, J., and Gumz, M.L. (2012) Advances in understanding the peripheral circadian clocks. *FASEB J* **26**: 3602–3613.
- Rieber, N., Giel, K.E., Meile, T., Enck, P., Zipfel, S., and Teufel, M. (2013) Psychological dimensions after laparoscopic sleeve gastrectomy: reduced mental burden, improved eating behavior, and ongoing need for cognitive eating control. *Surgery for Obesity and Related Diseases* **9**: 569–573.
- Rohde, K., Keller, M., Cour Poulsen, L. la, Blüher, M., Kovacs, P., and Böttcher, Y. (2019) Genetics and epigenetics in obesity. *Metabolism* **92**: 37–50.
- Rosenwasser, A.M., McCulley, W.D., Hartmann, M.C., Fixaris, M.C., and Crabbe, J.C. (2020) Suppression of voluntary ethanol intake in mice under constant light and constant darkness. *Alcohol* **83**: 37–46.
- Rosenwasser, A.M., and Turek, F.W. (2015) Neurobiology of Circadian Rhythm Regulation. *Sleep Medicine Clinics* **10**: 403–412.
- Rubin, N.H., Singh, P., Alinder, G., Greeley, G.H., Rayford, P.L., Rietveld, W.J., and Thompson, J.C. (1988) Circadian rhythms in gastrin receptors in rat fundic stomach. *Digest Dis Sci* **33**: 931–937.

- Ruiz-Lozano, T., Vidal, J., Hollanda, A. de, Canteras, M., Garaulet, M., and Izquierdo-Pulido, M. (2016a) Evening chronotype associates with obesity in severely obese subjects: interaction with CLOCK 3111T/C. *Int J Obes* **40**: 1550–1557.
- Ruiz-Lozano, T., Vidal, J., Hollanda, A. de, Scheer, F. a. J.L., Garaulet, M., and Izquierdo-Pulido, M. (2016b) Timing of food intake is associated with weight loss evolution in severe obese patients after bariatric surgery. *Clin Nutr* **35**: 1308–1314.
- Ruiz-Tovar, J., Boix, E., Bonete, J.M., Martínez, R., Zubiaga, L., Díez, M., and Calpena, R. (2015) Effect of Preoperative Eating Patterns and Preoperative Weight Loss on the Short- and Mid-term Weight Loss Results of Sleeve Gastrectomy. *Cirugía Española (English Edition)* **93**: 241–247.
- Ryan, K.K., Tremaroli, V., Clemmensen, C., Kovatcheva-Datchary, P., Myronovych, A., Karns, R., *et al.* (2014) FXR is a molecular target for the effects of vertical sleeve gastrectomy. *Nature* **509**: 183–188.
- Saeidi, N., Meoli, L., Nestoridi, E., Gupta, N.K., Kvas, S., Kucharczyk, J., *et al.* (2013) Reprogramming of intestinal glucose metabolism and glycemic control in rats after gastric bypass. *Science* **341**: 406–410.
- Saini, C., Liani, A., Curie, T., Gos, P., Kreppel, F., Emmenegger, Y., *et al.* (2013) Real-time recording of circadian liver gene expression in freely moving mice reveals the phase-setting behavior of hepatocyte clocks. *Genes Dev* **27**: 1526–1536.
- Salgado-Delgado, R., Ángeles-Castellanos, M., Buijs, M.R., and Escobar, C. (2008) Internal desynchronization in a model of night-work by forced activity in rats. *Neuroscience* **154**: 922–931.
- Sandi, C., and Haller, J. (2015) Stress and the social brain: behavioural effects and neurobiological mechanisms. *Nat Rev Neurosci* **16**: 290–304.
- Sato, S., Solanas, G., Peixoto, F.O., Bee, L., Symeonidi, A., Schmidt, M.S., *et al.* (2017) Circadian Reprogramming in the Liver Identifies Metabolic Pathways of Aging. *Cell* **170**: 664-677.e11.
- Saunders, K.H., Umashanker, D., Igel, L.I., Kumar, R.B., and Aronne, L.J. (2018) Obesity Pharmacotherapy. *Medical Clinics of North America* **102**: 135–148.
- Schmid, B., Helfrich-Förster, C., and Yoshii, T. (2011) A new ImageJ plug-in “ActogramJ” for chronobiological analyses. *J Biol Rhythms* **26**: 464–467.
- Schmutz, I., Ripperger, J.A., Baeriswyl-Aebischer, S., and Albrecht, U. (2010) The mammalian clock component PERIOD2 coordinates circadian output by interaction with nuclear receptors. *Genes Dev* **24**: 345–357.
- Schwartz, M.W., Seeley, R.J., Zeltser, L.M., Drewnowski, A., Ravussin, E., Redman, L.M., and Leibel, R.L. (2017) Obesity Pathogenesis: An Endocrine Society Scientific Statement. *Endocrine Reviews* **38**: 267–296.
- Schwartz, W.J., Tavakoli-Nezhad, M., Lambert, C.M., Weaver, D.R., and Iglesia, H.O. de la (2011) Distinct patterns of Period gene expression in the suprachiasmatic nucleus underlie circadian clock photoentrainment by advances or delays. *Proc Natl Acad Sci U S A* **108**: 17219–17224.
- Scott, E.M., Carter, A.M., and Grant, P.J. (2008) Association between polymorphisms in the Clock gene, obesity and the metabolic syndrome in man. *Int J Obes* **32**: 658–662.

Seelbach, C.L., and D'Almeida, M.J. (2020) Post-Op Assessment and Management Of Obesity Surgery. In *StatPearls*. StatPearls Publishing, Treasure Island (FL). <http://www.ncbi.nlm.nih.gov/books/NBK563131/>. Accessed January 7, 2021.

Segall, L.A., Perrin, J.S., Walker, C.-D., Stewart, J., and Amir, S. (2006) Glucocorticoid rhythms control the rhythm of expression of the clock protein, Period2, in oval nucleus of the bed nucleus of the stria terminalis and central nucleus of the amygdala in rats. *Neuroscience* **140**: 753–757.

Sen, S., Raingard, H., Dumont, S., Kalsbeek, A., Vuillez, P., and Challet, E. (2017) Ultradian feeding in mice not only affects the peripheral clock in the liver, but also the master clock in the brain. *Chronobiol Int* **34**: 17–36.

Shah, H., and Shin, A.C. (2020) Meal patterns after bariatric surgery in mice and rats. *Appetite* **146**: 104340.

Shannon, P., Markiel, A., Ozier, O., Baliga, N.S., Wang, J.T., Ramage, D., *et al.* (2003) Cytoscape: a software environment for integrated models of biomolecular interaction networks. *Genome Res* **13**: 2498–2504.

Sharma, S., and Fulton, S. (2013) Diet-induced obesity promotes depressive-like behaviour that is associated with neural adaptations in brain reward circuitry. *Int J Obes* **37**: 382–389.

Sharp, G.C., Lawlor, D.A., Richmond, R.C., Fraser, A., Simpkin, A., Suderman, M., *et al.* (2015) Maternal pre-pregnancy BMI and gestational weight gain, offspring DNA methylation and later offspring adiposity: findings from the Avon Longitudinal Study of Parents and Children. *Int J Epidemiol* **44**: 1288–1304.

Shearman, L.P., Sriram, S., Weaver, D.R., Maywood, E.S., Chaves, I., Zheng, B., *et al.* (2000) Interacting molecular loops in the mammalian circadian clock. *Science* **288**: 1013–1019.

Shi, S., Ansari, T.S., McGuinness, O.P., Wasserman, D.H., and Johnson, C.H. (2013) Circadian Disruption Leads to Insulin Resistance and Obesity. *Current Biology* **23**: 372–381.

Shimizu, H., Arima, H., Watanabe, M., Goto, M., Banno, R., Sato, I., *et al.* (2008) Glucocorticoids Increase Neuropeptide Y and Agouti-Related Peptide Gene Expression via Adenosine Monophosphate-Activated Protein Kinase Signaling in the Arcuate Nucleus of Rats. *Endocrinology* **149**: 4544–4553.

Shimizu, H., Hatao, F., Imamura, K., Takanishi, K., and Tsujino, M. (2017) Early Effects of Sleeve Gastrectomy on Obesity-Related Cytokines and Bile Acid Metabolism in Morbidly Obese Japanese Patients. *OBES SURG* <http://link.springer.com/10.1007/s11695-017-2756-9>. Accessed January 10, 2021.

Sideleva, O., Suratt, B.T., Black, K.E., Tharp, W.G., Pratley, R.E., Forgione, P., *et al.* (2012) Obesity and Asthma: An Inflammatory Disease of Adipose Tissue Not the Airway. *Am J Respir Crit Care Med* **186**: 598–605.

Sioka, E., Tzovaras, G., Oikonomou, K., Katsogridaki, G., Zachari, E., Papamargaritis, D., *et al.* (2013) Influence of Eating Profile on the Outcome of Laparoscopic Sleeve Gastrectomy. *OBES SURG* **23**: 501–508.

Sjöström, L., Narbro, K., Sjöström, C.D., Karason, K., Larsson, B., Wedel, H., *et al.* (2007) Effects of bariatric surgery on mortality in Swedish obese subjects. *N Engl J Med* **357**: 741–752.

- Skene, D.J., Skorniyakov, E., Chowdhury, N.R., Gajula, R.P., Middleton, B., Satterfield, B.C., *et al.* (2018) Separation of circadian- and behavior-driven metabolite rhythms in humans provides a window on peripheral oscillators and metabolism. *Proc Natl Acad Sci U S A* **115**: 7825–7830.
- Slenter, D.N., Kutmon, M., Hanspers, K., Riutta, A., Windsor, J., Nunes, N., *et al.* (2018) WikiPathways: a multifaceted pathway database bridging metabolomics to other omics research. *Nucleic Acids Res* **46**: D661–D667.
- Smith, K.B., and Smith, M.S. (2016) Obesity Statistics. *Primary Care* **43**: 121–135, ix.
- Son, G.H., Chung, S., Choe, H.K., Kim, H.-D., Baik, S.-M., Lee, H., *et al.* (2008) Adrenal peripheral clock controls the autonomous circadian rhythm of glucocorticoid by causing rhythmic steroid production. *Proc Natl Acad Sci U S A* **105**: 20970–20975.
- Song, Z., Xiaoli, A.M., and Yang, F. (2018) Regulation and Metabolic Significance of De Novo Lipogenesis in Adipose Tissues. *Nutrients* **10**.
- Soták, M., Bryndová, J., Ergang, P., Vagnerová, K., Kvapilová, P., Vodička, M., *et al.* (2016) Peripheral circadian clocks are diversely affected by adrenalectomy. *Chronobiology International* **33**: 520–529.
- Spek, R. van der, Fliers, E., Fleur, S.E. la, and Kalsbeek, A. (2018) Daily Gene Expression Rhythms in Rat White Adipose Tissue Do Not Differ Between Subcutaneous and Intra-Abdominal Depots. *Front Endocrinol (Lausanne)* **9**: 206.
- Spengler, M.L., Kuropatwinski, K.K., Comas, M., Gasparian, A.V., Fedtsova, N., Gleiberman, A.S., *et al.* (2012) Core circadian protein CLOCK is a positive regulator of NF- κ B-mediated transcription. *Proc Natl Acad Sci U S A* **109**: E2457–2465.
- Spiro, D., Raman, J., and Smith, E. (2020) Psychological outcomes following surgical and endoscopic bariatric procedures: A systematic review. *Obesity Reviews* **21** <https://onlinelibrary.wiley.com/doi/abs/10.1111/obr.12998>. Accessed December 4, 2020.
- Srivastava, G., and Apovian, C.M. (2018) Current pharmacotherapy for obesity. *Nat Rev Endocrinol* **14**: 12–24.
- Stefater, M.A., Pérez-Tilve, D., Chambers, A.P., Wilson-Pérez, H.E., Sandoval, D.A., Berger, J., *et al.* (2010) Sleeve gastrectomy induces loss of weight and fat mass in obese rats, but does not affect leptin sensitivity. *Gastroenterology* **138**: 2426–2436, 2436.e1–3.
- Stenvers, D.J., Jongejan, A., Atiqi, S., Vreijling, J.P., Limonard, E.J., Endert, E., *et al.* (2019) Diurnal rhythms in the white adipose tissue transcriptome are disturbed in obese individuals with type 2 diabetes compared with lean control individuals. *Diabetologia* **62**: 704–716.
- Stephens, J.W., Min, T., Dunseath, G., Churm, R., Barry, J.D., and Prior, S.L. (2019) Temporal effects of laparoscopic sleeve gastrectomy on adipokines, inflammation, and oxidative stress in patients with impaired glucose homeostasis. *Surgery for Obesity and Related Diseases* **15**: 2011–2017.
- Stokkan, K.A., Yamazaki, S., Tei, H., Sakaki, Y., and Menaker, M. (2001) Entrainment of the circadian clock in the liver by feeding. *Science* **291**: 490–493.
- Storch, K.-F., Lipan, O., Leykin, I., Viswanathan, N., Davis, F.C., Wong, W.H., and Weitz, C.J. (2002) Extensive and divergent circadian gene expression in liver and heart. *Nature* **417**: 78–83.

- Stott, N.L., and Marino, J.S. (2020) High Fat Rodent Models of Type 2 Diabetes: From Rodent to Human. *Nutrients* **12**.
- Stoynev, A.G., Ikononov, O.C., and Usunoff, K.G. (1982) Feeding pattern and light-dark variations in water intake and renal excretion after suprachiasmatic nuclei lesions in rats. *Physiol Behav* **29**: 35–40.
- Su, Y., Foppen, E., Zhang, Z., Fliers, E., and Kalsbeek, A. (2016) Effects of 6-meals-a-day feeding and 6-meals-a-day feeding combined with adrenalectomy on daily gene expression rhythms in rat epididymal white adipose tissue. *Genes Cells* **21**: 6–24.
- Sujino, M., Furukawa, K., Koinuma, S., Fujioka, A., Nagano, M., Iigo, M., and Shigeyoshi, Y. (2012) Differential Entrainment of Peripheral Clocks in the Rat by Glucocorticoid and Feeding. *Endocrinology* **153**: 2277–2286.
- Sumova, A., Maywood, E.S., Selva, D., Ebling, F.J.P., and Hastings, M.H. (1996) Serotonergic antagonists impair arousal-induced phase shifts of the circadian system of the Syrian hamster. *Brain Research* **709**: 88–96.
- Sun, X., Dang, F., Zhang, D., Yuan, Y., Zhang, C., Wu, Y., *et al.* (2015) Glucagon-CREB/CRTC2 Signaling Cascade Regulates Hepatic BMAL1 Protein. *J Biol Chem* **290**: 2189–2197.
- Sutton, E.F., Beyl, R., Early, K.S., Cefalu, W.T., Ravussin, E., and Peterson, C.M. (2018) Early Time-Restricted Feeding Improves Insulin Sensitivity, Blood Pressure, and Oxidative Stress Even without Weight Loss in Men with Prediabetes. *Cell Metabolism* **27**: 1212–1221.e3.
- Svane, M.S., Bojsen-Møller, K.N., Martinussen, C., Dirksen, C., Madsen, J.L., Reitelseder, S., *et al.* (2019) Postprandial Nutrient Handling and Gastrointestinal Hormone Secretion After Roux-en-Y Gastric Bypass vs Sleeve Gastrectomy. *Gastroenterology* **156**: 1627–1641.e1.
- Tahara, Y., Otsuka, M., Fuse, Y., Hirao, A., and Shibata, S. (2011) Refeeding after Fasting Elicits Insulin-Dependent Regulation of *Per2* and *Rev-erba* with Shifts in the Liver Clock. *J Biol Rhythms* **26**: 230–240.
- Taira, A., Arita, E., Matsumoto, E., Oohira, A., Iwase, K., Hiwasa, T., *et al.* (2019) Systemic oscillator-driven and nutrient-responsive hormonal regulation of daily expression rhythms for gluconeogenic enzyme genes in the mouse liver. *Chronobiology International* **36**: 591–615.
- Takahashi, J.S. (2017) Transcriptional architecture of the mammalian circadian clock. *Nat Rev Genet* **18**: 164–179.
- Takase, K., Tsuneoka, Y., Oda, S., Kuroda, M., and Funato, H. (2016) High-fat diet feeding alters olfactory-, social-, and reward-related behaviors of mice independent of obesity: High-Fat Diet-Induced Behavioral Changes. *Obesity* **24**: 886–894.
- Tannenbaum, B.M., Brindley, D.N., Tannenbaum, G.S., Dallman, M.F., McArthur, M.D., and Meaney, M.J. (1997) High-fat feeding alters both basal and stress-induced hypothalamic-pituitary-adrenal activity in the rat. *Am J Physiol* **273**: E1168–1177.
- Tarasco, E., Boyle, C.N., Pellegrini, G., Arnold, M., Steiner, R., Hornemann, T., *et al.* (2019) Body weight-dependent and independent improvement in lipid metabolism after Roux-en-Y gastric bypass in ApoE*3Leiden.CETP mice. *Int J Obes* **43**: 2394–2406.
- Tognini, P., Murakami, M., Liu, Y., Eckel-Mahan, K.L., Newman, J.C., Verdin, E., *et al.* (2017) Distinct Circadian Signatures in Liver and Gut Clocks Revealed by Ketogenic Diet. *Cell Metab* **26**: 523–538.e5.

- Toledo, M., Batista-Gonzalez, A., Merheb, E., Aoun, M.L., Tarabra, E., Feng, D., *et al.* (2018) Autophagy Regulates the Liver Clock and Glucose Metabolism by Degrading CRY1. *Cell Metab* **28**: 268–281.e4.
- Torquati, L., Mielke, G.I., Brown, W.J., Burton, N.W., and Kolbe-Alexander, T.L. (2019) Shift Work and Poor Mental Health: A Meta-Analysis of Longitudinal Studies. *Am J Public Health* **109**: e13–e20.
- Toth, I., and Neumann, I.D. (2013) Animal models of social avoidance and social fear. *Cell Tissue Res* **354**: 107–118.
- Travnickova-Bendova, Z., Cermakian, N., Reppert, S.M., and Sassone-Corsi, P. (2002) Bimodal regulation of mPeriod promoters by CREB-dependent signaling and CLOCK/BMAL1 activity. *Proceedings of the National Academy of Sciences* **99**: 7728–7733.
- Tschoner, A., Sturm, W., Engl, J., Kaser, S., Laimer, M., Laimer, E., *et al.* (2012) Plasminogen activator inhibitor 1 and visceral obesity during pronounced weight loss after bariatric surgery. *Nutrition, Metabolism and Cardiovascular Diseases* **22**: 340–346.
- Tuero, C., Valenti, V., Rotellar, F., Landecho, M.F., Cienfuegos, J.A., and Frühbeck, G. (2020) Revisiting the Ghrelin Changes Following Bariatric and Metabolic Surgery. *OBES SURG* **30**: 2763–2780.
- Tulipani, S., Griffin, J., Palau-Rodriguez, M., Mora-Cubillos, X., Bernal-Lopez, R.M., Tinahones, F.J., *et al.* (2016) Metabolomics-guided insights on bariatric surgery versus behavioral interventions for weight loss. *Obesity (Silver Spring)* **24**: 2451–2466.
- Turek, F.W., Joshu, C., Kohsaka, A., Lin, E., Ivanova, G., McDearmon, E., *et al.* (2005) Obesity and metabolic syndrome in circadian Clock mutant mice. *Science* **308**: 1043–1045.
- Ubaldo-Reyes, L.M., Buijs, R.M., Escobar, C., and Ángeles-Castellanos, M. (2017) Scheduled meal accelerates entrainment to a 6-h phase advance by shifting central and peripheral oscillations in rats. *Eur J Neurosci* **46**: 1875–1886.
- Um, J.H., Yang, S., Yamazaki, S., Kang, H., Viollet, B., Foretz, M., and Chung, J.H. (2007) Activation of 5'-AMP-activated kinase with diabetes drug metformin induces casein kinase Iepsilon (CKIepsilon)-dependent degradation of clock protein mPer2. *J Biol Chem* **282**: 20794–20798.
- Unamuno, X., Gómez-Ambrosi, J., Rodríguez, A., Becerril, S., Frühbeck, G., and Catalán, V. (2018) Adipokine dysregulation and adipose tissue inflammation in human obesity. *Eur J Clin Invest* **48**: e12997.
- Unger, R.H., and Orci, L. (2000) Lipotoxic diseases of nonadipose tissues in obesity. *Int J Obes Relat Metab Disord* **24 Suppl 4**: S28–32.
- Upadhyay, J., Farr, O., Perakakis, N., Ghaly, W., and Mantzoros, C. (2018) Obesity as a Disease. *Medical Clinics of North America* **102**: 13–33.
- Valladares, M., Obregón, A.M., and Chaput, J.-P. (2015) Association between genetic variants of the clock gene and obesity and sleep duration. *J Physiol Biochem* **71**: 855–860.
- Van Harmelen, V., Reynisdottir, S., Eriksson, P., Thorne, A., Hoffstedt, J., Lonnqvist, F., and Arner, P. (1998) Leptin secretion from subcutaneous and visceral adipose tissue in women. *Diabetes* **47**: 913–917.

- Varela-Rodríguez, B.M., Juiz-Valiña, P., Varela, L., Outeiriño-Blanco, E., Bravo, S.B., García-Brao, M.J., *et al.* (2020) Beneficial Effects of Bariatric Surgery-Induced by Weight Loss on the Proteome of Abdominal Subcutaneous Adipose Tissue. *J Clin Med* **9**.
- Velingkaar, N., Mezhnina, V., Poe, A., Makwana, K., Tulsian, R., and Kondratov, R.V. (2020) Reduced caloric intake and periodic fasting independently contribute to metabolic effects of caloric restriction. *Aging Cell* **19**: e13138.
- Vitaterna, M.H., Shimomura, K., and Jiang, P. (2019) Genetics of Circadian Rhythms. *Neurologic Clinics* **37**: 487–504.
- Vollmers, C., Gill, S., DiTacchio, L., Pulivarthy, S.R., Le, H.D., and Panda, S. (2009) Time of feeding and the intrinsic circadian clock drive rhythms in hepatic gene expression. *Proc Natl Acad Sci U S A* **106**: 21453–21458.
- Walker, W.H., Walton, J.C., DeVries, A.C., and Nelson, R.J. (2020) Circadian rhythm disruption and mental health. *Transl Psychiatry* **10**: 28.
- Walter, W., Sánchez-Cabo, F., and Ricote, M. (2015) GOpot: an R package for visually combining expression data with functional analysis. *Bioinformatics* **31**: 2912–2914.
- Wang, C.-Y., and Liao, J.K. (2012) A mouse model of diet-induced obesity and insulin resistance. *Methods Mol Biol* **821**: 421–433.
- Wang, D., Opperhuizen, A.-L., Reznick, J., Turner, N., Su, Y., Cooney, G.J., and Kalsbeek, A. (2017) Effects of feeding time on daily rhythms of neuropeptide and clock gene expression in the rat hypothalamus. *Brain Research* **1671**: 93–101.
- Wang, F., Li, C., Yongluo, and Chen, L. (2016) The Circadian Gene Clock Plays an Important Role in Cell Apoptosis and the DNA Damage Response *In Vitro*. *Technol Cancer Res Treat* **15**: 480–486.
- Wang, Q., Yin, Y., and Zhang, W. (2018) Ghrelin Restores the Disruption of the Circadian Clock in Steatotic Liver. *IJMS* **19**: 3134.
- Watson, R.A., Pride, N.B., Thomas, E.L., Fitzpatrick, J., Durighel, G., McCarthy, J., *et al.* (2010) Reduction of total lung capacity in obese men: comparison of total intrathoracic and gas volumes. *Journal of Applied Physiology* **108**: 1605–1612.
- Wehrens, S.M.T., Christou, S., Isherwood, C., Middleton, B., Gibbs, M.A., Archer, S.N., *et al.* (2017) Meal Timing Regulates the Human Circadian System. *Curr Biol* **27**: 1768-1775.e3.
- Weng, T.-C., Chang, C.-H., Dong, Y.-H., Chang, Y.-C., and Chuang, L.-M. (2015) Anaemia and related nutrient deficiencies after Roux-en-Y gastric bypass surgery: a systematic review and meta-analysis. *BMJ Open* **5**: e006964.
- Werdermann, M., Berger, I., Scriba, L.D., Santambrogio, A., Schlinkert, P., Brendel, H., *et al.* (2021) Insulin and obesity transform hypothalamic-pituitary-adrenal axis stemness and function in a hyperactive state. *Mol Metab* **43**: 101112.
- West, A.C., Smith, L., Ray, D.W., Loudon, A.S.I., Brown, T.M., and Bechtold, D.A. (2017) Misalignment with the external light environment drives metabolic and cardiac dysfunction. *Nat Commun* **8**: 417.

- Wharton, S., Bonder, R., Jeffery, A., and Christensen, R.A.G. (2020) The safety and effectiveness of commonly-marketed natural supplements for weight loss in populations with obesity: A critical review of the literature from 2006 to 2016. *Crit Rev Food Sci Nutr* **60**: 1614–1630.
- White, M.A., Kalarchian, M.A., Levine, M.D., Masheb, R.M., Marcus, M.D., and Grilo, C.M. (2015) Prognostic Significance of Depressive Symptoms on Weight Loss and Psychosocial Outcomes Following Gastric Bypass Surgery: A Prospective 24-Month Follow-Up Study. *Obes Surg* **25**: 1909–1916.
- WHO (2020) Obesity and overweight. <https://www.who.int/news-room/fact-sheets/detail/obesity-and-overweight>. Accessed February 18, 2021.
- Wiater, M.F., Mukherjee, S., Li, A.-J., Dinh, T.T., Rooney, E.M., Simasko, S.M., and Ritter, S. (2011) Circadian integration of sleep-wake and feeding requires NPY receptor-expressing neurons in the mediobasal hypothalamus. *Am J Physiol Regul Integr Comp Physiol* **301**: R1569–1583.
- Wilms, B., Leineweber, E.M., Mölle, M., Chamorro, R., Pommerenke, C., Salinas-Riester, G., *et al.* (2019) Sleep Loss Disrupts Morning-to-Evening Differences in Human White Adipose Tissue Transcriptome. *J Clin Endocrinol Metab* **104**: 1687–1696.
- Wilson-Pérez, H.E., Chambers, A.P., Ryan, K.K., Li, B., Sandoval, D.A., Stoffers, D., *et al.* (2013a) Vertical Sleeve Gastrectomy Is Effective in Two Genetic Mouse Models of Glucagon-Like Peptide 1 Receptor Deficiency. *Diabetes* **62**: 2380–2385.
- Wilson-Pérez, H.E., Chambers, A.P., Sandoval, D.A., Stefater, M.A., Woods, S.C., Benoit, S.C., and Seeley, R.J. (2013b) The effect of vertical sleeve gastrectomy on food choice in rats. *Int J Obes* **37**: 288–295.
- Winer, S., Chan, Y., Paltser, G., Truong, D., Tsui, H., Bahrami, J., *et al.* (2009) Normalization of obesity-associated insulin resistance through immunotherapy. *Nat Med* **15**: 921–929.
- Withrow, D., and Alter, D.A. (2011) The economic burden of obesity worldwide: a systematic review of the direct costs of obesity: The direct healthcare costs of obesity. *Obesity Reviews* **12**: 131–141.
- Woods, C.P., Corrigan, M., Gathercole, L., Taylor, A., Hughes, B., Gaoatswe, G., *et al.* (2015) Tissue specific regulation of glucocorticoids in severe obesity and the response to significant weight loss following bariatric surgery (BARICORT). *J Clin Endocrinol Metab* **100**: 1434–1444.
- Yamamoto, T., Nakahata, Y., Tanaka, M., Yoshida, M., Soma, H., Shinohara, K., *et al.* (2005) Acute Physical Stress Elevates Mouse *Period1* mRNA Expression in Mouse Peripheral Tissues via a Glucocorticoid-responsive Element. *J Biol Chem* **280**: 42036–42043.
- Yamamoto, Y., Tanahashi, T., Kawai, T., Chikahisa, S., Katsuura, S., Nishida, K., *et al.* (2009) Changes in behavior and gene expression induced by caloric restriction in C57BL/6 mice. *Physiological Genomics* **39**: 227–235.
- Yamamuro, D., Takahashi, M., Nagashima, S., Wakabayashi, T., Yamazaki, H., Takei, A., *et al.* (2020) Peripheral circadian rhythms in the liver and white adipose tissue of mice are attenuated by constant light and restored by time-restricted feeding. *PLoS One* **15**: e0234439.
- Yamazaki, S., Numano, R., Abe, M., Hida, A., Takahashi, R., Ueda, M., *et al.* (2000) Resetting central and peripheral circadian oscillators in transgenic rats. *Science* **288**: 682–685.

- Yang, Q.-Y., Liang, J.-F., Rogers, C.J., Zhao, J.-X., Zhu, M.-J., and Du, M. (2013) Maternal Obesity Induces Epigenetic Modifications to Facilitate Zfp423 Expression and Enhance Adipogenic Differentiation in Fetal Mice. *Diabetes* **62**: 3727–3735.
- Yannielli, P.C., Molyneux, P.C., Harrington, M.E., and Golombek, D.A. (2007) Ghrelin Effects on the Circadian System of Mice. *Journal of Neuroscience* **27**: 2890–2895.
- Yasumoto, Y., Hashimoto, C., Nakao, R., Yamazaki, H., Hiroshima, H., Nemoto, T., *et al.* (2016) Short-term feeding at the wrong time is sufficient to desynchronize peripheral clocks and induce obesity with hyperphagia, physical inactivity and metabolic disorders in mice. *Metabolism* **65**: 714–727.
- Yeh, T.-L., Chen, H.-H., Tsai, S.-Y., Lin, C.-Y., Liu, S.-J., and Chien, K.-L. (2019) The Relationship between Metabolically Healthy Obesity and the Risk of Cardiovascular Disease: A Systematic Review and Meta-Analysis. *JCM* **8**: 1228.
- Yi, C.-X., Vliet, J. van der, Dai, J., Yin, G., Ru, L., and Buijs, R.M. (2006) Ventromedial Arcuate Nucleus Communicates Peripheral Metabolic Information to the Suprachiasmatic Nucleus. *Endocrinology* **147**: 283–294.
- Yin, D.P., Boyd, K.L., Williams, P.E., Abumrad, N.N., and Wasserman, D.H. (2012) Mouse Models of Bariatric Surgery. In *Current Protocols in Mouse Biology*. Auwerx, J., Brown, S.D., Justice, M., Moore, D.D., Ackerman, S.L., and Nadeau, J. (eds). John Wiley & Sons, Inc., Hoboken, NJ, USA. p. mo120087 <http://doi.wiley.com/10.1002/9780470942390.mo120087>. Accessed November 17, 2020.
- Yokoyama, Y., Nakamura, T.J., Yoshimoto, K., Ijyuin, H., Tachikawa, N., Oda, H., *et al.* (2020) A high-salt/high fat diet alters circadian locomotor activity and glucocorticoid synthesis in mice. *PLoS One* **15**: e0233386.
- Yoo, S.-H., Yamazaki, S., Lowrey, P.L., Shimomura, K., Ko, C.H., Buhr, E.D., *et al.* (2004) PERIOD2::LUCIFERASE real-time reporting of circadian dynamics reveals persistent circadian oscillations in mouse peripheral tissues. *Proc Natl Acad Sci U S A* **101**: 5339–5346.
- Yoshida, J., Eguchi, E., Nagaoka, K., Ito, T., and Ogino, K. (2018) Association of night eating habits with metabolic syndrome and its components: a longitudinal study. *BMC Public Health* **18**: 1366.
- Yoshitane, H., Asano, Y., Sagami, A., Sakai, S., Suzuki, Y., Okamura, H., *et al.* (2019) Functional D-box sequences reset the circadian clock and drive mRNA rhythms. *Commun Biol* **2**: 300.
- Young, T., Skatrud, J., and Peppard, P.E. (2004) Risk Factors for Obstructive Sleep Apnea in Adults. *JAMA* **291**: 2013.
- Yumuk, V., Tsigos, C., Fried, M., Schindler, K., Busetto, L., Micic, D., and Toplak, H. (2015) European Guidelines for Obesity Management in Adults. *Obes Facts* **8**: 402–424.
- Zafar, U., Khaliq, S., Ahmad, H.U., Manzoor, S., and Lone, K.P. (2018) Metabolic syndrome: an update on diagnostic criteria, pathogenesis, and genetic links. *Hormones* **17**: 299–313.
- Zhang, E.E., Liu, Y., Dentin, R., Pongsawakul, P.Y., Liu, A.C., Hirota, T., *et al.* (2010) Cryptochrome mediates circadian regulation of cAMP signaling and hepatic gluconeogenesis. *Nat Med* **16**: 1152–1156.
- Zhang, R., Lahens, N.F., Ballance, H.I., Hughes, M.E., and Hogenesch, J.B. (2014) A circadian gene expression atlas in mammals: Implications for biology and medicine. *Proc Natl Acad Sci USA* **111**: 16219–16224.

- Zhang, R., Yan, C., Zhou, X., Qian, B., Li, F., Sun, Y., *et al.* (2013) Association of Rev-erb α in adipose tissues with Type 2 diabetes mellitus amelioration after gastric bypass surgery in Goto-Kakizaki rats. *Am J Physiol Regul Integr Comp Physiol* **305**: R134-146.
- Zhang, Y., Proenca, R., Maffei, M., Barone, M., Leopold, L., and Friedman, J.M. (1994) Positional cloning of the mouse obese gene and its human homologue. *Nature* **372**: 425–432.
- Zhang, Z., Li, L., Yang, M., Liu, H., Boden, G., and Yang, G. (2012) Increased Plasma Levels of Nesfatin-1 in Patients with Newly Diagnosed Type 2 Diabetes Mellitus. *Exp Clin Endocrinol Diabetes* **120**: 91–95.
- Zhou, M., Kim, J.K., Eng, G.W.L., Forger, D.B., and Virshup, D.M. (2015) A Period2 Phosphoswitch Regulates and Temperature Compensates Circadian Period. *Mol Cell* **60**: 77–88.
- Zhu, Z., Hua, B., Xu, L., Yuan, G., Li, E., Li, X., *et al.* (2016) CLOCK promotes 3T3-L1 cell proliferation via Wnt signaling. *IUBMB Life* **68**: 557–568.
- Zierath, J.R., Livingston, J.N., Thörne, A., Bolinder, J., Reynisdottir, S., Lönnqvist, F., and Arner, P. (1998) Regional difference in insulin inhibition of non-esterified fatty acid release from human adipocytes: relation to insulin receptor phosphorylation and intracellular signalling through the insulin receptor substrate-1 pathway. *Diabetologia* **41**: 1343–1354.
- Zvonic, S., Ptitsyn, A.A., Conrad, S.A., Scott, L.K., Floyd, Z.E., Kilroy, G., *et al.* (2006) Characterization of Peripheral Circadian Clocks in Adipose Tissues. *Diabetes* **55**: 962–970.
- Zylka, M.J., Shearman, L.P., Weaver, D.R., and Reppert, S.M. (1998) Three period homologs in mammals: differential light responses in the suprachiasmatic circadian clock and oscillating transcripts outside of brain. *Neuron* **20**: 1103–1110.

Supplements

List of rhythmic and differently expressed genes

Table S1: Relevant genes for the WAT transcriptome analysis. Common cycler are written bold, VSG only cycler italic, and sham only cycler underlined. Genes that were upregulated following VSG are written in green, that were downregulated in blue.

<i>0 - Dpp4</i>	<i>Dpp9 - Invs</i>	<i>Ipo9 - Ripk4</i>	<i>Rit1 - Zyx</i>
<u>0610010F05Rik</u>	<u>Dpp9</u>	<u>Ipo9</u>	<u>Rit1</u>
<u>0610040J01Rik</u>	<u>Dpy19l3</u>	<u>Ippk</u>	<u>Rmnd1</u>
<u>1110002E22Rik</u>	<u>Dpysl2</u>	<i>Iqcc</i>	Rmnd5b
<u>1110032F04Rik</u>	<u>Dpysl3</u>	<i>Iqsec1</i>	<u>Rn18s-rs5</u>
<u>1500002C15Rik</u>	<u>Dscr3</u>	<u>Irak1bp1</u>	<u>Rn7sk</u>
<u>1500011B03Rik</u>	<u>Dsg1a</u>	<u>Irak2</u>	<u>Rnase10</u>
<u>1500015A07Rik</u>	<u>Dsg1b</u>	<u>Irf2bp2</u>	<u>Rnase2a</u>
<u>1700001J03Rik</u>	<i>Dst</i>	<u>Irg1</u>	<u>Rnase6</u>
<u>1700010I14Rik</u>	<u>Dtl</u>	<u>Irgc1</u>	<u>Rnd1</u>
<u>1700025N21Rik</u>	Dtx4	<i>Irgm1</i>	Rnd3
<u>1700026L06Rik</u>	<u>Duox2</u>	Irs1	<i>Rnf113a1</i>
<u>1700028E10Rik</u>	<u>Duoxa1</u>	<u>Irs2</u>	Rnf122
<u>1700028K03Rik</u>	<u>Dusp6</u>	<u>Isca1</u>	Rnf125
<u>1700036A12Rik</u>	<u>Dusp8</u>	<u>Itga10</u>	Rnf144a
<u>1700041G16Rik</u>	<i>Dut</i>	<u>Itgad</u>	<i>Rnf150</i>
<u>1700041M05Rik</u>	<u>Dync1li1</u>	<u>Itgal</u>	<u>Rnf157</u>
<u>1700047G03Rik</u>	<u>Dynlrb2</u>	<u>Itgb2l</u>	<u>Rnf181</u>
<u>1700048O20Rik</u>	<u>Dzip1l</u>	<u>Itgb7</u>	<u>Rnf208</u>
<u>1700055D18Rik</u>	<u>E030018B13Rik</u>	<i>Itgbl1</i>	<u>Rnf214</u>
<u>1700056N10Rik</u>	<u>E030030I06Rik</u>	<u>Itih1</u>	<u>Rnf220</u>
<u>1700113A16Rik</u>	<u>E030042O20Rik</u>	<u>Itih3</u>	<u>Rnf24</u>
<u>1700123M08Rik</u>	<u>E230013L22Rik</u>	<i>Itpkc</i>	Rnf6
<u>1810011H11Rik</u>	E2f2	<u>Itpr1</u>	<u>Robo3</u>
<u>1810013L24Rik</u>	<u>E2f4</u>	<u>Itpripl2</u>	<u>Rora</u>
<u>1810059H22Rik</u>	E2f6	<u>Izumo1r</u>	<u>Rorc</u>
<u>2010003K11Rik</u>	<u>E330011M16Rik</u>	<u>Izumo4</u>	<u>RP23-124O24.4</u>
<u>2010007H06Rik</u>	<u>E330020D12Rik</u>	Jakmip1	<u>RP23-144N15.8</u>
<u>2010016I18Rik</u>	<u>E4f1</u>	<i>Jakmip3</i>	<u>RP23-225M4.1</u>
<u>2010107G23Rik</u>	<u>Ebf3</u>	<u>Jam3</u>	<i>RP23-285C18.7</i>
<u>2010109I03Rik</u>	<u>Ebi3</u>	<u>Jchain</u>	<i>RP23-335G1.1</i>
<u>2010110K18Rik</u>	<i>Ecd</i>	<u>Jdp2</u>	<u>RP23-339B16.2</u>
<u>2010111I01Rik</u>	<u>Ecscr</u>	<u>Jph2</u>	<u>RP23-366O14.6</u>
<u>2310015A10Rik</u>	Ednra	<u>Kalrn</u>	<u>RP23-366O14.9</u>
<u>2310065F04Rik</u>	<u>Eef1a1</u>	<u>Kat2b</u>	<u>RP23-419K14.8</u>
<u>2410131K14Rik</u>	<u>Eef1b2</u>	<u>Kat6b</u>	<u>RP23-423B21.6</u>

2500002B13Rik	Eef1d	Kbtbd11	RP23-457F4.3
2500004C02Rik	Eef2	Kbtbd4	RP23-466P2.3
2610002M06Rik	Eef2k	Kcna5	RP23-474B13.5
2610020C07Rik	Eefsec	Kcnab3	RP23-54G8.1
2610203C20Rik	Efcab11	Kcnd3	RP23-64D23.8
2610301B20Rik	Efcab8	Kcne1l	RP23-8M3.5
2610307P16Rik	Efhc2	Kcne3	RP24-172K3.1
2610507B11Rik	Efhd1	Kcne4	RP24-173K12.5
2610507I01Rik	Efhd2	Kcnh1	RP24-330M21.1
2610528A11Rik	Efna3	Kcnj14	RP24-365N15.2
2810001G20Rik	Efna5	Kcnj2	RP24-445D7.1
2810004N23Rik	Efnb1	Kcnj8	RP24-503A2.6
2810029C07Rik	Efr3a	Kcnn3	RP24-72H18.2
2810030D12Rik	Eftud2	Kcnq1	RP24-88J19.2
2810405F17Rik	Egfem1	Kcnq4	Rp9
2810407A14Rik	Egr1	Kcnrg	Rpa2
3000002C10Rik	Ehbp1	Kcnt1	Rpap3
3110056K07Rik	Ehhadh	Kctd13	Rpf1
3110083C13Rik	Eif2ak1	Kctd19	Rpl13a
3222401L13Rik	Eif3d	Kctd21	Rpl13a-ps1
3300005D01Rik	Eif3f	Kdelr2	Rpl17
3930402G23Rik	Eif3k	Kdelr3	Rpl18
4430402I18Rik	Eif4e3	Kdm1a	Rpl18a
4632404H12Rik	Eif4ebp3	Kdm4a	Rpl26
4731419I09Rik	Eif4g1	Kdm5b	Rpl27a
4732471J01Rik	Eif4g3	Kif13b	Rpl3
4732490B19Rik	Elac1	Kif18b	Rpl32
4831440E17Rik	Elane	Kif1b	Rpl34
4833403J16Rik	Eldr	Kif1bp	Rpl36a-ps2
4833407H14Rik	Elk1	Kif3c	Rpl37
4833417C18Rik	Elk3	Kifc2	Rpl37a
4930404I05Rik	Elk4	Kifc3	Rpl3-ps1
4930412C18Rik	Elmod1	Kin	Rpl41
4930422M22Rik	Elmod2	Kiss1r	Rpl6
4930426I24Rik	Elmod3	Kit	Rpl7
4930458D05Rik	Elmsan1	Klb	Rplp0
4930538K18Rik	Elp6	Klf13	Rpp14
4930539E08Rik	Emg1	Klf15	Rprd1a
4930555A03Rik	Eml3	Klf16	Rps12
4930562F07Rik	Emp1	Klf2	Rps14
4930570G19Rik	Emp3	Klf6	Rps15
4931406P16Rik	Enc1	Klf8	Rps15a

4932441J04Rik	Endov	Klf9	Rps16-ps2
4933404O12Rik	Eno1b	Klhdc3	Rps2
4933406C10Rik	Enpp6	Klhdc7a	Rps20
4933406P04Rik	Entpd5	Klhdc8a	Rps24
4933407L21Rik	Ep400	Klhdc8b	Rps5
4933424M12Rik	Epb41	Klhl15	Rps6ka1
4933428G20Rik	Epb41l1	Klhl22	Rps6kb1
5031414D18Rik	Epb41l4b	Klhl25	Rps9
5031425F14Rik	Epgn	Klhl29	Rpsa-ps1
5430416O09Rik	Epha2	Klhl35	Rpsa-ps11
5730405O15Rik	Eps8l2	Klhl7	Rras2
5730585A16Rik	Erbb4	Kmo	Rreb1
5930403N24Rik	Ercc2	Kmt2e	Rrp8
5930412G12Rik	Erf	Krt19	Rsad1
5930430L01Rik	Erlin1	Krt20	Rsad2
6330403L08Rik	Ermard	Krt222	Rsl24d1
6330416G13Rik	Ero1l	Krt36	Rtn4ip1
6330562C20Rik	Errfi1	Krt79	Rufy3
6430511E19Rik	Esm1	L1cam	Rundc3a
6430531B16Rik	Esyt3	L2hgdh	Runx1
6430550D23Rik	Etl4	Lalba	Rusc1
6430571L13Rik	Etv3	Lamb3	Rusc2
6430590A07Rik	Etv4	Lao1	Rwdd3
6530402F18Rik	Evi2a	Laptm5	Ryr1
6820431F20Rik	Exd1	Larp7	S100a3
8030453O22Rik	Exd2	Lars2	S100a4
9030407P20Rik	Exo5	Layn	S100a8
9030617O03Rik	Exoc3l4	Lbh	S100a9
9030619P08Rik	Exosc7	Lbp	S100b
9130011E15Rik	Exosc8	Lcat	S1pr2
9130017K11Rik	F10	Lcn2	S1pr3
9130221H12Rik	F2rl3	Lcp1	Safb
9330159F19Rik	F3	Lcp2	Samd4b
9530052E02Rik	Faap20	Ldlrad4	Samd8
9830107B12Rik	Fabp1	Ldlrap1	Samhd1
9930014A18Rik	Fabp5	Lef1	Sap30bp
A130071D04Rik	Fabp9	Leng8	Sapcd2
A230050P20Rik	Fads6	Leo1	Sash3
A230056P14Rik	Faim2	Lep	Sav1
A230072C01Rik	Faiml	Leprot	Scaf4
A230083G16Rik	Fam101a	Lgalsl	Scand1
A330040F15Rik	Fam101b	Lhcgr	Scarna13

<u>A330094K24Rik</u>	<u>Fam102a</u>	<u>Lhfp13</u>	<u>Scfd1</u>
<u>A430093F15Rik</u>	<u>Fam102b</u>	<u>Lif</u>	<u>Scmh1</u>
<u>A430105I19Rik</u>	Fam107a	<u>Lig4</u>	Scml4
<u>A430110L20Rik</u>	<u>Fam110c</u>	<u>Lilr4b</u>	<u>Scn4a</u>
A530020G20Rik	<u>Fam111a</u>	<u>Lilrb4a</u>	<u>Scn5a</u>
<u>A530072M11Rik</u>	<u>Fam120b</u>	<u>Lima1</u>	Scnm1
<u>A530076I17Rik</u>	Fam120c	<u>Limd2</u>	<u>Scnn1b</u>
<u>A630072L19Rik</u>	<u>Fam122b</u>	<u>Lin37</u>	<u>Scrg1</u>
<u>A630077J23Rik</u>	Fam124a	<u>Lin52</u>	<u>Sct</u>
A730017L22Rik	Fam124b	Lin7a	<u>Sctr</u>
<u>A730056A06Rik</u>	<u>Fam134a</u>	<u>Lin7b</u>	<u>Scx</u>
A830008E24Rik	Fam13a	<u>Lipf</u>	<u>Sdc1</u>
<u>A930004D18Rik</u>	<u>Fam150b</u>	<u>Litaf</u>	<u>Sdf2</u>
<u>A930004J17Rik</u>	<u>Fam160a1</u>	<u>Lmbrd2</u>	<u>Sec11c</u>
<u>A930005H10Rik</u>	<u>Fam160a2</u>	<u>Lmo2</u>	<u>Sec14l1</u>
<u>A930016O22Rik</u>	<u>Fam161b</u>	Ln timer	<u>Sec22a</u>
<u>A930018M24Rik</u>	<u>Fam163b</u>	<u>Lonp2</u>	Sec31b
<u>A930024E05Rik</u>	<u>Fam167b</u>	Lonrf1	<u>Sec61a2</u>
<u>A930024N18Rik</u>	<u>Fam168a</u>	Loxl2	<u>Sele</u>
<u>AA413626</u>	<u>Fam188b</u>	<u>Lpar3</u>	Sell
<u>AA474331</u>	<u>Fam193b</u>	<u>Lpar6</u>	<u>Selp</u>
<u>Aacs</u>	<u>Fam195b</u>	<u>Lpin1</u>	<u>Selplg</u>
<u>Aadac</u>	<u>Fam19a1</u>	Lpin3	<u>Sema3c</u>
<u>Aaed1</u>	<u>Fam19a3</u>	<u>Lrch3</u>	<u>Sema4a</u>
<u>Aarsd1</u>	<u>Fam209</u>	<u>Lrig1</u>	<u>Sema6d</u>
<u>Abca13</u>	<u>Fam20b</u>	<u>Lrig2</u>	<u>Sema7a</u>
Abca8a	<u>Fam20c</u>	<u>Lrig3</u>	<u>Senp1</u>
<u>Abca8b</u>	<u>Fam21</u>	<u>Lrp12</u>	Senp3
Abcb1a	<u>Fam212b</u>	<u>Lrp3</u>	<u>Sept1</u>
<u>Abcc1</u>	Fam214a	<u>Lrp8</u>	<u>Sept11</u>
<u>Abcc12</u>	<u>Fam214b</u>	<u>Lrrc15</u>	<u>Sept9</u>
<u>Abcc2</u>	<u>Fam220a</u>	<u>Lrrc25</u>	<u>Serac1</u>
<u>Abcc3</u>	<u>Fam46a</u>	<u>Lrrc27</u>	<u>Sergef</u>
<u>Abcc4</u>	<u>Fam46b</u>	<u>Lrrc36</u>	<u>Serpina12</u>
<u>Abcc5</u>	Fam58b	<u>Lrrc3b</u>	<u>Serpina1a</u>
<u>Abcc9</u>	<u>Fam63a</u>	<u>Lrrc41</u>	<u>Serpina1d</u>
<u>Abcd2</u>	<u>Fam64a</u>	<u>Lrrc4c</u>	<u>Serpina3b</u>
<u>Abcf2</u>	Fam65b	<u>Lrrc55</u>	<u>Serpina3k</u>
Abcg2	<u>Fam65c</u>	<u>Lrrc57</u>	<u>Serpina3m</u>
<u>Abhd5</u>	<u>Fam71d</u>	<u>Lrrc59</u>	<u>Serpinb1a</u>
<u>Abi3</u>	<u>Fam71e1</u>	Lrrc8a	<u>Serpine1</u>
<u>Ablim1</u>	<u>Fam71f2</u>	<u>Lrriq3</u>	<u>Serpinf1</u>

Acacb	<u>Fam73b</u>	<u>Lrrn4</u>	<u>Sertad1</u>
<u>Acad10</u>	Fam76a	<u>Lrrtm1</u>	<u>Sertad3</u>
<u>Acap3</u>	<u>Fam78a</u>	<u>Lrrtm3</u>	<u>Set</u>
<u>Accs1</u>	<u>Fam83a</u>	<u>Lsamp</u>	<u>Setd1b</u>
Acer2	<u>Fam83d</u>	<u>Lsm6</u>	<u>Setd4</u>
<u>Ache</u>	<u>Fam83f</u>	<u>Lsmem1</u>	<u>Setd7</u>
<u>Acin1</u>	<u>Fam84a</u>	<u>Lsp1</u>	<u>Sez6l</u>
<u>Ackr1</u>	Fan1	<u>Lst1</u>	<u>Sez6l2</u>
<u>Acot4</u>	<u>Fancb</u>	<u>Lta4h</u>	<u>Sf1</u>
<u>Acot9</u>	Fancc	<u>Ltb</u>	<u>Sfmbt2</u>
<u>Acoxl</u>	<u>Fank1</u>	<u>Ltbp1</u>	<u>Sfn</u>
<u>Acr</u>	<u>Fasl</u>	<u>Ltbp2</u>	<u>Sfxn2</u>
<u>Acs13</u>	<u>Faxc</u>	<u>Ltbr</u>	<u>Sfxn3</u>
Acsm5	Fbn1	<u>Ltf</u>	<u>Sgcg</u>
<u>Acss2</u>	Fbn2	<u>Lxn</u>	<u>Sgol1</u>
Acss3	<u>Fbx113</u>	<u>Ly6d</u>	<u>Sgol2a</u>
<u>Actb</u>	<u>Fbx116</u>	<u>Ly6g</u>	<u>Sgtb</u>
<u>Actn4</u>	Fbx17	<u>Ly6g6d</u>	<u>Sh2b3</u>
<u>Actr3b</u>	<u>Fbxo24</u>	<u>Ly6i</u>	<u>Sh2d1b1</u>
<u>Acvr1</u>	<u>Fbxo3</u>	<u>Lyl1</u>	Sh2d4b
<u>Acvr1b</u>	<u>Fbxo32</u>	<u>Lypd1</u>	<u>Sh2d6</u>
<u>Acvrl1</u>	<u>Fbxo40</u>	<u>Lypd6</u>	<u>Sh3bgrl3</u>
<u>Acy1</u>	<u>Fbxo45</u>	<u>Lymr1</u>	<u>Sh3bp2</u>
<u>Ada</u>	<u>Fbxw10</u>	<u>Lysmd3</u>	Sh3d21
<u>Adal</u>	<u>Fbxw8</u>	<u>Lyst</u>	Sh3pxd2a
<u>Adam19</u>	<u>Fcer1g</u>	<u>Lztr1</u>	<u>Sh3yl1</u>
Adam1a	Fcer2a	Lzts1	<u>Sharpin</u>
<u>Adamts1</u>	<u>Fcgr1</u>	<u>Lzts3</u>	<u>Shc3</u>
<u>Adamts12</u>	<u>Fcgr2b</u>	<u>Mad1l1</u>	<u>Shisa5</u>
<u>Adamts14</u>	<u>Fcgr4</u>	Mad2l1bp	<u>Shisa6</u>
<u>Adamts15</u>	<u>Fcmr</u>	<u>Maea</u>	<u>Shroom1</u>
<u>Adamts16</u>	<u>Fcnb</u>	<u>Maf1</u>	<u>Shroom3</u>
<u>Adamts17</u>	<u>Fcrl1</u>	<u>Mafa</u>	Shroom4
Adamts4	<u>Fcrla</u>	<u>Maff</u>	<u>Siae</u>
<u>Adamts5</u>	<u>Fdft1</u>	<u>Mageb18</u>	<u>Sidt2</u>
<u>Adamts12</u>	<u>Ffar1</u>	<u>Maged2</u>	<u>Siglece</u>
Adap1	<u>Fgd3</u>	<u>Man2a2</u>	<u>Siglecg</u>
Adap2	<u>Fgf10</u>	<u>Mansc1</u>	<u>Sik1</u>
<u>Adap2os</u>	<u>Fgf21</u>	<u>Map1a</u>	Sik2
<u>Adarb1</u>	<u>Fgf9</u>	<u>Map2k3</u>	<u>Sik3</u>
<u>Adat1</u>	<u>Fgfr3</u>	<u>Map3k14</u>	<u>Sirpa</u>
<u>Adcy9</u>	<u>Fgr</u>	Map3k6	<u>Sirpb1b</u>

<u>Add3</u>	<u>Fhad1</u>	<u>Map3k7cl</u>	<u>Sirpb1c</u>
<u>Adgre1</u>	<u>Fhdc1</u>	<u>Map4k1</u>	<u>Sirt7</u>
<u>Adgrg2</u>	<u>Fhl3</u>	<u>Map7d2</u>	<u>Six1</u>
<u>Adgrg5</u>	Fhl5	<u>Mapk11</u>	<u>Six2</u>
<u>Adh1</u>	<u>Fibp</u>	Mapk12	<u>Six4</u>
<u>Adh6-ps1</u>	<u>Fig4</u>	<u>Mapk13</u>	<u>Skida1</u>
<u>Adipor2</u>	<u>Fign</u>	Mapk14	<u>Skil</u>
Adora1	<u>Fkbp10</u>	<u>Mapk6</u>	<u>Skiv2l2</u>
<u>Adora2a</u>	<u>Fkbp11</u>	<u>Mapkapk5</u>	<u>Slamf9</u>
<u>Adprm</u>	<u>Fkbp14</u>	<u>Mapre1</u>	Slc10a6
<u>Afap1l2</u>	Fkbp5	<u>Mapre2</u>	<u>Slc11a2</u>
Aff1	<u>Fkbp7</u>	<u>Mapre3</u>	<u>Slc12a2</u>
<u>Afg3l2</u>	<u>Flywch1</u>	<u>Mapt</u>	<u>Slc12a7</u>
<u>Agap2</u>	<u>Fmo1</u>	<u>Marcks</u>	<u>Slc13a3</u>
<u>Ager</u>	Fmo2	<u>Marcksl1</u>	<u>Slc13a4</u>
<u>Agmo</u>	<u>Fmo4</u>	<u>Marco</u>	<u>Slc14a1</u>
<u>Agtpbbp1</u>	<u>Fmr1os</u>	<u>Mark2</u>	<u>Slc15a3</u>
Ahctf1	<u>Fnbp1l</u>	Marveld1	<u>Slc16a1</u>
<u>Ahcyl1</u>	<u>Fntb</u>	<u>Masp2</u>	<u>Slc16a10</u>
Ahcyl2	<u>Folh1</u>	<u>Mat2a</u>	<u>Slc16a12</u>
<u>Ahdc1</u>	<u>Fosl2</u>	<u>Mavs</u>	<u>Slc16a13</u>
<u>Ahi1</u>	Foxd2	Mbd1	<u>Slc16a3</u>
Ahsa2	<u>Foxd4</u>	<u>Mbd5</u>	<u>Slc16a5</u>
<u>Al429214</u>	Foxk2	<u>Mbl1</u>	<u>Slc16a6</u>
Al464131	<u>Foxo1</u>	<u>Mboat1</u>	<u>Slc16a7</u>
<u>Al662270</u>	<u>Fpr1</u>	<u>Mbtps1</u>	<u>Slc17a9</u>
<u>Al846148</u>	<u>Fpr2</u>	<u>Mcemp1</u>	<u>Slc1a1</u>
<u>Aicda</u>	<u>Fras1</u>	Mcf2l	<u>Slc1a3</u>
<u>Aif1</u>	<u>Frat1</u>	<u>Mcm10</u>	Slc1a7
<u>Aif1l</u>	<u>Frmd4a</u>	<u>Mcm8</u>	<u>Slc20a1</u>
<u>Aifm3</u>	<u>Frmpd3</u>	<u>Mcoln2</u>	<u>Slc22a23</u>
<u>Ajuba</u>	<u>Frzb</u>	<u>Mcu</u>	<u>Slc22a3</u>
<u>Ak3</u>	<u>Fst</u>	<u>Mdga1</u>	<u>Slc24a1</u>
<u>Ak4</u>	<u>Fstl3</u>	<u>Mdk</u>	<u>Slc24a5</u>
Akap12	<u>Fto</u>	<u>Meaf6</u>	<u>Slc25a14</u>
<u>Akap2</u>	<u>Fut4</u>	<u>Med11</u>	<u>Slc25a16</u>
<u>Akr1c18</u>	Fut8	<u>Med18</u>	Slc25a30
<u>Akt2</u>	<u>Fv1</u>	Med24	<u>Slc25a33</u>
<u>Akt2-ps</u>	<u>Fxr2</u>	<u>Med27</u>	<u>Slc25a34</u>
<u>Aldh18a1</u>	<u>Fxyd3</u>	<u>Med28</u>	<u>Slc25a38</u>
<u>Aldh1a1</u>	<u>Fxyd5</u>	Med30	<u>Slc25a44</u>
<u>Alkbh4</u>	<u>Fyb</u>	<u>Med4</u>	Slc25a48

<i>Aloxe3</i>	<i>Fyco1</i>	<i>Med8</i>	<i>Slc26a1</i>
<i>Alpk1</i>	<i>Fyn</i>	<i>Mefv</i>	<i>Slc26a10</i>
Alpk3	<i>Fzd1</i>	<i>Meis1</i>	<i>Slc26a2</i>
<i>Als2</i>	<i>Fzd5</i>	<i>Meox1</i>	<i>Slc28a2</i>
<i>Alyref</i>	<i>G430095P16Rik</i>	<i>Meox2</i>	<i>Slc29a4</i>
<i>Alyref2</i>	<i>Gabra2</i>	<i>Mertk</i>	<i>Slc2a13</i>
<i>Amigo2</i>	<i>Gabrb3</i>	<i>Mest</i>	<i>Slc2a4</i>
<i>Amigo3</i>	<i>Gad1-ps</i>	<i>Met</i>	<i>Slc2a4rg-ps</i>
<i>Amot</i>	<i>Gal3st1</i>	Mettl16	<i>Slc2a6</i>
<i>Amotl2</i>	<i>Galm</i>	<i>Mettl17</i>	<i>Slc2a9</i>
<i>Ampd1</i>	<i>Galnt12</i>	<i>Mettl2</i>	<i>Slc35b2</i>
<i>Ampd3</i>	<i>Galnt14</i>	<i>Mettl21c</i>	<i>Slc35c2</i>
<i>Amt</i>	<i>Galnt15</i>	<i>Mettl23</i>	<i>Slc35d1</i>
<i>Amz1</i>	<i>Galnt18</i>	<i>Mettl5os</i>	<i>Slc36a4</i>
<i>Anapc1</i>	<i>Galt</i>	<i>Mettl7b</i>	<i>Slc38a3</i>
<i>Anapc10</i>	<i>Ganab</i>	<i>Mex3a</i>	<i>Slc39a14</i>
Angpt1	<i>Gapdh</i>	<i>Mfap1b</i>	<i>Slc39a8</i>
<i>Angpt4</i>	<i>Gapdhs</i>	<i>Mfap2</i>	<i>Slc3a2</i>
<i>Angptl1</i>	<i>Garnl3</i>	<i>Mfap4</i>	<i>Slc41a1</i>
Angptl2	Gart	<i>Mff</i>	Slc43a3
<i>Angptl4</i>	<i>Gas1</i>	<i>Mfn1</i>	<i>Slc4a4</i>
<i>Angptl8</i>	<i>Gas2l2</i>	<i>Mfn2</i>	<i>Slc4a8</i>
<i>Ank</i>	<i>Gatsl2</i>	Mfng	<i>Slc5a11</i>
Ankef1	Gatsl3	<i>Mgam</i>	<i>Slc5a6</i>
<i>Ankrd12</i>	<i>Gbas</i>	<i>Mgat4b</i>	<i>Slc5a7</i>
<i>Ankrd24</i>	<i>Gbe1</i>	<i>Mgp</i>	<i>Slc6a13</i>
<i>Ankrd46</i>	<i>Gcnt2</i>	<i>Mical1</i>	<i>Slc6a20a</i>
Ankrd50	<i>Gdap2</i>	Micall1	<i>Slc7a1</i>
<i>Ankrd6</i>	<i>Gdf5</i>	<i>Mid1ip1</i>	<i>Slc9a3r2</i>
<i>Ano2</i>	<i>Gdi1</i>	<i>Mief2</i>	<i>Slc9a9</i>
<i>Anp32a</i>	Gfm2	<i>Milr1</i>	<i>Slfn1</i>
<i>Anxa11</i>	<i>Gga2</i>	<i>Mios</i>	<i>Slfn4</i>
<i>Anxa3</i>	<i>Ggcx</i>	<i>Mipol1</i>	<i>Slit3</i>
<i>Anxa7</i>	<i>Gid4</i>	<i>Mir142hg</i>	Slmap
<i>Anxa8</i>	<i>Gid8</i>	<i>Mir143hg</i>	<i>Slpi</i>
<i>Aoah</i>	<i>Gigyf1</i>	<i>Mir145a</i>	<i>Slx1b</i>
<i>Aoc1</i>	<i>Gigyf2</i>	<i>Mir23a</i>	<i>Slx4ip</i>
<i>Aoc3</i>	<i>Gipc2</i>	<i>Mir3057</i>	<i>Smad3</i>
<i>Ap1g2</i>	<i>Gja1</i>	<i>Mir3060</i>	<i>Smad5</i>
<i>Ap1m1</i>	<i>Gja4</i>	<i>Mir365-2</i>	<i>Smad7</i>
<i>Ap1m2</i>	<i>Gjb1</i>	<i>Mir5125</i>	Smagp
<i>Ap3s2</i>	<i>Gjb5</i>	<i>Mir6236</i>	<i>Smagp2</i>

Ap4e1	<u>Gla</u>	<u>Mir6392</u>	Smarca2
<u>Ap4m1</u>	<u>Glce</u>	Mirg	Smarchb1
Ap5s1	Gldc	<u>Mis18a</u>	<u>Smarcc2</u>
<u>Apbb1ip</u>	Gli2	<u>Mkl2</u>	<u>Smarcd3</u>
<u>Apex2</u>	<u>Glpr2</u>	<u>Mkln1os</u>	<u>Smarce1</u>
<u>Aph1a</u>	<u>Glis1</u>	<u>Mkrn1</u>	<u>Smg9</u>
<u>Aph1b</u>	<u>Glis3</u>	<u>Mllt3</u>	<u>Smim24</u>
<u>ApIn</u>	<u>Glrp1</u>	<u>Mlph</u>	Smkr-ps
<u>Apoa1</u>	<u>Gls2</u>	<u>Mlxip1</u>	<u>Smoc1</u>
<u>Apobec2</u>	<u>Gltsr1</u>	<u>Mmp23</u>	<u>Smoc2</u>
<u>Apoc3</u>	Glul	<u>Mmp8</u>	<u>Smpdl3b</u>
<u>Apoc4</u>	<u>Glyat13</u>	<u>Mmp9</u>	<u>Smpx</u>
<u>Apol10b</u>	<u>Glycam1</u>	<u>Mms19</u>	<u>Smtnl2</u>
<u>Apol8</u>	<u>Glyctk</u>	<u>Mnat1</u>	<u>Smu1</u>
<u>Apol9b</u>	<u>Gm10032</u>	<u>Mocs1</u>	<u>Smyd3</u>
Apold1	<u>Gm10093</u>	<u>Mogat2</u>	<u>Smyd4</u>
<u>Aqp11</u>	<u>Gm10138</u>	<u>Morf4l1</u>	<u>Smyd5</u>
<u>Aqp7</u>	<u>Gm10167</u>	<u>Mphosph8</u>	<u>Snapc3</u>
<u>Aqr</u>	<u>Gm10364</u>	<u>Mpp2</u>	<u>Sncb</u>
<u>Arap1</u>	<u>Gm10392</u>	<u>Mpp4</u>	<u>Sned1</u>
<u>Arel1</u>	<u>Gm10399</u>	<u>Mpp6</u>	<u>Snf8</u>
<u>Arf2</u>	<u>Gm10406</u>	<u>Mrgprg</u>	<u>Snhg12</u>
<u>Arfgap1</u>	Gm10425	<u>Mrln</u>	<u>Snn</u>
<u>Arfgap2</u>	<u>Gm10441</u>	<u>Mrm1</u>	<u>Snora28</u>
<u>Arfgap3</u>	<u>Gm10463</u>	<u>Mrpl24</u>	<u>Snord49a</u>
<u>Arfip2</u>	<u>Gm10478</u>	<u>Ms4a1</u>	Snrk
<u>Arfrp1</u>	<u>Gm10602</u>	<u>Ms4a6c</u>	<u>Snrpb2</u>
<u>Arg2</u>	<u>Gm10642</u>	<u>Ms4a7</u>	<u>Snrpd2</u>
<u>Arhgap18</u>	<u>Gm10644</u>	<u>Msh2</u>	<u>Snrpd3</u>
<u>Arhgap20</u>	<u>Gm10654</u>	<u>Mstn</u>	<u>Snrpe</u>
<u>Arhgap21</u>	<u>Gm10658</u>	<u>Msto1</u>	<u>Snrpg</u>
<u>Arhgap24</u>	<u>Gm10699</u>	<u>Mt2</u>	<u>Snta1</u>
Arhgap28	Gm10710	<u>Mta3</u>	Sntb1
<u>Arhgap4</u>	<u>Gm10785</u>	<u>Mterf1b</u>	Snw1
<u>Arhgap42</u>	<u>Gm11266</u>	<u>Mthfd1</u>	<u>Snx15</u>
<u>Arhgap5</u>	<u>Gm11346</u>	<u>Mthfd1l</u>	<u>Snx18</u>
<u>Arhgdib</u>	<u>Gm11427</u>	Mthfr	<u>Snx20</u>
<u>Arhgef11</u>	<u>Gm11460</u>	<u>Mtl5</u>	<u>Snx29</u>
<u>Arhgef17</u>	<u>Gm11478</u>	<u>Mtm1</u>	<u>Snx33</u>
<u>Arhgef26</u>	<u>Gm11496</u>	Mtmr10	<u>Soat2</u>
<u>Arhgef39</u>	<u>Gm11537</u>	<u>Mtor</u>	<u>Sorbs1</u>
<u>Arhgef6</u>	<u>Gm11560</u>	<u>Mturn</u>	Sorbs3

<u>Arid3a</u>	Gm11730	<u>Mtx2</u>	<u>Sort1</u>
<u>Arid3b</u>	<u>Gm11734</u>	<u>Mup3</u>	<u>Sos2</u>
<u>Arid5b</u>	<u>Gm11772</u>	<u>Mut</u>	<u>Sowahc</u>
<u>Arl11</u>	<u>Gm11827</u>	<u>Mxd1</u>	<u>Sox12</u>
<u>Arl14ep1</u>	<u>Gm11837</u>	<u>Mxra7</u>	<u>Sox5</u>
<u>Arl16</u>	<u>Gm11839</u>	<u>Mybpc2</u>	<u>Sox5os4</u>
<u>Arl2bp</u>	<u>Gm12002</u>	Mycl	<u>Sp2</u>
<u>Arl4a</u>	<u>Gm12166</u>	<u>Mycn</u>	<u>Sparc</u>
<u>Arl4c</u>	<u>Gm12183</u>	<u>Myd88</u>	<u>Spata13</u>
<u>Arl5a</u>	<u>Gm12279</u>	<u>Myh2</u>	Spata2
<u>Arl5c</u>	<u>Gm12328</u>	<u>Myh7b</u>	<u>Spata24</u>
<u>Arl6ip1</u>	<u>Gm12419</u>	<u>Myl12b</u>	<u>Spata33</u>
<u>Armc8</u>	<u>Gm12473</u>	<u>Mylip</u>	<u>Spatc1</u>
<u>Armcx4</u>	<u>Gm12511</u>	<u>Mylpf</u>	<u>Spats2</u>
<u>Armcx6</u>	<u>Gm12596</u>	<u>Myo19</u>	<u>Spc25</u>
Arnt	<u>Gm12791</u>	<u>Myo1c</u>	Spen
Arntl	<u>Gm13021</u>	<u>Myo1g</u>	<u>Spi1</u>
<u>Arpc2</u>	<u>Gm13071</u>	<u>Myo6</u>	<u>Spib</u>
<u>Arpc3</u>	<u>Gm13110</u>	<u>Myom2</u>	<u>Spint2</u>
<u>Arpc4</u>	<u>Gm13372</u>	<u>Myot</u>	<u>Spire1</u>
<u>Arrb1</u>	<u>Gm13373</u>	Myrip	<u>Spn</u>
<u>Arrb2</u>	<u>Gm13387</u>	<u>Myzap</u>	<u>Spo11</u>
<u>Arrdc1</u>	<u>Gm13562</u>	<u>Mzb1</u>	<u>Spock1</u>
<u>Arrdc4</u>	<u>Gm13703</u>	Naa60	Spon1
Arsb	<u>Gm13709</u>	<u>Nab2</u>	Spon2
<u>Asap1</u>	<u>Gm13919</u>	<u>Nabp1</u>	<u>Spop</u>
<u>Asb12</u>	<u>Gm14027</u>	Nadk	<u>Spry3</u>
<u>Ascl2</u>	<u>Gm14232</u>	<u>Nadk2</u>	<u>Spry4</u>
Ash2l	<u>Gm14257</u>	Nampt	<u>Spsb1</u>
<u>Asic1</u>	<u>Gm14305</u>	<u>Nap1l1</u>	<u>Spsb2</u>
<u>Aspg</u>	<u>Gm14320</u>	<u>Napepld</u>	<u>Sptlc2</u>
Asph	Gm14403	<u>Napsa</u>	<u>Sqstm1</u>
Asxl3	Gm14420	<u>Narf</u>	<u>Sra1</u>
<u>Atf4</u>	<u>Gm14488</u>	<u>Nat14</u>	<u>Src</u>
<u>Atf6</u>	<u>Gm14812</u>	<u>Natd1</u>	<u>Srd5a3</u>
<u>Atg9a</u>	<u>Gm15228</u>	<u>Nav1</u>	<u>Srgap2</u>
<u>Atl2</u>	<u>Gm15327</u>	<u>Nav3</u>	<u>Srp68</u>
<u>Atn1</u>	<u>Gm15418</u>	<u>Nbas</u>	<u>Srp9</u>
<u>Atp11a</u>	<u>Gm15506</u>	<u>Nbea</u>	<u>Srpk2</u>
<u>Atp1a4</u>	<u>Gm15513</u>	<u>Nbr1</u>	<u>Srpr</u>
<u>Atp1b3</u>	<u>Gm15535</u>	<u>Ncan</u>	Srrd
<u>Atp2b4</u>	<u>Gm15564</u>	<u>Ncbp1</u>	<u>Srrm4</u>

<i>Atp6v0a2</i>	<i>Gm15587</i>	<i>Ncbp2</i>	<i>Srrt</i>
<i>Atp6v1c2</i>	<i>Gm15608</i>	<i>Ncf4</i>	<i>Srsf1</i>
<i>Atrn</i>	<i>Gm15650</i>	<i>Ncl</i>	<i>Srsf12</i>
<i>Atxn1</i>	<i>Gm15675</i>	<i>Ncoa1</i>	<i>Srsf3</i>
<i>Atxn2l</i>	<i>Gm15767</i>	<i>Ncoa4</i>	<i>Srxn1</i>
<i>Atxn7l1</i>	<i>Gm15788</i>	<i>Ncoa5</i>	<i>Ssfa2</i>
<i>Avil</i>	<i>Gm15848</i>	<i>Ncor1</i>	<i>Ssh1</i>
<i>Avpi1</i>	<i>Gm15894</i>	<i>Ncs1</i>	<i>Ssrp1</i>
<i>Avpr1a</i>	<i>Gm15987</i>	<i>Ndrg3</i>	<i>Ssu2</i>
<i>Avpr2</i>	<i>Gm16008</i>	<i>Nebi</i>	<i>Ssx2ip</i>
<i>AW209491</i>	<i>Gm16015</i>	<i>Nedd9</i>	<i>St6gal1</i>
<i>Azgp1</i>	<i>Gm16143</i>	<i>Nek3</i>	<i>St6galnac3</i>
<i>B130055M24Rik</i>	<i>Gm16156</i>	<i>Nek4</i>	<i>St6galnac4</i>
<i>B230354K17Rik</i>	<i>Gm16170</i>	<i>Nek9</i>	<i>St6galnac5</i>
<i>B230369F24Rik</i>	<i>Gm16172</i>	<i>Nelfb</i>	<i>St7l</i>
<i>B3galt1</i>	<i>Gm16174</i>	<i>Nepro</i>	<i>Stab2</i>
<i>B3galt2</i>	<i>Gm16185</i>	<i>Net1</i>	<i>Stac</i>
<i>B3gnt5</i>	<i>Gm16214</i>	<i>Neurl1a</i>	<i>Stap2</i>
<i>B3gnt7</i>	<i>Gm1627</i>	<i>Neurl3</i>	<i>Stard13</i>
<i>B3gntl1</i>	<i>Gm16353</i>	<i>Neurl4</i>	<i>Stat1</i>
<i>B430219N15Rik</i>	<i>Gm16536</i>	<i>Nexn</i>	<i>Stau1</i>
<i>B4galnt1</i>	<i>Gm16548</i>	<i>Nf2</i>	<i>Stbd1</i>
<i>Bace1</i>	<i>Gm16576</i>	<i>Nfe2</i>	<i>Stc1</i>
<i>Bace2</i>	<i>Gm16712</i>	<i>Nfe2l1</i>	<i>Stc2</i>
<i>Bag3</i>	<i>Gm16998</i>	<i>Nfic</i>	<i>Steap4</i>
<i>Bag6</i>	<i>Gm17055</i>	<i>Nfil3</i>	<i>Stfa2l1</i>
<i>Bak1</i>	<i>Gm17147</i>	<i>Nfkb1</i>	<i>Stil</i>
<i>Bambi</i>	<i>Gm17249</i>	<i>Nfkbid</i>	<i>Stim1</i>
<i>Bambi-ps1</i>	<i>Gm17296</i>	<i>Nfkbie</i>	<i>Stk32c</i>
<i>Bank1</i>	<i>Gm17315</i>	<i>Ngf</i>	<i>Stk35</i>
<i>Basp1</i>	<i>Gm17435</i>	<i>Ngfr</i>	<i>Stk39</i>
<i>Batf</i>	<i>Gm17484</i>	<i>Ngfrap1</i>	<i>Stk40</i>
<i>Bax</i>	<i>Gm17501</i>	<i>Ngp</i>	<i>Stkld1</i>
<i>Baz1b</i>	<i>Gm17586</i>	<i>Nhej1</i>	<i>Stmn2</i>
<i>Baz2a</i>	<i>Gm17597</i>	<i>Nhlrc1</i>	<i>Stmnd1</i>
<i>Bbs10</i>	<i>Gm17764</i>	<i>Nhlrc2</i>	<i>Stoml1</i>
<i>Bbs9</i>	<i>Gm18009</i>	<i>Nhs</i>	<i>Ston1</i>
<i>BC005624</i>	<i>Gm18336</i>	<i>Nid2</i>	<i>Stox2</i>
<i>BC017158</i>	<i>Gm18486</i>	<i>Nipal4</i>	<i>Stradb</i>
<i>BC023829</i>	<i>Gm1966</i>	<i>Nipsnap1</i>	<i>Strip1</i>
<i>BC035044</i>	<i>Gm19938</i>	<i>Nkain2</i>	<i>Strip2</i>
<i>BC049352</i>	<i>Gm20324</i>	<i>Nlrp3</i>	<i>Stx16</i>

<u>BC051226</u>	<u>Gm20457</u>	<u>Nmb</u>	<u>Stx3</u>
<u>BC064078</u>	<u>Gm20470</u>	<u>Nmt1</u>	<u>Stx6</u>
<u>BC067074</u>	<u>Gm20496</u>	<u>Nnt</u>	<u>Stx8</u>
<u>Bcar3</u>	<u>Gm20559</u>	Noct	<u>Sugct</u>
<u>Bcl2l1</u>	<u>Gm20604</u>	<u>Nol4l</u>	<u>Sulf1</u>
<u>Bcl2l10</u>	<u>Gm20658</u>	<u>Nol6</u>	<u>Sult1a1</u>
<u>Bcl2l11</u>	<u>Gm20684</u>	<u>Notch3</u>	<u>Sult2b1</u>
<u>Bcl3</u>	<u>Gm21451</u>	<u>Notch4</u>	<u>Sun1</u>
<u>Bcl6</u>	<u>Gm22</u>	<u>Nova1</u>	<u>Sun2</u>
<u>Bcor</u>	<u>Gm22175</u>	Npas2	<u>Susd1</u>
<u>Bcorl1</u>	<u>Gm22482</u>	<u>Npas4</u>	<u>Susd3</u>
<u>Bdnf</u>	<u>Gm23935</u>	<u>Npepps</u>	Sybu
Bean1	<u>Gm24074</u>	<u>Npffr1</u>	<u>Syde2</u>
Bend5	<u>Gm2415</u>	Npnt	Syn2
<u>Bet1l</u>	<u>Gm2619</u>	<u>Nprl2</u>	<u>Syne1</u>
Bhlhb9	<u>Gm26510</u>	<u>Nptx1</u>	<u>Syt12</u>
<u>Bhlhe40</u>	<u>Gm26516</u>	Npy1r	<u>Syt14</u>
<u>Bhlhe41</u>	Gm26532	<u>Npy4r</u>	<u>Syt2</u>
<u>Bid</u>	<u>Gm26616</u>	Nr1d1	<u>Syt5</u>
<u>Bin2</u>	<u>Gm26620</u>	Nr1d2	<u>Sytl1</u>
<u>Bin3</u>	<u>Gm26626</u>	<u>Nr1i3</u>	Sytl2
<u>Birc3</u>	<u>Gm26668</u>	<u>Nr2f2</u>	Tab1
<u>Blk</u>	<u>Gm26670</u>	<u>Nr4a1</u>	<u>Tacc1</u>
<u>Blzf1</u>	<u>Gm26684</u>	<u>Nr4a2</u>	<u>Tacc2</u>
<u>Bmp6</u>	<u>Gm26740</u>	<u>Nr5a2</u>	Taco1
<u>Bmp7</u>	<u>Gm26760</u>	<u>Nrbp1</u>	<u>Tada2b</u>
<u>Bmper</u>	<u>Gm26762</u>	<u>Nrbp2</u>	<u>Taf15</u>
<u>Bms1</u>	<u>Gm26772</u>	<u>Nrg4</u>	<u>Taf3</u>
<u>Bnc2</u>	<u>Gm26792</u>	<u>Nrip1</u>	<u>Taf4a</u>
<u>Bnip3</u>	<u>Gm26797</u>	<u>Nrros</u>	<u>Taf6</u>
<u>Bpifb6</u>	<u>Gm26801</u>	<u>Nsdhl</u>	<u>Tagln2</u>
<u>Brap</u>	<u>Gm26808</u>	<u>Nsg2</u>	<u>Tagln3</u>
<u>Brat1</u>	<u>Gm26813</u>	<u>Nsmce1</u>	<u>Tamm41</u>
<u>Brca2</u>	<u>Gm26840</u>	<u>Nsmce2</u>	Tap1
<u>Brd1</u>	<u>Gm26863</u>	<u>Nsmce4a</u>	<u>Tapbp</u>
<u>Brd2</u>	Gm26877	<u>Nsrp1</u>	<u>Tardbp</u>
<u>Brd9</u>	<u>Gm26982</u>	<u>Nsun2</u>	<u>Tarm1</u>
<u>Brinp1</u>	<u>Gm27028</u>	<u>Nt5c1b</u>	<u>Tars</u>
<u>Brinp2</u>	Gm27252	<u>Nthl1</u>	<u>Tarsl2</u>
<u>Bspry</u>	<u>Gm27616</u>	<u>Ntn4</u>	<u>Tatdn2</u>
<u>Bst1</u>	<u>Gm28035</u>	<u>Ntsr2</u>	<u>Tax1bp1</u>
<u>Btbd3</u>	<u>Gm28055</u>	<u>Nuak2</u>	<u>Tbc1d4</u>

<u>Btf3</u>	<u>Gm28154</u>	<u>Nub1</u>	<u>Tbc1d5</u>
<u>Btg1</u>	<u>Gm28230</u>	<u>Nucb2</u>	<u>Tbc1d8</u>
<u>Btg3</u>	<u>Gm28417</u>	<u>Nudcd2</u>	<u>Tbrg1</u>
<u>Btla</u>	<u>Gm28424</u>	<u>Nudt1</u>	<u>Tbx18</u>
<u>Btnl2</u>	<u>Gm2862</u>	<u>Nudt18</u>	<u>Tbx21</u>
<u>Bves</u>	<u>Gm28643</u>	<u>Nup188</u>	Tbx3os1
<u>C130012C08Rik</u>	<u>Gm2885</u>	<u>Nup210</u>	<u>Tcaim</u>
<u>C130060C02Rik</u>	<u>Gm28875</u>	<u>Nup210l</u>	<u>Tcea1-ps1</u>
<u>C130083M11Rik</u>	<u>Gm28876</u>	<u>Nup62</u>	Tceanc2
<u>C1d</u>	<u>Gm29101</u>	<u>Nup93</u>	<u>Tcerg1l</u>
<u>C1qa</u>	<u>Gm29443</u>	<u>Nup98</u>	<u>Tcf23</u>
<u>C1qb</u>	<u>Gm29585</u>	<u>Nutf2</u>	Tctn3
<u>C1qtnf6</u>	<u>Gm29669</u>	Nxn	<u>Tead1</u>
<u>C230062I16Rik</u>	<u>Gm30173</u>	<u>Nxpe5</u>	<u>Tead4</u>
C2cd2l	<u>Gm30557</u>	Nxph3	<u>Tec</u>
<u>C330007P06Rik</u>	<u>Gm3248</u>	<u>Nxt2</u>	<u>Tecpr1</u>
<u>C530043K16Rik</u>	<u>Gm3289</u>	<u>Nyx</u>	Tef
<u>C530050E15Rik</u>	<u>Gm3294</u>	<u>Oard1</u>	<u>Tekt1</u>
C6	Gm32999	<u>Oas1b</u>	<u>Ten1</u>
<u>C630043F03Rik</u>	<u>Gm33370</u>	<u>Oas1g</u>	<u>Tesk2</u>
<u>C920009B18Rik</u>	<u>Gm3468</u>	<u>Oas3</u>	<u>Tespa1</u>
<u>Cables2</u>	<u>Gm3511</u>	<u>Oaz2</u>	<u>Tet2</u>
<u>Cabyr</u>	<u>Gm35549</u>	<u>Obfc1</u>	<u>Tex40</u>
<u>Cacna1i</u>	<u>Gm3558</u>	<u>Ogt</u>	<u>Tfap4</u>
<u>Cacna2d4</u>	<u>Gm3636</u>	<u>Olfm1</u>	<u>Tfb2m</u>
<u>Cacnb3</u>	<u>Gm36638</u>	<u>Olfm2</u>	<u>Tfeb</u>
<u>Cacng1</u>	<u>Gm36981</u>	<u>Olfm1l</u>	<u>Tfpi2</u>
<u>Cacng5</u>	<u>Gm36995</u>	<u>Olfm13</u>	<u>Tfr2</u>
<u>Cacul1</u>	<u>Gm37019</u>	<u>Olfr1388</u>	<u>Tfrc</u>
<u>Calca</u>	<u>Gm37027</u>	<u>Olfr56</u>	<u>Tgm3</u>
<u>Calm2</u>	Gm37033	<u>Oma1</u>	<u>Tgoln1</u>
<u>Calr</u>	<u>Gm37078</u>	<u>Optc</u>	<u>Thada</u>
<u>Calr3</u>	<u>Gm37192</u>	Optn	<u>Thap2</u>
<u>Camkk2</u>	<u>Gm37296</u>	<u>Orai2</u>	<u>Thap4</u>
<u>Caml</u>	<u>Gm37309</u>	<u>Orc6</u>	<u>Them4</u>
<u>Camp</u>	<u>Gm37336</u>	<u>Orm1</u>	<u>Them5</u>
<u>Cap2</u>	<u>Gm37352</u>	Ormdl3	<u>Themis2</u>
<u>Capg</u>	<u>Gm37397</u>	<u>Osbp</u>	<u>Thnsl1</u>
<u>Capn12</u>	<u>Gm37452</u>	<u>Osbp2</u>	Thoc6
<u>Capn15</u>	Gm37474	Osbpl11	<u>Thrsp</u>
<u>Car11</u>	<u>Gm37510</u>	Osbpl1a	<u>Ticrr</u>
<u>Car12</u>	<u>Gm37592</u>	<u>Oscp1</u>	<u>Tifab</u>

<u>Car4</u>	<u>Gm37621</u>	<u>Osgep</u>	<u>Tigar</u>
<u>Car6</u>	<u>Gm37691</u>	Osgin1	<u>Timd4</u>
<u>Card6</u>	<u>Gm37716</u>	<u>Osgin2</u>	<u>Timp1</u>
<u>Cars2</u>	<u>Gm37755</u>	<u>Ostc</u>	Timp3
<u>Casc1</u>	<u>Gm38021</u>	<u>Ostf1</u>	Timp4
<u>Cask</u>	<u>Gm38043</u>	<u>Otos</u>	<u>Tinag</u>
<u>Caskin2</u>	<u>Gm38082</u>	<u>Otulin</u>	<u>Tipin</u>
<u>Casp4</u>	<u>Gm38102</u>	<u>Oxnad1</u>	<u>Tirap</u>
<u>Cast</u>	<u>Gm38158</u>	<u>Oxtr</u>	<u>Tk2</u>
<u>Cbfb</u>	<u>Gm38227</u>	<u>P2ry14</u>	Tle1
Ccbe1	<u>Gm38244</u>	P2ry2	<u>Tlr13</u>
<u>Ccdc114</u>	<u>Gm38313</u>	<u>P3h2</u>	<u>Tlr2</u>
<u>Ccdc12</u>	<u>Gm38342</u>	<u>P4ha1</u>	<u>Tlr6</u>
<u>Ccdc122</u>	<u>Gm38399</u>	<u>Pabpn1</u>	<u>Tm4sf5</u>
<u>Ccdc127</u>	<u>Gm4076</u>	<u>Padi4</u>	<u>Tmc5</u>
<u>Ccdc130</u>	<u>Gm4204</u>	<u>Pafah1b3</u>	<u>Tmc7</u>
<u>Ccdc137</u>	<u>Gm42487</u>	<u>Pank2</u>	<u>Tmc8</u>
<u>Ccdc144b</u>	<u>Gm42577</u>	<u>Pank3</u>	<u>Tmcc2</u>
<u>Ccdc148</u>	<u>Gm42582</u>	<u>Panx1</u>	<u>Tmed10</u>
<u>Ccdc157</u>	<u>Gm4262</u>	<u>Pappa</u>	<u>Tmem108</u>
<u>Ccdc158</u>	<u>Gm42783</u>	<u>Papss2</u>	<u>Tmem119</u>
Ccdc159	<u>Gm42797</u>	<u>Paqr9</u>	<u>Tmem128</u>
<u>Ccdc167</u>	Gm42798	<u>Pard3</u>	Tmem129
<u>Ccdc183</u>	<u>Gm42835</u>	Park2	<u>Tmem132b</u>
<u>Ccdc184</u>	<u>Gm42847</u>	<u>Parp11</u>	<u>Tmem138</u>
<u>Ccdc27</u>	<u>Gm42984</u>	<u>Parp16</u>	<u>Tmem150b</u>
<u>Ccdc71</u>	<u>Gm43006</u>	<u>Parp2</u>	<u>Tmem156</u>
Ccdc80	<u>Gm43012</u>	<u>Parp9</u>	Tmem17
Ccdc85a	Gm43076	<u>Pax5</u>	<u>Tmem173</u>
<u>Ccl11</u>	<u>Gm43080</u>	<u>Paxip1</u>	<u>Tmem176b</u>
<u>Ccl12</u>	<u>Gm43088</u>	<u>Pbk</u>	<u>Tmem178</u>
<u>Ccl2</u>	<u>Gm43091</u>	<u>Pbld2</u>	<u>Tmem179</u>
<u>Ccl25</u>	<u>Gm43105</u>	<u>Pcdh12</u>	<u>Tmem18</u>
<u>Ccl27a</u>	<u>Gm43148</u>	<u>Pcdh7</u>	<u>Tmem200b</u>
<u>Ccl4</u>	<u>Gm43172</u>	<u>Pcdhb11</u>	<u>Tmem216</u>
<u>Ccl8</u>	Gm43314	<u>Pcdhb16</u>	<u>Tmem221</u>
<u>Ccnb2-ps</u>	<u>Gm43328</u>	<u>Pcdhb21</u>	<u>Tmem229b</u>
<u>Ccndbp1</u>	<u>Gm43362</u>	<u>Pcdhga11</u>	<u>Tmem233</u>
<u>Ccng2</u>	<u>Gm43379</u>	<u>Pcdhga4</u>	<u>Tmem252</u>
<u>Ccny</u>	<u>Gm43412</u>	Pcdhga5	<u>Tmem255a</u>
<u>Ccp110</u>	<u>Gm43445</u>	<u>Pcdhga6</u>	<u>Tmem258</u>
<u>Cd101</u>	<u>Gm43568</u>	Pcdhga7	<u>Tmem40</u>

<u>Cd163</u>	<u>Gm43609</u>	<u>Pcdhgb2</u>	<u>Tmem41a</u>
<u>Cd177</u>	<u>Gm43618</u>	<u>Pcdhgb4</u>	<u>Tmem45a</u>
<u>Cd19</u>	<u>Gm4366</u>	<u>Pcdhgb6</u>	<u>Tmem52</u>
<u>Cd209b</u>	<u>Gm43681</u>	Pcdhgc3	<u>Tmem55b</u>
<u>Cd22</u>	<u>Gm43699</u>	<u>Pcdhgc5</u>	Tmem57
<u>Cd244</u>	<u>Gm43712</u>	<u>Pcid2</u>	<u>Tmem64</u>
Cd276	<u>Gm43808</u>	<u>Pcolce</u>	<u>Tmem79</u>
<u>Cd300a</u>	<u>Gm43819</u>	<u>Pcolce2</u>	<u>Tmem80</u>
<u>Cd300e</u>	<u>Gm43848</u>	<u>Pcyt1a</u>	<u>Tmem81</u>
<u>Cd300lf</u>	<u>Gm43852</u>	<u>Pdcd2l</u>	Tmem86a
<u>Cd37</u>	Gm43909	Pddc1	<u>Tmem88b</u>
<u>Cd3e</u>	<u>Gm43938</u>	<u>Pde11a</u>	<u>Tmem94</u>
<u>Cd40</u>	<u>Gm44026</u>	<u>Pde1b</u>	<u>Tmod2</u>
<u>Cd48</u>	<u>Gm44065</u>	Pde3a	<u>Tmod4</u>
<u>Cd5l</u>	<u>Gm44117</u>	<u>Pde3b</u>	<u>Tmprss6</u>
<u>Cd72</u>	<u>Gm44143</u>	Pde4c	<u>Tmsb4x</u>
Cd79a	<u>Gm44175</u>	<u>Pde6d</u>	Tmtc1
<u>Cd79b</u>	<u>Gm44246</u>	Pde7b	<u>Tnf</u>
<u>Cd8b1</u>	<u>Gm44250</u>	<u>Pdgfc</u>	<u>Tnfaip2</u>
<u>Cdadcl</u>	<u>Gm44276</u>	<u>Pdgfrb</u>	<u>Tnfaip8</u>
<u>Cdc20</u>	<u>Gm44291</u>	<u>Pdha1</u>	<u>Tnfaip8l2</u>
Cdc25b	<u>Gm44428</u>	<u>Pdlim7</u>	<u>Tnfrsf10b</u>
Cdc37l1	<u>Gm4462</u>	Pdp2	<u>Tnfrsf13b</u>
<u>Cdc42bpa</u>	<u>Gm4482</u>	<u>Pdzd2</u>	<u>Tnfrsf13c</u>
<u>Cdc42bpg</u>	<u>Gm4524</u>	<u>Pdzrn3</u>	<u>Tnfsf14</u>
<u>Cdc42ep2</u>	<u>Gm454</u>	<u>Pecam1</u>	<u>Tnk2</u>
<u>Cdc42ep4</u>	<u>Gm4604</u>	<u>Peg3</u>	<u>Tnks1bp1</u>
<u>Cdc73</u>	<u>Gm4673</u>	<u>Peli2</u>	<u>Tnnc1</u>
<u>Cdca4</u>	<u>Gm4779</u>	<u>Peli3</u>	<u>Tnni3</u>
<u>Cdh11</u>	<u>Gm4804</u>	Per1	<u>Tnnt3</u>
<u>Cdh19</u>	<u>Gm4912</u>	Per2	<u>Tnpo3</u>
<u>Cdh2</u>	<u>Gm5113</u>	Per3	<u>Tnrc18</u>
Cdipt	<u>Gm5150</u>	<u>Pex1</u>	Tns2
<u>Cdk18</u>	<u>Gm5276</u>	<u>Pex26</u>	<u>Tns4</u>
<u>Cdk9</u>	<u>Gm5460</u>	<u>Pex5</u>	<u>Tob2</u>
<u>Cdkl1</u>	<u>Gm5547</u>	<u>Pex5l</u>	<u>Tomm34</u>
<u>Cdkl5</u>	<u>Gm5627</u>	<u>Pfdn5</u>	<u>Tonsl</u>
<u>Cdkn2c</u>	<u>Gm568</u>	<u>Pfkfb3</u>	<u>Top3b</u>
Cdon	<u>Gm5763</u>	<u>Pfn1</u>	<u>Tor1a</u>
<u>Cdr2l</u>	<u>Gm5805</u>	<u>Pgam2</u>	<u>Tor1aip2</u>
<u>Ceacam10</u>	<u>Gm5970</u>	Pgbd5	<u>Tor2a</u>
<u>Cebpg</u>	<u>Gm6548</u>	<u>Pglyrp1</u>	<u>Tor4a</u>

<u>Cecr2</u>	<u>Gm684</u>	<u>Pgrmc2</u>	<u>Tox2</u>
<u>Cecr5</u>	<u>Gm6969</u>	<u>Phf11b</u>	<u>Tph2</u>
<u>Celsr2</u>	<u>Gm7120</u>	<u>Phf12</u>	<u>Tpm3</u>
<u>Cenpa</u>	Gm7160	<u>Phf2</u>	<u>Tpm4</u>
<u>Cenpf</u>	<u>Gm7180</u>	<u>Phf20</u>	<u>Tprn</u>
<u>Cep126</u>	<u>Gm7609</u>	<u>Phf21a</u>	<u>Tpst1</u>
Cep170b	<u>Gm7694</u>	<u>Phf23</u>	<u>Trabd2b</u>
<u>Cep41</u>	<u>Gm7964</u>	<u>Phf5a</u>	<u>Traf1</u>
<u>Cep44</u>	<u>Gm8066</u>	<u>Phkb</u>	<u>Traf3ip1</u>
<u>Cep70</u>	<u>Gm8250</u>	Phkg1	<u>Traf7</u>
<u>Ces1d</u>	<u>Gm8281</u>	<u>Phlda3</u>	<u>Traip</u>
<u>Ces4a</u>	Gm8606	Phldb1	<u>Tram1</u>
<u>Cfap20</u>	<u>Gm867</u>	<u>Phrf1</u>	<u>Trappc1</u>
<u>Cfap54</u>	<u>Gm8773</u>	<u>Phyhd1</u>	<u>Trappc10</u>
<u>Cfap69</u>	<u>Gm8895</u>	<u>Pi15</u>	<u>Trappc13</u>
<u>Cfl1</u>	<u>Gm9358</u>	<u>Picalm</u>	<u>Trappc8</u>
<u>Cflar</u>	<u>Gm9484</u>	<u>Piezo1</u>	<u>Trav8n-2</u>
<u>Cgref1</u>	<u>Gm960</u>	Pigg	<u>Trbj2-7</u>
<u>Ch25h</u>	<u>Gm9696</u>	Pigh	<u>Trbv13-1</u>
Chac1	<u>Gm9733</u>	<u>Pigl</u>	<u>Trbv29</u>
<u>Chaf1b</u>	<u>Gm9774</u>	<u>Pigo</u>	<u>Trem1</u>
<u>Chd3os</u>	Gm9821	<u>Pigu</u>	<u>Trem3</u>
<u>Chdh</u>	<u>Gm9889</u>	<u>Pih1d1</u>	<u>Trem2</u>
<u>Chga</u>	<u>Gm9899</u>	<u>Pik3cd</u>	<u>Trem14</u>
<u>Chil1</u>	<u>Gm9947</u>	Pik3r1	<u>Trhde</u>
<u>Chil3</u>	<u>Gm9951</u>	<u>Pim1</u>	<u>Trib1</u>
<u>Chkb</u>	<u>Gmfg</u>	<u>Pinx1</u>	<u>Trim2</u>
<u>Chl1</u>	<u>Gnas</u>	<u>Pirb</u>	Trim24
<u>Chmp4c</u>	<u>Gnat2</u>	<u>Pisd</u>	<u>Trim26</u>
<u>Chn1</u>	<u>Gnat3</u>	<u>Pisd-ps1</u>	<u>Trim30b</u>
<u>Chp2</u>	<u>Gnb1</u>	<u>Pitpna</u>	<u>Trim32</u>
Chpf2	<u>Gnb1l</u>	<u>Pitpnb</u>	<u>Trim43c</u>
<u>Chrac1</u>	<u>Gnb2l1</u>	Pitrm1	<u>Trim44</u>
<u>Chrna5</u>	<u>Gng3</u>	<u>Pja1</u>	Trim5
Chst1	<u>Gng4</u>	<u>Pkd1</u>	<u>Trip10</u>
<u>Chtf8</u>	<u>Gng7</u>	<u>Pkd2l2</u>	<u>Trip13</u>
Ciart	<u>Gng8</u>	<u>Pkp1</u>	<u>Trip6</u>
<u>Cidec</u>	Gngt2	<u>Pkp4</u>	<u>Trit1</u>
<u>Cipc</u>	<u>Gnpat</u>	<u>Pla2g15</u>	<u>Trmt1l</u>
<u>Cirbp</u>	<u>Gnptab</u>	<u>Pla2g2e</u>	<u>Trmt2a</u>
<u>Cish</u>	<u>Golga3</u>	<u>Pla2g4e</u>	Trnau1ap
<u>Cit</u>	Golga4	<u>Pla2g5</u>	<u>Trp53bp2</u>

<u>Cited2</u>	<u>Golt1b</u>	<u>Plaa</u>	<u>Trp53i11</u>
<u>Ciz1</u>	<u>Gorab</u>	<u>Plac8</u>	<u>Trp53inp2</u>
<u>Ckap2</u>	<u>Gp9</u>	<u>Platr26</u>	<u>Trp63</u>
<u>Ckm</u>	Gpam	<u>Plaur</u>	<u>Tsc22d1</u>
<u>Clca2</u>	<u>Gpat4</u>	<u>Plcb3</u>	Tsc22d3
Clcn2	<u>Gpatch2l</u>	<u>Plcb4</u>	<u>Tsen54</u>
Cldn10	<u>Gpatch3</u>	<u>Plce1</u>	<u>Tshz3</u>
Cldn12	<u>Gpatch4</u>	<u>Plch2</u>	<u>Tsku</u>
<u>Cldn15</u>	<u>Gpatch8</u>	Plcl1	<u>Tsnax</u>
<u>Cldn22</u>	<u>Gpc1</u>	<u>Plcl2</u>	<u>Tspan13</u>
<u>Clec12a</u>	<u>Gpc3</u>	<u>Pld4</u>	<u>Tspan14</u>
<u>Clec4a1</u>	<u>Gpc4</u>	<u>Pld5</u>	<u>Tspan18</u>
<u>Clec4a4</u>	<u>Gpd1l</u>	<u>Plekha5</u>	<u>Tspan32</u>
<u>Clec4d</u>	<u>Gpd2</u>	<u>Plekha6</u>	Tspan4
<u>Clec4e</u>	<u>Gper1</u>	<u>Plekha8</u>	<u>Tspan5</u>
<u>Clec4g</u>	<u>Gpld1</u>	<u>Plekhg1</u>	Tssk4
<u>Clec4n</u>	<u>Gpr132</u>	Plekhg3	<u>Tstd2</u>
<u>Clic1</u>	<u>Gpr141</u>	<u>Plekho2</u>	<u>Ttc1</u>
<u>Clic6</u>	Gpr146	<u>Plgrkt</u>	<u>Ttc13</u>
<u>Clmn</u>	<u>Gpr153</u>	<u>Plin3</u>	<u>Ttc26</u>
<u>Clmp</u>	<u>Gpr156</u>	<u>Plin4</u>	<u>Ttc37</u>
Clock	<u>Gpr157</u>	<u>Plin5</u>	<u>Ttc39a</u>
<u>Clptm1l</u>	<u>Gpr179</u>	<u>Plk3</u>	<u>Ttc4</u>
<u>Clta</u>	<u>Gpr18</u>	<u>Plk5</u>	<u>Ttc5</u>
<u>Cmah</u>	<u>Gpr183</u>	<u>Plk-ps1</u>	<u>Ttc8</u>
Cmklr1	<u>Gpr19</u>	<u>Plod2</u>	<u>Ttll12</u>
<u>Cml3</u>	<u>Gpr27</u>	<u>Plpp6</u>	<u>Ttll5</u>
<u>Cmtm3</u>	Gpr34	<u>Plppr4</u>	Ttll7
<u>Cmtm6</u>	<u>Gpr35</u>	<u>Plrg1</u>	<u>Ttn</u>
<u>Cmtm7</u>	<u>Gpr75</u>	<u>Pm20d1</u>	<u>Tuba1a</u>
<u>Cnbd2</u>	<u>Gpr84</u>	<u>Pm20d2</u>	<u>Tuba1c</u>
<u>Cnn2</u>	<u>Gprc5a</u>	Pmepa1	Tubd1
<u>Cnn3</u>	<u>Gprc5b</u>	<u>Pmfbp1</u>	<u>Tubgcp4</u>
<u>Cnnm2</u>	<u>Gprin3</u>	<u>Pml</u>	<u>Tubgcp6</u>
<u>Cnot3</u>	<u>Gpsm1</u>	<u>Pnma5</u>	<u>Tulp3</u>
<u>Cnppd1</u>	<u>Gpsm3</u>	<u>Pnp</u>	<u>Tusc3</u>
<u>Cnrip1</u>	<u>Gpx7</u>	<u>Pnpla5</u>	Tusc5
<u>Cnst</u>	Gramd1b	Podn	<u>Twist1</u>
<u>Cntfr</u>	<u>Gramd4</u>	<u>Polg</u>	<u>Txlna</u>
Cntnap1	<u>Grb10</u>	<u>Polm</u>	Txlng
<u>Coa7</u>	<u>Grb14</u>	<u>Poln</u>	<u>Txnl1</u>
<u>Cobll1</u>	<u>Grb7</u>	<u>Polr2b</u>	<u>Txnrd1</u>

<u>Cog2</u>	<u>Grem2</u>	<u>Polr2d</u>	<u>Tyro3</u>
<u>Col10a1</u>	<u>Gria3</u>	<u>Polr2j</u>	<u>Tyrobp</u>
<u>Col12a1</u>	<u>Grid1</u>	<u>Polr3b</u>	<u>U2af1l4</u>
<u>Col15a1</u>	<u>Grik4</u>	<u>Polr3c</u>	<u>Uap1</u>
Col28a1	<u>Grrp1</u>	<u>Pop4</u>	<u>Uba1</u>
<u>Col4a3</u>	<u>Grsf1</u>	Por	<u>Uba7</u>
<u>Col4a4</u>	<u>Gsap</u>	<u>Pou2af1</u>	Ubb
<u>Col4a5</u>	<u>Gsdma</u>	<u>Pou2f2</u>	Ubc
<u>Col6a6</u>	<u>Gsdma2</u>	<u>Pparg</u>	<u>Ube2j1</u>
<u>Col7a1</u>	<u>Gsdma3</u>	<u>Ppcdc</u>	Ube2l6
<u>Commd4</u>	<u>Gsdmd</u>	<u>Ppfia2</u>	<u>Ube2s</u>
Commd7	<u>Gsg1l</u>	<u>Ppfia4</u>	<u>Ubl5</u>
<u>Copg2</u>	<u>Gtf2h3</u>	<u>Ppfibp2</u>	<u>Ubqln1</u>
<u>Copz2</u>	Gtf2i	<u>Ppic</u>	<u>Ubqln4</u>
Coq10b	<u>Gtf2ird1</u>	<u>Ppie</u>	<u>Ubr2</u>
<u>Coro1a</u>	<u>Gtse1</u>	<u>Ppil3</u>	<u>Ubr7</u>
<u>Coro2b</u>	<u>Gucy1b3</u>	<u>Ppip5k1</u>	<u>Ubxn2a</u>
<u>Cotl1</u>	<u>Gypc</u>	<u>Ppm1b</u>	<u>Ubxn4</u>
<u>Cox4i2</u>	<u>Gys2</u>	<u>Ppm1d</u>	<u>Uckl1os</u>
<u>Cox7a2l</u>	<u>H2-Ab1</u>	<u>Ppm1g</u>	<u>Ucp2</u>
<u>Cp</u>	<u>H2afy</u>	<u>Ppm1j</u>	Ugt1a6a
<u>Cpa2</u>	<u>H2-DMb2</u>	<u>Ppm1l</u>	<u>Ugt3a2</u>
<u>Cpa5</u>	<u>H2-K1</u>	<u>Ppme1</u>	<u>Ulbp1</u>
<u>Cpeb1</u>	<u>H2-M11</u>	<u>Ppp1r12a</u>	<u>Unc119</u>
<u>Cpeb3</u>	<u>H2-M9</u>	<u>Ppp1r12b</u>	<u>Unc119b</u>
<u>Cped1</u>	<u>H2-Ob</u>	<u>Ppp1r18</u>	<u>Unc13d</u>
<u>Cplx1</u>	<u>H2-Q5</u>	<u>Ppp1r26</u>	<u>Unc45bos</u>
Cplx2	<u>H2-Q6</u>	<u>Ppp1r27</u>	<u>Unc79</u>
<u>Cpne7</u>	<u>H2-T24</u>	Ppp1r3c	<u>Unc80</u>
<u>Cpne9</u>	<u>H3f3b</u>	<u>Ppp1r3e</u>	<u>Unk</u>
<u>Cpped1</u>	<u>H6pd</u>	<u>Ppp1r3fos</u>	Unkl
<u>Cpt1b</u>	<u>Haa0</u>	<u>Ppp2r1b</u>	<u>Use1</u>
<u>Cpt1c</u>	<u>Hacd2</u>	Ppp2r2d	<u>Usf2</u>
<u>Creb3l3</u>	<u>Haghl</u>	<u>Ppp2r3a</u>	<u>Usp10</u>
<u>Creb3l4</u>	<u>Hapln1</u>	<u>Ppp2r3c</u>	<u>Usp2</u>
<u>Crebl2</u>	<u>Hapln4</u>	<u>Ppp4c</u>	<u>Usp3</u>
<u>Creg2</u>	<u>Haus1</u>	<u>Pqlc2</u>	<u>Usp30</u>
<u>Creld2</u>	Haus4	<u>Prcp</u>	<u>Usp31</u>
<u>Crip1</u>	Hcar1	<u>Prdm1</u>	Usp33
<u>Crisp2</u>	<u>Hck</u>	<u>Prdm8</u>	<u>Usp34</u>
<u>Crkl</u>	<u>Hcls1</u>	<u>Prelid2</u>	<u>Usp40</u>
<u>Crmp1</u>	<u>Hcst</u>	<u>Prepl</u>	<u>Usp47</u>

<u>Crot</u>	<u>Hdac3</u>	<u>Prex1</u>	<u>Usp50</u>
<u>Crtac1</u>	<u>Hdac7</u>	<u>Prickle4</u>	<u>Usp7</u>
<u>Crtc1</u>	<u>Hdc</u>	<u>Prim2</u>	<u>Ust</u>
Cry1	<u>Hddc3</u>	<u>Primpol</u>	<u>Utrn</u>
<u>Cryl1</u>	<u>Heatr5b</u>	<u>Prkaa2</u>	<u>Vamp8</u>
<u>Csf2rb</u>	Hecw2	<u>Prkab1</u>	<u>Vangl2</u>
<u>Csf2rb2</u>	<u>Heg1</u>	<u>Prkcd</u>	<u>Vapa</u>
<u>Csf3r</u>	<u>Heph11</u>	Prkce	<u>Vash1</u>
<u>Csk</u>	Herpud1	<u>Prkcq</u>	<u>Vash2</u>
<u>Csnk2a2</u>	<u>Hes1</u>	<u>Prkd1</u>	<u>Vasn</u>
<u>Cspg4</u>	<u>Hexim1</u>	<u>Prkra</u>	<u>Vat1l</u>
<u>Cspp1</u>	<u>Heyl</u>	<u>Prmt1</u>	<u>Vcl</u>
<u>Csrnp1</u>	<u>Hfe</u>	<u>Prmt10</u>	<u>Vcp-rs</u>
<u>Csrp3</u>	<u>Hhat</u>	<u>Prob1</u>	<u>Vgl14</u>
<u>Cst6</u>	<u>Hhipl1</u>	Prodh	<u>Vhl</u>
<u>Ctage5</u>	<u>Hif3a</u>	<u>Prok2</u>	<u>Vil1</u>
<u>Ctbs</u>	<u>Hilpda</u>	<u>Proser3</u>	<u>Vipr2</u>
Ctcf1	<u>Hip1</u>	<u>Prpf19</u>	<u>Vkorc1l1</u>
<u>Ctgf</u>	Hipk1	<u>Prpf4b</u>	<u>Vldlr</u>
Cth	<u>Hipk4</u>	<u>Prpf8</u>	Vmp1
<u>Ctrl</u>	Hira	<u>Prps1</u>	<u>Vnn1</u>
<u>Ctsa</u>	<u>Hist1h1d</u>	<u>Prps1l1</u>	<u>Vpreb3</u>
<u>Ctse</u>	<u>Hk2</u>	Prr13	Vps13a
<u>Ctsg</u>	Hlf	<u>Prr16</u>	<u>Vps13c</u>
<u>Ctsh</u>	<u>Hmg20a</u>	<u>Prr36</u>	<u>Vps16</u>
<u>Ctsw</u>	Hmgb2	<u>Prrc2a</u>	<u>Vrk3</u>
<u>Cuedc1</u>	<u>Hmgcs1</u>	<u>Prrg3</u>	<u>Vsig2</u>
<u>Cul1</u>	<u>Hmgcs2</u>	<u>Prrt3</u>	<u>Vstm4</u>
<u>Cutal</u>	<u>Hmgxb3</u>	<u>Prss12</u>	Vta1
<u>Cwc27</u>	<u>Hmha1</u>	<u>Prss23</u>	Vti1a
<u>Cx3cl1</u>	<u>Hmox2</u>	<u>Prss55</u>	<u>Vwa3a</u>
<u>Cx3cr1</u>	<u>Hn1</u>	<u>Prune</u>	<u>Wash1</u>
<u>Cxcl11</u>	<u>Hnrnph3</u>	<u>Psma1</u>	<u>Wasl</u>
<u>Cxcl13</u>	<u>Hnrnp1</u>	<u>Psma6</u>	Wbp5
<u>Cxcl16</u>	<u>Hnrnp1l</u>	<u>Psma8</u>	<u>Wdfy2</u>
<u>Cxcl9</u>	<u>Homer1</u>	<u>Psmb10</u>	<u>Wdr1</u>
<u>Cxcr2</u>	<u>Homez</u>	<u>Psmb8</u>	<u>Wdr11</u>
<u>Cxcr5</u>	<u>Hook2</u>	<u>Psmb9</u>	Wdr13
<u>Cyb561</u>	<u>Hopx</u>	<u>Psmc1</u>	<u>Wdr45b</u>
<u>Cyba</u>	Hoxa6	<u>Psmc10</u>	<u>Wdr73</u>
<u>Cygb</u>	<u>Hoxa9</u>	<u>Psmc8</u>	Wdr75
<u>Cyp2b10</u>	<u>Hoxb4</u>	<u>Psmc1</u>	Wdr82

Cyp2b9	Hoxb6	Psmc2	Wdr90
Cyp2c44	Hoxc10	Psmf1	WDR97
Cyp2e1	Hoxc5	Pstpip1	Wee1
Cyp2f2	Hoxc6	Ptcd1	Wfdc17
Cyp2u1	Hoxc9	Ptcd3	Wfdc21
Cyp4f17	Hoxd4	Ptchd4	Whamm
Cyp4f18	Hp	Pten	Wisp2
Cyp4v3	Hpca	Ptger2	Wnt16
Cyp7b1	Hpcal1	Ptger3	Wnt8b
Cyr61	Hpgds	Ptgir	Wwc2
Cys1	Hps5	Ptgis	Wwox
Cysltr2	Hpx	Ptp4a3	Wwp2
Cystm1	Hr	Ptpn18	Xab2
Cyth4	Hrh2	Ptpn3	Xdh
Cytip	Hrk	Ptprb	Xkr4
D2hgdh	Hsd11b1	Ptprd	Xlr4b
D630045J12Rik	Hsd17b1	Ptpru	Xpa
D830025C05Rik	Hsd17b14	Pum3	Xpnpep3
D930048N14Rik	Hsh2d	Purg	Xrcc1
Dag1	Hsp90ab1	Pus7	Xrcc3
Dagla	Hspa1b	Pxdc1	Xrra1
Dapk1	Hspa1l	Pxylp1	Xylt1
Dapl1	Hspa2	Pycr1	Ydic
Dars2	Hspa4l	Pydc3	Yeats2
Dazap2	Hspa8	Pydc4	Ypel1
Dbil5	Hspb1	Pyhin1	Ywhaz
Dbnl	Hspb7	Qsox2	Zadh2
Dbp	Hspb8	Qtrt1	Zbed5
Dbt	Hspd1-ps4	Rab10	Zbtb14
Dcaf10	Htra3	Rab19	Zbtb16
Dcaf12	Hus1	Rab20	Zbtb24
Dcaf13	Huwe1	Rab27a	Zbtb26
Dcaf15	Hyal1	Rab37	Zbtb37
Dchs2	Hydin	Rab3gap2	Zbtb39
Dclk3	Hyou1	Rab3il1	Zbtb4
Dcps	Hypk	Rab44	Zbtb40
Dctd	I830077J02Rik	Rab13	Zbtb7a
Dctn2	I830127L07Rik	Rab16	Zc3h12d
Dctn4	I830134H01Rik	Rac2	Zc3h18
Dcun1d2	Icam2	Rad18	Zc3h7b
Dcun1d3	Ick	Ralb	Zcchc14
Dcun1d4	Idi1	Ralgapa1	Zcchc4

<u>Ddhd2</u>	<u>Ier2</u>	<u>Ralgapa2</u>	<u>Zdhhc24</u>
<u>Ddias</u>	Iffo2	Ralgps1	Zdhhc5
<u>Ddit4</u>	<u>Ifi30</u>	<u>Ralgps2</u>	<u>Zfhx2</u>
Ddo	<i>Ifit1b1</i>	<u>Raly</u>	<i>Zfp119b</i>
<u>Ddost</u>	<u>Ifit3b</u>	<u>Ramp2</u>	<u>Zfp14</u>
Ddr1	<i>Ifitm1</i>	<i>Ranbp9</i>	Zfp142
<i>Ddx11</i>	<u>Ifitm5</u>	<i>Rapgef4</i>	<u>Zfp143</u>
<u>Ddx17</u>	<u>Ifnar2</u>	<u>Rapgef5</u>	<u>Zfp185</u>
<u>Ddx19b</u>	Ifngr1	<u>Rara</u>	<u>Zfp2</u>
<u>Ddx39</u>	<u>Ifngr2</u>	<u>Rasa3</u>	<u>Zfp26</u>
<u>Ddx39b</u>	<u>Ift74</u>	<i>Rasal1</i>	<i>Zfp273</i>
<u>Ddx47</u>	Igbp1	<u>Rasal2</u>	<u>Zfp277</u>
<i>Ddx49</i>	<i>Igfals</i>	<u>Rasd1</u>	<i>Zfp28</i>
<u>Ddx56</u>	<u>Ighd</u>	<i>Rasgef1a</i>	<u>Zfp30</u>
<i>Def8</i>	<i>Ighg1</i>	<u>Rasgef1c</u>	<u>Zfp330</u>
<i>Depdc7</i>	<i>Ighg2b</i>	<u>Rasgrp1</u>	Zfp335
<u>Derl3</u>	<i>Ighg3</i>	Rasgrp3	<u>Zfp365</u>
<u>Det1</u>	<i>Ighj2</i>	<u>Rasl11a</u>	<i>Zfp366</i>
<i>Dfna5</i>	<i>Ighm</i>	<u>Rasl11b</u>	<u>Zfp361l1</u>
<i>Dgat2</i>	<i>Ighv11-2</i>	<u>Rasl12</u>	<i>Zfp382</i>
Dgcr8	Ighv1-22	<u>Raver2</u>	Zfp414
<u>Dgke</u>	<u>Ighv1-76</u>	<u>Rbm14</u>	Zfp433
<u>Dgkh</u>	<i>Ighv6-6</i>	Rbm45	<u>Zfp442</u>
Dgkq	<i>Igkc</i>	<u>Rbms2</u>	<i>Zfp446</i>
<i>Dhcr24</i>	<i>Igkj2</i>	<u>Rbpms</u>	<u>Zfp449</u>
<u>Dhdh</u>	<u>Igkj5</u>	<u>Rbsn</u>	<i>Zfp462</i>
<u>Dhps</u>	<i>Igkv1-110</i>	<i>Rcan2</i>	<u>Zfp493</u>
<u>Dhrs3</u>	<u>Igkv1-122</u>	<i>Rchy1</i>	<u>Zfp503</u>
<u>Dhx16</u>	Igkv12-46	<i>Rcl1</i>	<i>Zfp511</i>
<u>Dhx35</u>	<i>Igkv17-121</i>	<u>Rcor2</u>	<u>Zfp512</u>
<u>Diaph3</u>	<u>Igkv3-7</u>	<i>Rd3</i>	Zfp526
<u>Dido1</u>	<u>Igkv5-39</u>	<u>Rdh14</u>	<i>Zfp575</i>
<i>Dio2</i>	<u>Igkv6-15</u>	Reep4	<u>Zfp583</u>
<u>Dis3l2</u>	<u>Igkv8-19</u>	Rela	<u>Zfp593</u>
Dixdc1	<i>Iglc1</i>	<u>Relb</u>	<i>Zfp598</i>
<u>Dlc1</u>	<u>Iglc2</u>	<u>Relt</u>	<u>Zfp608</u>
<u>Dlg4</u>	<u>Iglc3</u>	<u>Rere</u>	<u>Zfp609</u>
<i>Dll1</i>	<u>Igli3</u>	<i>Ret</i>	<i>Zfp612</i>
<u>Dlx5</u>	<u>Iglv2</u>	<i>Retnlg</i>	Zfp623
<u>Dmrt2</u>	<u>Igsf10</u>	Rev1	<u>Zfp655</u>
<u>Dmtf1</u>	<i>Igsf6</i>	<u>Rfc1</u>	<u>Zfp697</u>
<i>Dmxl2</i>	<i>Igtp</i>	<u>Rfc3</u>	<i>Zfp704</i>

Dnaaf5	<u>Ikake</u>	<u>Rftn1</u>	<u>Zfp74</u>
Dnah3	<u>Ikzf1</u>	<u>Rftn2</u>	<u>Zfp740</u>
Dnah6	<u>Il13</u>	<u>Rfx3</u>	<u>Zfp783</u>
<u>Dnaic1</u>	<u>Il17ra</u>	<u>Rfxank</u>	<u>Zfp810</u>
<u>Dnaja1</u>	<u>Il17re</u>	<u>Rgag1</u>	<u>Zfp827</u>
<u>Dnaja2</u>	<u>Il18bp</u>	<u>Rgma</u>	<u>Zfp862-ps</u>
<u>Dnaja3</u>	<u>Il18r1</u>	<u>Rgs14</u>	<u>Zfp938</u>
Dnaja4	<u>Il1b</u>	<u>Rgs16</u>	<u>Zfp94</u>
Dnajib1	<u>Il1f9</u>	<u>Rgs4</u>	<u>Zfp946</u>
<u>Dnaib4</u>	<u>Il1r1</u>	<u>Rgs7bp</u>	<u>Zfp948</u>
<u>Dnaic8</u>	<u>Il21r</u>	<u>Rhbdd2</u>	<u>Zfp949</u>
<u>Dnase1l1</u>	<u>Il2rg</u>	<u>Rho</u>	<u>Zfp955a</u>
<u>Dnase2a</u>	<u>Il34</u>	<u>Rhog</u>	<u>Zfyve9</u>
<u>Dnm3os</u>	<u>Il4ra</u>	<u>Rhoh</u>	<u>Zgpat</u>
<u>Dnmbp</u>	<u>Il6st</u>	<u>Rhoj</u>	<u>Zhx2</u>
<u>Dnmt3l</u>	<u>Ilk</u>	<u>Rhot1</u>	Zhx3
<u>Dntt</u>	<u>Impact</u>	<u>Rhot2</u>	<u>Zim1</u>
<u>Doc2b</u>	<u>Ina</u>	<u>Rhov</u>	<u>Zmym1</u>
Dock1	<u>Inafm2</u>	<u>Rhpn1</u>	<u>Zmym6</u>
<u>Dock9</u>	<u>Incenp</u>	<u>Ric8b</u>	<u>Zmynd11</u>
<u>Dok2</u>	<u>Inf2</u>	<u>Riid1</u>	<u>Zmynd15</u>
Dok3	<u>Ing4</u>	<u>Rin1</u>	<u>Zmynd8</u>
<u>Dok7</u>	<u>Inpp5j</u>	<u>Rinl</u>	<u>Zpr1</u>
<u>Dopey1</u>	<u>Inpp1</u>	<u>Rint1</u>	<u>Zscan29</u>
<u>Dopey2</u>	<u>Ints2</u>	<u>Riok1</u>	<u>Zswim4</u>
<u>Dph5</u>	<u>Ints6</u>	<u>Ripk1</u>	<u>Zyg11a</u>
<u>Dpm2</u>	<u>Ints8</u>	<u>Ripk3</u>	<u>Zyg11b</u>
<u>Dpp4</u>	<u>Invs</u>	Ripk4	<u>Zyx</u>

Other supplements

Table S2: Number of genes per amplitude (FC) interval

	Sham	VSG
0-0.1	3	2
0.1-0.2	35	36
0.2-0.3	64	58
0.3-0.4	58	67
0.4-0.5	43	65
0.5-0.6	48	44
0.6-0.7	37	28
0.7-0.8	25	25
0.8-0.9	17	17
0.9-1.0	17	16
>1.0	58	47

Table S3: Mean ZT expression data and diurnal fold change (dFC) for core clock genes

Gene		ZT1		ZT7		ZT13		ZT19		dFC
Arntl	Sham	855.4	± 51.92	209.2	± 19.84	112.9	± 12.54	706.4	± 54.08	1.58
	VSG	798.7	± 43.01	230.4	± 39.23	153.9	± 21.43	739.7	± 106.92	1.34
Dbp	Sham	173.6	± 21.78	1427.3	± 172.01	1342.8	± 132.22	268.9	± 33.04	1.56
	VSG	293.0	± 98.46	2078.7	± 347.24	1375.8	± 289.36	300.8	± 84.44	1.76
Clock	Sham	1732.2	± 80.47	1509.1	± 103.47	1379.4	± 33.63	1604.8	± 42.72	0.23
	VSG	1370.3	± 79.63	1260.0	± 64.28	1088.2	± 59.27	1630.5	± 132.53	0.41
Per1	Sham	1109.8	± 92.85	2946.2	± 125.92	3343.6	± 484.58	2093.7	± 515.50	0.94
	VSG	1174.8	± 51.77	1996.2	± 243.73	3213.2	± 178.30	2210.6	± 548.91	0.95
Per2	Sham	233.1	± 20.03	613.6	± 30.55	1687.1	± 173.88	893.4	± 125.87	1.70
	VSG	276.9	± 11.61	562.7	± 43.46	1391.9	± 259.33	832.8	± 73.04	1.46
Npas2	Sham	210.6	± 22.93	20.3	± 2.82	10.9	± 0.86	80.6	± 8.49	2.48
	VSG	214.2	± 17.89	36.2	± 3.86	20.1	± 3.93	133.5	± 8.81	1.92
Nr1d1	Sham	2928.6	± 586.19	7546.7	± 624.16	4037.0	± 253.12	1168.0	± 192.74	1.63
	VSG	2631.1	± 380.08	7568.3	± 844.39	3393.3	± 114.57	1074.7	± 236.58	1.77
Nr1d2	Sham	621.0	± 108.12	1600.1	± 171.37	1613.3	± 100.73	482.2	± 42.08	1.05
	VSG	616.8	± 50.30	1746.5	± 237.64	1422.3	± 85.37	530.7	± 61.68	1.13
Cry1	Sham	360.8	± 29.89	280.1	± 16.17	501.7	± 10.59	675.3	± 54.19	0.87
	VSG	351.5	± 17.94	251.9	± 30.25	381.0	± 27.12	674.9	± 78.23	1.02

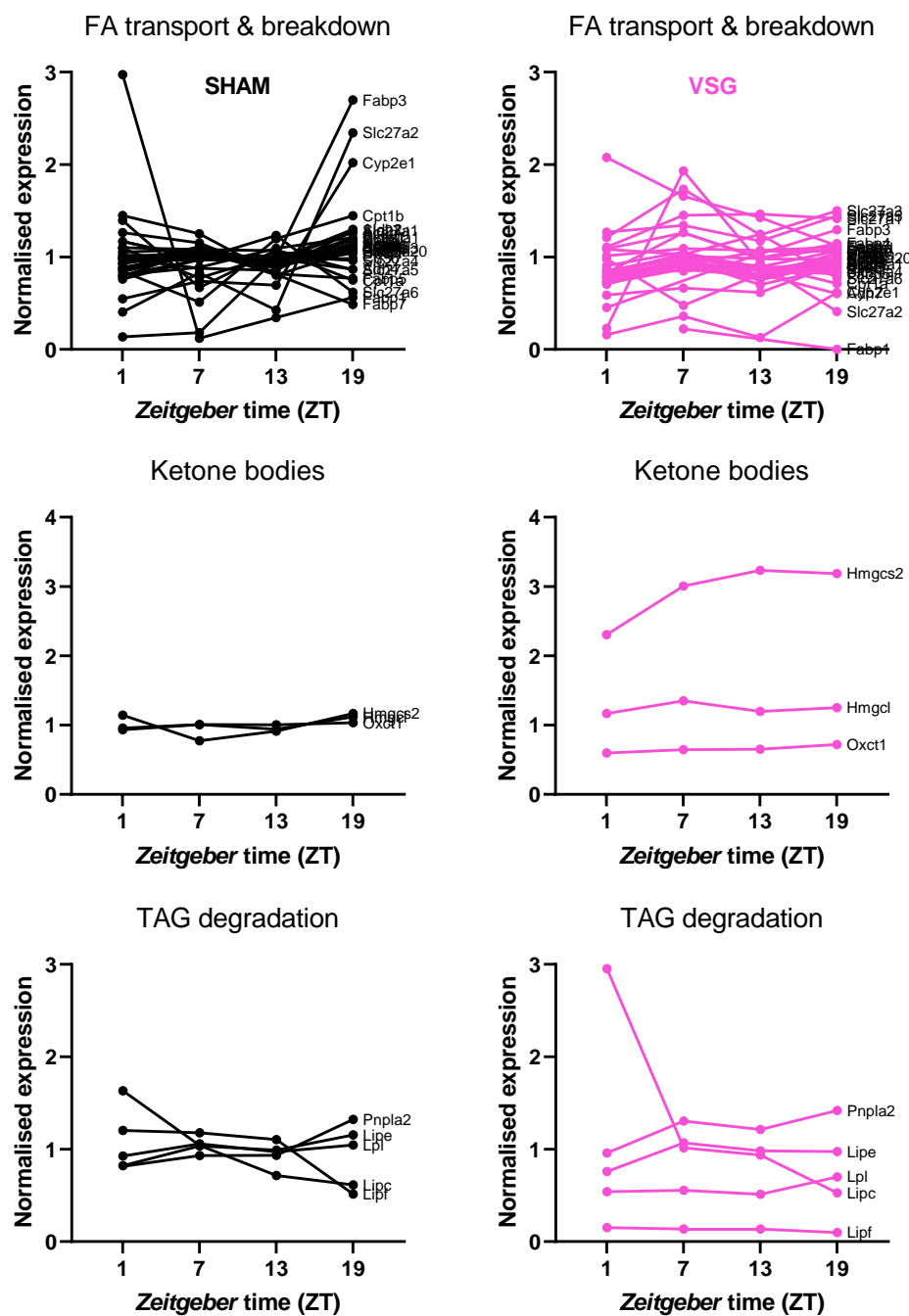


Figure S1: Breakdown of fatty acids. Sham-normalised expression data for pathway-associated genes.

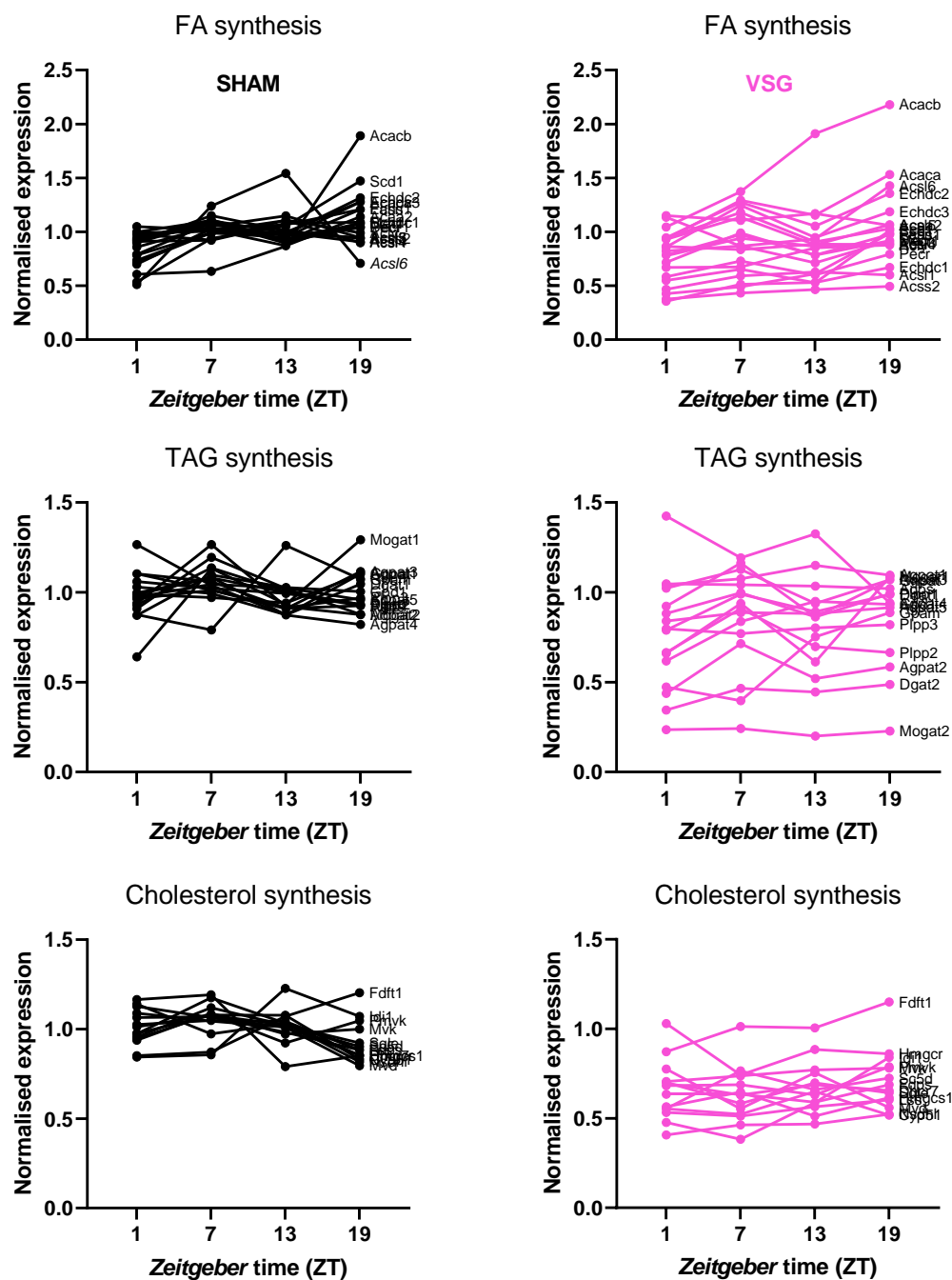


Figure S2: Lipid synthesis pathways. Sham-normalised expression data for pathway-associated genes.

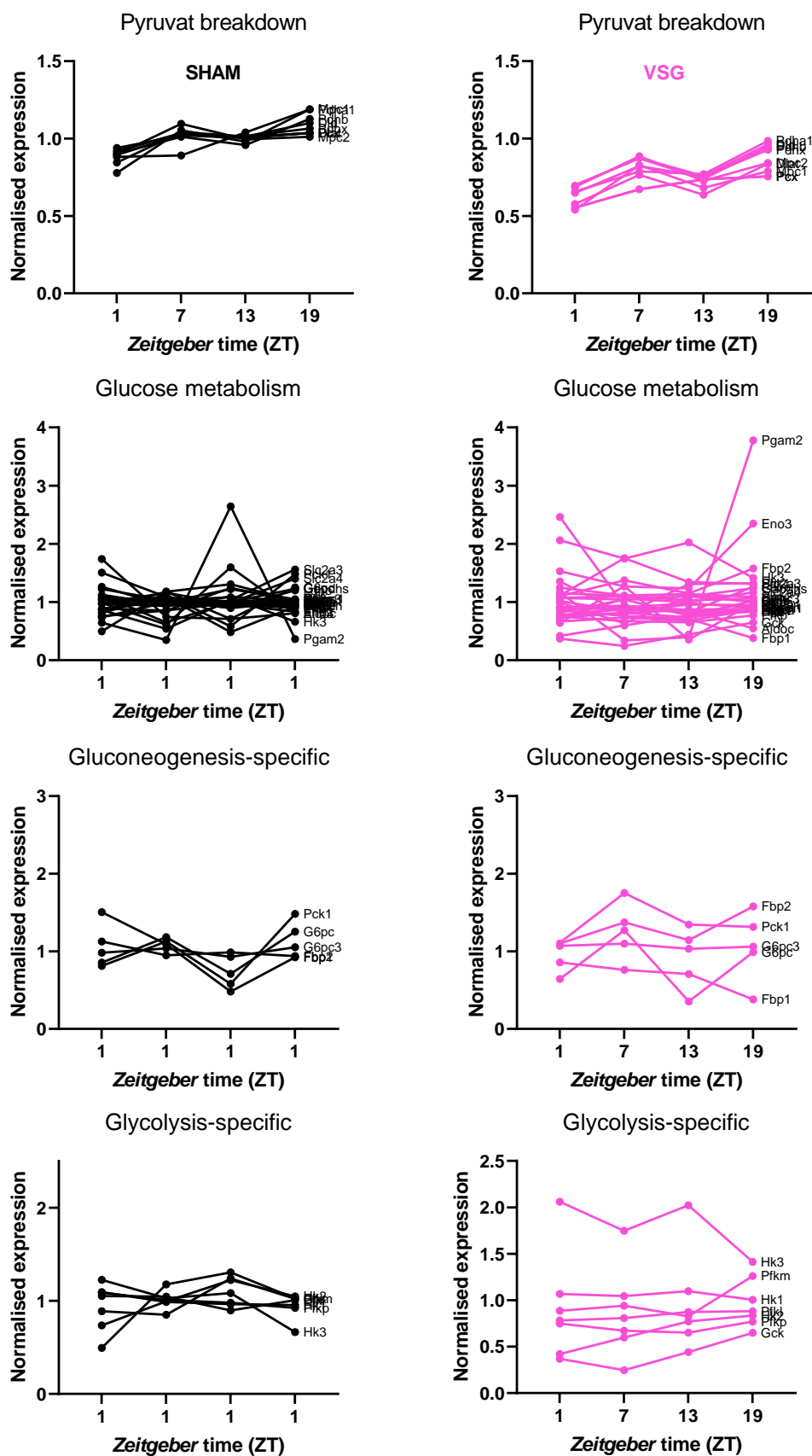


Figure S3: Glucose metabolism pathways. Sham-normalised expression data for pathway-associated genes.

Table S4: Mean ZT expression data and diurnal fold change (dFC) for exemplary genes of specific lipid pathways.

Gene		ZT1	ZT7	ZT13	ZT19	dFC
<i>Lpl</i>	Sham	235557.8 ± 24668.43	269295.0 ± 15157.97	247459.8 ± 9992.06	265801.5 ± 40888.88	0.13
	VSG	137214.6 ± 25075.63	141136.0 ± 34041.40	130310.7 ± 29447.18	178275.0 ± 32228.84	0.33
<i>Pnpla3</i>	Sham	14660.1 ± 3553.15	16265.6 ± 1212.96	19366.0 ± 1535.02	23993.6 ± 2799.51	0.50
	VSG	7207.0 ± 1812.81	7277.6 ± 2305.95	8627.1 ± 2833.89	14408.5 ± 4892.69	0.77
<i>Lipf</i>	Sham	797.4 ± 166.87	780.9 ± 148.28	732.2 ± 130.12	341.6 ± 162.93	0.69
	VSG	98.5 ± 29.98	89.8 ± 34.96	88.1 ± 25.36	63.0 ± 6.70	0.42
<i>Hmgcs1</i>	Sham	11926.8 ± 1139.24	12203.1 ± 1292.02	8093.7 ± 564.68	8720.7 ± 710.87	0.40
	VSG	5793.2 ± 829.88	6621.2 ± 1317.20	5238.9 ± 441.71	6299.8 ± 1051.60	0.23
<i>Hmgcr</i>	Sham	516.8 ± 82.77	441.0 ± 31.60	467.2 ± 17.27	387.2 ± 27.25	0.29
	VSG	466.1 ± 55.65	336.8 ± 24.22	401.2 ± 28.88	389.3 ± 26.83	0.32
<i>Sqle</i>	Sham	549.4 ± 78.19	606.2 ± 59.39	575.7 ± 43.56	519.0 ± 88.73	0.16
	VSG	395.0 ± 48.38	328.0 ± 62.10	391.0 ± 72.75	362.1 ± 32.65	0.18
<i>Hmgcs2</i>	Sham	3162.5 ± 1467.93	2146.0 ± 380.68	2526.4 ± 416.24	3232.5 ± 710.14	0.39
	VSG	6382.6 ± 966.54	8324.9 ± 2627.01	8947.9 ± 2306.57	8805.3 ± 1387.19	0.32
<i>Hmgcl</i>	Sham	1563.2 ± 78.37	1690.7 ± 42.65	1578.4 ± 38.16	1880.0 ± 295.19	0.19
	VSG	1959.4 ± 43.98	2265.2 ± 167.93	2010.3 ± 161.80	2099.9 ± 115.58	0.15
<i>Oxct1</i>	Sham	9298.2 ± 1346.83	9813.0 ± 344.09	9764.9 ± 380.61	10057.7 ± 1022.37	0.08
	VSG	5800.1 ± 522.13	6274.2 ± 595.29	6373.0 ± 636.11	7025.4 ± 580.79	0.19

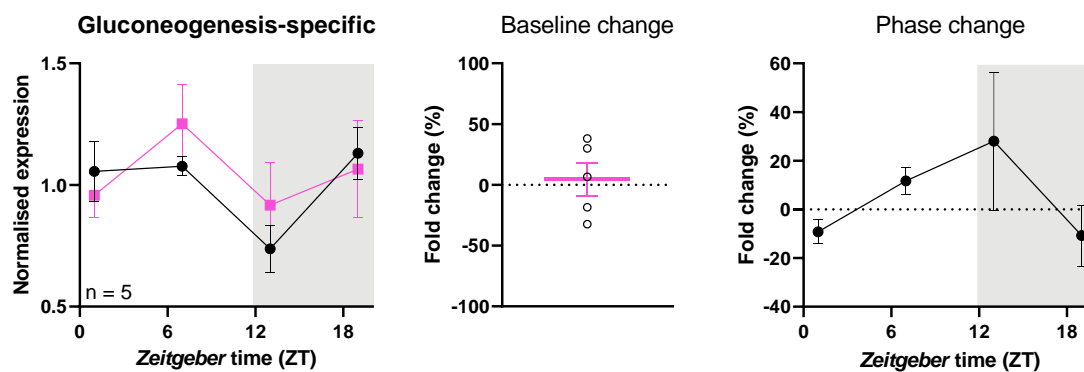
**Figure S4: Gluconeogenesis-specific genes show no phase- or baseline-dependent changes in expression.**

Table S5: Mean ZT expression data and diurnal fold change (dFC) for selected adipokines

Gene		ZT1		ZT7		ZT13		ZT19		dFC
<i>Lep</i>	<i>Sham</i>	113169.5 ±	13817.85	117786.7 ±	5837.05	142189.4 ±	4169.70	111051.2 ±	29051.11	0.26
	<i>VSG</i>	36636.7 ±	9386.33	40724.7 ±	11712.24	51244.3 ±	15632.93	53959.7 ±	6932.03	0.38
<i>Adipoq</i>	<i>Sham</i>	108737.9 ±	15621.67	109243.4 ±	5551.16	103646.7 ±	3138.95	107379.1 ±	3645.80	0.05
	<i>VSG</i>	80367.8 ±	7451.40	105876.1 ±	5270.18	87977.9 ±	3136.51	96549.9 ±	6882.54	0.28
<i>Apln</i>	<i>Sham</i>	1603.1 ±	493.72	1576.6 ±	250.58	1304.0 ±	60.17	933.8 ±	226.90	0.49
	<i>VSG</i>	408.2 ±	73.06	456.2 ±	114.36	395.7 ±	87.82	510.5 ±	68.46	0.26
<i>Rarres2</i>	<i>Sham</i>	7672.3 ±	719.36	10282.2 ±	244.78	8958.3 ±	88.98	9494.2 ±	794.30	0.29
	<i>VSG</i>	9576.7 ±	1132.80	11116.5 ±	532.11	11642.8 ±	948.42	10858.7 ±	312.49	0.19
<i>Serpine1</i>	<i>Sham</i>	2706.2 ±	572.22	6123.6 ±	878.60	2093.2 ±	432.26	609.0 ±	136.92	1.91
	<i>VSG</i>	749.4 ±	230.69	2155.8 ±	469.12	1132.1 ±	164.74	330.5 ±	32.76	1.67
<i>Ccl2</i>	<i>Sham</i>	1338.3 ±	177.17	758.2 ±	60.91	594.0 ±	67.77	591.1 ±	228.69	0.91
	<i>VSG</i>	776.8 ±	144.85	886.2 ±	222.26	624.0 ±	83.83	568.1 ±	65.68	0.45

Acknowledgements

“There’s been trials and tribulations, you know I’ve had my share,
but I’ve climbed the mountain, crossed the river and I’m almost there!”

Tiana, *The Princess and the Frog*

Und angekommen wäre ich nicht ohne die Unterstützung einiger Menschen, bei denen ich mich an dieser Stelle bedanken möchte – für das Wegweisen, die Ratschläge, den Rückhalt und die vielen schönen Momente dazwischen.

Zuallererst möchte ich mich bei meinem Doktorvater, Henrik Oster, bedanken für die beste Betreuung, die ich mir vorstellen kann, für die Möglichkeit mich wissenschaftlich weiterzubilden und auszuprobieren, eine immer offene Tür und ein Arbeitsklima, das seinesgleichen sucht. Im Institut für Neurobiologie gilt tatsächlich „In jeder Arbeit, die erledigt werden muss, steckt ein gewisses Maß an Spaß“ (Mary Poppins) und das wusste ich immer sehr zu schätzen. Mir wird in Zukunft ein Chef fehlen, mit dem man so ausführlich sowohl über Wissenschaft als auch japanische Kultur und Science-Fiction-Filme reden kann.

Weiterhin möchte ich mich bei meinen beiden Zweitbetreuern, Henriette Kirchner und Christian Sina, bedanken für ihre Starthilfe und Ideen zum Projekt. Ich empfand es als persönliche Bereicherung, direkten Zugang zu einer jungen, weiblichen Führungskraft zu haben, und viele unserer Unterhaltungen halfen mir, mich und meine Zukunftsvorstellungen weiterzuentwickeln. Mein Dank geht ebenso an all die Personen, die im Rahmen des GRK jederzeit Fragen beantworteten (speziell Chaoqun Jiang), Hilfe vermittelten oder wissenschaftliche Empfehlungen gaben. Furthermore, I would like to thank Violetta Pilorz, Orr Shomroni, and Iwona Olejniczak. Your professional support, legwork, and cooperation helped shaping crucial parts of this thesis. Violetta, danke dir vor allem für das Anleiten in der Gewebekultur, das Aufarbeiten des SCN sowie die vielen sehr hilfreichen wissenschaftlichen Beiträge. Isa Kolbe, danke, dass du mir geholfen hast, meinen Weg in die Transkriptomanalysen zu finden.

Ein besonderer Dank geht an all die anderen Mitarbeiterinnen der „AG Chronobiologie“ und freundlichen Gesichter des CBBMs. Die manchmal langen und stressigen Tage sind nicht immer einfach wegzustecken, aber wenn man mit so großartigen Leuten zusammenarbeiten (und Mittagessen) darf, ist es doch auch immer irgendwie schön. Viele von euch wurden im Laufe der Zeit zu weit mehr als Kolleg*innen und wir konnten gemeinsam Erinnerungen schaffen, die lange halten werden. Die regelmäßigen Disneyabende sind hoffentlich noch nicht am Ende ihrer Zeit angekommen.

“We stick together and can see it through. ‘Cause you’ve got a friend in me.”

Toy Story

Cathleen, wir haben uns zwar nicht unbedingt gesucht, aber definitiv gefunden. Wie oft hat jemand wohl das Glück, dass man eine neue Arbeitsstelle antritt, mit einer anderen Person zusammenarbeiten soll und dann so sehr auf einer Wellenlänge ist wie wir beide? Wir kannten uns kaum, flogen um die halbe Welt um eine Technik zu lernen und erkundeten wie jahrzehntelange Freunde Ann Arbor. Danke, dass mit dir diese langen OP-Tage so angenehm waren, für all deine Hinweise und Ratschläge zu vor allem den metabolischen Fragen und natürlich diesen unendlich wundervollen Trip nach Paris zu Rapunzel, Winnie und Stitch.

Isa, du hast mir immer auf ganz besondere Art deine Zuneigung gezeigt und ich möchte dies nun nicht mehr missen. Danke, dass du sofort so freundlich und hilfsbereit auf mich zugekommen bist, dass du immer ein offenes Ohr hattest und wir gemeinsam über so ziemlich alles ausgiebig reden konnten,

professionell wie privat und egal wie einig man sich war. Uns verbindet „The Greatest Showman“ ebenso wie „Bautzner Senf“ und das will schon etwas heißen.

Jana, deine direkte No-Nonsense-Art war mir sofort sympathisch. Es hat sich im Laufe der Zeit bestätigt, dass wir uns gut verstehen würden. Danke für deine Meinungen, das Philosophieren über Superhelden (inklusive des Unverständnisses über Isas Vergessen von „Bucky Barnes“) sowie die gemeinsame Reise in das wundervolle Oz. „For Good“ werde ich nun auf ewig mit dir verbinden.

Sandro, though we have not directly worked all that much together, you were a constant positive presence on all things related to the GRK, together, we managed to go through quite some professional ups and downs and I am very grateful for it. Your additional presence in my private life was also much appreciated and I fondly remember our Pokémon Go breaks and Star Wars discussions.

Brinja, danke, dass ich mir bei dir immer noch einmal eine andere Perspektive einholen konnte, für jeden guten Ratschlag und die gemeinsamen Spaziergänge. Irgendwann schaffen wir auch noch einen gemeinsamen Spieleabend. Lisbeth, als du ins Büro eingezogen bist, hat es recht schnell zwischen uns gefunkt. Danke für deine Hilfe beim Präparieren, deine immer ehrliche Art und die gemeinsamen YARE-Momente. Kimberly, mit dir zusammen das Projekt für die Austauschstudentinnen zu planen und anschließend durchzuführen, hat wirklich Freude bereitet. Danke, dass ich vor allem am Ende immer zu dir kommen konnte, mich aufregen durfte und du mich runtergeholt hast. Xenia, ohne dich wäre der Einstieg in die Chronobiologie tausendmal frustrierender gewesen. Danke, für deine Hilfe in der Zellkultur und die vielen abendlichen Diskussionen.

“If everybody got somebody by the hand, maybe everyone could learn and understand.”

Sebastian, *The Little Mermaid*

An dieser Stelle möchte ich mich bei meinen anderen Freunden und natürlich bei meiner immer größer werdenden Familie bedanken. Ihr habt immer hinter mir gestanden und an mich geglaubt. Danke, dass ihr Verständnis hattet, dass ich mal wieder nicht zu Event XY kommen kann, weil ich am Wochenende oder nachts arbeiten musste, und dass ihr Interesse gezeigt habt, mein Projekt zu verstehen, und mir dann spannende, kritische Fragen aus ganz anderen Blickwinkeln gestellt habt.

Es gab einen prägenden Moment in meinem Leben. Als junge Heranwachsende beschloss ich, später in die medizinische Forschung zu gehen und einen Dokortitel zu machen. Jemand entgegnete darauf, ich solle doch bitte realistisch bleiben. Danke Mama, dass du mir beigebracht hast, nicht auf solche Menschen zu hören und meinen Weg zielstrebig zu gehen, dass du immer daran geglaubt hast, dass ich erreiche, was ich mir vornehme und mich dann in all diesen Unterfangen unterstützt hast.

“Love is putting someone else’s needs before yours.”

Olaf, *Frozen*

Zuletzt möchte ich mich bei meinem Partner, Felix, bedanken für seine tägliche Unterstützung. Du warst schon nach kurzer Zeit bereit mit mir irgendwo nach Europa auszuwandern. Es ist dann „nur“ Lübeck geworden, aber es war für mich die richtige Entscheidung und du hast das begrüßt. Alles hast du mitgemacht – meine ungewöhnlichen Arbeitszeiten, meine Launen, wenn ich müde und gestresst war, meine „Hangry“-Momente, mich morgens zur Arbeit fahren, wenn es „zu doll regnet“ oder abends abholen, wenn ich keine Lust auf Fahrradfahren hatte oder der letzte Bus ohne mich gefahren ist. Ohne die Mopsenergie und das Umarmen nach einem schlechten Tag wäre das ganze hier wahrscheinlich nur halb so gut geworden, wenn überhaupt etwas. Vielen Dank, du bist der Beste.

Curriculum vitae

Name: Anne-Marie Neumann
Birth: 1990/01/16
Nationality: German
E-Mail: anne-marie.neumann@gmx.de



WORK

Research Fellow **2017-2020** University Hospital Schleswig-Holstein, Lübeck, Germany
 Institute of Neurobiology

2015-2017 University of Rostock, Rostock, Germany
 Institute for Anatomy / Biomechanics & Implant Technology Research

Research Assistant **2011-2014** University of Rostock, Rostock, Germany
 Institute for Immunology / Institute for Physiology

EU Fulltime Volunteer **2008-2009** Dublin Simon Community, Dublin, Ireland
 Emergency shelter for homeless (Assistant, Reception)

Temporary Help Sales (Real,- 2015; Wupatki Toy Store 2011 & 2013)
 Housekeeping (Hotel Sonne 2009)

EDUCATION

PhD **Since 2017** University of Lübeck, Neuroscience

MS **2012-2014** University of Rostock, Medical Biotechnology (finale grade 1.6)

BS **2009-2012** University of Rostock, Medical Biotechnology (finale grade 1.9)

Secondary School **2000-2008** Käthe-Kollwitz-Gymnasium Rostock, Abitur (finale grade 1.5)

SKILLS

Training Animal handling course at University of Lübeck, Animal surgery workshop at the University of Michigan, Good scientific practice, Presentation skills, Scientific presentation, Scientific writing, Project management, Advanced biostatistics, Intercultural competence, 360° Leadership

Teaching Physiology Seminar Tutor (Winter 2017/18, 2018/19, 2019/20),
 Anatomy Preparation Course Help (2016)

Supervision **2020** MS thesis Clara Ritter
2019 RISE internship student Ryann Carpenter
2018 MD thesis Ruth Merle Brockmann
2017 internship Ann-Engelke Timm

Engagement Young Active Research in Endocrinology (Active Board Member)
 Research Training Group GRK1957 (Vice student speaker until 2020)

Languages German (native), English (European C1), Latin (proficiency), Japanese (basics)

SCIENTIFIC ACCOMPLISHMENTS

Publications

Geißler C, Krause C, **Neumann AM**, et al. Induction and reversal of obesity and insulin resistance is associated with changes in Fgf21 DNA methylation in liver of mice. (In preparation 2021)

Neumann AM, Geißler C, Pilorz V, et al. Restructuring of circadian rhythms after bariatric surgery in male mice. J. Endocrinol. (In revision 2021)

Begemann K, **Neumann AM**, Oster H. Regulation and function of extra-SCN circadian oscillators in the brain. Acta Physiol (Oxf). 2020 May.

Neumann AM. The trouble with stumbling upon circadian clocks. Physiology News. 2019 Jan.

Neumann AM*, Schmidt X*, Brockmann RM, Oster H. Circadian Regulation of Endocrine Systems. Auton Neurosci. 2019 Jan. (*contributed equally)

Streckenbach F, Klose R, Langner S, et al. Ultrahigh-Field Quantitative MR Microscopy of the Chicken Eye In Vivo Throughout the In Ovo Period. Mol Imaging Biol. 2019 Feb.

Landgraf D*, **Neumann AM***, Oster H. Circadian clock-gastrointestinal peptide interaction in peripheral tissues and the brain. Best Pract Res Clin Endocrinol Metab. 2017 Dec. (*contributed equally)

Neumann AM*, Abele J*, Kirschstein T*, et al. Mycophenolate mofetil prevents the delayed T cell response after pilocarpine-induced status epilepticus in mice. PLoS One. 2017 Nov. (*contributed equally)

Hawlichschka A, Holzmann C, Witt S, et al. Intrastrially injected botulinum neurotoxin-A differently effects cholinergic and dopaminergic fibers in C57BL/6 mice. Brain Res. 2017 Sep.

Lindner T, Klose R, Streckenbach F, et al. Morphologic and biometric evaluation of chick embryo eyes in ovo using 7 Tesla MRI. Sci Rep. 2017 Jun.

Conferences

2018-2020

Poster (First-Author): Virtual FENS Forum, July 2020

Talk (First-author): The 42th Annual Meeting of the Japan Neuroscience Society; July, 2019; Niigata, Japan.

*Invited Talk (First-author): "Sektion Angewandte Endokrinologie" Annual meeting; June 2019; Nuremberg, Germany.

Talk (First-author): ABC Symposium 2019; March 2019; Lübeck, Germany.

Poster (First-author): German Clock Club 2019, March 2019; Lübeck, Germany.

Talk (First-author): 20th Annual Meeting Young Active Research in Endocrinology; October 2018; Munich, Germany.

Poster (First-author): German Clock Club 2018, March 2018; Würzburg, Germany.

2014-2017

Poster (First-author): 25th Annual Meeting of the European Orthopaedic Research Society; September 2017; Munich, Germany.

Conference paper (Co-author): European Congress on Computational Methods in Applied Sciences and Engineering 2016; June 2016; Crete, Greece.

Talk (Co-author): The 37th Annual Meeting of the Japan Neuroscience Society; September 2014; Yokohama, Japan.

Awards & Grants

DDG stipend to attend "Diabetes Herbsttagung 2020"
NWG stipend to attend "Virtual FENS Forum 2020"
FENS travel grant to attend "Neuroscience2019" in Niigata, Japan
DAAD stipend to pursue my master thesis abroad in Japan (2014)

Research Stays

2019 Murcia, Spain: University of Murcia, Department of Physiology (3 Months, Collaborations, PhD program)

2014 Kodaira (Tokyo), Japan: National Institute of Neuroscience, Department for Neurodegenerative Diseases (9 Months, MS thesis)

Lübeck, den 24.02.2020

A handwritten signature in black ink, appearing to read 'A. Den'.

“There is just no telling how far I will go.”
Moana